Senescence and Oxidative Stress
in Wallflowers and Arabidopsis

A thesis submitted for the degree of

Doctor of Philosophy

Cardiff University, Wales

by

Faezah Mohd Salleh

2011

UMI Number: U585489

UMI U585489

DECLARATION

This work has not previously been accepted in substance for any degree and is not concurrently submitted in candidature for any degree.

Signed ....[signature]........ (candidate)   Date ....24/06/2011....

STATEMENT 1

This thesis is being submitted in partial fulfillment of the requirements for the degree of
.......PhD.......(insert MCh, MD, MPhil, PhD etc, as appropriate)

Signed ....[signature]........ (candidate)   Date ....24/06/2011....

STATEMENT 2

This thesis is the result of my own independent work/investigation, except where otherwise stated.
Other sources are acknowledged by explicit references.

Signed ....[signature]........ (candidate)   Date ....24/06/2011....

STATEMENT 3

I hereby give consent for my thesis, if accepted, to be available for photocopying and for inter-library loan, and for the title and summary to be made available to outside organisations.

Signed ....[signature]........ (candidate)   Date ....24/06/2011....

ACKNOWLEDGEMENTS

ABSTRACT

Reactive oxygen species (ROS) together with other signalling molecules including phytohormones regulate plant growth and senescence as well as responses to abiotic stress and pathogens. One aim of this thesis was to investigate how ROS and phytohormones regulate progression of senescence in wallflower petals. A second aim of this thesis was to investigate how *SAG21*, previously found to be elevated in wallflower petals, functions during development, senescence and stress in the model plant, *Arabidopsis thaliana*. In wallflowers (Chapter 3), onset of petal senescence was characterized by a rise in ethylene and auxin, followed by ROS accumulation. In parallel, transcript levels for markers of senescence, ethylene biosynthesis and auxin-response also increased with age. However, *SAG21* peaked earlier, before visible senescence. Treatments that aimed to increase cytokinin levels or reduce ethylene delayed progression of senescence and time to petal abscission compared to controls. In contrast, ethylene hastened both processes. Marker genes analysed displayed differential expression patterns. Patterns of ROS-related enzyme activity (catalase, ascorbate peroxidase and superoxide dismutase) were also investigated in relation to wallflower petal and leaf senescence. SAG21 (previously named AtLEA5 in Arabidopsis) belongs to the late embryogenesis-associated (LEA) protein family, implicated in growth and redox responses. A SAG21-YFP fusion was localized to Arabidopsis mitochondria (Chapter 4). Over-expression (OEX) of *SAG21* in Arabidopsis resulted in increased root and shoot biomass, whereas antisense (AS) lines exhibited reduced biomass. Root and shoot development, flowering and senescence were altered in transgenic lines. Transgenic lines exhibited marked root hair phenotypes (Chapter 5). Abiotic stress induced stress induced *SAG21* expression in roots but not leaves. Growth of *B. cinerea* and of a virulent bacterial pathogen (*Pseudomonas syringae* pv. tomato) was affected by *SAG21* expression, however growth of an avirulent *P.syringae* strain was unaffected (Chapter 6). These data show that *SAG21* is regulated by a complex signalling network.

301 words

CONTENTS

Chapter 1: General Introduction

Senescence is a key stage of normal plant development regulated by both internal and external signals (Thomas et al., 2003; Lim, Kim and Nam, 2007). In some organs such as flowers, plant growth regulators are key regulators of senescence (Rogers, 2006; Tripathi and Tuteja, 2007; van Doorn and Woltering, 2008). However, environmental responses are a key feature of plant growth due to their sessile habit and adverse environmental conditions such as abiotic and biotic stresses can induce premature senescence, especially in leaves (Quirino et al., 2000; Lim et al., 2007; Zentgraf, 2007). This suggests common signalling processes between senescence and stress responses (Lim et al., 2007). Both senescence and stress responses are governed by highly regulated processes occurring at structural, biochemical and transcript levels (Cheong et al., 2002; Buchanan-Wollaston et al., 2003; Chinnusamy, Schumaker and Zhu, 2004; Buchanan-Wollaston et al., 2005; Fujita et al., 2006). Hence understanding how growth, stress and senescence signalling interact is important.

Reactive oxygen species (ROS) are elevated by both stress and senescence (Apel and Hirt, 2004; Foyer and Noctor, 2005; Zentgraf, 2007; Foyer and Noctor, 2009; Jaspers and Kangasjärvi, 2010). Recent advances in plant research especially in the model plant, *Arabidopsis thaliana* have shown that cellular redox homeostasis governed mainly by ROS, antioxidative systems and other signalling molecules is considered to be a key integrator of information from metabolism and environment controlling plant growth and acclimation response, as well as senescence and cell death (Foyer and Noctor, 2009b).

1.1 Senescence

Senescence is an age-dependent deterioration process that occurs at cellular, tissue, organ and organism levels. At the organism level this leads to death marking the terminal point of its life span (Nooden et al., 1988). For example, monocarpic annual plants such as many crop plants (e.g. maize, wheat, rice, soybean) undergo leaf senescence followed by organism-level senescence following seed production. On the other hand, in many perennial plants such as trees, senescence is seen as the splendid autumn scenery of colour changes in leaves while the whole plant survives and new leaves are produced the following year (Lim et al., 2007). At

an organ-level, different or similar events may occur upon senescence depending on organ, structure and function. It is worth noting that the function of leaves and flowers are very different, as are the development and signalling mechanisms that trigger their senescence. However, organs including petals and siliques that were thought to evolve from leaves (Friedman et al., 2004) share some common distinctive events during senescence (Thomas et al., 2003; Thomas et al., 2009).

Senescence is not a passive and unregulated decay process but is highly regulated by various internal and environmental factors (Lim et al., 2007). It involves a massive nutrient remobilization of nitrogen, phosphorus and metal ions from ageing leaves or other photosynthetic organs and petals to younger tissues or developing seeds. This contributes to the fitness of the whole plant by ensuring optimum production of offspring and better plant survival thus marking a crucial phase in the plant life cycle (Quirino et al., 2000; Rogers, 2006; van Doorn and Woltering, 2008). In both petals and leaves, remobilization comprises a carefully orchestrated dismantling of the cellular machinery to prevent cell death until remobilization is complete. Microarray results also showed that a large proportion of remobilization-related genes are up regulated in both leaves and petals during senescence (Buchanan-Wollaston et al., 2003; Wagstaff et al., 2003; Hoeberichts et al., 2007; Price et al., 2008; Wagstaff et al., 2009; Bai et al., 2010).

From an agricultural point of view, leaf senescence may limit crop yield by limiting the growth phase. In addition, it also causes postharvest spoilage including leaf yellowing and nutrient loss in vegetable crops such as lettuce and spinach (Lim et al., 2007). Therefore, studying senescence will not only improve our knowledge of the fundamental biological process, but also provide alternatives to improve agricultural traits of crop plants.

1.1.1 Senescence associated events

1.1.1.1 Morphology and structural changes

The most pronounced feature of cell structural change in senescing tissues is the disintegration of intracellular organelles (Thomson et al., 1987). In leaves, yellowing represents the first sign of visible senescence and is due to chloroplast breakdown, the organelle that contains 70% of the leaf protein (Lim et al., 2007). On the other hand, mitochondria and the nucleus remain intact until the last stages of senescence in order to maintain energy production and regulate gene expression respectively (Yen et al., 1998; Simeonova et al., 2000).This indicates that the leaf cell has to remain functional throughout the later stages of senescence suggesting that it might be crucial for effective remobilization of cellular material (Lim et al., 2007). Typical programmed cell death (PCD) hallmarks can be observed during the later stages of leaf senescence. These can be described as vacuolar collapse, chromatin condensation and DNA laddering (Nooden et al., 1988; Cao et al., 2003; Yen et al., 1998). Finally, the loss of plasma membrane integrity disrupts the cellular homeostasis, thus resulting in cell death (Simeonova et al., 2000). These observations indicate that leaf senescence involves cellular events that lead to PCD (Lim et al., 2007; van Doorn and Woltering, 2008).

Visible petal senescence symptoms in many flowers are petal wilting due to loss of turgor and withering associated with colour change and slow dehydration (van Doorn and Woltering, 2008). In several flowers including carnation, iris and gypsophila, visible petal wilting coincided with epidermal cell collapse (Smith et al., 1992; van Doorn et al., 2003; Zhou et al., 2005). In several other species such as *Alstroemeria*, mesophyll cells die earlier than epidermal cells (Wagstaff et al., 2003). Closure of plasmodesmata, important for small molecule transfer including sugars and hormones, is one of the earliest structural changes detected in iris followed by loss of most endoplasmic reticulum (ER), attached ribosomes and Golgi bodies (van Doorn et al., 2003). In addition, senescing petal cells of carnation exhibit a reduction in the number of small vacuoles and an increase in vacuolar size ending with vacuolar collapse (Smith et al., 1992). In tobacco flowers, most mitochondria degrade but a small portion remains until vacuolar collapse (Serafini-Fracassini et al., 2002). The nucleus remains functional until a late stage of senescence however in some species (e.g. *Ipomoea*) it

3

shows several morphological changes such as nuclear blebbing, similar to that observed during animal apoptosis (Yamada, Ichimura and van Doorn, 2006a; Yamada et al., 2006b). Overall, in petal senescence, ultrastructural changes seem similar to those elicited by large-scale autophagy (Rogers, 2006; van Doorn and Woltering, 2008).

1.1.1.2 Metabolical and biochemical changes

A reduction in anabolism including photosynthesis and increase in catabolism such as breakdown of chlorophyll and macromolecules (proteins, membrane lipids and nucleic acids) is the main feature of senescence-associated events (Quirino et al., 2000; Thomas et al., 2003). This massive increase in catabolic activity is responsible for mediating the conversion of cellular materials accumulated during the growth phase into simpler exportable nutrients that will be supplied to other growing organs (Lim et al., 2007; Tripathi and Tuteja, 2007). Hydrolysis of proteins into free amino acids is achieved by the increase of endo and exo-peptidase levels upon senescence (Rubinstein, 2000; Jones et al., 2005). Protein degradation is particularly associated with the accumulation of cysteine proteases in vacuoles (Chichkova et al., 2004; Xu and Zhang, 2009). Loss of membrane lipid phosphate due to lipid-degrading enzyme activity is to date one of the best documented processes in membrane lipid metabolism during senescence (Leverentz et al., 2002). Most of the fatty acids are either oxidized to produce energy for the senescence process to take place or converted to α-ketoglutarate via the glyoxylate cycle which later can later be converted to phloem-mobile sugars (Hörtensteiner and Feller, 2002). Another key event is the massive breakdown of nucleic acids in particular RNA. Total RNA levels are rapidly degraded with the progression of senescence due to the increased activity of several RNases (Rubinstein, 2000; van Doorn and Woltering, 2008).

1.1.1.3 Gene expression changes

Plant senescence is tightly programmed and many genes have been identified whose expression changes during the initiation and/or the execution of normal and induced senescence (Quirino et al., 2000; Buchanan-Wollaston et al., 2003; Tripathi and Tuteja, 2007). In leaf senescence for example, expression of genes related to photosynthesis (e.g. RuBisCO) and protein synthesis are down-regulated. In contrast, expression of genes

4

involved in protein degradation, nucleic acid breakdown, lipid remobilization, chlorophyll breakdown, nitrogen remobilization and antioxidative signalling is increased (Buchanan-Wollaston, 1997; Buchanan-Wollaston et al., 2003). Due to the large number of genes that change in expression, a broader approach has to be taken to obtain a global view of gene expression changes during senescence. Recent technologies have made possible identification of Senescence-Associated Genes (SAGs) on a genome-wide scale. In Arabidopsis, microarray analysis revealed 800 SAGs out of the 24 000 genes screened in the Affymetrix Genechip array, illustrating the dramatic change in gene expression occurring during senescence (van der Graaff et al., 2006).

The expression pattern of several SAGs was studied in more detail in natural senescence and in response to stress and hormone treatments (Weaver et al., 1998; Miller, Arteca and Pell, 1999; Weaver and Amasino, 2001). These studies revealed that the gene expression changes differed between treatments suggesting that SAG expression is regulated by various factors and is not restricted to senescent-specific tissues (Weaver et al., 1998). For example, *SAG12*, a well-known senescence marker which encodes a cysteine protease and is specifically expressed in senescing tissues such as yellow leaves, does not exhibit a strong induction upon stress treatment and does not cause visible leaf yellowing (Weaver et al., 1998; Miller et al., 1999; Pegadaraju et al., 2005). *SAG13, SAG2* and *SAG27,* on the other hand, are also expressed in younger leaves and respond to various stresses (Weaver et al., 1998; Miller et al., 1999; Pegadaraju et al., 2005; Tosti et al., 2006). These findings suggest that all stress-responsive genes are certainly not SAGs and not all SAGs respond to premature senescence, induced by stress or/and hormones. Thus, the regulation of stress-induced senescence probably differs from regulation of natural senescence (Lim et al., 2007). Moreover, comparative transcriptome analysis reveals distinctive gene expression patterns and signalling pathways between natural senescence and dark/starvation-induced senescence in Arabidopsis (Buchanan-Wollaston et al., 2005).

5
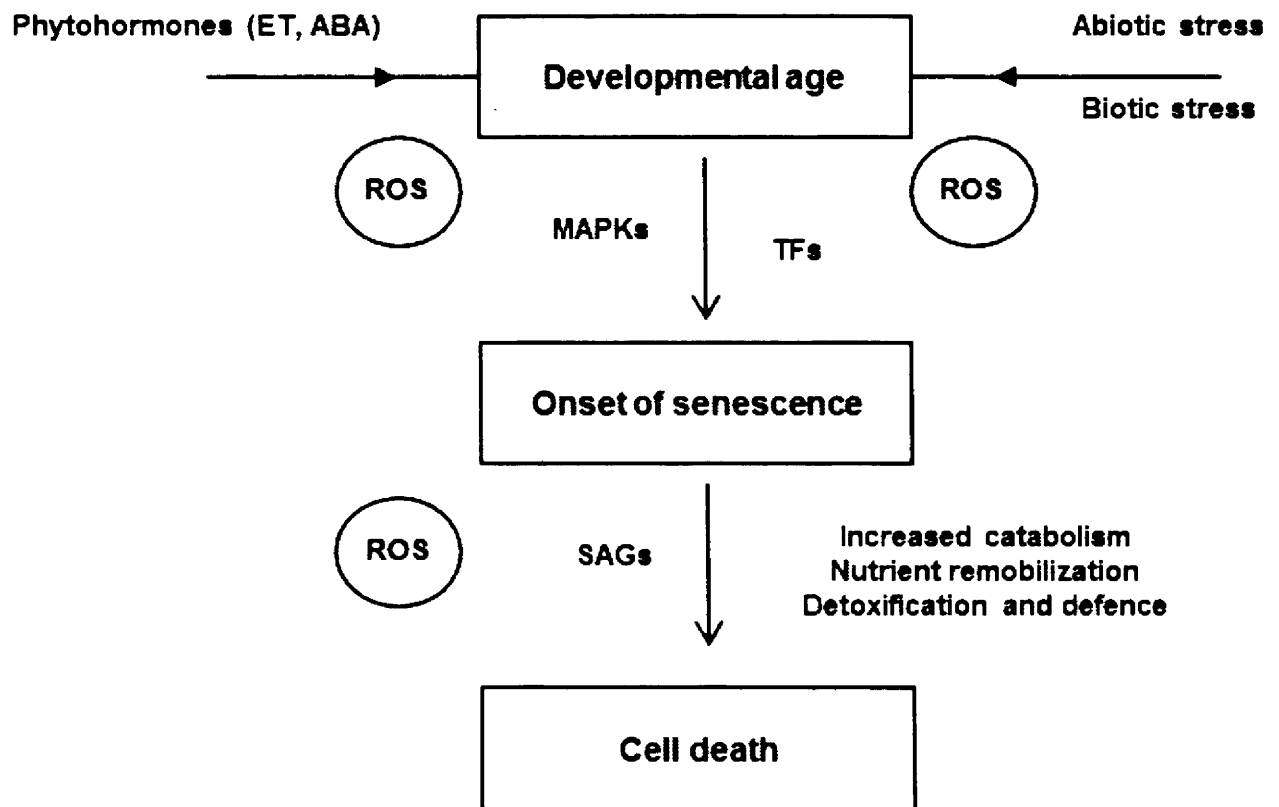
Figure 1-1: A model for senescence integrative response. Senescence is tightly reg various internal (e.g. phytohormones) and external factors (abiotic stress and biotic str plays an important role as a signalling molecule at different phases. The integration c regulatory elements forms a complex network which finally leads to the onset of senes cell death.

1.1.2.1 Phytohormones and senescence or stress-related pathways

Cytokinins and ethylene are the best studied hormones involved in senescence control (Buchanan-Wollaston et al., 2003; Guo and Gan, 2005; van Doorn and Woltering, 2008). Cytokinin appears to be involved in the onset of developmental senescence (Eisinger, 1977). It is widely known that treatment with exogenous cytokinin delays leaf senescence and petal senescence in some ethylene-sensitive flowers (Mor, Spiegelstein and Halevy, 1983; Chang et al., 2003; Hoeberichts et al., 2007; Price et al., 2008). Expression of the cytokinin biosynthesis gene, *Agrobacterium isopentynyl transferase* (*ipt*) gene in tobacco and lettuce under the control of the *SAG12* promoter delayed the time to senescence as well as other senescence markers including chlorophyll breakdown and protein degradation. More recently, a *SAG12* homologue, *SAG39* was identified in a monocot crop plant, rice (Liu et al., 2010). The *SAG39* promoter driving *ipt* expression in rice also elicited similar effects. Transgenic plants also showed earlier flowering due to the altered endogenous cytokinin content, thus also resulting in slower sugar breakdown and nitrogen remobilization during senescence (Liu et al., 2010). Although, the delay in leaf senescence in this kind of crop plant does not result in an improvement in crop yield (seeds) it might be useful in vegetable crops where, prior to harvesting nutrients are retained in the leaves longer.

Ethylene on the other hand which is an essential signal for fruit ripening has also been shown to play a key role in both leaf and petal senescence (Buchanan-Wollaston, 2003; Rogers, 2006). Exogenous application of ethylene promotes premature senescence in older leaves on the plant that are induced to yellowing, and older flowers wilt faster and more severely compared to the untreated ones (Buchanan-Wollaston, 1997; ten Have and Woltering, 1997).

Current knowledge of the phytohormone relationship between stress responses and leaf senescence is mainly based on senescence studies in response to abscisic acid (ABA), jasmonic acid (JA), salicylic acid (SA) and ethylene (ET) (Lim et al., 2007; Tripathi and Tuteja, 2007). These phytohormones are extensively involved in responses to various abiotic and biotic stresses (Anderson et al., 2004; Yasuda et al., 2008). Plants respond to the various external environmental stresses by activating certain stress-hormonal pathways thus triggering the synthesis and expression of stress responsive genes (Seki et al., 2001; Seki et al., 2002; Shinozaki, Yamaguchi-Shinozaki and Seki, 2003). Mutants in ET and JA

7

signalling, and transgenic *NahG* plants defective in SA signalling, all showed delayed senescence (Buchanan-Wollaston et al., 2005). More detail on hormonal regulation during senescence and stress responses is provided in Chapters 3 and 6, respectively.

1.1.2.2 WRKY Transcription Factors (TFs)

In Arabidopsis, genes for 96 transcription factors are up-regulated at least three fold in senescing leaves (Buchanan-Wollaston et al., 2003). WRKYs constitute the second largest transcription factor family in the senescence transcriptome (Guo and Gan, 2005) but the individual function of WRKYs is largely unknown (Zentgraf, Laun and Miao, 2010). The WRKY domain is defined by the conserved WRKYGQK motif in its N-terminal region, and was shown to interact with the *cis*-acting W-box which contains a (C/T)TGAC(T/C) core element (Eulgem et al., 2000; Ulker and Somssich, 2004). The WRKY TFs were initially believed to be plant specific (Eulgem et al., 2000) but recently have been discovered in non-photosynthetic eukaryotes (Berri et al., 2009). WRKY TFs are involved in transcriptional regulation of many plant genes associated with pathogen elicitors, abiotic stress, ROS-regulated processes, senescence and development (Eulgem et al., 2000; Miao et al., 2004). WRKYs that have been shown to regulate senescence include *AtWRKY4, 6, 11* (Eulgem et al., 2000), *53* (Hinderhofer and Zentgraf, 2001) and *70* (Ulker, Shahid Mukhtar and Somssich, 2007). *AtWRKY53* positively regulates developmental senescence while *WRKY70* is a negative regulator (Miao et al., 2004; Ulker et al., 2007).

AtWRKY53 was identified in a suppressive subtractive hybridization experiment specifically designed to isolate genes expressed early in leaf senescence (Hinderhofer and Zentgraf, 2001). *AtWRKY53* mRNA expression was rather unique in that in 6-week-old rosettes, it was only expressed in the oldest leaves before the expression of *SAG12* (senescence marker) became detectable. However, at 7 weeks, expression was detected in all leaves independent of the leaf developmental age, and decreased again in 8-week-old plants (Hinderhofer and Zentgraf, 2001). This finding suggests that this gene might play a key role in early events of leaf senescence. Moreover, the *AtWRKY53* RNAi and knock-out lines showed delayed senescence, whereas overexpression of *AtWRKY53* resulted in precocious senescence, confirming its role as a positive regulator of leaf senescence (Miao et al., 2004). This TF also appears to work antagonistically with a JA-inducible protein EPITHIOSPECIFYING

SENESCENCE REGULATOR (ESR/ESP) to mediate negative crosstalk between senescence and pathogen resistance, which is regulated by a JA and SA counterbalance (Miao and Zentgraf, 2007). Furthermore, another WRKY TF, AtWRKY6 which exhibits induced expression in senescing leaves, also shows enhanced expression upon wounding and pathogen infection (Robatzek and Somssich, 2001, 2002). However, in AtWRKY6 knockout mutants, no obvious senescence-related phenotype was observed despite a change of expression pattern of some SAGs (Robatzek and Somssich, 2001). In addition, senescence phenotypes were not reported for nine other WRKY knock-outs even though expression of these WRKY TFs is up-regulated during senescence (Zentgraf et al., 2010). This implies that altered expression of SAGs in the knockout mutation is not sufficient to affect the phenotype. This might be due to the functional redundancy that exists among the numerous members of the WRKY family (Rushton et al., 2010).

A genomic pull-down assay using recombinant AtWRKY53 proteins identified several SAGs as its direct target proteins: other WRKYs including AtWRKY70, PR genes, stress related genes and auxin-induced genes (Miao et al., 2004). This demonstrates that AtWRKY53 regulates SAG expression and acts in an upstream position in a WRKY signalling cascade (Zentgraf et al., 2010). Moreover, W-boxes are present in the promoters of other WRKY genes and various stress-related proteins suggesting that the WRKY factors act in a regulatory network instead of a linear signalling cascade (Zentgraf et al., 2010). In addition, AtWRKY53 and AtWRKY70 are also up-regulated by ROS accumulation and hydrogen peroxide (H_2O_2) which resulted in oxidative stress (Miao et al., 2004; Ulker et al., 2007).WRKYs are characterized by their redox-sensitive finger DNA-binding domain in which two cysteines together with two histidines interact electrostatically with a zinc atom to form a 'zinc finger', which makes them excellent candidates for redox regulation (Miao et al., 2004).

1.1.3 ROS-antioxidant signalling

Plants, being aerobic, utilize molecular dioxygen (O_2) as their main terminal electron acceptor in both photosynthesis and photorespiration processes. In these events, O_2 is reduced into highly reactive free radicals called reactive oxygen species (ROS) (Zimmermann and Zentgraf, 2005). ROS are continuously produced as by-products of many processes associated with plant growth and development and their overproduction in cells is often referred to as oxidative stress which causes oxidative damage to proteins, DNA and lipids (Apel and Hirt, 2004). However, growing evidence indicates that ROS accumulation acts as a vital subset of the signal perception and transduction that plants adopt to make appropriate adjustments of transcriptional expression and cell structure in response to developmental cues (e.g hormones) and environmental changes (Foyer and Noctor, 2005; Pitzschke and Hirt, 2006) hence affecting diverse developmental such as senescence and acclimation processes upon stress (Zimmermann and Zentgraf, 2005; Foyer, Faragher and Thornalley, 2009; Foyer and Noctor, 2009). In addition, transcript levels of eight out of twelve Arabidopsis SAGs were induced by ozone (Weaver et al., 1998) and expression of many other SAGs was also enhanced dramatically by increased levels of ROS (Navabpour et al., 2003) indicating that alteration of internal redox state might act as signal to promote senescence.

The sophisticated ROS network consists of Reactive Oxygen Intermediates (ROIs), ROS-producing enzymes (eg; NADPH oxidases), antioxidative enzymes (e.g catalases, ascorbate peroxidases, superoxide dismutase) and antioxidants (ascorbate, glutamate) (Pitzschke and Hirt, 2009). Upon ROS induction, ROS sensors located at the cell surface (Foyer and Noctor, 2009) are activated, transducing the signal via kinase signalling cascades (e.g. Arabidopsis *OXI1* (Rentel et al., 2004) that then translate this information into biological output programmes (Pitzschke and Hirt, 2009). Oxidative signals are then transmitted in both plants and animals by a mitogen-activated protein kinase (MAPK) cascade (Foyer and Noctor, 2005; Foyer et al., 2009). The specificity of the biological response is highly dependent on several factors: chemical identity of the ROS, intensity of the signal, production site, plant developmental stage, previous stresses encountered and finally interactions with other signalling molecules such as phytohormones (Foyer and Noctor, 2009).

1.1.3.1 ROIs

ROS can appear in several forms depending on the catalytic steps they undergo. The first step of O_2 reduction results in the formation of superoxide (O_2^-) or hyperoxide (HO_2^-). The second step leads to the formation of hydrogen peroxide (H_2O_2) (Foyer and Noctor, 2009). Chemical attributes of specific ROS members such as half-life have a significant effect on the severity of oxidative stress caused. For example, H_2O_2 has a longer half life than O_2^- thus making it an excellent candidate to act as a signalling molecule (Apel and Hirt, 2004; Zimmermann and Zentgraf, 2005). Hydrogen peroxide (H_2O_2) is the most stable ROS, being the only intermediate that could cross plant membranes and therefore directly function in cell-cell signalling (Gadjev et al., 2006; Pitzschke and Hirt, 2006). The oxidizing power of these free radicals can serve as a potential hazard to the surrounding cellular environment. H_2O_2 can inactivate enzymes by oxidizing their thiol groups leading to functional impairment of major processes. Upon binding with metal ions such as Fe^{3+} or Cu^{2+}, the destructive properties of O_2^- and H_2O_2 are significantly enhanced by the formation of the most reactive radical in the ROS family, hydroxyl radical (OH^-) through the Fenton/Haber Weiss reaction (Apel and Hirt, 2004). Interaction of OH^- with any molecules including nucleic acids, proteins and lipids contributes to the highest degree of damage involving macromolecule degradation (Foyer and Noctor, 2009) and lipid peroxidation which are main events associated with senescence (Leverentz et al., 2002). Lipid peroxidation leads to the generation of more free radicals, which in turn initiates an increase in ethylene formation resulting in early senescence signals (van Doorn and Woltering, 2008).

1.1.3.2 ROS perception and signal transduction

MAPK cascades minimally comprise a MAPKKK-MAPKK-MAPK module (activated via reversible sequential phosphorylation) that is linked in various ways to upstream receptors and downstream targets (Rodriguez, Petersen and Mundy, 2010). In Arabidopsis, the characterization of MAPKKK *MEKK1* as a regulator of redox homeostasis with MAPKK *MKK1/2* (Gao et al., 2008) and MAPKK *MPK4* being its downstream regulators (Nakagami et al., 2006) has improved our understanding of its importance in plant ROS signalling (Pitzschke et al., 2009). Figure 1-2 represents a putative model of ROS signalling by this MAPK cascade upon stress in Arabidopsis.
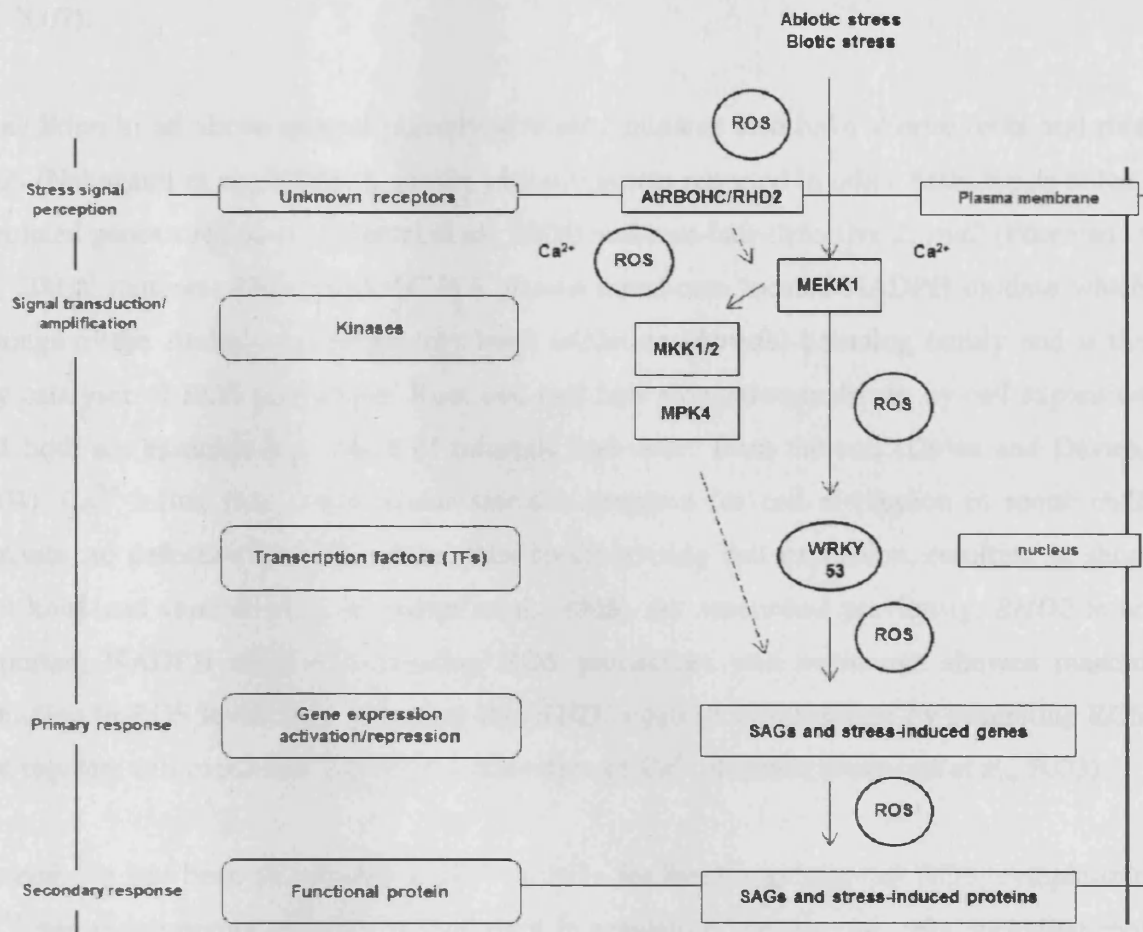
Figure 1-2: A model for MAPK cascade: MEKK1-MKK1/2-MPK4 regulation upon stress in Arabidopsis. ROS could act as a signalling molecule at different regulation points thus affecting the expression of TFs (e.g *WRKY53*) and the downstream stress/senescence induced genes (e.g. *SAGs*, *LEA* proteins).

MEKK1 transcripts are up-regulated by cold, salt, drought, wounding and touch (Mizoguchi et al., 1996) and have been implicated in biotic stress signalling (Suarez-Rodriguez et al., 2007). *mekk1* knockout plants show severe lethal dwarfism, accumulate a high level of ROS and display a mis-regulation of a number of redox-regulatory enzymes (Nakagami et al., 2006). In addition, *MEKK1* may also be involved in the regulation of senescence, in part by direct transcriptional regulation of its key transcription factor, *WRKY53* (Miao et al., 2007) through a H_2O_2 induced pathway. *In vitro* experiments confirmed that MEKK1 can interact directly

with *WRKY53* and binds to a MYC-related binding motif in the *WRKY53* promoter (Miao et al., 2007).

In addition to an above-ground phenotype, *mekk1* mutants also have shorter roots and root hairs (Nakagami et al., 2006). A similar phenotype was reported in other Arabidopsis redox-regulated genes such as *oxi1*(Rentel et al., 2004) and root-hair-defective 2, *rhd2* (Foreman et al., 2003), mutants. *RHD2/AtrbohC* is a plasma membrane located NADPH oxidase which belongs to the Arabidopsis respiratory burst oxidative (*Atrboh*) homolog family and is the key catalyser of ROS production. Root and root hair elongation is driven by cell expansion and both are essential for uptake of minerals and water from the soil (Dolan and Davies, 2004). Ca^{2+} influx from extracellular stores is required for cell elongation in roots. *rhd2* mutants are defective in Ca^{2+} uptake, thus compromising cell expansion, resulting in short root hairs and stunted roots (Foreman et al., 2003). As mentioned previously, *RHD2* is an important NADPH oxidase stimulating ROS production, and its mutant showed marked reduction in ROS levels thus indicating that RHD2 controls development by generating ROS that regulate cell expansion through the activation of Ca^{2+} channels (Foreman et al., 2003).

Recently, it has been shown that a local positive feedback regulation of ROS, cytoplasmic Ca^{2+} and redox-regulated genes is important in regulating tip-growing cells including root hair, pollen tube and fungal hyphae (Knight, 2007; Lee and Yang, 2008; Takeda et al., 2008). GFP-*RHD2* driven by its own promoter localised to all epidermal cells of the elongation zone but became restricted to trichoblasts (specialized cells that form root hairs) in the zone just before hair outgrowth occurred (Takeda et al., 2008). *RHD2* remained at the site of growth during hair elongation and disappeared when growth stopped, suggesting that *RHD2* restricts ROS production to the growth points of the cell (Takeda et al., 2008). A similar focusing of ROS-production at the tips of immature root hairs has also been described in maize (Carol and Dolan, 2006). Exogenous ROS application to *rhd2* mutants only partially rescued the phenotype by stimulating growth from *rhd2* trichoblasts but led to depolarized root-hair growth which resulted in the formation of spherical bulges instead of typical thin, long WT hairs (Foreman et al., 2003; Carol and Dolan, 2006). Taken together, these findings show that maintaining the correct redox homeostasis, specific ROS production site and polarized-ROS production is critical for correct plant development.

1.1.3.3 ROS scavenging enzymes and antioxidants

Plants possess a carefully regulated system to prevent ROS toxicity and ensure accurate execution of their signalling functions (Foyer and Noctor, 2005). They have evolved two main pathways comprising an enzymatic and non-enzymatic antioxidant system, which work together with the ROS-producing enzymes in order to maintain ROS homeostasis in different cellular compartments (Foyer and Noctor, 2009). The enzymatic system is governed by three main enzymes, catalases (CAT), superoxide dismustase (SOD) and ascorbate peroxidase (APX). An efficient regulation of these enzyme levels is essential to maintain and restrict the level of superoxide (O_2^-) and H_2O_2 in different cell compartments (Zimmermann and Zentgraf, 2005). SODs are the only plant enzymes capable of scavenging O_2^- while CAT and APX work together during H_2O_2 catabolism. In Arabidopsis, measurement of hydrogen peroxide (H_2O_2) content in leaves revealed that H_2O_2 levels increased during development and peaked exactly when the plants started to bolt (Miao et al., 2004; Zimmermann et al., 2006). All three Arabidopsis catalase isoforms (CAT1, CAT2 and CAT3) and one APX isoform (APX1) showed differential regulation of enzyme activity during bolting time. The decrease in CAT2 activity and mRNA level at bolting time has been proposed to be an integral part of H_2O_2-triggered leaf senescence (Zimmermann et al., 2006; Smykowski, Zimmermann and Zentgraf, 2010).

Besides the enzymatic antioxidant system, the complex ROS network is also governed by low molecular weight non-enzymatic antioxidants such as ascorbate, glutathione, tocopherol and carotenoids (Foyer et al., 2009). They are mainly divided into water-soluble antioxidants and lipid-soluble antioxidants and play an important role in specific cell compartments (Foyer and Noctor, 2005). In addition, comparative transcriptome analyses reveal an up-regulation of various antioxidants, metal binding (metallothionein-like) and stress-detoxification (heat shock proteins, glutathione-S-transferase) genes in both natural and dark-induced leaf senescence, and petal senescence (Buchanan-Wollaston et al., 2005; Price et al., 2008; Wagstaff et al., 2009), which may have a role in modulating ROS levels.

1.2 Abiotic stress responses

Abiotic stress responses are crucial for sessile organisms such as plants because without this mechanism, plants would be unable to survive and cope with the constantly changing environment. The term 'abiotic stress' comprises various stresses including osmotic stress, drought, high salinity, high and low temperature, freezing, ultraviolet (UV) light, heavy metals and hypoxia (Nakashima, Ito and Yamaguchi-Shinozaki, 2009; Hirayama and Shinozaki, 2010). Besides inducing premature senescence as mentioned earlier, overall agricultural productivity is also compromised when crop plants are subjected to such stresses, particularly drought and high salinity due to their magnitude of impact and prevalence (Bray, 1993; Bartels, 2005). Thus, understanding abiotic stress responses is now thought to be one of the major topics in plant science.

Plants respond and adapt to abiotic stresses at all levels: molecular, cellular, physiological and biochemical (Urano et al., 2010). The regulatory circuit includes a complex integration of stress receptors/sensors, various signalling pathways, transcription factors and promoters and finally the output proteins or metabolites (Bartels, 2005). The completion of the genome sequence for the model plant, *Arabidopsis thaliana* and a major crop plant *Oryza sativa* spp. *Japonica* cv *Nipponbare*, allowed genome-wide expression profiling in response to numerous stresses using microarray technology thus identifying various stress-induced genes. Moreover, comprehensive transcriptome analyses revealed clear relationships between stress-regulated transcript expression profiles, and their 5'-*cis*-regulatory motifs (Yamaguchi-Shinozaki and Shinozaki, 2005). These findings revealed that stress-regulated genes are governed by a complicated regulatory network (Hirayama and Shinozaki, 2010). The function of stress-inducible genes can be categorised into two major groups: one involved in direct stress tolerance (e.g. LEA proteins, enzymes for osmolyte biosynthesis and detoxification enzymes) while the other contains regulators for intracellular signalling and gene expression such as protein kinases (MAPKs), phosphatases, transcription factors and phospholipid metabolic enzymes (Shinozaki, Yamaguchi-Shinozaki and Seki, 2003; Shinozaki and Yamaguchi-Shinozaki, 2007).

Abscisic acid (ABA) is synthesized under water-deficit conditions. It thus plays an important role in seed maturation and seed dormancy and in inducing stress responses in vegetative tissues, particularly responses to drought and high salinity (Bray, 1993; Cutler et al., 2010). Many stress-inducible genes are induced by ABA but some are not, indicating that both ABA-dependent and ABA independent regulatory networks are involved in the abiotic stress-induced gene expression (Shinozaki et al., 2003; Bartels, 2005). Promoter analyses of drought and/or cold induced genes revealed at least four regulatory systems for gene expression, two are ABA-dependent while the other two are ABA-independent (Yamaguchi-Shinozaki and Shinozaki, 2005). Since many genes are up-regulated by various stresses at the same time (e.g. cold, drought, salt), this shows that there is crosstalk between the different stress-regulatory systems (Fig.1-3) implying interactions between the corresponding cis-regulatory elements (Shinozaki and Yamaguchi-Shinozaki, 2007; Nakashima et al., 2009).

1.2.1 Transcriptional regulation of gene expression

1.2.1.1 ABA-dependent gene expression
1.2.1.1.1 The ABA-responsive element (ABRE) regulon

A large number of drought and salt-inducible genes respond to exogenous ABA application in Arabidopsis and rice (Bray, 1993; Seki et al., 2002; Rabbani et al., 2003). Promoter regions of these ABA-inducible genes were compared and analysed which lead to the identification of a conserved sequence, PyACGTGGC/TC (Bartels, 2005). This sequence was first identified in a wheat LEA *Em* gene (Guiltinan, Marcotte and Quatrano, 1990) and later in a rice LEA gene, *RAB16* (Mundy, Yamaguchi-Shinozaki and Chua, 1990) and was named an ABA responsive element (ABRE). Both of these *LEA* genes are expressed in dehydrated tissues and maturing seeds. ABRE is a major cis-acting element in ABA-responsive genes (Nakashima et al., 2009). However, a single copy of ABRE is not sufficient for ABRE-dependent transcription. For ABA activation, ABRE requires another cis-element referred to as the coupling element (CE). In the promoters of barley genes *HVA22* and *HVA1*, the coupling elements CE1 and CE3 are necessary for ABA activation (Shen and Ho, 1995; Shen, Zhang and Ho, 1996). However in the Arabidopsis dehydration-responsive gene promoter, *RD29B*, two ABRE sequences are required for its expression in seeds and for

ABA-induced expression in vegetative tissues and one of the ABRE cis-elements probably acts as a coupling element (Uno et al., 2000). Most of the known coupling elements identified so far are similar to ABREs and composed of the A/GCGT motif (Yamaguchi-Shinozaki and Shinozaki, 2005).

Arabidopsis cDNAs encoding basic-domain leucine zipper (bZIP) TFs, referred to as ABRE binding proteins (AREB) or ABRE binding factors (ABF), were isolated using yeast one-hybrid screening (Choi et al., 2000). The AREB/ABF binds to the ABRE cis-elements and activates ABA-dependent gene expression. Arabidopsis *AREB1/ABF2*, *AREB2/ABF4* and *ABF3* are mainly induced by dehydration and high salinity in vegetative tissues but are absent in seeds (Yamaguchi-Shinozaki and Shinozaki, 2005). In fact, overexpression of *AREB1* in transgenic plants results in ABA hypersensitivity, reduced transpiration rate and enhanced drought tolerance (Fujita et al., 2005). On the other hand, promoters of both *ABF3* and *ABF4* showed highest expression in roots and guard cells which is consistent with their proposed role in stomatal regulation and water stress response (Kang et al., 2002). The *areb1 areb2 abf3* triple mutant showed significant down-regulation of various genes responding to dehydration, high salinity and ABA treatments which included 13 LEA genes, ABA-regulated genes and MYB TF genes (Yoshida et al., 2010). These results are in agreement with the previous finding which indicates that AREB1, AREB2 and ABF3 act as positive regulators in ABA/water-stress signalling.

In many plant systems, transcriptional regulation is controlled by phosphorylation (Colcombet and Hirt, 2008). AREB/ABF proteins in Arabidopsis and TRAB1 of rice are regulated via phosphorylation of the multiple Ser/Thr residues (Chae et al., 2007). Bimolecular fluorescence complementation (BiFC) analysis confirmed that SNF1-related kinase 2 (SnRK2)-type protein kinases interact with these TFs upon water-stress and co-localize in plant cell-nuclei (Bucholc et al., 2011). In addition, AREB1 was also shown to interact with a key determinant of ABA sensitivity, SRKD2 (Choi et al., 2000). These observations suggest that the ABA-dependent phosphorylation of AREB/ABF type TFs by SnRK2 protein kinases may play an important role in regulating the AREB/ABF activation in both monocot and dicot plants . Thus, clarification of the AREB/ABF-SnRK2 system may lead to better strategies for creating drought-tolerant plants.

Time course   Biotic stress   Osmotic stress   Cold
                wounding   (drought/salt)

                                JA   ABA   DREB2

Rapid response

                                                    DREB1/
                                                    CBF

                                          AREB/   DRE/
                                          ABF   CRT

Slow and adaptive   MYC2   MYB2
response
                     MYC   MYB   ABRE

Stress-induced gene expression
(e.g. LEA proteins, metabolic enzymes)
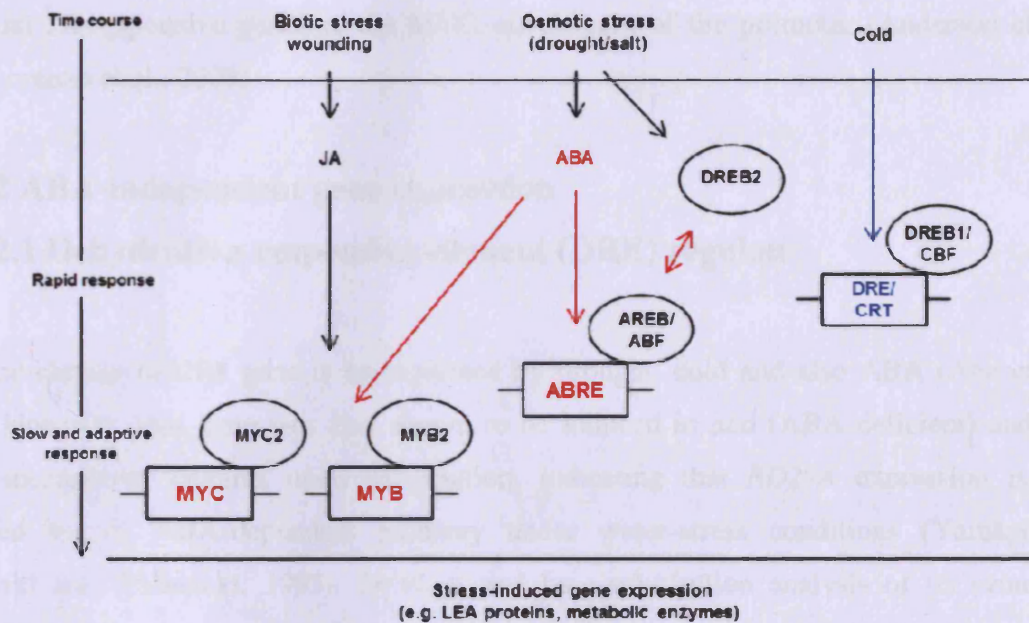
Figure 1-3: Major transcriptional regulatory networks of *cis*-acting elements and transcription factors (TFs) involved in abiotic stress-responsive gene expression in Arabidopsis. Two major pathways contribute to abiotic stress regulation: an ABA-dependent pathway (in red) and an ABA-independent pathway (in blue). *Cis*-acting elements are shown in boxes; TFs are represented by ovals.

1.2.1.1.2 The MYC and MYB regulon

Some ABA-induced genes are not regulated by ABRE-like motifs. In a dehydration responsive gene promoter, *RD22*, ABA-dependent expression is regulated by MYC and MYB *cis*-elements upon water-stress (Abe et al., 1997). Two TFs, a MYC-like basic helix-loop helix (bHLH), *AtMYC2* and a MYB TF, *AtMYB2* were shown to bind to the MYB and MYC recognition sites in the *RD22* promoter, thus regulating the expression of *RD22* (Abe et al., 2003). Both TFs are synthesized after the accumulation of ABA upon water-stress indicating a later response compared to the ABRE (Boter et al., 2004). Microarray analysis revealed that transgenic plants overexpressing both TFs (which have higher sensitivity towards ABA and higher osmotic tolerance) show an increase in genes encoding ABA-inducible genes which also includes a jasmonic acid (JA) inducible gene (Lorenzo et al., 2004). In addition, AtMYC2 was demonstrated to play a role in JA-regulation (induced by biotic stress and wounding) in plant defence in Arabidopsis suggesting a crosstalk between

ABA and JA-responsive genes at the MYC *cis*-element of the promoter (Anderson et al., 2004; Lorenzo et al., 2004).

1.2.1.2 ABA-independent gene expression
1.2.1.2.1 Dehydration responsive element (DRE) regulon

The Arabidopsis *RD29A* gene is up-regulated by drought, cold and also ABA (Abe et al., 1997). However, this gene was also shown to be induced in *aba* (ABA deficient) and *abi* (ABA insensitive) mutants upon dehydration, indicating that *RD29A* expression is not regulated by an ABA-dependent pathway under water-stress conditions (Yamaguchi-Shinozaki and Shinozaki, 1993). Deletion and base-substitution analysis of its promoter identified a 9-bp conserved sequence, TACCGACAT, known as a dehydration responsive element (DRE) which is the most important *cis*-regulatory element regulating *RD29A* expression in response to dehydration and cold in the absence of ABA induction (Yamaguchi-Shinozaki and Shinozaki, 1994). Unlike ABRE, a single copy of DRE is sufficient to trigger ABA-independent stress responsive genes without coupling with other elements. DRE plays a crucial role in the regulation of gene expression in response to drought, high salinity and cold stresses in Arabidopsis (Yamaguchi-Shinozaki and Shinozaki, 19931994). Similar DRE-like *cis*-acting elements consisting of an A/GCCGAC motif referred to as a C-repeat (CRT) and low temperature responsive element (LTRE) were also reported to be involved in cold-inducible promoters in various plants including Arabidopsis and grasses such as rice, wheat, barley, maize and sorghum (Seki et al., 2001).

Three Arabidopsis cDNAs encoding DRE-binding proteins were isolated via yeast one-hybrid screening: C-repeat binding factor 1 (CBF1), the DRE binding proteins 1A (DREB1A) and DREB2A (Liu et al., 1998). These proteins contain an APETALA2 (AP2/ethylene responsive element binding factor) motif and bind specifically to the DRE/CRT recognition sites thus regulating the activation of genes whose transcription is regulated by the DRE/CRT sequence in Arabidopsis (Singh, Foley and Oñate-Sánchez, 2002). *DREB1* expression is rapidly induced by cold, but not by dehydration or high salinity. Conversely, *DREB2* transcription is induced by dehydration and salinity (Maruyama et al., 2004). This specificity in the response of the DRE-binding proteins indicates the presence of

cross-talk between drought and cold-responsive expression in the DRE *cis*-regulatory element. In addition, the DRE/CRT sequence may also serve as a coupling element (CE) of ABRE in response to ABA (Narusaka et al., 2003), implying the presence of crosstalk between the two regulons (Seki et al., 2002).

Constitutive expression of the *DREB1/CBF1* TF in Arabidopsis resulted in enhanced tolerance towards drought, high salinity and freezing demonstrating that DREBs/CBFs target multiple genes (Seki et al., 2001). Furthermore, microarray analysis successfully identified more than 40 target genes including LEA proteins, carbohydrate-metabolism related proteins, sugar transport proteins, osmoprotectant biosynthesis proteins and also protease inhibitors. Most of the target genes detected known to function in stress regulation and also senescence. Metabolomic analysis of transgenic lines also charted an increase in osmoprotectants, such as proline and various sugars (Zhou et al., 2005; Zhou et al., 2010). Over expression of *DREB/CBF* homologues identified in rice, maize, barley and wheat in Arabidopsis or tobacco confer similar tolerance to drought, salinity and freezing and also the accumulation of osmoprotectants (Nakashima et al., 2009). However, overexpression of the *DREB/CBF* gene also caused severe growth retardation under optimal growth conditions. *DREB/CBF* transgenic lines driven by the stress-inducible promoter, *RD29A* resulted in normal plant growth and was then implemented for *DREB1* overexpression studies (Qin et al., 2004). These data suggested the over-expression of DRE regulons in a variety of grasses could possibly be used to improve crop tolerance towards drought, high salinity and cold (Nakashima et al., 2009).

1.2.1.1.2 Other regulons

Besides the DRE and ABRE *cis*-regulatory elements described earlier, there are several drought-inducible genes which do not respond either to cold or ABA. This suggests the existence of another ABA-independent gene expression response upon dehydration stress. The *EARLY RESPONSIVE TO DEHYDRATION 1 (ERD1)* gene which encodes a proteolytic regulatory subunit is an example of a drought-inducible gene not regulated by cold or ABA (Nakashima et al., 1997; Simpson et al., 2003). *ERD1* is also up-regulated during natural senescence and dark/starvation induced senescence (Weaver, Froehlich and Amasino, 1999; Simpson et al., 2003). The expression of the *ERD1* gene is regulated by the activation of *cis*-

acting elements NACR and a zinc-finger homeodomain (ZFHD) present in the *ERD1* promoter (Tran et al., 2004).

1.3 Late Embryogenesis Abundant (LEA) proteins

The ability of numerous animals, plants and microorganisms to survive in extreme environments has long been of interest to understand the underlying mechanisms (Tunnacliffe and Wise, 2007; Battaglia et al., 2008; Tunnacliffe et al., 2010). One of the most dramatic results of evolution is the capability of anhydrobiotic organisms to withstand almost complete water loss (up to ~7% of normal water content), yet remain viable (Tunnacliffe and Wise, 2007). Some anhydrobiotic organisms include invertebrates such as nematodes, (*Aphelenchus avenea*), bdelloid rotifers (*Adenita ricciae, Brachionus plicatilis*), microorganisms (*Saccharomyces cerevisiae)* and the resurrection plant *(Craterostigma plantagineum)* (Browne et al., 2004; Bartels, 2005; Pouchkina-Stantcheva et al., 2007; Denekamp et al., 2009). In addition, most plant seeds are dessication tolerant, as are other propagules such as pollen (Hoekstra, Golovina and Buitink, 2001; Alpert, 2006). Upon dehydration, these organisms and propagules are able to resume life processes into the metabolically active state without experiencing any severe damage. This phenomenon is described as 'anhydrobiosis' or dessication tolerance. In addition to water stress, organisms with this attribute are also highly resistant to extreme temperature (Hand et al., 2010).

Due to their special survival traits, some of these organisms are able to remain viable for a very long time in a dry state and unfavourable conditions. Some invertebrates can revive successfully after decades of activity suspension (Guidetti and Jonsson, 2002). Moreover, some seeds that had been dormant for thousands of years, germinated successfully when rehydrated (Shen-Miller et al., 1995). In contrast, the opposite effect was reported in desiccation-sensitive maize where severe damage was observed at all levels following drying (Leprince et al., 1995). In this state, membrane structures are modified resulting in leakiness and fusion, followed by loss of correct protein structural confirmation which finally causes failure of various functions. Besides that, desiccation-sensitive organisms also experience nucleic acid rearrangement thus compromising their RNA, DNA and chromatin stability (Kanias, Wong and Acker, 2007).

The mechanism underlying desiccation tolerance or anhydrobiosis has been investigated for the past few decades (Wise and Tunnacliffe, 2004). The most prominent event observed in these organisms is the increase in non-reducing disaccharides such as trehalose in animals and fungi (Crowe, Carpenter and Crowe, 1998; Grelet et al., 2005), and sucrose; in plants (Cacela and Hincha, 2006) offering protection against desiccation through physical intercalation with phospholipid membranes. Trehalose has a more complex structure than monosaccharides such as glucose and is shown to act as both a water replacement molecule and a vitrification agent (Buitink and Leprince, 2004; Yamaguchi et al., 2007). However, it is important to note that these protective sugars are absent in some anhydrobiotic organisms such as bdelloid rotifers (Lapinski and Tunnacliffe, 2003); McGee, 2006) and are non-essential in *S.cerevisiae* (Ratnakumar and Tunnacliffe, 2006) indicating that tolerance can also be conferred by other elements/molecules (Tunnacliffe et al., 2010). This interesting difference led to the discovery of other key genes up-regulated by these two similar processes, desiccation and anhydrobiosis. Most anhydrobiotic organisms produce substantial amounts of highly hydrophilic proteins called 'hydrophilins' (Battaglia et al., 2008). The most well-studied sub group of these proteins are known as Late Embryogenesis Abundant (LEA) proteins since they were initially detected in mature cotton seeds upon desiccation (Dure, 1989). Recent findings have also shown that LEA proteins accumulate in anhydrobiotic nematodes, bdelloid rotifers, brine shrimp cysts, micro-organism, and the resurrection plant and in various plant seeds (Tunnacliffe et al., 2010). Moreover, LEA proteins have also been classified as stress-induced genes upon abiotic stress in plants, having a direct function in stress tolerance (Shinozaki and Yamaguchi-Shinozaki, 2007). The discovery of LEA proteins in non-plant systems suggests that similar mechanisms mediate anhydrobiosis and desiccation tolerance across kingdoms.

All the findings to date suggest that LEA proteins might play an important role in several developmental processes (germination, tuberization, senescence, symbiosis, PCD), as well as responding towards a wide-range of stresses either water-stress related (dehydration and osmotic stress), extreme temperature (heat and cold) and/or ROS-stress related (ozone, oxidant, pathogen attack, wounding) (Tunnacliffe and Wise, 2007; Hand et al., 2010; Tunnacliffe et al., 2010; Urano et al., 2010). Overexpression of LEA proteins using *in vivo* and *in vitro* systems improves tolerance against stress suggesting a protective role at both protein and membrane level (Wise and Tunnacliffe, 2004). Although there has been research

into LEA proteins for almost 30 years, their molecular function is still unknown (Hundertmark and Hincha, 2008; Tunnacliffe et al., 2010). Major characteristics of LEA proteins are their high hydrophilicity and structurally disordered state in solution (hydrated form) (Kovacs, Agoston and Tompa, 2008a). This structural plasticity might contribute to their versatile roles in the non-optimal environments (Tompa and Kovacs, 2010).

1.3.1 LEA characteristics

1.3.1.1 Hydrophilicity and protein structure

As mentioned above, LEA proteins are generally small highly hydrophilic molecules. The first hydrophilic feature of canonical LEA proteins is mainly contributed by their bias in amino acid composition in which hydrophilic amino acids are generally overrepresented (Hundertmark and Hincha, 2008). This characteristic is usually expressed as their grand average hydrophathy value (GRAVY) (Kyte and Doolittle, 1982). An average score for a typical hydrophilic LEA e.g. Group 3 LEA (refer to section 1.3.2 for LEA classification) is - 0.97 (Wise, 2003) which is significantly lower than a 'normal/well-structured' globular protein such as bovine serum albumin (-0.43). Due to their high hydrophilicity, most LEA proteins are predicted to be highly unstructured in solution or usually referred to as intrinsically disordered proteins (IDPs) (Tompa and Kovacs, 2010; Tunnacliffe et al., 2010; Hundertmark et al., 2011). This means that LEA proteins are also a part of another large group of proteins that has been compiled in a DisProt database available online (http://www.disprot.org/). This database shows experimental evidence for 5-15% of proteins being fully disordered, and about 50% of proteins having at least one long disordered region (Kovacs et al., 2008a).

The lack of structure of LEA proteins has only become understandable with the advent of the concept of disorder (Tompa, 2002; Tompa and Kovacs, 2010). A recent report showed that the functional state of many proteins or protein domains are actually in an intrinsically disordered state (Hoekstra et al., 2001; Kovacs et al., 2008b). IDP can be best described as a structured assembly of rapidly interconverting alternative conformations (Kovacs et al., 2008a; Shih, Hoekstra and Hsing, 2008). Interestingly, it was found that several chaperones are fully disordered (e.g., α-synuclein, β-synuclein, α- and β-casein) and RNA and protein

chaperones in general contain high levels of disorder (with 40% and 15% of their residues falling into disordered regions of >30 consecutive residues (Radivojac et al., 2004; Radivojac et al., 2007)). This fits with the accumulating evidence that LEA proteins are structurally disordered in solution but undergo a large conformational shift to α-helixes upon dessication (Radivojac et al., 2007; Tompa and Kovacs, 2010). Disordered regions are directly involved in chaperone function, which has led to the formulation of the "entropy transfer" model of chaperone function (Kovacs et al., 2008a; Tompa and Kovacs, 2010). The key elements of this mechanism are that disorder in chaperones may play a role in non-specific recognition, whereas it may also promote solubilization and assist local unfolding of misfolded parts of the client protein (Hoekstra et al., 2001; Shih et al., 2008). Some of these functional elements are similar to "molecular shield" and "space filler" functions of LEA proteins that will be described in more detail in the LEA functions section (1.3.4).

1.3.2 LEA classification

LEA proteins constitute a divergent family, initially classified by its two main co-founders (Dure et al., 1989; Bray, 1993) into three loosely defined groups; Group 1, Group 2 and Group 3. It was clustered according to the presence of similar sequence motifs between the different LEA proteins identified in different plants at that time. Group 1 proteins are characterized by a hydrophilic 20 amino acid motif; GGQTRREQLGEEGYSQMQRK while Group 2 proteins contain at least two of the three distinct motifs (Y: DEYGNP, S: S_n, K: EKKGIMDKIKEKLPG). On the other hand, Group 3 LEA proteins are identified by the presence of an 11–mer amino acid motif: TAQAAKEKAXE (Wise, 2003).

An alternative naming scheme was introduced by Dure (1999) corresponding to the prototypical cotton seed, *Gossipium hirsutum* LEA as follows: D19 (Group 1), D11 (Group 2) and D7 (Group 3). Nevertheless, most researchers used the first nomenclature system to classify their proteins. Besides the major LEA groups, there are also other minor groups assigned as Group 4 (D113), Group 5 (D29), Group 6 (D34), Lea5 (D73) and Lea14 (D95) (Bray, 1993; Galau, Wang and Hughes, 1993). Group 6 and Group Lea5 are also known as atypical LEA proteins due to their more average grand hydrophobicity that might result in a more structured protein in its hydrated form therefore affecting its possible structural-function roles upon cellular stress (Tunnacliffe and Wise, 2007). This peculiar feature of

atypical LEAs was supported by the outcome of several secondary structure prediction programmes that predicts most LEA proteins from this group not to be IDPs (Tunnacliffe et al., 2010).

The LEA protein groups were then further classified according to the corresponding Pfam domain families which are summarised in Table 1-1. Each Pfam domain in the database is represented by multiple sequence alignments which corresponds to specific protein domains or functional regions which therefore provide insights into their possible function (Bateman et al, 2004). To date, the Pfam classification seems to be the most appropriate way of classifying LEA proteins since it is more consistent and universal across different organisms (Hunault and Jaspard, 2010; Tunnacliffe et al., 2010). For instance, it is clearly more sensible to compare a rotifer protein to proteins from other animals than to a domain present only in cotton seed (Tunnacliffe and Wise, 2007). I have chosen to adopt the latest classification of corresponding Pfam families throughout this work to avoid confusion and name contradiction between authors.

Table 1-1. LEA protein classification according to Pfam families, species distribution and main characteristics.

Pfam	Distribution	Characteristics	Examples	References
LEA_1 (Group 4) PF 03790	Plant	Highly hydrophilic, Predicted to be IDPs Largely uncharacterized		
LEA_2 (Group Lea14) PF 03168	Plant Bacteria	Predicted not to be IDPs However, 3D structure available for 1 protein No functional information available	*AtLEA14* (*A.thaliana*)	(Singh et al., 2005)
LEA_3 (Group Lea5) PF 03242	Plant	Average hydrophobicity but some are more hydrophilic Mostly predicted not to be IDPs Stabilization of macromolecules membranes	*AtLEA5/SAG21* (*A. thaliana*) *LjIDP1* (*L. japonicus*) *C-Lea5* (Citrus) *AtDi21* (*A. thaliana*)	(Mowla et al., 2006) *(Haaning et al., 2008)* (Naot et al., 1995) (Jackson et al., 1997)
LEA_4 (Group 3) PF 02987	Plant Metazoa Fungi Bacteria Archae	Hydrophilic 11-mer repeat motifs Mainly IDPs Transition to α-helix upon dessication Stabilization of macromolecules and membranes Ion-binding property	*PsLEAM* (Pea) *GmPM16* (Soybean) *HVA1* (Barley) *Afrlea3* (Brine shrimp) *AavLEA* (Nematode)	(Grelet et al., 2005) (Shih et al., 2004) (Xu et al., 1996) (Menze et al., 2009) (Browne et al., 2004)

Table 1-1. (continued)

Pfam	Distribution	Characteristics	Examples	References
LEA_5 (Group 1) PF 00477	Plant metazoa, bacteria	Hydrophilic 20-residue motif Mainly IDPs Stabilization of macromolecules	*Em* (Wheat)	(Litts et al., 1987)
Dehydrin (Group 2) PF 00257	Plant	Hydrophilic, contains several distinctive motifs; (K, Y, S segments) Mainly IDPs Stabilization of macromolecules Chaperone activity, Antioxidant Metal-binding property DNA/RNA-binding	*COR47 (A.thaliana)* *LT129 (A.thaliana)* *RAB18 (A.thaliana)* *ERD14 (A.thaliana)*	(Nylander et al., 2001) (Puhakainen et al., 2004) (Svensson et al., 2000) (Kovacs et al., 2008)
SMP (Group 6) PF 04927	Plant Fungi	Most hydrophobic LEA protein group Mostly predicted not to be IDPs Largely uncharacterized	*MtPM25 (M. truncatula)*	(Boucher et al., 2010)

1.3.3 LEA expression profiles and their involvement in abiotic stresses

As defined by their name, many LEA proteins are expressed abundantly during seed maturation in embryonic tissue and their expression decreases gradually upon germination (Wise and Tunnacliffe, 2004). This pattern which was first observed in cotton seeds (Dure and Galau, 1981) is associated with desiccation tolerance. In addition, LEA proteins are also detected in non-embryonic or vegetative tissues upon stress, not limited to desiccation (Wise, 2003). Expression of LEA proteins is enhanced by a wide range of stresses (mainly abiotic) which include cold, dehydration, salt and osmotic stress (Wise and Tunnacliffe, 2004; Hundertmark and Hincha, 2008). Like many drought-induced genes, several LEA proteins were also shown to respond to abscisic acid (ABA), a well-known stress hormone in plants (Wise and Tunnacliffe, 2004; Tunnacliffe and Wise, 2007). However, ABA response involves complex interacting signalling pathways with other phytohormones and other signalling molecules (Finkelstein, Gampala and Rock, 2002) hence reflecting expression patterns which are not uniform and vary between individual members within the same LEA family (Galau et al., 1993); Parcy et al., 1994, Delseny et al., 2001). It is also worth noting that LEA proteins are not induced by heat unlike other well-studied stress proteins; e.g. heat shock proteins (HSPs) (Battaglia et al., 2008).

In non-plant systems such as invertebrates or microorganisms, LEA expression clearly cannot be related directly to the seed maturation event since these organisms lack this developmental process. Most of the LEA proteins from these species were initially identified by conserved domains which were also present in most plant LEA proteins (Dure et al., 1989; Bray, 1993; Wise, 2003). LEA expression in both plant and non-plant systems is linked to dehydration, referred to desiccation tolerance and anhydrobiosis, respectively (Goyal, Walton and Tunnacliffe, 2005). However, it must be stressed that LEA expression alone is not sufficient to confer dehydration tolerance since LEA expression is also found in dessication-sensitive seeds (Finch-Savage et al., 1994). Moreover, LEA proteins are constitutively expressed in other tissues, up-regulated by other stresses besides dehydration, and can be involved in other developmental processes such as tuberization and senescence (Tunnacliffe and Wise, 2007).

More recently, a large scale global analysis of transcriptomes from *Arabidopsis thaliana* identified 51 LEA protein encoding genes that could be further classified into nine groups (Hundertmark and Hincha, 2008). The findings charted individual LEA gene expression patterns in different developmental stages, different organs and responses to different stress and hormone treatments (ABA and giberrelic acid). There was however only a little overlap between genes expressed only in seeds and those expressed in other vegetative tissues. Most LEA-encoding genes contain ABRE and LTRE *cis*-elements within their promoter region and most genes having the respective promoter element were shown to be induced by ABA, cold and/or drought (Hundertmark and Hincha, 2008). This comprehensive analysis serves as an important starting point to further elucidate specific LEA functions.

In general, most LEA proteins fall into the typical LEA (highly hydrophilic and unstructured) protein group (Group 1, 2, 3, 4, 5; Table 1-1) with Group 3 having representatives from both plants and non-plants, thus also resulting in the best characterized group so far (Tunnacliffe et al., 2010). On the other hand, the atypical LEA protein group (Group Lea14, Lea5, 6) has received less attention, and has fewer members although they have started to increase more recently. These two main groupings might further link to their expression pattern and proposed role during different developmental stages and response towards stress.

1.3.3.1 Expression profiles of typical LEA proteins

To date, most typical LEA proteins being studied belong to Group 3, followed by Group 2 and 1. Thus this section focuses on the differential expression profiles of these LEA groups in relation to their proposed function.

1.3.3.1.1 Group 3 LEA (Pfam: LEA_4)

Group 3 LEA proteins are the best studied and largest category of LEA proteins and are thought to be involved in protein stabilization of macromolecules and membranes (Wise and Tunnacliffe, 2004). They are found in diverse organisms (plants, invertebrates, and microorganisms). One of the classical examples of this group is the *HVA1* gene isolated from barley (*Hordeum vulgare L.*) that is induced significantly by ABA and water deficit (Shen et al., 2004). Expression of this gene regulated by the rice *actin* 1 gene promoter led to high-level, constitutive accumulation of the protein in both leaves and roots of transgenic rice

29

plants. The transgenic rice from this line showed a significantly increased tolerance to water deficit and salinity (Xu et al., 1996). In wheat, constitutive expression of this gene improves biomass productivity and water use efficiency (Sivamani et al., 2000). Moreover, overexpression of this gene also improved the same traits in transgenic mulberry, *Morus indica* (Lal, Gulyani and Khurana, 2008).

Another group 3 LEA protein was isolated from roots of rice seedlings (*Oryza sativa*), *OsLea3* accumulates in roots and is up-regulated strongly by salt and ABA, but not jasmonic acid (Moons, De Keyser and Van Montagu, 1997). *In vivo* studies overexpressing an LEA Group 3 homologue from *Chlorella vulgaris (hiC6)* in yeast, proved that its expression is effective in the development of freezing tolerance (Honjoh et al., 2001). This gene was further studied in transgenic tobacco The results confirmed that freezing tolerance was improved in the transgenic overexpressing lines (Honjoh et al., 2001). Due to this special characteristic, *hiC6* is referred to as a cryoprotective protein. Another cold-regulated LEA gene from this group, *WCS19* from wheat *(Triticum aestivum)* was also shown to play a role in enhancement of freezing tolerance. Furthermore, homologues were isolated from rye (*Secale cereale*) and *Arabidopsis* (NDong et al., 2002). This gene responds specifically towards cold and light but not towards water stress or exogenous ABA (NDong et al., 2002). In addition, a new member of group 3 LEAs, *cw80lea3* was isolated from the halotolerant green alga *Chlamydomonas sp.* strain W80 by a functional expression screening with cyanobacterial cells based on the acquisition of NaCl salt-tolerance. Its expression was significantly induced by salt and cold but not by ABA treatment (Tanaka, Ikeda and Miyasaka, 2004).

In non-plants, one of the earliest Group 3 LEA proteins discovered was from an anhydrobiotic nematode, *Aphelenchus avenea* (Browne, Tunnacliffe and Burnell, 2002). The protein called, *AavLEA1* is up-regulated by severe dehydration and osmotic upshift but not by cold and oxidative stress (Browne et al., 2004). A gene isolated from the juvenile larval stage in the model nematode *Caenorhabditis elegans, Ce-lea-1* encodes an LEA-like protein and showed increased expression in the dehydrated state. Furthermore, the *Ce-lea-1* RNA interference lines resulted in a significant increase of mortality rate upon desiccation (Gal, Glazer and Koltai, 2004). Another desiccation tolerance LEA protein was identified from an

anhydrobiotic chrinomid, *Polypedilum vanderplanki* (*PvLEA*), and *PvLEA* was also induced by hypersalinity (Kikawada et al., 2006).

Group 3 LEA proteins are also found in desiccation-tolerant bdelloid rotifers (Lapinski and Tunnacliffe, 2003). *In silico* analysis showed that four EST candidates from the collembolan species, *Megaphorura arctica* matched Group 3 domains and are involved in dehydration stress (Bahrndorff et al., 2009). The first mitochondrially-targeted animal LEA, *AfrLEA3m* was reported from the brine shrimp cyst, *Artemia franciscana* that shows high tolerance towards freezing (Menze et al., 2009). The latest additions to this group are two genes expressed exclusively in diapausing embryos (resting eggs) of rotifers (*Brachionus plicatilis*) that disappear upon hatching (Denekamp et al., 2009). They are called *bpa-leaa* and *bpa-leab*. These proteins are absent in other male or female forms suggesting that their expression is developmentally programmed during resting egg formation and hatching. Their high expression only in resting eggs also denotes that they might be involved in desiccation during dormancy (Denekamp et al., 2009).

1.3.3.1.2 Group 2 LEA (Pfam: Dehydrin)

Group 2 LEA proteins are often referred to as dehydrins (Tunnacliffe and Wise, 2007). Members of this group can be further divided into group 2a (containing the Y motif with canonical expression in seeds) and group 2b (containing the K or S motif whose expression is cold-regulated and phospho-regulated, respectively). A tomato gene from this latter group, *le25,* is also capable of conferring salt and freezing tolerance when overexpressed in yeast (Imai et al., 1996). In Arabidopsis, five dehydrins (*COR47, LT129, ERD14, LT130, RAB18*) have been identified. They show clear differences in their responses towards ABA, low temperature and salinity (Steponkus et al., 1998; Nylander et al., 2001; Kovacs et al., 2008b). Immunohistochemical staining showed that they localized to different cells and tissues under stress with *ERD14* accumulating in vascular tissues and bordering parenchymal cells, *LT129* and *ERD14* localized to the root tip while *RAB18* is expressed in stomatal guard cells. Interestingly, *LT130* was absent in unstressed plants but accumulates mainly in primary vascular tissues and anthers upon cold stress (Nylander et al., 2001). In addition, overexpression of *RAB18* and *COR47* in Arabidopsis conferred freezing tolerance when co-expressed together. Both genes are also expressed in rapidly dividing tissues such as root tips

and leaves (Puhakainen et al., 2004). Another Arabidopsis dehydrin pair that confer cold tolerance when overexpressed together are *LTI29* and *LTI30* (Thomashow, 1998). These findings suggest a functional specialization of the different members of this LEA family (Tunnacliffe et al., 2010).

1.3.3.1.3 Group 1 LEA (Pfam: LEA_5)

Group 1 LEA proteins are prevalent in plants but rare in metazoans (Tunnacliffe et al., 2010). They are typified by the wheat *Em* protein (Litts et al., 1987). Its expression is abundant in mature embryos but then disappears rapidly upon the onset of germination which fits with its proposed function as a nutritional storage protein. *Em*-like proteins were further identified in a number of plants including cotton, rice, maize, sunflower, barley, radish, carrot, mungbean and Arabidopsis (Swire-Clark and Marcotte, 1999). Expression of these *Em*-like proteins can also be induced in vegetative tissues upon osmotic stress and by ABA (Morris et al., 1990). However, wheat *Em* could function as an osmoprotective molecule when overexpressed in yeast suggesting a possible dual role as storage protein and osmoprotectant (Swire-Clark and Marcotte, 1999).

1.3.3.2 Expression profiles of atypical LEA protein
1.3.3.2.1 Group Lea5 (Pfam: LEA_3)

Lea5 Group constituents identified so far indicate that this LEA group is specific to the plant kingdom suggesting that it might have appeared later in evolution. Its best characterized member so far is the *LJIDP1*, *a* protein from the legume, *Lotus japonicus*. This protein is highly expressed in functional nitrogen-fixing root nodules and in roots inoculated with the compatible endosymbiotic *Mesorhizobium loti* (Haaning et al., 2008). Both of these processes require high respiration rate (up to 70% of total respiration rate is associated with nitrogen fixation) resulting in high production of ROS (Haaning et al., 2008). Members of the Lea5 Group have also been identified in cotton (*lea5 and lea14*), citrus (*c-lea5*), potato (*clone 32B*), tobacco (*NtLea5*), *Tamarix androssowii* (*TaLea5*), *Prosopis juliflora* (*PjLEA3*) and Arabidopsis (Dure and Galau, 1981; Naot et al., 1995; Jackson et al., 1997; Mowla et al., 2006; Hundertmark and Hincha, 2008; George, Usha and Parida, 2009). The citrus c-*lea5* transcripts increased when plants were grown in the presence of high salt, drought and heat

stress (Galau et al., 1993; Naot et al., 1995). Furthermore potato *clone 32B* transcript expression seems to peak during tuberization, while the expression pattern of a homologue of a *clone 32B* from tomato is expressed strongly in green fruits but disappears upon ripening (Jackson et al., 1997).

1.3.3.2.1.1 *AtLea5/SAG21* homologues and expression pattern

In Arabidopsis, four LEA proteins encoding genes including AtLEA5/SAG21 (At4g02380; hereafter referred to as SAG21) studied in this work are assigned to Group LEA_3. The other three members encode drought-responsive proteins, AtDi21 (At4g15910), At1g02820 and At3g53770. These encoded proteins are exclusively targeted to either plastids or mitochondria, and are more hydrophobic than other Arabidopsis LEA proteins (Hundertmark and Hincha, 2008). Multiple sequence analysis reveals that AtLEA5 share sequence homology to other Lea5 member at their C-terminal end (Fig. 1-4).
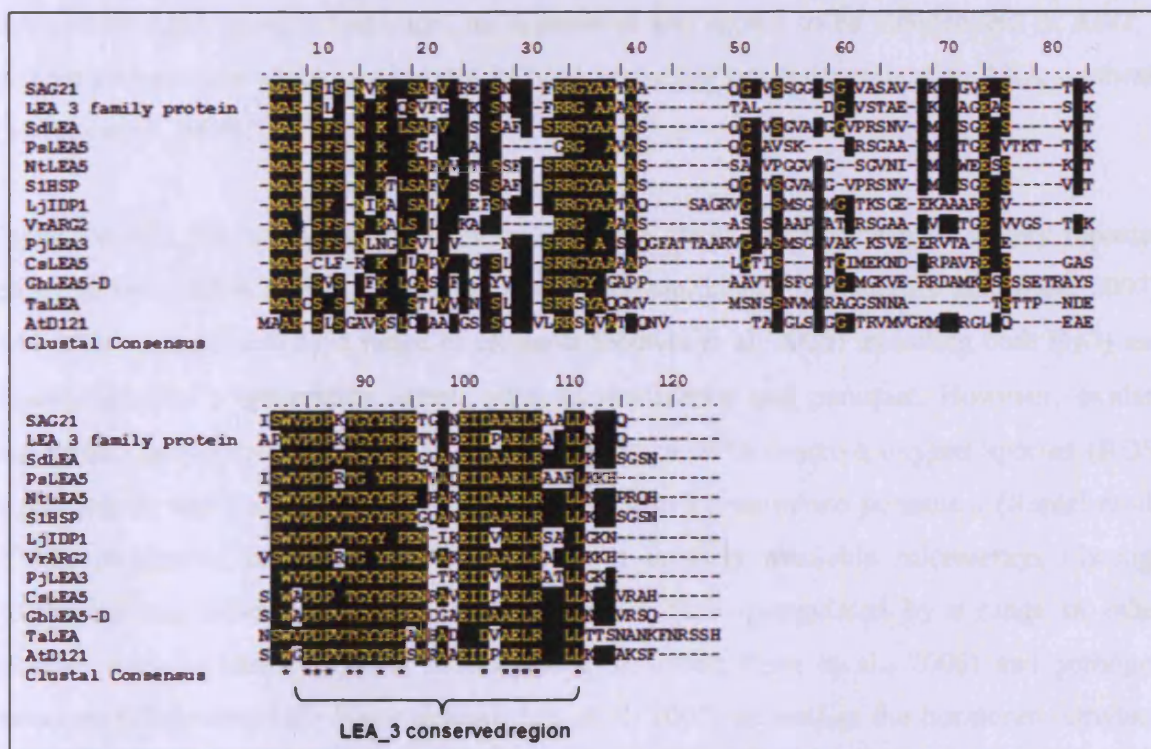
Figure 1-4: Alignment showing homologues of SAG21 in plants. Peptide sequences were aligned using COBALT and optimized with CLUSTALW. Accession number of sequences used to perform the alignments are as follows: SAG21 (NP_567231.1), LEA 3 family protein (NP_171781.1), SdLEA (CAA66948.1), PsLEA5 (ABF29697.1), NtLEA5 (AAC06242.1), S1HSP (AAA34193.1), LjIDP1 (ACJ46652.1), VrARG2 (XP_002523101.1), PjLEA3 (ABG66530.1), CsLEA5 (ABD93882.1), GhLEA5-D (P46522.1), TaLEA (ABG54481.1), AtDi21 (At4g15910). Asterisk (*) indicates the conserved region retained between the species.

SAG21 was first identified as a senescence-associated gene (SAG), expressed transiently at an early stage of leaf senescence just as leaves begin to yellow (Weaver et al., 1998), which coincides with the increase in endogenous level of hydrogen peroxide in Arabidopsis plants (Zimmermann et al., 2006). In addition, *SAG21* expression is shown to be light-regulated, specifically induced by darkness (Weaver et al., 1998; Mowla et al., 2006) and was most abundant in roots and flowers (Mowla et al., 2006).

Although dehydration is identified as a common inducer of most LEA proteins in Arabidopsis, RT-PCR analysis revealed that among the LEA_3 members, only *SAG21* showed high induction followed by a slight increase in *AtDi21* expression. Expression was not detected in At1g02820 and At3g53770 upon any stress (Hundertmark and Hincha, 2008). Furthermore, only *SAG21* was induced by cold, salt and ABA (Weaver et al., 1998; Seki et al., 2001; Mowla et al., 2006; Hundertmark and Hincha, 2008) suggesting that different LEA proteins within each group might play a distinctive role in Arabidopsis. Although *SAG21* was induced by ABA upon dehydration, its expression was shown to be independent of *ABI1*, a protein phosphatase which participates in ABA signalling but is dependent on ABA synthesis (Mowla et al, 2006).

Induction of LEA protein expression by oxidative stress has not been as widely reported although some LEA proteins may have a role as antioxidants (Tunnacliffe and Wise, 2007). *SAG21* is up-regulated by a range of oxidants (Mowla et al, 2006) including both H_2O_2 and superoxide ($O_2^{\bullet-}$) -generating agents such as menadione and paraquat. However, oxidant induction was independent of *OXI1*, a gene implicated in reactive oxygen species (ROS) signalling in root hair growth and basal resistance to *Peronospora parasitica* (Rentel et al., 2004). Numerous reports, including data from publicly available microarrays (through AtgenExpress) indicate that *SAG21* expression is also up-regulated by a range of other stresses such as ozone (Miller, Arteca and Pell, 1999; Tosti et al., 2006) and pathogen infection (*Colletotrichum higginsianum,* Liu et al, 2007) as well as the hormones, ethylene (Weaver et al, 1998; De Paepe et al. 2004), jasmonate (Jung et al, 2007) and by sugar signalling (Xiao et al, 2000).

Thus the role of *SAG21* remains enigmatic. Although its light-repression and predominant expression in non-photosynthetic tissues (flowers and roots) do not suggest a direct antioxidant role in photosynthesis, its up-regulation in response to oxidants and the reduced sensitivity to H_2O_2 in over-expressing plants (Mowla et al, 2006) suggests a potential function in ROS-mediated signalling. However, its lack of dependence on *OXI1* indicates that the *SAG21* signalling pathway differs from that established for root hair growth and pathogen attack. A role in redox signalling is nevertheless possible in response to stresses such as drought, although its *ABI1*-independent expression suggests that the signalling pathway converging on ROS-induced *SAG21* is not exclusively via the ABA-dependent pathway.

1.3.4 LEA functions

Despite their up-regulation in response to a wide range of stresses and successful production of more robust (abiotic stress tolerant) transgenic plants over-expressing LEA proteins, the mechanism underlying their action is still poorly understood. They have been suggested to play a role in protein stabilization, hydration buffering, membrane protection, antioxidant signalling/action and ion sequestration (Tunnacliffe and Wise, 2007). Structural characterization of their protein structure and expression profiling has provided some insights towards a better understanding of these enigmatic proteins (Tompa and Kovacs, 2010).

1.3.4.1. Protein stabilization

In vitro studies have demonstrated that LEA proteins are able to provide a protective effect to other proteins such as enzymes by acting as a 'molecular shield' or sometimes referred to as 'space fillers' (Tunnacliffe and Wise, 2007; Hand et al., 2010). Many enzymes such as lactate dehydrogenase (LDH) and citrate synthase (CS) form aggregates upon freezing or desiccation (Haaning et al., 2008; Tolleter, Hincha and Macherel, 2010). Exogenous application (*in vitro*) of any LEA protein from the three major typical LEA groups reduced protein aggregation significantly (Hand et al., 2010). *ERD10* and *ERD14* from Group 2 are also able to prevent heat-induced aggregation (Kovacs et al., 2008b). The Group 3 *PsLEAm* protein from *Pisum sativum* is able to protect two mitochondrial enzymes, fumarase and rhodanase during drying (Grelet et al., 2005). Furthermore, some LEA proteins are also capable of preventing

35

inactivation of a wide-range substrates (lysozyme, ADH, CS, luciferase) which is a similar role played by *Hsp90*, a heat-induced chaperone (Kovacs et al., 2008a; Kovacs et al., 2008b).

The property of anti-aggregation property is probably due to the hydrophilic, unstructured nature (IDP) of LEA proteins that enables not to be susceptible to aggregation on dehydration, freezing or even boiling (Tompa, 2002; Hand et al., 2010; Tompa and Kovacs, 2010). This special feature facilitates correct protein folding of other proteins and assists in the formation of functioning protein complexes. Besides preventing protein aggregation, LEA proteins also exhibit other chaperone-like properties such as becoming involved in transient protein-protein interaction with their client proteins (Chakrabarty, Chatterjee and Datta, 2007; Chakrabortee et al., 2007; Tompa and Kovacs, 2010). This interaction is typically created via hydrophobic patches of interaction between molecules (Radivojac et al., 2004; Radivojac et al., 2007). Although such specific interactions are unlikely to occur in typical LEAs due to their hydrophilic structure in the hydrated state, this might lead to another possible role of the atypical group which has more average hydrophobic properties (Tunnacliffe et al., 2010).

LEA protein activity is suggested to be less complicated than that of molecular chaperones (Goyal et al., 2005; Tompa and Kovacs, 2010). They suggest LEA proteins act as 'molecular shields' by decreasing interaction between partially denatured polypeptides and potential aggregates in a dehydrating environment (cytoplasm). The molecular shield effect also mimics the function of entropic bristles of the microtubule-associated protein, MAP2, and neurofilament side arms which play an important role in preventing aggregation of microtubules and microfilaments by allocating adequate space between them (Mukhopadhyay et al., 2004).

1.3.4.2. Membrane protection

During dehydration, maintaining cellular and organellar integrity is essential. Group 2 LEA proteins (dehydrins) are localized close to the membrane upon dehydration suggesting that they might be involved in membrane stabilization (NDong et al., 2002). The K segment, a Lys-rich 15-mer sequence of the conserved domain of dehydrins was suggested to be involved in membrane-binding (Close, 1996). In addition, two other dehydrins from

Arabidopsis, *ERD10* and *ERD14* also bind anionic phospholipid vesicles, suggesting peripheral electrostatic interactions upon membrane binding (Kovacs et al., 2008b).

Functional characterization of the Group 3 *PsLEAm* protein found in pea seed mitochondria revealed a possible mechanism for LEA protein-membrane interaction (Grelet et al., 2005). Upon dehydration, *PsLEAm* formed an amphiphatic α-helix structure which showed strong propensity to interact with dry phospholipid. This interaction protects liposomes during drying by preventing membrane fusion events and lysis (Tolleter et al., 2007; Tolleter et al., 2010). Another member of this group, *ArLEA1B* from a bdelloid rotifer which formed an α-helical structure in the dry state is also able to interact with dry phospholipid membranes (Pouchkina-Stantcheva et al., 2007).

1.3.4.3. Ion sequestration and antioxidant capacity

Another major event resulting from desiccation is ion accumulation that leads to an increase in intracellular ion concentrations. Without an effective ion sequestration mechanism, this could cause severe damage to macromolecular structure and function (Tunnacliffe and Wise, 2007). Due to the bias in amino acid composition of LEA proteins that is generally largely composed of charged amino acids, LEA proteins might act as important ion chelators (Svensson, Palva and Welin, 2000; Tunnacliffe and Wise, 2007). A Group 2 LEA protein was successfully purified by exploiting its binding affinity to the divalent cation, Ca^{2+} (Svensson, Palva and Welin, 2000). The same approach was used to isolate an iron-binding protein from castor bean which shows high homology to Group 2 LEA proteins (Kruger et al., 2002). Furthermore, the structure of several Group 2 LEA proteins analysed using NMR and differential scanning calorimetry, showed that they have a general propensity for binding solute ions, which agrees with the broader concept of these proteins serving as an ion sink (Tompa et al., 2006).

Water deficit could also lead to accumulation of catalytic metal ions in plants. A Group 2 citrus LEA protein, *CuCOR19* was reported to have an antioxidant property by binding to metal ions, which protected liposomes from peroxidation (Hara et al., 2003; Hara et al., 2009). In addition, this gene also reduced electrolyte leakage in cold-treated transgenic tobacco (Hara et al., 2003), and exhibited scavenging activity for hydroxyl and peroxyl

radicals (Hara, Fujinaga and Kuboi, 2004). It is widely accepted that hydroxyl radicals could react with singlet oxygens which are main components of ROS. On the other hand, treatment with ozone also induced the expression of *AtLEA5/SAG21* which suggests that this protein might also possess an ion-binding property (Miller et al., 1999; Tosti et al., 2006). Thus, LEA proteins might play a crucial role in reducing oxidative stress in cellular compartments either directly (by ROS scavenging) or indirectly (by metal ion sequestration).

LEA proteins clearly exhibit a versatility of form and function which act beyond their historical expression during late embryogenesis. These special characteristics make them excellent candidates as downstream proteins that play various roles during unfavourable stress conditions. They also may play an important role in regulating developmental processes such as growth and senescence, which involve ROS in their complex signalling network.

1.4 Experimental Aims

This work aims to study the regulation of reactive oxygen species (ROS) during plant growth, stress and senescence. Initial work was focused on senescence and redox regulation in wallflowers (*Erysimum linifolium*) where expression of *SAG21*, a senescence associated gene was previously found to be elevated in senescent petals. Further work then focused on the elucidation of the role of this gene in the model plant *Arabidopsis thaliana*. Below are the approaches that were taken:

1) In order to understand the hormonal and redox control in wallflowers senescence, the role of ethylene, cytokinins, auxin, hydrogen peroxide and several antioxidative enzymes were investigated. In parallel, the differential expression pattern of two SAGs (*SAG12* and *SAG21*), an ethylene biosynthetic gene and auxin-induced gene were also determined. These genes could then act as markers to test whether perturbation of floral senescence signals had affected senescence progression in a uniform manner.

2) In order to elucidate the function of *SAG21* in Arabidopsis, several approaches were implemented. Firstly various tools were used to try to identify the subcelllular localization of this protein. This is important in understanding its potential *in vivo* role. Using bioinformatics analysis, SAG21 protein characteristics, promoter elements and potential subcellular localization were predicted and identified. Using transgenic lines transformed with *SAG21*-YFP fusions driven by the 35S constitutive promoter, the compartment-specific expression was confirmed. A second step in elucidating SAG21 function was to define its tissue-specific, spatial and temporal expression during development and stress conditions. This was analyzed in transgenic lines transformed with *SAG21* promoter-GUS constructs. Finally, phenotypic characterization of the *SAG21* over-expressor (OEX), and *SAG21* antisense (AS) plants compared to WT plants grown under various conditions were carried out to identify how *SAG21* perturbation affected growth, development and plant defence. This enabled tentative models to be proposed for the signalling pathways regulating *SAG21* expression and a working model for the role of SAG21 in development and stress responses.

39

Chapter 2: General Materials and Methods

This chapter describes the general methods that we employed in more than one chapter of this thesis. Additional methods required for certain experiments are described in relevant chapters. All chemicals and reagents were purchased from Sigma-Aldrich (UK) unless specified.

2.1 Plant materials

Plants of *Erysimum linifolium* (wallflowers) cv. Bowles Mauve (2n==2x =32) were grown either outdoors or in a greenhouse at *Tal-y-bont*, Cardiff. For later, plants were grown under natural light and temperature, which was monitored to be between 21 °C and 24 °C to promote flowering. The plants were collected and staged into 7 developmental stages according to Price et al. (2008) (Appendix A). Complete experimental design involving this plant is described in Chapter 3.

All studies in Chapter 4, 5 and 6 utilized *Arabidopsis thaliana* ecotype Col-0 as a model system. Plants were grown in a controlled growth room or Sanyo-Gallenkamp growth chamber at 21°C under long days (LD) conditions; 16 h light (300-400 μmol m^{-2} s^{-1}) and 8 h dark unless stated. Plants were watered 3-4 times per week to retain soil humidity. Under these parameters, flowers developed within 7 weeks after germination and mature seeds were harvested at 12 weeks.

2.2 Bacterial strains

Organism	Strain	Origin
E. coli *	DH5 α	Rogers, H.J. lab, Cardiff Uni.
	DB3.1	Invitrogen
A. tumefaciens *	GV3101	Rogers, H.J. lab, Cardiff Uni.

(*E.coli: Escherichia coli; A. tumefaciens: Agrobacterium tumefaciens*

2.3 Plasmids

All plasmids were in *E.coli* strain DH5α except pMDC162 which was propagated in *E.coli* strain DB3.1. Plasmids were selected either on Ampicilin (Amp) or Kanamycin (Kan) at 100 µg/mL or 50 µg/mL respectively.

Type	Name	Selection	Chapter	Origin
Cloning	pGEM-T Easy:: SAG21 ORF	Amp	4	Mowla, 2006
template	pGEM-T Easy:: SAG21 1685 promoter	Amp	5, 6	This work
	pGEM-T Easy:: SAG21 1685 promoter NcoI	Amp	4	This work
	pGEM-T:: NcoI SAG21 ORF 6xHis TAG	Amp	4	This work
	pDONR221:: SAG21 300 promoter	Amp	5, 6	This work
Expression	pGREEN::35Sp::SAG21::YFP::nosT	Amp	4	This work
construct	pGPTV-KAN::SAG21 1685 promoter::GUS	Kan	5, 6	This work
	pMDC162::SAG21 300 promoter::GUS	Kan	5, 6	This work
	pGREEN::SAG21 1685 promoter::SAG21His TAG	Kan	4	This work
	pDHA::TP pre-23K::GFP	Amp	4	Robinson, C. Warwick Uni.
Empty	pGEM-T Easy	Amp	4, 5, 6	Promega
plasmid	pGEM-T	Amp	5, 6	Promega
	pGREEN::35Sp::YFP nosT	Amp	4	de. Graaf, B. Cardiff Uni.
	pGREEN0029	Amp	4	de. Graaf, B. Cardiff Uni.
	pGPTV-KAN::GUS	Kan	5, 6	Becker, 1992
	pDONR221	Amp	5	Invitrogen
	pMDC162	Kan	5, 6	Invitrogen

2.4 Arabidopsis seed stocks

In order to obtain homozygous lines, transgenic plants were selected for 2-3 generations either on kanamycin (Kan) or hygromycin (Hyg) at 50 µg/mL or 20 µg/mL respectively.

Analysis type	Name	Selection/ Description	Chapter	Origin
Cell localization	35S::SAG21::YFP	Kan, HM*, OEX*, Lines: T2-1-1 T2-1-2	4	This work
Spatial expression during development and upon stress	SAG21(1685)::GUS	Kan, HM*, Lines: T3-2-6 T2-3-5	5, 6	This work
	SAG21(325)::GUS	Hyg, HZ*, Lines: T2-5-6 T2-5-7 T2-5-8	5, 6	This work
	SAG12::GUS	Kan, HM*	5, 6	Buchanan, V. Warwick Uni.
Phenotyping	SAG21-OEX	Kan, HM*, OEX* Line: SAG21-OEX-2-4	5	Mowla thesis, 2006
	SAG21-AS	Kan, HZ*, AS* Lines: SAG21-AS-1 SAG21-AS-2 SAG21-AS-8	5	Mowla thesis, 2006
Control	WT*	Ecotype Col-0	4, 5, 6	This work

(*HM: homozygous; HZ: heterozygous; OEX: overexpressor; AS: antisense; WT: wild type)

2.5 Primers

All desalted-grade (scale 0.025) primers were obtained from Sigma (sigma.com/oligos). For primer description and exact PCR conditions, please refer to specified chapters.

2.5.1 Primers used for work on wallflowers

Analysis type	Primer set	Sequence (5'-3')	Tm (^{O}C)	Product size (bp)	Chapter
Semi-quantitative RT-PCR	PUV 2 F PUV 4 R	TTCCATGCTAATGTATTCAGAG ATGGTGGTGACGGGTGAC	55	459	3
	Wf SAG21 F Wf SAG21 R	TCCGAGCAGCTCTCTTGAAC GGAAACCAAACGGTTCTCAA	60	525	3
	Wf SAG12 F Wf SAG12 R	TTGCCGGTTTCTGTTGAYTGG TGGTGTGCCACTGCYTTCAT	60	339	3
	WLS73 F WLS 73 R	GGCACCTAGACCGAGGATTT TTCCATCGAGGCCTTTCTTA	60	163	3
	WPS 46 F WPS 46 R	GCTCCGATCATTGAGCTTTT TTCAAATGGGACTAGAAACCTTC	60	156	3
	WPS 96 F WPS 96 R	GGGGACGCATCATTCATT GCCGAGGTACTGCTTCACA	55	226	3

2.5.2 Primers used for work on Arabidopsis

Analysis type	Primer set	Sequence (5'-3')	Tm (°C)	Product size (bp)	Chapter
Cloning and transformant screening	SAG21 YFP F	CGGATCCATGGCTCGTTCTATCTCTAACG	60	303	4
	SAG21 YFP R	TAATATAATAGCGGCCGCCTGCTTGTTGT TCAAGAG			
	35Sp F	GATTGATGTGATATCTCCACTGAC	55	535	4
	YFP R	GCTAGTTATGCTCAGCGG			
	4A Sall F	AAGTCGACTAATCTCCAAAACATTGTGA	60	1695	4
	A1-2 NcoI R	AGCCATGGTCGAAGTAAGTGG			
	B1-2NcoI F	CGACCATGGCTCGTTCTATCTCTAACG	60	322	4
	4B 6xHis	TAGCGGCCGCTCAGTGGTGGTGGTGGT			
	TGA Not 1 R	GGTGCTGCTTGTTGTTTCAA			
	SAG21 P Sall F	AATTGTCGACTAATCTCCAAAACATTGTG	60	1697	5, 6
	SAG21 P XbaI R	ACTGTCTAGATTTCGAAGTAAGTGGTTTC			
	attBSAG21 F	GGGGACAAGTTTGTACAAAAAAGCAGGC TTCGGGTCAAAAGACTCAAAGGC	67	341	5, 6
	attBSAG21 R	GGGGACCACTTTGTACAAGAAAGCTGGG TCTTTCGAAGTAAGTGGTTTCT			
	M13 F	GTTTTCCAGTCACGACGTTG	50	511	4, 5, 6
	M13 R	TGAGCGGATAACAATTTCACACAG			
	GUS 1 F	GAAACCCCAACCCGTGAAATCA	55	730	5
	GUS 2 R	AACCTTCACCCGGTTGCCAGA			
Genotyping	CaMV 1F	CGTAAGGGATGACGCACA	55	564	5
	AtSAG21 F	ATCTTCCGACGTGGTTATGC			
	CaMV 1F	CGTAAGGGATGACGCACA	55	534	5
	AtSAG21 R	CCGGTTTCGGGTCTGTAATA			
Semi-quantitative RT-PCR	PUV 2 F	TTCCATGCTAATGTATTCAGAG	55	459	5
	PUV 4 R	ATGGTGGTGACGGGTGAC			
	AtSAG21 F	ATCTTCCGACGTGGTTATGC	55	137	5
	AtSAG21 R	CCGGTTTCGGGTCTGTAATA			

2.6 DNA extraction from Arabidopsis

2.6.1 Edwards et al. (1991) method

This method served as a simple and rapid DNA extraction protocol for genotyping purposes. Fresh plant material (10-50 mg) was ground with liquid nitrogen using a sterile Eppendorf grinder in a sterile microcentrifuge tube. Extraction buffer of 200 μL (200 mM Tris-HCl pH 7.5, 250 mM NaCl, 25 mM EDTA, 0.5% (w/v) SDS) was added to the homogenate and centrifuged at 13 000 rpm, RT for 5 min using a Eppendorf MiniSpin plus® microcentrifuge. The clear supernatant was transferred into a fresh sterile microcentrifuge tube. An equal volume of 100% isopropanol was added to the same tube, followed by 5 min incubation on ice. Then, the tube was centrifuged again at 13 000 rpm, RT, for 10 min. The supernatant was discarded and pellet was allowed to dry at 60 ^{0}C for 5-10 min. The dried pellet was resuspended in 50 μl sterile distilled water.

2.6.1 CTAB method (adapted from Saghai-Maroof et al. 1984)

This method yielded more DNA of higher purity and was preferable for cloning purposes in order to obtain a good DNA template.

Prior to extraction, 40 μL of 1.42 M β-mercaptoethanol was added to 10 mL of 2x CTAB (Cetyl trimethylammonium bromide) isolation buffer (100 mM Tris-HCl pH 8, 1.4 M NaCl, 20 mM EDTA, 2% CTAB) in a fume hood and pre-heated at 65 ^{0}C for 15 min. Sterile 30 mL round bottom centrifuge tubes, pestle and mortar were also pre-heated under the same conditions. Fresh or frozen plant material (0.5 - 1.5 g) was ground in a mortar with liquid nitrogen forming a fine powder. The pre-heated CTAB isolation buffer was added and grinding continued until a homogenous paste was obtained. The mix was incubated at 65 ^{0}C for 10 min. SEVAG of 10 mL (24:1 chloroform:isoamylalcohol) was added to the paste and mixed gently. The extract was then carefully transferred into sterile 30 mL centrifuge tubes that had been pre-heated earlier, sealed with nesco film and then incubated on a shaker at 125 rpm for 30 min at RT.

The filled centrifuge tubes were inserted into a JA-20 rotor, and spun at 8000 rpm, RT, for 10 min in a Beckman Coulter Avanti® J-E centrifuge. The top aqueous layer was transferred to a sterile 50 mL Falcon tube and further processed using the QIAquick PCR purification Kit (QIAGEN) according to the instructions provided in QIAquick® Spin Handbook (QIAGEN). DNA concentration was quantified using a spectrophotometer (section 2.10.1) and the remaining sample was stored in -20 ^{0}C until further use.

2.7 RNA extraction

2.7.1 RNA extraction from Wallflowers

Due to the limited amount of material, total RNA isolation from wallflowers was done by using a small scale isolation kit; RNAqueous® Kit (Ambion, Inc.). All instructions were provided in the RNAqueous® Kit manual.

2.7.2 RNA extraction from Arabidopsis

Prior to extraction, a sterile pestle and mortar were pre-chilled at -20 ^{0}C overnight. Approximately 200 mg of fresh or frozen material were ground thoroughly with liquid nitrogen in a mortar forming fine powder. Tri® Reagent (2 mL) was added and grinding was resumed until a homogenous paste was formed. Equal amounts of extract was transferred into two sterile microcentrifuge tubes, vortexed briefly for 5 s and allowed to stand at RT for 5 min. The samples were centrifuged at 12 000 rpm, 4 ^{0}C, for 10 min in a pre-cooled Beckman Coulter AllegraTH 21R centrifuge fitted with a F2402H rotor. The supernatant was transferred into fresh sterile microcentrifuge tubes leaving the plant debris behind. Chloroform (0.2 mL) was added, vortexed for 15 s and the mixture was allowed to stand at RT for 5 min before centrifuging at 12 000 rpm, 4 ^{0}C, for 15 min. Then, the resulting aqueous layer was carefully transferred to fresh sterile microcentrifuge tubes, followed by the addition of 0.5 mL isopropanol. The samples were gently mixed and incubated on ice for 10 min then centrifuged again at 12 000 rpm, 4 ^{0}C, for 10 min. The supernatant was removed and discarded, 1 mL of 75% Ethanol (EtOH) was added, vortexed for 15 s before the final centrifugation at 12 000 rpm, 4 ^{0}C, for 10 min. Subsequently, the supernatant was discarded

and the pellet was allowed to dry at 60 ^{0}C for 5-10 min. The dried pellets from both tubes were resuspended in sterile distilled water and combined to a final volume of 50 μL. RNA quality and purity was assessed by running 5 μL of the sample on a 1% agarose gel (section 2.10.2) and quantified using a spectrophotometer (section 2.10.1). The remaining samples were stored at -80 ^{0}C until further use.

2.8. DNase treatment

For wallflower RNA samples, DNase treatment was carried out using RNAqueous® Kit (Ambion, Inc.) as described by the manufacturer.

For Arabidopsis samples, a 20 μL reaction mix containing 2 μg of total RNA, in 1x RQ1 DNase buffer (Promega; 40 mM Tris-HCl pH 8, 10 mM $MgSO_4$, 1 mM $CaCl_2$), 2 μL of RQ1 RNase-Free DNase (Promega; 1 unit/μL) was set up for each DNase treatment. The reaction was incubated for 30 min at 37 ^{0}C. Afterwards, 2 μL of RQ1 Stop Solution (Promega; 20 mM EGTA pH 8) was added to the mix and further incubated at 70 ^{0}C to terminate the DNAse digestion.

2.9 cDNA synthesis

DNase-Free RNA (~2 μg) from the previous step was mixed with 500 ng of Oligo(dt)15 primer (Promega) to a final volume of 20 μl. The mix was incubated at 70 ^{0}C for 10 min followed by another 10 min incubation at 4 ^{0}C. For every reaction, 6 μL of 5x M-MLV RT buffer (Promega; 250 mM Tris-HCl pH 8.3, 375 mM KCl, 15 mM $MgCl_2$, 50 mM DTT), 2 μL of 0.1 M DTT and 1 μL of 10 mM dNTP mix were added. The reaction was incubated at 42 ^{0}C for 2 min before adding 1 μL of M-MLV Reverse Transcriptase (Promega; 200 units/μL) and further incubated for 50 min at the same temperature. To inactivate the reaction, the mix was incubated at 70 ^{0}C for 15 min. The samples were then stored at -20 ^{0}C until further use.

The quality of the single-stranded cDNA produced was checked via PCR (section 2.11) with PUV primers (section 2.5) that bind to the 18S ribosomal RNA before proceeding to semi-quantitative RT-PCR (section 2.11.1) or used as a DNA template in cloning (section 2.12).

2.10 Nucleic acid quantification

2.10.1 Spectrophotometer

Both DNA and RNA concentration were determined with a Nanodrop UV spectrophotometer (Thermo Scientific) by reading 1 µL of the sample at 260 nm. The final unit was expressed as ng/µL.

2.10.2 Agarose gel electrophoresis

For 1% (w/v) agarose gel, 0.5 g of agarose (Bioline) was added to 50 mL of 1x TAE buffer (4.84 g/L Tris, 1.142 ml/L glacial acetic acid, 2 ml/L 0.5 M EDTA pH 8), boiled in the microwave and cooled down to approximately 50 ^{0}C under running tap water. Then, 4 µL of 10 mg/mL EtBr was added, mixed and poured to a tray to allow gel to solidify. The percentage of agarose used was adjusted depending on the size of the nucleic acid to be separated. For RNA, the gel tank, comb and tray were soaked in 0.1 M NaOH for 20 min and rinsed with distilled water before gel preparation to prevent RNA degradation. Samples were prepared in 10x loading buffer (50 mM Tris pH 7.6, 60% glycerol, bromophenol blue) prior to loading. The gel was run at 100 V for 15-20 min in 1x TAE buffer. Ladder 1 kb of 500 ng (Invitrogen) was run in parallel with the samples for band size determination. DNA was visualized under UV illumination using a Gene Genius Bioimaging System (Syngene Ltd). For semi-quantitative purposes, the intensity of PCR product bands was quantified in arbitrary units using Gene Tools Software package (Syngene Ltd.).

2.11 Polymerase Chain Reaction (PCR)

All PCR reactions were cycled either on a GeneAmp® 2700 PCR System (Applied Biosystems) or a PTC-10 Thermocycler (MJ Research) machine. PCR conditions were optimised individually according to the parameters e.g. type of Taq polymerase used. For general PCR (non-quantitative), either in-house purified Taq polymerase or a commercial GoTaq® DNA polymerase (Promega) was used or the PCR conditions were stated as below. For semi-quantitative RT-PCR and cloning purposes, the conditions are described in section 2.11.2 and 2.12, respectively.

A standard 25 µL PCR reaction mix consisted of approximately 10 ng of template (genomic DNA, cDNA or plasmid DNA), 2.5 µL of 10x PCR buffer (100 mM Tris-HCl pH 9, 500 mM KCl, 15 mM MgCl$_2$), 1 µL of 10 µM primers, 0.5 µL of 10 mM dNTP mix, 0.125 µL Taq polymerase, made to 25 µL with sterile distilled water. The mix was subjected to the following thermocycling programme: 95 ^{0}C, 2 min initial denaturation, 40x (95 ^{0}C, 1 min, 55 ^{0}C, 1 min, 72^{0}C, 1 min), 72 ^{0}C, 5 min final extension.

PCR products were run on 1 – 1.5 % agarose gels depending on product size and analysed as described in section 2.10.2.

2.11.1 Semi-quantitative RT-PCR

It is crucial to ensure that the same amount of cDNA is used in each sample in order to obtain reproducible semi-quantitative results. In order to achieve this, the amount of transcript abundance of the specific gene of interest was normalised against a housekeeping gene that is known to be present ubiquitously in the plant system. In this work, a PUV primer set (section 2.5) which binds to the 18S ribosomal RNA was used. These procedures have been published (Price et al. 2008) and have proved to be reliable and acceptable in the Cardiff laboratory.

First, individual PCR reactions were set up using cDNA as template and PUV primers or specific primers. Reactions were terminated at varying cycle number between 16 and 40

cycles. PCR products were quantified (section 2.10.2) and plotted against the cycle number. The exponential phase (the region when the production of PCR product increased linearly with the cycle number) was identified from the slope. The cycle number that coincided with the exponential phase before entering the stationary phase was determined and selected as the optimum cycle number. Optimum cycle number was verified by using template dilution of cDNA (100%, 50%, 25%) and checking for linear response between template concentration and product abundance at that cycle number and with the specific primers used. The template dilution series was included in each set of PCR reaction experiment.

After establishing the optimum cycle number for each primer set and cDNA batch, the relative expression pattern was charted by normalising the product obtained from the specific primer of interest (at optimum cycle number), against the product obtained using the PUV primer set (at optimum cycle number). The final values were expressed as percentage of maximum giving a value of 100% to highest product in each reaction set. At least three reproducible replicates were considered for the final transcript abundance quantification.

2.12 Cloning

In this section, general cloning steps involved in construct making that are further discussed in Chapters 4 and 5 are described. Specific cloning details for each construct are described in the individual chapters.

2.12.1 Insert amplification and purification

Insert was amplified via PCR using specific primers for the target gene under defined optimal parameters (Chapter 4: section 4.2, Chapter 5: section 5.2). Larger fragments required a longer extension time depending on the efficiency of the Taq polymerase being used. Choosing the correct Taq and minimizing the cycle number are critical points to consider in each amplification step to minimize non-specific amplification thus preventing mutations introduced by PCR. The amplified PCR product was run on an agarose gel and the band of interest of correct size was identified, excised using a razor blade and transferred into a fresh sterile microcentrifuge tube. DNA was purified from gel fragment using a QIAquick Gel

Extraction Kit (QIAGEN) according to the instructions provided in QIAquick® Spin Handbook (QIAGEN). Afterwards, 4 μL of purified insert was run on an agarose gel to check for DNA presence and estimated quantity of the DNA.

2.12.2 Insert and vector restriction digestion

All restriction enzymes and buffers were purchased from Promega. The 10x Reaction Buffer supplied with each restriction enzyme was selected to give 100% activity. In addition, good activity was also obtained by MULTI-CORE® 10x buffer for multiple enzyme digestion. Information on buffer selection was provided by the manufacturer.

For a single digestion reaction, 30 μL of gel-purified insert or 2 μg of vector was mixed with 4.0 μL 10x Reaction Buffer, 0.4 μL of 10 mg/mL BSA, 1 μL Restriction enzyme (10 units/μL) and made up to 40 μL with sterile distilled water. The reaction mix was incubated at 37 ^{0}C for an hour. For double digestion reactions requiring two different buffers, 5 μL mix of the first digestion was first checked on an agarose gel for full digestion. Subsequently, the remaining digest was purified with QIAquick PCR purification Kit. Thirty μL of purified product was further digested with the second enzyme with the respective buffer as described above.

The digested product was either directly purified with a Qiaquick PCR purification Kit or gel-purified using a QIAquick Gel Extraction Kit according to the instructions provided in QIAquick® Spin Handbook (QIAGEN).

2.12.3 Phosphatase

Following digestion, the vector was phosphatased in the following mix: 40 μL digested vector, 5 μL 10x CIAP buffer (Promega), 1 μL CIAP enzyme (Promega; 0.01 units/μL) made up to 50 μL with sterile distilled water. The mix was incubated at 37 ^{0}C for 30 min. Another 1 μL of CIAP enzyme (Promega; 0.01 units/μL) was added to the reaction and incubated at 37 ^{0}C for an additional 30 min to ensure complete dephosphorylation. The reaction was

stopped by purifying the mix through the QIAquick PCR purification Kit as described in the previous section.

2.12.4 Ligation

For a 10 μL ligation reaction into pGEM-T/ Easy vector systems (Promega), the setup was as follows: 1 μL pGEM-T/Easy vector (50 ng/μL), 7 μL digested insert, 1 μL 10x Rapid Ligation buffer (Promega; 60 mM Tris-HCl pH 7.8, 20 mM $MgCl_2$, 20 mM DTT, 2 mM ATP, 10% Polyethyleneglycol), 1 μL T4 DNA ligase (Promega; 3 units/μL) incubated overnight at 4 ^{0}C. As controls, a ligation reaction was performed without insert to check for plasmid religation and another ligation reaction was set up without insert and ligase to check whether the vector had undergone complete or partial digestion.

For ligations with other vectors (10 – 15 μl reaction volumes), the ratio between the vector and insert was calculated using the formula below:

$$\frac{\text{length of insert (in bp)}}{\text{length of vector (in bp)}} \times \text{ng of vector} = \text{ng of insert needed for a 1:1 ratio}$$

2.12.5 Bacterial transformation

A heat shock transformation method was used for transforming competent cells of two E.Coli strains; DH5α or DB3.1 and A. tumafaciens strain GV3101.

For competent cell preparation, please refer to Appendix E.

2.12.5.1 Transformation into E. coli

Competent cells (100 μL aliquots) were removed from the -80 ^{0}C, thawed on ice for several minutes prior to transformation. Ligation mix or purified plasmid (2 μL) were pipetted into the microcentrifuge tubes containing the thawed cells and incubated on ice for 20 min.

Subsequently, the mix was heat shocked at 42 ^{0}C for 45 s and transferred back immediately to ice for 2 min. LB of 900 μL (10 g/L Bacto-Tryptone, 5 g/L Bacto Yeast extract, 10 g/L NaCl; pH 8, autoclaved prior to use) was added to the cells and they were incubated at 37 ^{0}C, 200 rpm for 1 hour in a Gallenkamp cooled orbital incubator. For plasmid DNA transformation, 50 μL of transformed cells were plated on LB agar (LB with the addition of 15g/L Difco™ Agar (Becton, Dickinson and Company)) with appropriate antibiotic selection. For ligation transformation, the transformed cells were spun in an Eppendorf MiniSpin plus® microcentrifuge at 13 000 rpm, RT, for 1 min, the supernatant was removed and the pellet was resuspended in 100 μL LB prior to plating on LB agar with antibiotics. Selection plates were incubated at 37 ^{0}C overnight. The following day, transformed colonies were screened via PCR with specific primers (section 2.12.6).

2.12.5.2 Transformation into *Agrobacterium tumefaciens* (GV3101)

Competent cells (100 μL aliquots) were removed from the -80 ^{0}C and thawed on ice for several minutes prior to transformation. Approximately 0.5 μg of plasmid DNA was added per cell aliquot, quick frozen in liquid nitrogen for 10 s and immediately thawed at 37 ^{0}C for 5 min. Subsequently, 1 ml of LB was added to the cells and they were incubated at 30 ^{0}C, 100 rpm for 4 hours in a Gallenkamp cooled orbital incubator. Following incubation, the transformed cells were centrifuged at 13 000 rpm, RT for 30 s in an Eppendorf MiniSpin plus® microcentrifuge to harvest the cells. The supernatant was removed and the pellet was resuspended in 100 μL of LB and plated on LB agar containing appropriate antibiotic selection. Plates were incubated at 30 ^{0}C for 2 -3 days. This step was followed by colony PCR with specific primers (section 2.12.6).

2.12.6 Colony screening

Five to six colonies were selected from each plate for screening. Colonies were inoculated in 3 mL LB containing appropriate antibiotic and incubated at 37 ^{0}C, (*E. coli*) or 30 ^{0}C (*A. tumefaciens*), with shaking at 200 rpm overnight in a Gallenkamp cooled orbital incubator. The overnight culture (1 μL) was used as template for PCR reactions (section 2.11) with specific internal primers (section 2.5) to select clones for plasmid purification.

2.12.7 Plasmid purification and glycerol stock preparation

Two mL of the overnight cultures was used for plasmid purification using a QIAprep Spin Miniprep Kit (QIAGEN) according to the QIAprep® Miniprep Handbook. The remaining 1 mL of culture was centrifuged at 13 000 rpm, RT for 1 min, supernatant was removed and the pellet was resuspended in 80% glycerol in LB and stored at -80 ^{0}C as a glycerol stock. For large-scale plasmid preparation (up to 250 µg), a QIAGEN Plasmid Mid Kit was used following instructions provided in the QIAGEN® Plasmid Purification Handbook.

Plasmid DNA quality was checked on a 1% agarose gel (2.10.2) and the concentration was determined via spectrophotometry (section 2.10.1) before sequencing.

2.13 Sequencing

Sequencing reactions were performed using the BigDye Terminator Cycle Sequencing Kit (Applied Biosystems) with specified primers in an ABI Prism 3100 capillary sequencer by the Cardiff School of Biosciences Molecular Biology Unit.

2.14 Growth condition

2.14.1 *In vitro* growth and seed sterilization

For *in vitro* plant growth, a seed sterilization step was necessary to ensure all seeds were free from any source of contamination. All sterilization steps were performed in a sterile Microflow Laminar flow workstation.

Small scale sterilization (~100 seeds) was performed in microcentrifuge tubes. First, 1 mL of 10% (v/v) sodium hypochlorite was added to the tube containing the seeds. The tube was inverted thoroughly to ensure all seeds came into contact with the solution, and then allowed to stand at RT for 5 min to allow the seeds to settle to the bottom. Next, most of the solution (~900 µL) was removed from the tube and 1 mL of EtOH mix (EtOH:sterile water: sodium hypochlorite at 7:2:1 ratio) was added. The tube was inverted thoroughly again, allowed to

stand for 5 min. The EtOH mix was then removed and the seeds were washed with 1 mL of sterile distilled water. This was repeated three times to ensure all traces of bleach had been completely removed. The surface sterilized seeds were then sown on 1% strength MS agar (4.708 g/L MS salt (Duchefa Biochemicie), 30g/L sucrose, 1% (w/v) Difco™ agar; pH to 6 and autoclaved prior to use) in 9 mm diameter petri dishes.

For large scale sterilization (usually used for T_0 seed selection) following transformation, 500 mg of seed were transferred to a sterile 50 mL Falcon tube. The seeds were first treated with 30 mL of 70% EtOH for 7 min, then this was replaced with 30 mL bleach mix (sterile water:sodium hypochlorite:Tween-20 at ratio 8:2:0.05) for 7 min. This was followed by thorough washing with 5x 30 mL sterile distilled water for 5 min each. The surface sterilized seeds in the final 30 mL of water were then divided into several sterile 14 mL Falcon tubes (~5 mL/tube). The water was discarded from the tube, leaving the seeds to settle at the bottom. Five mL of 0.8% MS agar was added to each tube. Seeds and agar were mixed and poured evenly onto 1% strength MS agar in 9 mm diameter petri dishes. For transgenic selection, the 1% strength MS medium contained appropriate antibiotics for selection.

The agar plates with the seeds were allowed to dry for several minutes, sealed with nesco film or 3M™ Micropore™ Medical Tape 1530-0 (BM, USA) and stratified at 4 ^{0}C for 48 h to promote uniform germination before being transferred to a controlled chamber and grown under long day conditions (section 2.1). After two weeks, the seedlings were transferred onto soil for further growth. For genotyping of transgenic lines, DNA was extracted from plant tissues and checked via PCR with specific primers (section 2.11).

2.14.2 Growth in soil

WT or homozygous transgenic Arabidopsis seeds were sown directly on to soil mix (compost:sand; 3:1) either in individual pots or using the ARASYSTEM (Betatech) as directed by the manufacturer. Each pot was filled with moist soil mix and grown under optimal growth conditions as described in section 2.1.

2.15 Stable transformation into Arabidopsis

The floral dip technique (Clough and Bent, 1998); a simplified *Agrobacterium*-mediated transformation method for *A. thaliana* was used in this work.

Two to three pots (~30 seeds/pot) of soil-grown Arabidopsis WT were required for each transformation. Plants were grown normally or in domes, for four weeks and then and used when maximum number of flowers was produced.

On day 1, a single colony from a freshly streaked transformed *A. tumefaciens* culture was inoculated into a 50 mL sterile flask containing 10 mL LB with appropriate antibiotics and incubated at 30 ^{0}C, 100 rpm in a Gallenkamp cooled orbital incubator overnight; serving as a starter culture. The following day, the starter culture was further inoculated into a sterile 2 L flask containing 500 mL of LB with appropriate antibiotics and incubated overnight under the same conditions. On the third day, the cells were harvested via centrifugation at 5500 g, RT for 20 min in a Beckman Coulter Avanti® J-E centrifuge fitted with a JA-20 rotor. The supernatant was removed and the pellet was carefully resuspended in a solution containing 5% sucrose and 0.05% Silwett 77 (Lehle Seeds). The resuspended bacterial solution was transferred into an appropriate container and 4-week-old WT Arabidopsis plants were dipped in the solution for approximately 10 s and then covered with black plastic bags overnight to retain the humidity. Subsequently, the transformed plants were grown for 4-5 weeks in a controlled growth chamber under optimum conditions (section 2.1) until the seeds were ready to be collected. These seeds, known as T_0 (Generation 0) were then sown on selective MS agar to identify transgenic plants (section 2.14.1).

2.16 Protein extraction and quantification

Several extraction methods using different buffers were used in this work. Nevertheless, the general approach was similar, with some additional purification steps that are described in specific chapters.

Protein extract	Buffer composition	Centrifugation parameters	Chapter
Catalase and Superoxide dismutase isoforms	100 mM Tris-HCl pH 8, 30 mM DTT, 20% (v/v) glycerol	Beckman Coulter AllegraTH 21R centrifuge fitted with a F2402H rotor 14 000 g, 4 ^{0}C, 30 min	3
Ascorbate peroxidise isoforms	100 mM Potassium phosphate pH 8, 5 mM ascorbate, 1 mM EDTA	Beckman Coulter AllegraTH 21, centrifuge fitted with a F2402H rotor 14 000 g, 4 ^{0}C, 30 min	3
GUS extraction buffer	50 mM sodium phosphate pH 7, 1 mM EDTA pH 8, 10 mM DTT, 0.1% (w/v) sarcosyl, 0.1% (v/v) Triton X-100	Eppendorf MiniSpin plus® microcentrifuge 13000 rpm, RT, 5 min	5, 6

Protein was extracted by grinding plant material in a pre-cooled mortar with liquid nitrogen followed by the addition of extraction buffer. The samples were transferred into microcentrifuge tubes, vortexed briefly and centrifuged. The supernatant was aliquoted into small volumes and kept at -20 °C until further use.

The protein content was quantified using the Bradford assay (Bradford, 1976). First, a BSA dilution standard ranging from from 0.125 to 1 mg/mL was prepared in extraction buffer. Then, 5 µL of sample or BSA dilution standards were loaded into White-Opaque Optiplate-96 microplate (Perkin Elmer). Bradford reagent (Biorad) (250 µL) were added to each sample, mixed gently by pipetting up and down, and incubated at RT between 10-30 minutes. The absorbance was measured at 590 nm using a MRX Revelation Microplate Reader

(Dynex) and the output was analyzed with the MRX Revelation software (Dynex). The unknown protein sample concentration was determined from the BSA standard curve. The final unit was expressed as mg/mL.

2.17 Promoter GUS (β-glucuronidase) analysis

In this section, I describe qualitative and quantitative GUS expression analyses used for three Arabidopsis transgenic lines used in this work; SAG21 1685 promoter::GUS, SAG21 300 promoter::GUS and SAG12 promoter::GUS. Details on experimental designs to study the spatial expression during developmental and upon stress are given in Chapters 5 and 6, respectively.

All 5-bromo-4-chloro-3-indolyl-β-D-glucuronide cyclohexylammonium (X-GlcA) salt, 4-methyl umbelliferyl glucuronide (MUG) and 4-methyl umbelliferone (MU) used in this work were purchased from Melford, UK.

2.17.1 GUS staining (Qualitative approach)

Seedlings grown *in vitro* as described in section 2.1 were transferred to tubes containing X-Gluc staining solution (0.5 M sodium phosphate pH 7, 200 mM potassium ferricyanide, 20 mg/mL chloroamphenicol, 0.01% Triton X-100, 5 mg/mL X-GlcA salt/DMSO), vacuum infiltrated using an A.C. motor (AEI Ltd) for 2-3 min and incubated at 37 ^{0}C for 2-6 hours. The amount of staining solution and tube size were dependent on the age of seedlings and treatment set up. Following incubation, GUS-stained seedlings were decolorized by replacing the staining solution with 96% EtOH for 2-3 hours. This step was repeated several times until all chlorophyll was completely removed. GUS spatial expression in different tissues was observed using light microscopy (section 2.19.1).

2.17.2 GUS fluorogenic assay (Quantitative approach)

Prior to GUS assay, proteins extracted from seedlings were quantified as described in section 2.16. The fluorogenic reaction was adapted from Jefferson *et al* (1987) and carried out as follows: 5 μL of protein extract was added to 50 μL GUS assay buffer (1 mM MUG in GUS extraction buffer; section 2.16) and incubated at 37 °C. Ten μL of reaction mix was removed at time 0, 5 and 30 min of incubation, and the reaction was terminated by the addition of 90 μL Stop buffer (0.2 M Na_2CO_3). The addition of Na_2CO_3 served the dual purposes of stopping the enzyme (β-glucuronidase) reaction and developing the fluorogenic product, MU. Fluorescence was then measured in a Black-Opaque Optiplate-96 microplate (Perkin Elmer) with excitation at 365 nm and emission at 455 nm using BIO-TEK FL600 fluorometer (BIO-TEK®) and the output was analysed using the KC4 software (BIO-TEK®). The instrument was calibrated with freshly prepared MU dilution standards (ranging from 100 nM to 1 μM MU in Stop buffer). In order to calculate the activity in the unknown samples, relative fluorescence units (F.U.) produced by the MU standards were plotted against concentration (with the assumption of 1 μM MU is equivalent to 1000 F.U.). The unknown sample concentration was determined from the standard curve. This value was further normalised against the incubation time and total protein. The final GUS activity was expressed as nmoles MU/min/mg of protein.

2.18 Hydrogen peroxide (H_2O_2) quantification

An Amplex Red Hydrogen Peroxide/Peroxidase assay Kit (Molecular Probes, Invitrogen) was used to measure H_2O_2 production in wallflower petals/leaves (Chapter 3) and Arabidopsis seedlings (Chapter 6). Plant tissues were frozen in liquid nitrogen and then ground. Then, 200 μL of phosphate buffer (20 mM K_2HPO_4, pH 6.5) was added to the ground frozen tissue and centrifuged at 13000 rpm, RT, 5 min. After centrifugation, 50 μL of the supernatant was incubated with 100 μM Amplex Red reagent (10-acetyl-3,7-dihydrophenoxazine) and 0.2 units/mL horseradish peroxidase at RT for 30 min under dark conditions. The fluorescence was quantified using BIO-TEK FL600 fluorometer (BIO-TEK®) (excitation at 650 nm and emission at 590 nm). The final unit was expressed as pmol mg^{-1} protein.

2.19 Imaging

2.19.1 Light microscopy

Arabidopsis seedlings were examined and images captured using a VMS-001 USB Microscope (Veho).

2.19.2 Confocal microscopy

Transient and stable expression was studied by confocal laser scanning microscopy using a Leica TCS SP2 AOBS spectral confocal microscope (Leica Microsystems). YFP/GFP was excited at 514 nm and detected in the 525 to 583 nm range. Chlorophyll autofluorescence was detected in the 660 to 700 nm range.

2.20 Bioinformatics

Primers were designed with Primer 3 software and analysed using Oligoanalyzer before purchased. Two main freely available databases that were used extensively as major reference in this work were The Arabidopsis Information Resource (TAIR) and National Center for Biotechnology Information (NCBI). Bioedit and Chromas Lite were used primarily for sequence alignment analyses.

2.21 Statistical analysis

Data were assessed by Student's t-test (significant differences were expressed as P-value <0.05).

Chapter 3: Hormonal and redox regulation in wallflowers

3.1 Introduction

Plant senescence is a developmentally regulated and genetically programmed process that ultimately leads to death of particular organs such as flowers and leaves, or the whole plant (Tripathi and Tuteja, 2007). Flower parts such as petals have a finite life span and serves as an excellent model for the study of senescence and abscission because both processes are irreversible and are under precise developmental control (Rogers, 2006; van Doorn and Woltering, 2008). Unlike the reversible leaf senescence, petal senescence which ends with cell death can be considered as a subset of developmental PCD (Thomas et al., 2003; van Doorn and Woltering, 2008).

Two main events associated with senescence include the down-regulation of biosynthetic pathways and the up-regulation of catabolic events which hydrolyse polymers such as carbohydrates, proteins, lipids and nucleic acids producing simple mobile products that will be remobilized to newly growing tissues (Lim, Kim and Nam, 2007). Numerous genes involved in these processes such as senescence associated genes (SAGs) become transiently up-regulated while many other genes are down-regulated (van Doorn and Woltering, 2008). The expression of these genes is also regulated by a complex hormone interplay mainly between ethylene and cytokinins (Lim et al., 2007; van Doorn and Woltering, 2008) and is often accompanied by a change in redox balance.

3.1.1 Wallflower as model species

Although leaf senescence has been extensively studied in Arabidopsis due to the availability of genomic resources and transgenic lines, Arabidopsis has not proved to be very tractable for the study of flower senescence due to the size limitation of its flowers and asynchrony of floral development making staging difficult. Wallflowers (*Erysimum linifolium*) provide a good alternative model species as they are closely related to *Arabidopsis thaliana* and *Brassica* spp., both of which provide a useful resource of information regarding leaf senescence due to the extensive studies that have been done with them. The advantages of wallflowers are that they have longer lasting relatively large pigmented petals whose

development and senescence are easily staged (Price et al., 2008) and can be easily sourced being commercially relevant ornamental plants. The variety of wallflowers selected for this work is also a perennial evergreen plant with a long flowering season making it possible to collect samples throughout the year. Besides that, this variety is sterile, and, thus, petal senescence is unaffected by pollination which is well known as one of the main senescence inducers in most flowers (Van Doorn, 1997; O'Neil, 1997; Woltering et al., 1994; Stead, 1992). Moreover, a recent microarray analysis comparing wallflower petals and leaves revealed a number of common and distinct patterns in their gene expression. A large proportion of genes up-regulated during senescence in both tissues includes genes involved in remobilization, hormonal regulation and ROS signalling (Price et al., 2008).

3.1.2 Hormonal regulation of petal senescence

Ethylene is the major regulator of petal senescence in ethylene-sensitive flowers such as carnation, petunia, and rose, and orchid while in ethylene-insensitive species (daylily and *Iris*), abscisic acid (ABA) seems to play a major role (van Doorn and Woltering, 2008). Ethylene hastens petal senescence by accelerating petal in-rolling resulting in petal wilting and colour changes and affecting the time to abscission. For example in detached carnation, ethylene increases with the progression of petal senescence and peaks just before abscission (ten Have and Woltering, 1997; Shibuya et al., 2000). In Arabidopsis, ethylene was shown to be essential for normal floral organ abscission (Patterson and Bleecker, 2004; Butenko et al., 2006). Furthermore, flower lifespan in carnation was improved when cut flowers were treated with an ethylene receptor inhibitor, silver thio-sulphate (STS) (Hoeberichts et al., 2007a). This treatment also prevents the up-regulation of *SAGs* in carnation (Hoeberichts et al., 2007a), confirming that their expression is regulated by ethylene at a transcriptional level.

Increase in endogenous ethylene production in carnation flower senescence was accompanied by sequential expression of the ethylene biosynthetic genes; *ACC* synthase (*ACS*) and *ACC* oxidase (*ACO*) (ten Have and Woltering, 1997). In carnations, both genes were rapidly induced by ethylene indicating that ethylene is the main regulator of these genes (autocatalytic feedback) and responsible for their expression during natural senescence (ten Have and Woltering, 1997). However, *ACS* expression was not altered in petals and leaves of Arabidopsis during natural senescence but *ACO* increased dramatically only in stage 15

senescing petals (Wagstaff et al., 2009). *ACO* genes were also down-regulated in *Alstroemeria* (Wagstaff et al., 2005) and up-regulated in petunia flower senescence (Tang et al.,1996).

In contrast to ethylene, cytokinins delays senescence in floral tissues (van Doorn and Woltering, 2008). An inverse relationship between cytokinin content and senescence was established in transgenic petunias overexpressing the *isopentenyltransferase* (*ipt*) gene. These transgenics had high levels of cytokinins, a delayed ethylene rise and extended petal lifespan (Chang et al., 2003). In addition, treatment with the synthetic cytokinin; kinetin or the natural cytokinin, zeatin delayed petal senescence in detached carnation and also resulted in a slower rise in ethylene production, possibility through a decrease in ethylene sensitivity (Eisinger, 1977; Mor, Spiegelstein and Halevy, 1983).

Cytokinin levels can be regulated by synthesis, inactivation or degradation. In carnation and Arabidopsis, genes encoding cytokinin oxidase which plays a role in cytokinin degradation showed increased expression during petal senescence (Hoeberichts et al., 2007a; Wagstaff et al., 2009). Detached carnation supplied with 6-metylpurine (6-MP); an inhibitor of cytokinin oxidase resulted in higher cytokinin content and much longer petal life span (Taverner et al., 2000) which mirrored the effect of STS. Taken together, these data strongly suggest that cytokinin could interact with ethylene during flower senescence. Moreover, a cytokinin insensitive Arabidopsis mutant; *ckr1*, which is allelic to the ethylene-insensitive mutant; *ein2*, provides evidence that cytokinin action involves some overlap with the ethylene-signalling pathway (Su and Howell, 1992; Cary, Liu and Howell, 1995).

Auxins also affect ethylene production but their role during petal senescence is still unclear (van Doorn and Woltering, 2008). A synthetic auxin (2,4-dichlorophenoxyacetic acid; 2,4-D) induced the expression of ACC synthase genes in the styles, ovaries and petals of carnation (Jones and Woodson, 1999). Application of IAA also hastened the rise of ethylene production and petal wilting in cut carnation flowers (van Staden, 1995). *Aux/IAA* transcripts are transiently increased in carnation petal senescence (Hoeberichts et al., 2007a) and Arabidopsis leaf senescence (Buchanan-Wollaston et al., 2005) but down-regulated in Arabidopsis senescing petals (Wagstaff et al., 2009). A putative orthologue of the Arabidopsis auxin-responsive like protein *DFL1; (Dwarf in Light)* (IAA amido synthase

involved in auxin signal transduction (Nakazawa et al., 2001) is up-regulated during pollination-induced corolla senescence in petunia (Bai et al., 2010).

3.1.3 ROS signalling in petal and leaf senescence

ROS are thought to play an essential role in senescence in both animals and plants (Mhamdi et al., 2010). This is consistent with a loss in antioxidative capacity during the progression of senescence, which has been reported in many different plants (Panavas and Rubinstein, 1998; Orendi et al., 2001), implying that this might be a general phenomenon for many aerobic organisms. Two main antioxidant enzymes responsible for H_2O_2 scavenging in plants are catalase and ascorbate peroxidase (Foyer, Faragher and Thornalley, 2009). In Arabidopsis, measurement of hydrogen peroxide (H_2O_2) content in leaves revealed that H_2O_2 levels increased during development and peaked exactly when the plants started to bolt (Miao et al., 2004; Zimmermann et al., 2006). All three Arabidopsis catalase isoforms; CAT1, CAT2 and CAT3 showed senescence-specific activity. CAT2 activity decreased with bolting time in parallel with a decrease in APX1 activity coinciding with the H_2O_2 peak. Following the oxidative burst, the ROS-inducible CAT3 isoform was activated and APX1 activity was recovered, accompanied by a decline of the H_2O_2 content (Zimmermann et al., 2006). The decrease in CAT2 activity and mRNA level at bolting time has been proposed to be an integral part of H_2O_2-triggered leaf senescence (Zimmermann et al., 2006; Smykowski, Zimmermann and Zentgraf, 2010). In addition to the ROS-inducible property of the CAT3 isoform, eight out of twelve SAGs characterized in Arabidopsis leaf senescence could also be induced by ozone (Miller, Arteca and Pell, 1999) and expression of many other SAGs was also enhanced by increased levels of ROS (Navabpour et al., 2003), indicating that the elevation of H_2O_2 level might serve as a signal to promote leaf senescence (Zimmermann and Zentgraf, 2005; Zentgraf, 2007). Moreover, the timing of senescence is also altered in an ascorbate-deficient Arabidopsis mutant (Barth et al., 2004).

In petal senescence, the role of ROS remains debatable. It is still not known if the increase in ROS levels may have a regulatory signalling function or is merely a consequence of deregulation of the antioxidant system as cells enter PCD (van Doorn and Woltering, 2008). An increase in H_2O_2 levels was reported upon flower opening in daylily (Panavas and Rubinstein, 1998), chrysanthemum (Chakrabarty, Chatterjee and Datta, 2007) and rose (Xue

et al., 2008). In addition, a H_2O_2 peak could also be observed quite late in petal senescence in tulip after the occurrence of key senescence markers such as a rise in proteases and release of cytochrome c from the mitochondria (Azad et al., 2008). A similar peak was also reported in daylily taking place after the sharp rise in ion leakage associated with membrane degradation (Panavas and Rubinstein, 1998). These findings suggest that the rise in ROS levels are more likely to be associated with PCD rather than senescence. However, it might not be a universal feature in all species.

The activity of anti-oxidative enzymes such as superoxide dismutase (SOD), CAT and APX have thus far mainly been assessed crudely in petals via spectrometric methods (van Doorn and Woltering, 2008). In general, total activities of these antioxidative enzymes appear to increase during flower development and then fall as senescence progresses although in some species CAT activity remained high at later stages (Droillard and Paulin, 1990); Bailly et al., 2001; Panavas and Rubinstein, 1998). A decline in APX activity has been suggested to be a pre-requisite for inducing cell death in Gladiolus (Hossain et al, 2006). Very few studies have compared the activity of individual isozymes using in-gel zymogram analyses. In these studies, in daylily (Chakrabarty et al., 2009) and chrysanthemum (Chakrabarty et al., 2007), the findings clearly revealed a more complex redox regulation exhibiting distinct and differential changes in activity levels of specific isozymes of the different enzymes through petal senescence. Differences in antioxidant regulation between species may reflect the relative importance of different ROS scavenging systems or the significance of the role of ROS itself during the progression of petal senescence.

In the work reported in this chapter, the aim was to understand hormonal and redox regulation of wallflower petal and leaf senescence. Harvested wallflowers (detached flowers) were subjected to several treatments and monitored for senescence and abscission progression. The production of specific hormones was quantified in different petal stages (attached flowers). In parallel, the expression of a number of SAGs and hormone-regulated genes was also determined in both petals and leaves. Further confirmation of ROS involvement was obtained by measuring H_2O_2 production and analysing the antioxidant enzyme activities using zymograms.

3.2 Materials and methods

3.2.1 Plant material

Wallflowers *(Erysimum linifolium* cv Bowles Mauve) were grown at the University botanical and research garden of Cardiff University (Cardiff, UK) either outside or in a greenhouse with temperature set at a minimum of 14 °C. Humidity and light were not controlled. Petals and leaves were collected and staged into seven defined developmental stages according to Price et al. (2008) (Appendix-A).

Material for protein extraction was immediately frozen in liquid nitrogen and stored at –80 °C until required.

3.2.2 Hormone analysis

3.2.2.1 Detached flower treatments

Individual flowers were detached from the raceme at stage 1 and the pedicel was immediately submerged in water. Flowers were held continuously at $20°$ C 16 h light either in water, or in solutions of kinetin (1.0 or 0.1 mM) or 6-methyl purine (0.1mM) or 2-chloroethylphosphonic acid; CEPA (SIGMA-ALDRICH, Dorset, UK). For ethylene inhibitor treatment, flowers were held in STS (4 mM $AgNO_3$:32 mM NaS_2O_3) for 1 hour and then transferred to water. Each experiment consisted of ten replicate flowers which were monitored daily to record senescence stage and day of petal abscission.

3.2.2.2 Endogenous auxin content

3.2.2.2.1. Extraction and purification of indolacetic acid (IAA)

For indolacetic acid (IAA) quantification, approximately 2 g of floral tissue were used for each stage. Samples were homogenised with a mortar and pestle in cold 70% (v/v) acetone (1:5 w/v). The homogenate was supplemented with 50 ng of $[^{13}C]_6$IAA (Olchemim Ltd) as an internal standard, then stirred for 4 h at 4°C, before centrifugation at 2000 g for 15 min. The

supernatant was recovered and stored at 4°C while the pellet was re-extracted twice (4 h each extraction) and then left overnight stirring at 4°C. The supernatant containing solvent was reduced to the aqueous phase (approximately to a volume of 10 mL) under vacuum at 35°C, adjusted to pH 2.8 with 0.1 N HCl and partitioned 5 times against equal volumes of ethyl ether. The pooled ethyl ether extracts were kept at –20°C overnight, to freeze and separate traces of water. Ethyl ether was then evaporated, the dried samples were dissolved in a small volume of 10% (v/v) aqueous acetonitrile containing 0.1% (v/v) acetic acid and purified by HPLC.

IAA samples were purified by reverse phase HPLC using a Kontron PUMP 422 (Kontron, Germany). The detector was operated at 254 nm wavelength. A C18 Hypersil column (Thermo) 150 x 4.6 mm i.d. particle size 5 μm, eluted at a flow rate of 1 mL min-1 was used. Samples were applied to the column and the fraction containing IAA was collected while the column was being eluted with a linear gradient of acetonitrile in water and 0.1% acetic acid, from 10% to 30% for 15 min and then from 30% to 100% in 40 min. The fraction was dried under vacuum, dissolved with 30% (v/v) aqueous methanol containing 0.5% (v/v) acetic acid and purified by HPLC equipped with a Nucleosil $N(CH3)2$ column (Macherey-Nagel) and eluted with a flow rate of 1 mL min^{-1} Samples were applied to the column and the fraction containing IAA was collected while the column was being eluted continuously with 30% (v/v) methanol in water containing 0.5% (v/v) acetic acid. The fractions containing IAA were dried, eluted with 250 μL of 100% acetone, transferred into capillary tubes and dried under vacuum. After adding 100 μL of 100% diazomethane the capillary tubes were dried to remove water residues and silylated with bis(trimethylsilyl)trifluoroacetamide containing 1% trimethylchlorosilane (Sigma) for 1 h at 70°C.

3.2.2.2.2. Quantification of indolacetic acid (IAA) with GC-MS

Gas chromatography-mass spectrometry analysis was performed on a Saturn 2200 quadrupole ion trap mass spectrometer coupled to a CP-3800 gas chromatograph (Varian, Palo Alto, CA) equipped with a MEGA 1 capillary column (MEGA, Legnano, Italy) 25 m x 0.25 mm ID x 0.25 mm film thickness, coated with 100% dimethylpolysiloxane. The injection was splitless with 2 min purge off, at 250°C. The temperature of the transfer line between the gas chromatograph and the mass spectrometer was set at 250°C.

For IAA analysis, oven temperature was 120°C for 2 min, followed by a gradient from 120°C to 190°C at 35°C min^{-1}, then from 190°C to 210°C at 6°C min^{-1} and a final ramp from 210°C to 300°C at 35°C min^{-1} with a final hold of 10 min. Full scan mass spectra were obtained in EI+ mode with an emission current of 30 μA, an axial modulation of 4 V and the electron multiplier set at −1500 V. Data acquisition was from 70 to 350 Da at a speed of 1.4 scan s-1. The following ions were monitored for IAA analysis: m\z 202 and 319 for IAA, and 208 and 325 for the 13C-labelled internal standard. Quantification of IAA was carried out by reference to a calibration plot obtained from the GC-MS analysis of a series of mixtures of the standard hormone with its labelled form.

3.2.3. ROS analysis

3.2.3.1 H$_2$O$_2$ quantification

Fluorometric H$_2$O$_2$ analysis using an Amplex-Red Hydrogen Peroxide/Peroxidase Assay Kit (Molecular probes, Eugene, USA) was performed as described in section 2.18.

3.2.3.2 Enzyme analyses

3.2.3.2.1 Protein extraction

To determine the CAT and SOD activities, 1 leaf or 16 petals of Arabidopsis and wallflowers of all stages were homogenized in 200 μl extraction buffer (100 mM Tris-HCl pH 8.0, 20% glycerol and 30 mM dithiothreitol (DTT)) with liquid nitrogen at 4^{0}C. For the analyses of APX activities, the samples were ground with liquid nitrogen in 200 μl extraction buffer 100 mM (potassium phosphate buffer, pH 7.0, containing 5 mM ascorbate and 1 mM EDTA) at 4^{0}C. Homogenized samples were then centrifuged at 14000 g for 30 min at 4^{0}C and the resulting supernatant used directly for zymograms. Protein content of samples was quantified as described in section 2.16.

3.2.3.2.2 Zymograms

For CAT zymograms (Zimmermann et al., 2006), a serial dilution of a commercially available bovine CAT (ICN Biochemicals) was prepared (~0.1% - 3%) and used to confirm a linear relationship between the concentration and relative activity of the enzymes, having equated 0.1 units with 0.1% relative activity. Ten µl of protein extracts of each samples were separated in 7.5% native polyacrylamide gels (0.375 M Tris-HCl, pH 8.8, as gel buffer) with a 3.5 % stacking gel (0.125 M Tris-HCl, pH 6.8, as gel buffer) for 3 h (70-80 V) at 18 ^{0}C using 250 mM glycine and 25 mM Tris-HCl, pH 8.3, as electrophoresis buffer. The gels were subsequently stained for CAT activity according to Chandlee & Scandalios (1983) as follows: The gels were soaked in 0.01% H_2O_2 solution for 5 min, washed twice in water and incubated for 5 min in 1% $FeCl_3$ and $K_3[Fe(CN)_6]$ with shaking. After staining, the green-coloured gels were washed once more in water and illuminated in white light.

For APX zymograms (Zimmermann et al., 2006), the protein extracts were separated on 10% native polyacrylamide gels (0.375 M Tris–HCl, pH 8.8, as gel buffer) with a 5% stacking gel (0.137 M Tris–HCl, pH 6.8, as gel buffer) for 3 h (120 V) at 4°C using 2 mM ascorbate, 250 mM glycine, and 25 mM Tris–HCl, pH 8.3, as electrophoresis buffer. After electrophoresis, the gels were soaked in 50 mM potassium phosphate buffer, pH 7.0, containing 2 mM ascorbate for 10 min (3×) and, subsequently, in 50 mM potassium phosphate buffer, pH 7.0, containing 4 mM ascorbate, and 1 mM H_2O_2 for 20 min. After rinsing in water, the gels were stained in 50 mM potassium phosphate buffer, pH 7.8, containing 14 mM TEMED and 2.45 mM NBT for 10–30 min and followed by illumination in white light.

For SOD zymograms (Orendi et al., 2001), the protein extracts were separated 13% native polyacrylamide gels (0.375 M Tris–HCl, pH 8.8, as gel buffer) with a 5% stacking gel (0.137 M Tris–HCl, pH 6.8, as gel buffer) for 3 h (120 V) at 4°C using 250 mM glycine, and 25 mM Tris–HCl, pH 8.3, as electrophoresis buffer. After electrophoresis, the gels were soaked in 50 mM potassium phosphate buffer, pH 7.8, containing 1 mM EDTA, 0.2% TEMED (N,N,N',N'-tetramethylethylenediamine), 2.6 µM riboflavin, and 1.2 mM NBT (nitroblue tetrazolium) for 30 min, rinsed in water, and illuminated in white light.

3.3 Results

3.3.1 Hormonal regulation of petals and leaves senescence in wallflowers

3.3.1.1 Effect on wallflower petal senescence and abscission of exogenous cytokinin and ethylene and perturbation of endogenous ethylene and cytokinin levels through STS and 6MP.

To elucidate how individual hormones regulate petal senescence, individual detached flowers harvested at stage 1 (first opened flower) were subjected to several treatments. Where flowers were held in water, the progression of senescence and abscission time mimicked the time taken in attached flowers (Fig 3-1). Time to abscission in cut flowers held in water was approximately 7 days. Both in detached flowers held in water and on the plant, flowers took 1 day to progress between stages. However, when pulsed for 1 hour with STS (ethylene inhibitor) on the day of harvest, abscission was delayed by 2 days (Fig 3-1a). STS-pulsed flowers also senesced more slowly, taking 4 days to progress from stage 3 to stage 5 (Fig 3-3b), instead of 2 days when held in water (Fig 3-3a). In contrast, petal abscission was accelerated by continuous exposure to 125 ppm CEPA (which releases ethylene) resulting in petal abscission occurring 2 days before those in water (Fig 3-1b), whilst those at a higher concentration of CEPA (250 ppm) lost their petals in about half the time compared with those in water. A lower concentration of CEPA (5ppm) did not affect time to abscission indicating a dose-dependent effect of the CEPA. CEPA-treated flowers also experienced accelerated senescence by skipping two stages at stage 3 and stage 5 (Fig 3-3c).

Continuous treatment with either 0.1 or 1.0 mM kinetin (Fig 3-2b) or with 0.1 mM 6-methyl purine (cytokinin oxidase inhibitor) (Fig 3-2a) also delayed abscission of flowers harvested at stage 1 by 2 days. 6-MP-treated flowers exhibited a similar senescence progression pattern to STS-pulsed flowers (Fig 3-3d). However, kinetin-treated flowers senesced similarly to flower held in water until stage 3, followed by a slower senescence progression, taking 3 days to progress from stage 3 to 5 (Fig 3-3e), instead of 2 days in the control.

(a)

(b)
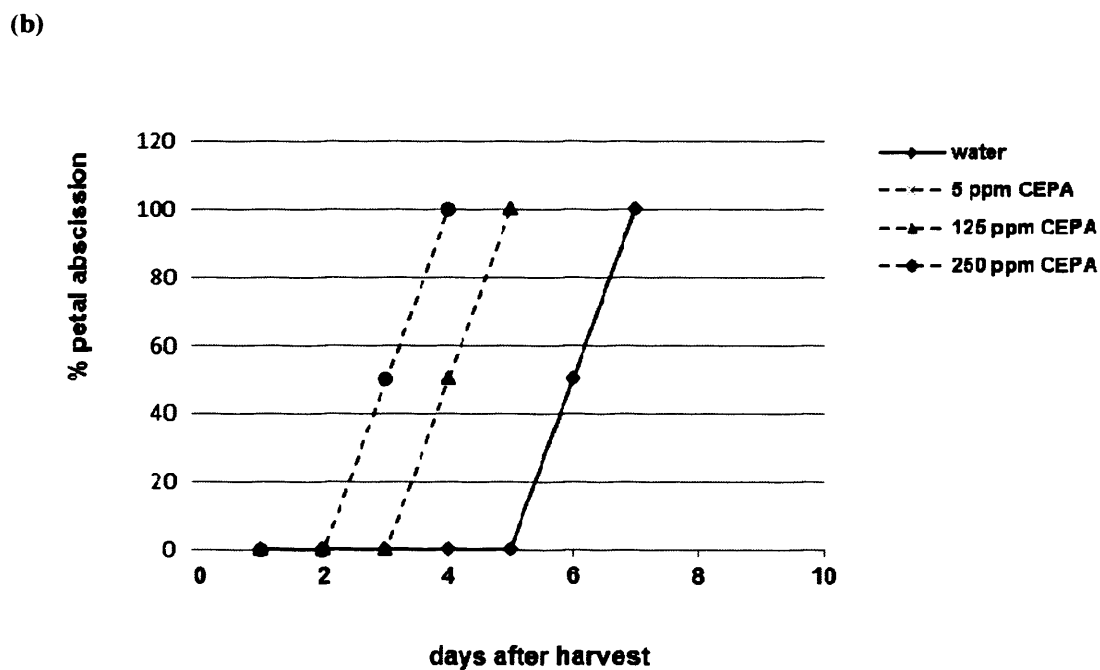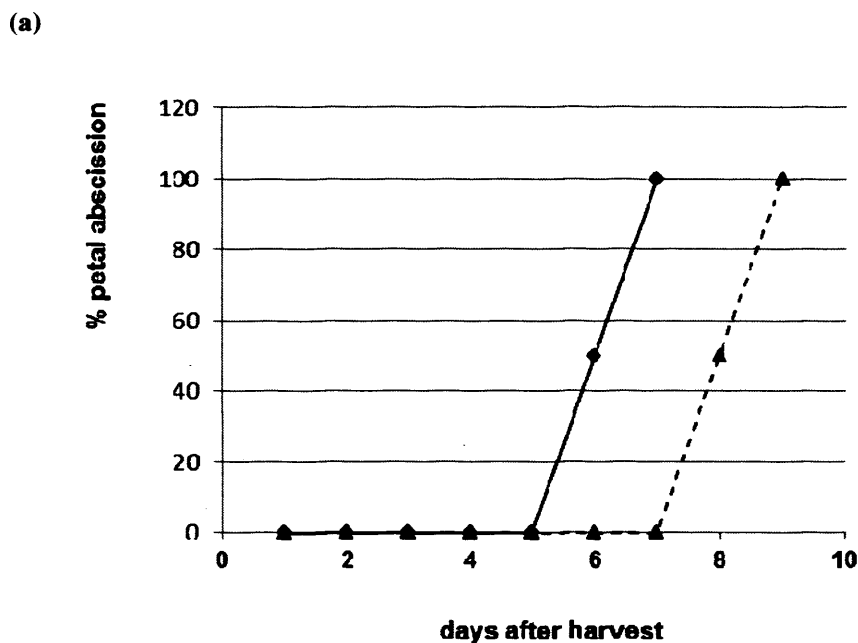
Figure 3-1. Effects on abscission time of cut wallflowers treated with: (a) STS (4 mM AgNO$_3$:32 mM NaS$_2$O$_3$) (b) CEPA (2-chloroethylphosphonic, produces ethylene) compared to water control.

(a)
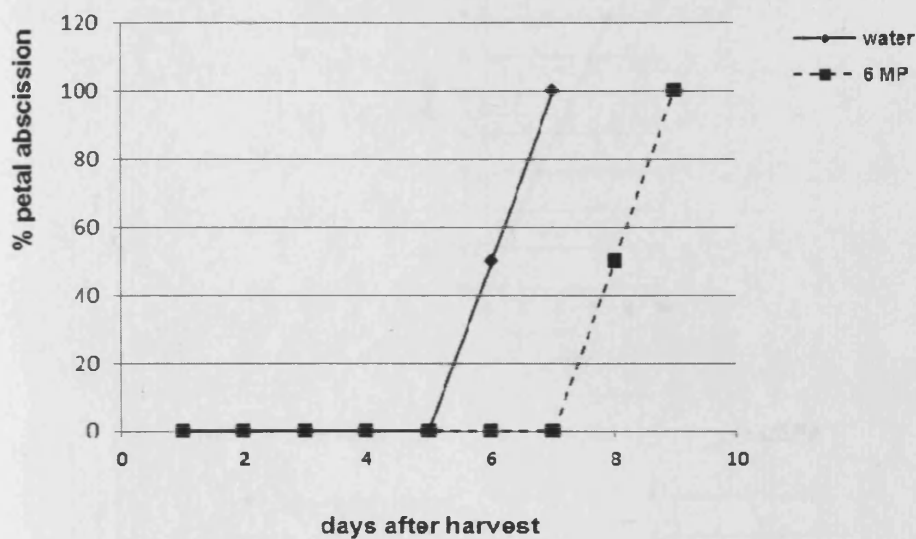
(b)
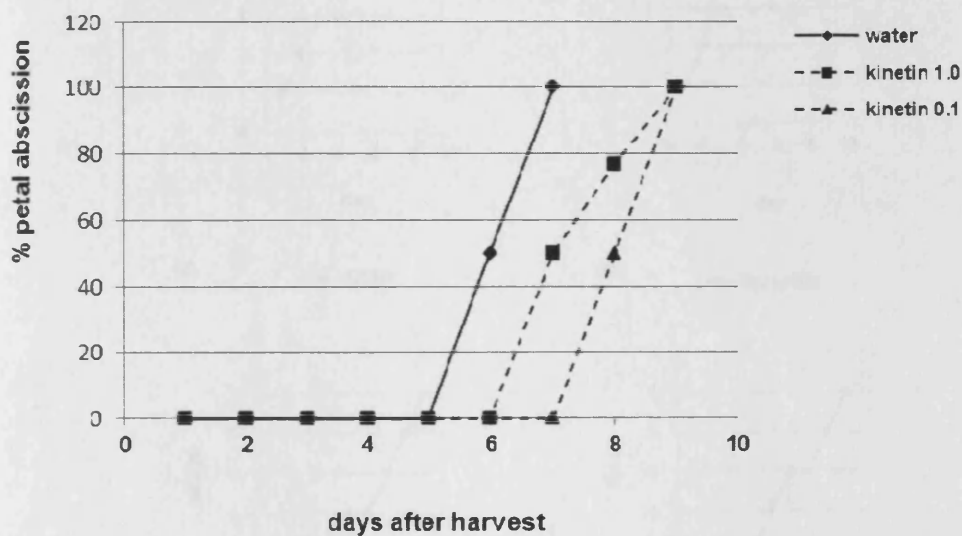
Figure 3-2. Effects on abscission time of cut wallflowers treated with: (a) 6-methyl purine (0.1 mM) (b) kinetin (1.0 or 0.1 mM), compared to water control.
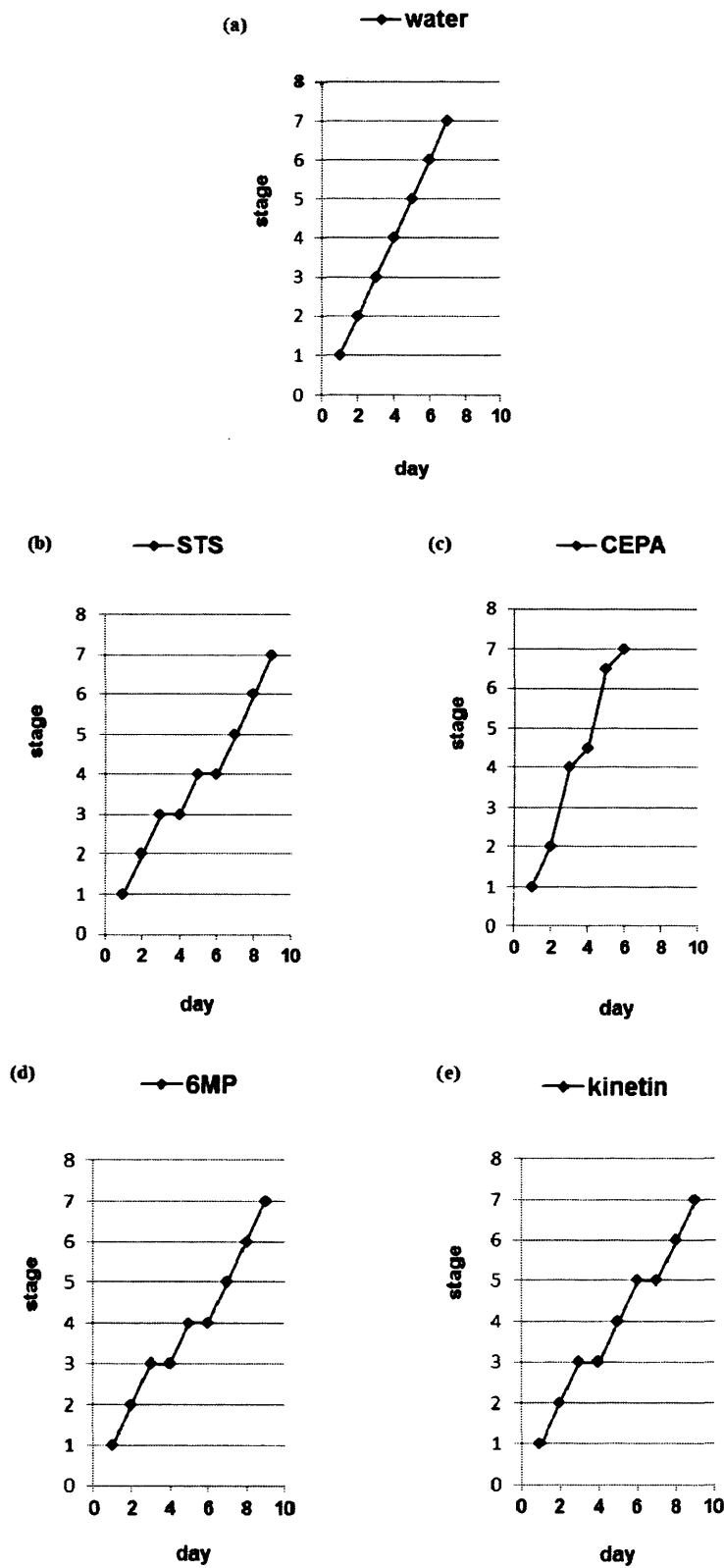
Figure 3-3. Effects on progression of petal development and senescence in cut wallflowers treated with: (a) water; (b) STS; (c) 125 ppm CEPA; (d) 6-methyl purine; (e) 1.0 mM kinetin.

3.3.1.2 Ethylene and auxin production during petal development

Ethylene production was detectable from the youngest unopened flower although the amount produced was quite low (4.21 $nLg^{-1}FW\ h^{-1}$) (Figure 3-4). Ethylene production increased with flower opening at stage 1 and reached the highest peak at stage 3 (25 $nLg^{-1}FWh^{-1}$), just before visible senescence. Ethylene remained high at stage 4 but declined sharply at stage 6 in late senescence.
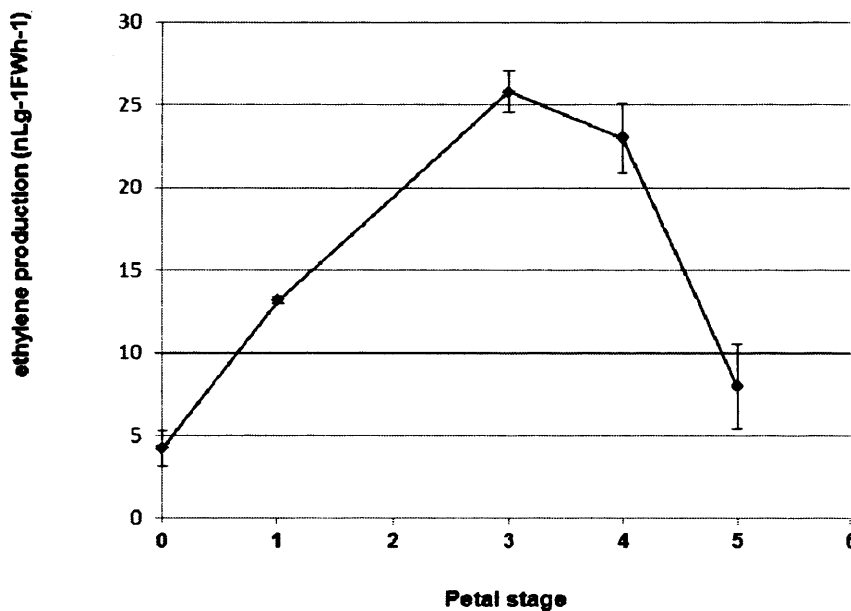
Figure 3-4. Ethylene production from isolated wallflowers detected by gas chromatography. Mean (±SE, n=9).

The endogenous content of auxin was determined by quantifying two types of IAA, free IAA and conjugate IAA 7N from attached flowers. The amount of free IAA was relatively lower than conjugates IAA with the highest content of 168.67 ngg^{-1} FW and 600.84 ngg^{-1} FW (Fig. 3-5), respectively. However, both IAA forms gave a distinct pattern of auxin content at different stages of flower development and senescence. Free IAA was high in young buds, fell slightly (P<0.001) in older buds then increased (P<0.001) once entering stage 3 (Fig. 3-5a). The free IAA continued to increase significantly (P<0.001) with age and peaked at the stage 5. Conversely, conjugate IAA 7N displayed almost the opposite pattern with the highest content in the youngest flowers decreasing as senescence progressed (Fig. 3-5b).

(a)
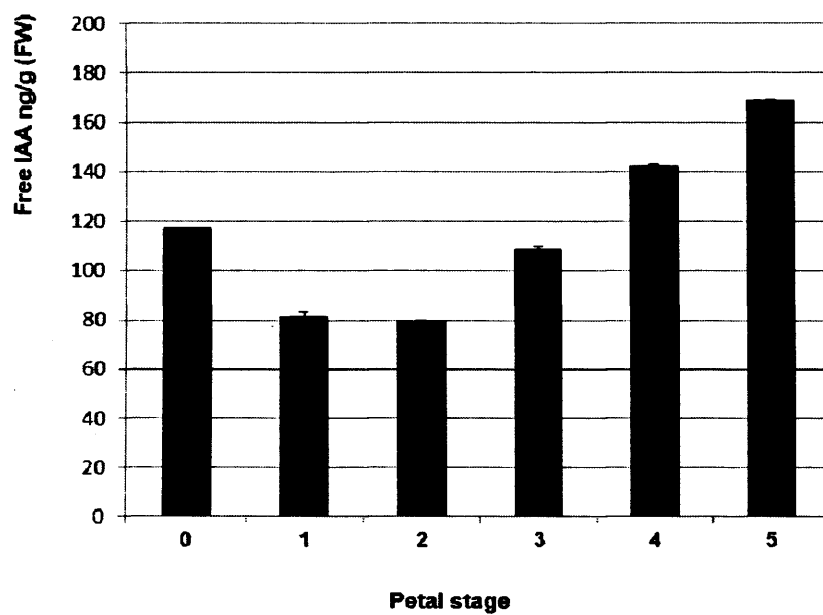
(b)
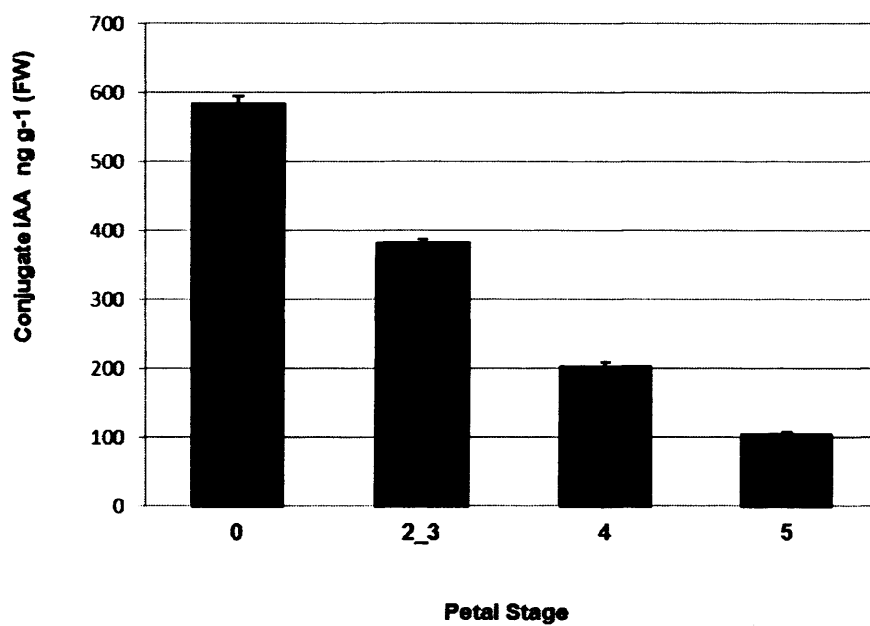
Figure 3-5. Auxin production from isolated wallflowers detected by gas chromatography.
(a) Free IAA (b) Conjugated IAA . Mean (±SE, n=3).

3.3.1.3 Expression pattern of SAGs and hormonally-regulated genes in wallflower petals and leaves

Three genes; *SAG21* (ROS responsive gene), *WLS73* (ethylene synthesis, putative ACC oxidase activity) and *WPS46* (auxin transport) were selected for expression analysis based on their putative function and to confirm the microarray data results (Price et al., 2008). Semi-quantitative RT-PCR analysis revealed that *SAG21* expression peaked in open flowers, stage 1 (P<0.001) (Fig. 3-6a). Expression then reduced significantly (P<0.001) at stage 3 and stage 4 when visible senescence started, followed by a sharp decrease (P<0.001) in the final two stages of senescence (stages 5 and 6).
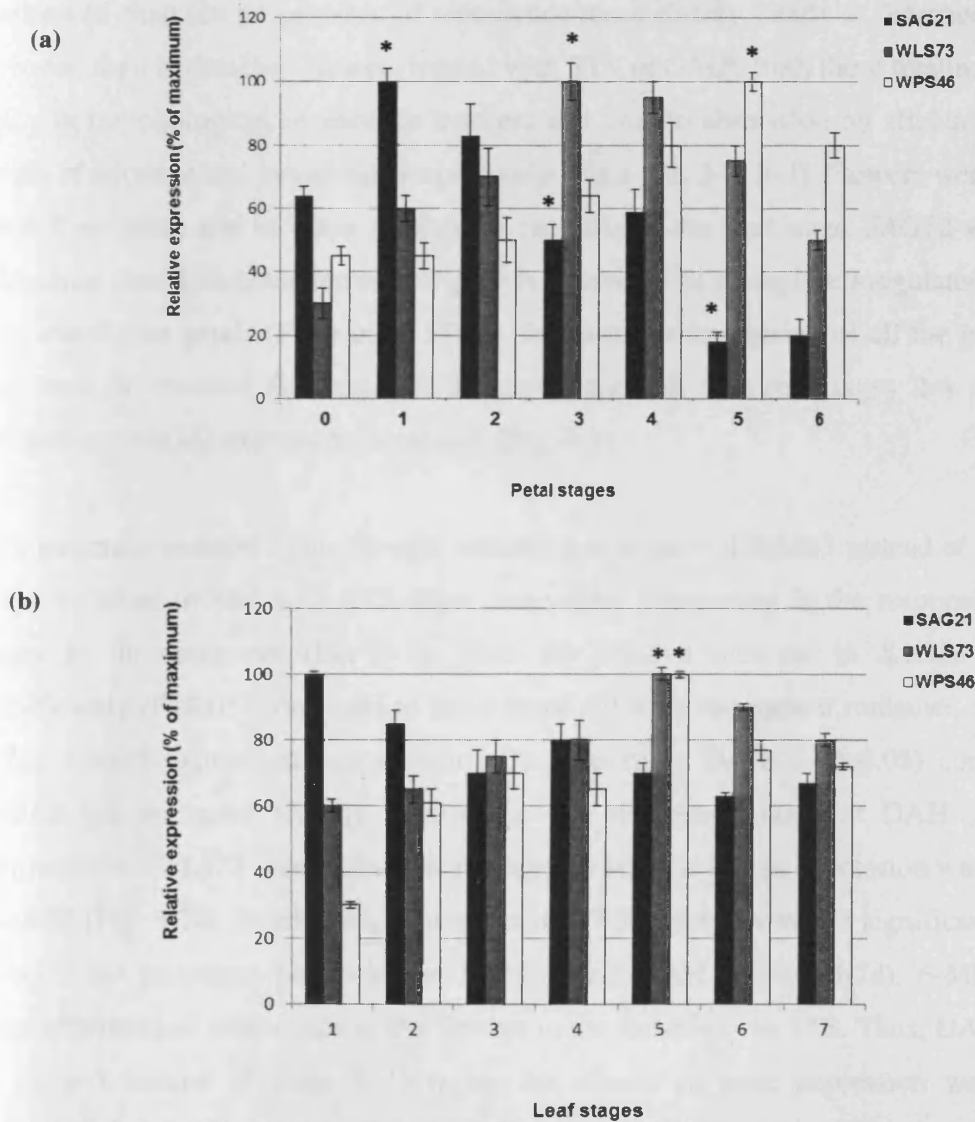
Figure 3-6. Semi-quantitative RT-PCR analysis of *SAG21*, *WLS73* and *WPS46* in different stages of petals (a) and leaves (b). Significant differences of relative expressions were indicated by asterisk (*P<0.001).

76

WLS73 transcript was relatively low in younger flowers but increased significantly (P<0.001) with age (Fig. 3-6a). The highest expression was observed at stages 3 and 4, and then decreased gradually in later stages of senescence. On the other hand, *WPS46* remained low during the first three stages followed by a significant up-regulation (P<0.001) in stages 4 and 5 and a slight drop at stage 6 (Fig. 3-6a). In leaves, *SAG21* expression was relatively higher in the youngest leaves but showed a slight decrease at stage 2 (Fig. 3-6b). The expression level was maintained at a constant level in senescing tissues. *WLS73* and *WPS46* increased gradually as leaves aged and peaked at the same time (stage 5) (Fig. 3-6b).

Having established the patterns of expression in attached flowers these genes were used as markers to chart the progression of senescence more closely, firstly in detached flowers held in water, then in detached flowers treated with STS or 6-MP. Both these treatments result in a delay in morphological senescence markers and time to abscission by affecting endogenous levels of ethylene and cytokinins respectively (Fig.s 3-1, 3-2, 3-3). Flowers were harvested at stage 1 as before and in water progressed each day to the next stage. *SAG12* was used as an additional senescence marker as this gene is known to be strongly up-regulated around stage 2 in wallflower petals (Price et al, 2008). In water the expression of all the genes followed that seen in attached flowers: *SAG21* expression fell between stages 2-4 while *WLS73*, *WPS46* and *SAG12* expression increased (Fig. 3-7).

STS treatment resulted in the flowers remaining at stage 3 at DAH 3 instead of progressing to stage 4. When treated with STS, there were clear differences in the responsiveness of the genes to the treatment (Fig 3-7). Thus the relative increase in *SAG12* was reduced significantly (P<0.05) compared to the control although the pattern remained the same (Fig. 3-7a). *SAG21* expression was significantly reduced at DAH 1 (P<0.05) compared to the control but increased slightly at DAH 2 and remained higher at DAH 3 (Fig. 3-7b). Expression of *WLS73* was affected at all stages where the rise in expression was abolished by the STS (Fig. 3-7c). In contrast, expression of *WPS46* only showed a significant reduction at DAH 1 but remained unaffected at DAH 2 and DAH 3 (Fig. 3-7d). 6-MP and kinetin treatment delayed senescence in the flowers in the same way as STS. Thus, DAH 3 remained at stage 3 instead of stage 4. However the effects on gene expression were much less pronounced than those elicited by STS (Fig 3-7). *SAG12* and *WLS73* levels increased at a

slightly lower levels seen in the control (Fig 3-7a) while *SAG21* and *WPS46* expression was essentially unaffected (Fig 3-7b, d).

(a)

SAG12

(b)
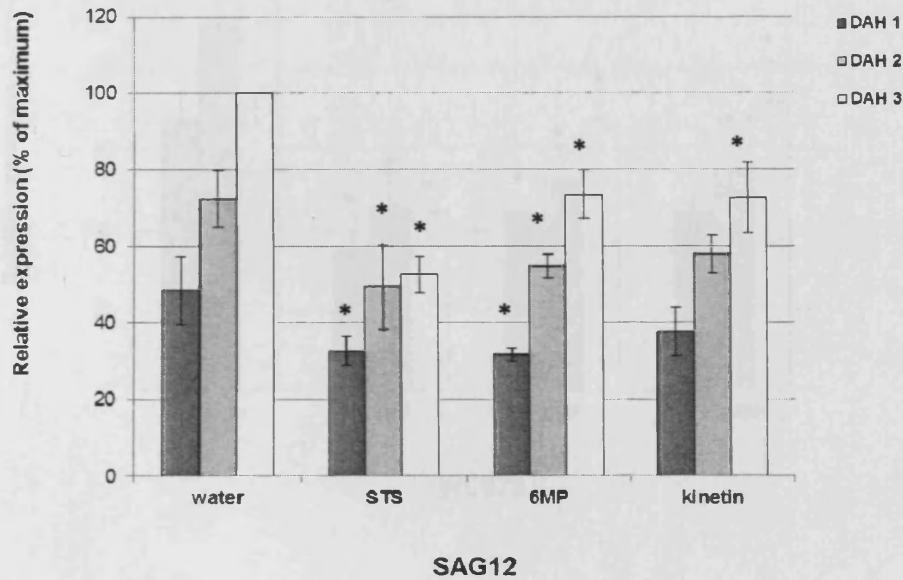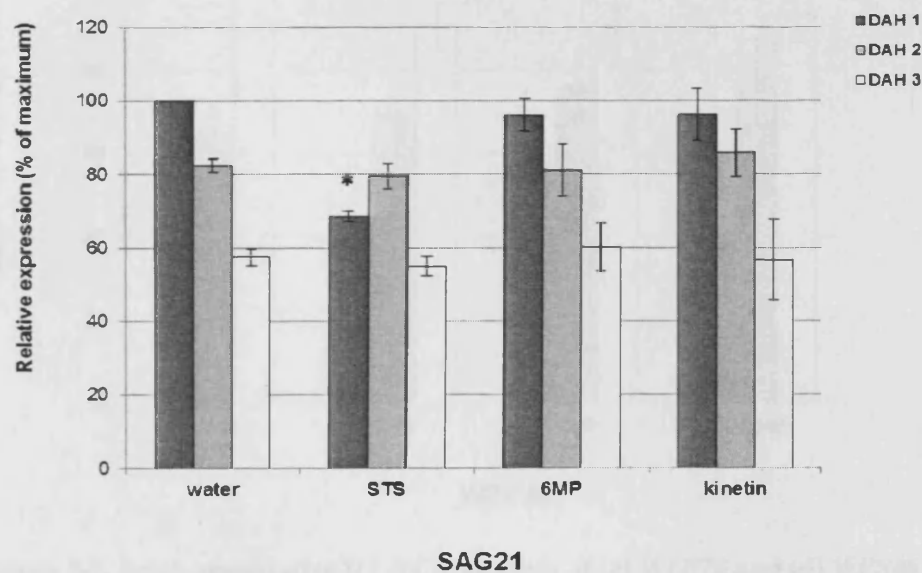
SAG21

Figure 3-7. Semi-quantitative RT-PCR analysis of (a) *SAG12* and (b) *SAG21* in detached flowers treated with water (control), STS, 6-MP and 1.0 M kinetin. For water-treated flowers DAH 1, DAH 2, DAH 3 corresponds to stage 2, 3 and 4 respectively. For STS/6MP/kinetin treated flowers DAH 1, DAH 2, DAH 3 corresponds to stage 2, 2 and 3 respectively. Significant differences of relative expression compared to control were indicated by asterisk (*P<0.05).

78

(c)

WLS73

(d)
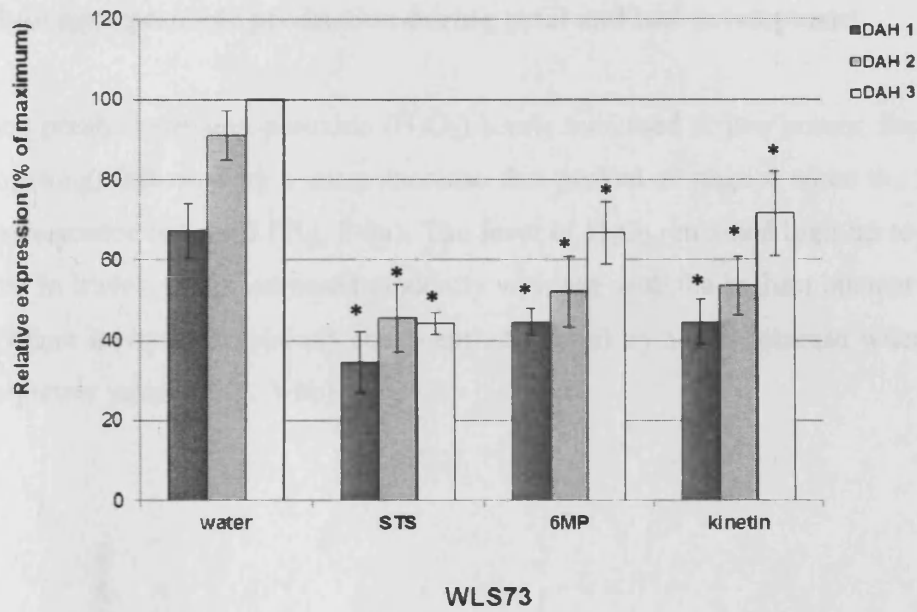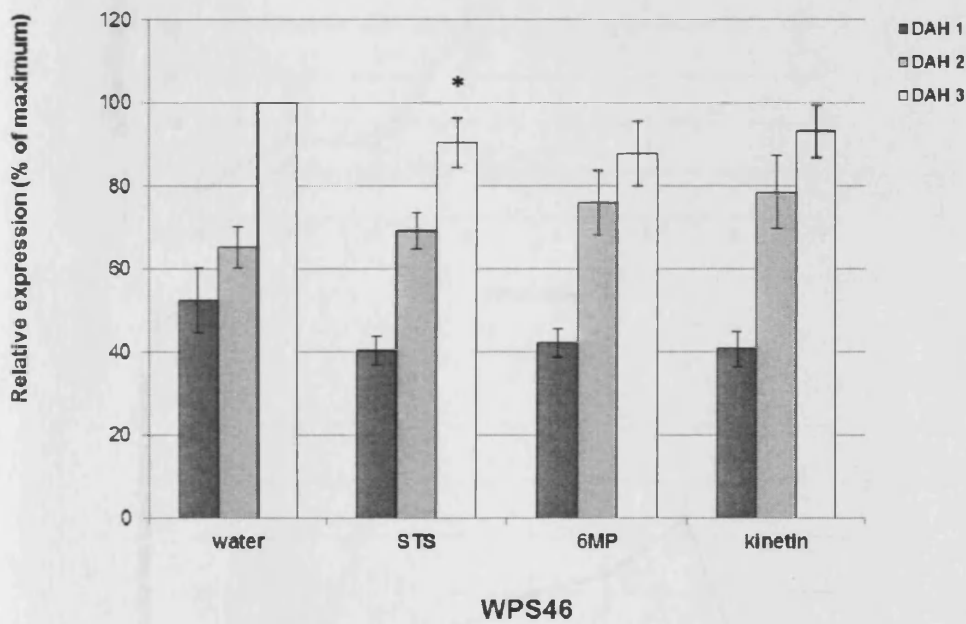
WPS46

Figure 3-7. Semi-quantitative RT-PCR analysis of (c) *WLS73* and (d) *WPS46* in detached flowers treated with water (control), STS, 6-MP and 1.0 M kinetin. For water-treated flowers DAH1, DAH2, DAH3 corresponds to stage 2, 3 and 4 respectively. For STS/6MP/kinetin treated flowers DAH1, DAH2, DAH3 corresponds to stage 2, 2 and 3 respectively. Significant differences of relative expression compared to control were indicated by asterisk (*P<0.05).

3.3.2 Redox regulation of wallflowers

3.3.2.1 Hydrogen peroxide production during petal and leaf development

In attached petals, hydrogen peroxide (H_2O_2) levels increased at two points; first at stage 1 (flower opening) followed by a sharp increase that peaked at stage 4 when the first visible signs of senescence occurred (Fig. 3-8a). The level of H_2O_2 remained high up to the time of abscission. In leaves, H_2O_2 increased gradually with age with the highest content recorded at stage 6 (where leaves were already senescent), followed by sharp decrease when the leaves were completely yellow (Fig. 3-8b).
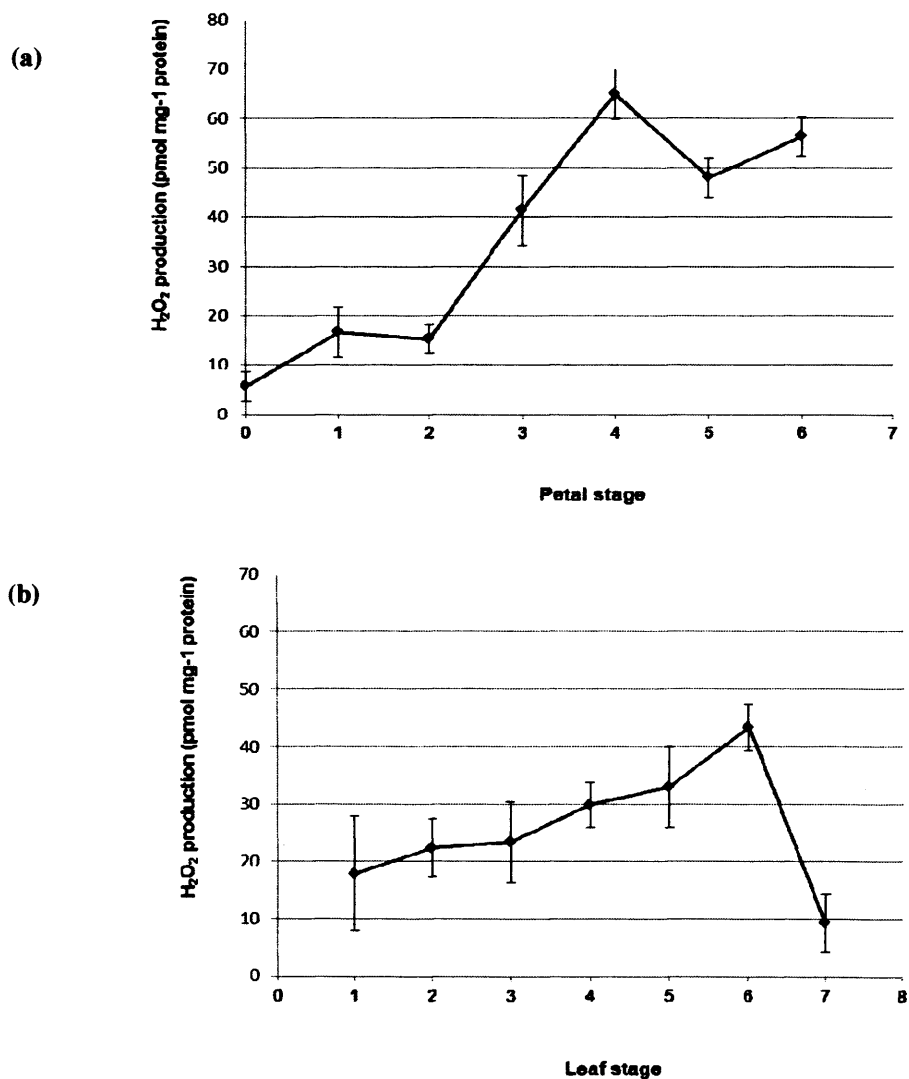
Figure 3-8. Quantification of relative H_2O_2 production in wallflower petals (a) and leaves (b). Mean (±SE, n=3).

The production of H_2O_2 in detached STS and 6-MP treated flowers was also quantified compared to controls held in water (Fig 3-9). In both treatments, the H_2O_2 production remained significantly lower than controls ($P<0.001$).
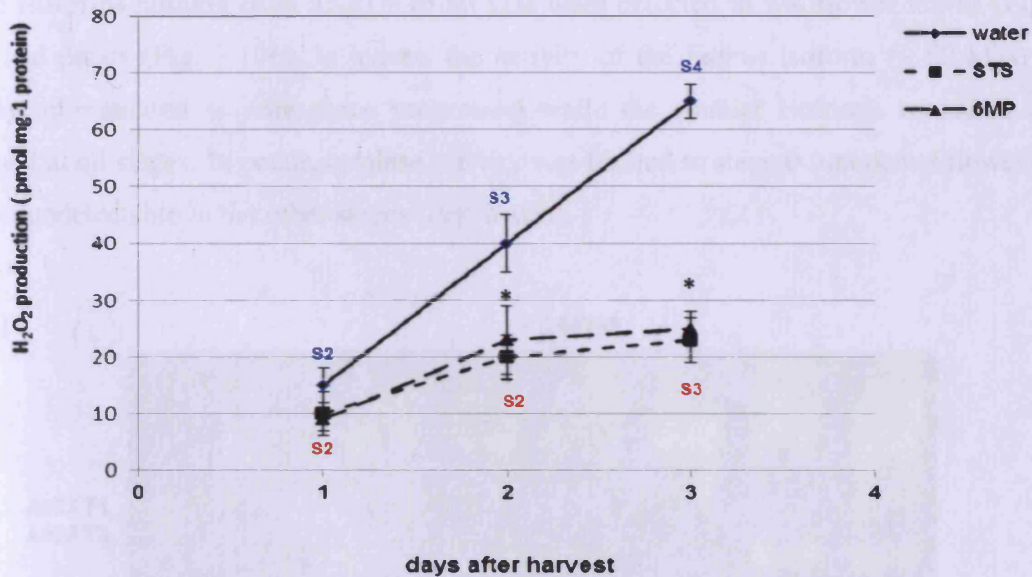
Figure 3-9. Quantification of relative H_2O_2 production in detached wallflower petals following STS/6-MP/water treatment. The blue text indicates the petal stage for water (control) while the red text indicates the petal stage for STS/6MP treated flowers. Mean ($\pm$SE, n=3). Significant differences of transcript level compared to control is indicated by asterisk (*$P<0.001$).

3.3.2.2 Antioxidant enzyme activities during petal and leaf development

Enzyme activities of three antioxidant enzymes, catalase (CAT), ascorbate peroxidase (APX) and superoxide dismutase (SOD) were determined by native PAGE. For catalase activity in leaves, protein extracted from senescing Arabidopsis leaves was used as a positive control. Three isoforms ranging from 45 kDa to 80 kDa were detected in wallflower leaves (Fig. 3-10a) and petals (Fig. 3-10b). In leaves, the activity of the largest isoform (~ 80 kDa) was clearly up-regulated as senescence progressed while the smaller isoforms remained quite constant at all stages. In petals, catalase activity was limited to stage 0 (unopened flower) and almost undetectable in the other stages (Fig. 3-10b).
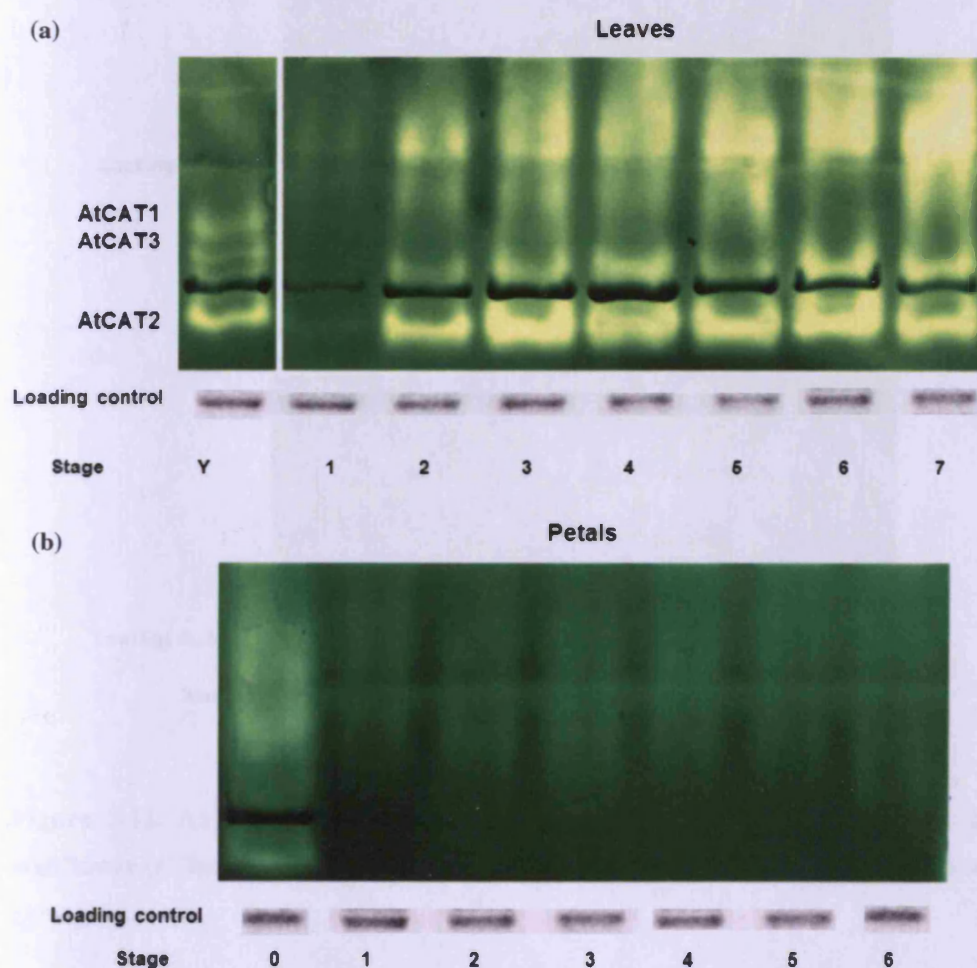
Figure 3-10. Catalase (CAT) zymograms during leaf and petal development: (a) CAT activities of leaves represented by three isoforms of Arabidopsis (control); AtCAT1, AtCAT2, AtCAT3 and wallflower (b) CAT activities of petals represented by three isoforms of wallflowers. Loading control gel images are shown beneath each zymogram

One isoform and two different isoforms of ascorbate peroxidase were detected in leaves and petals, respectively. The activity of APX increased in young leaves followed by a dramatic drop at stage 5 when the senescence symptoms became more pronounced (Fig. 3-11a). On the other hand, both isoforms activities were relatively low in younger flowers, but increased in late senescing petals (Fig. 3-11b).
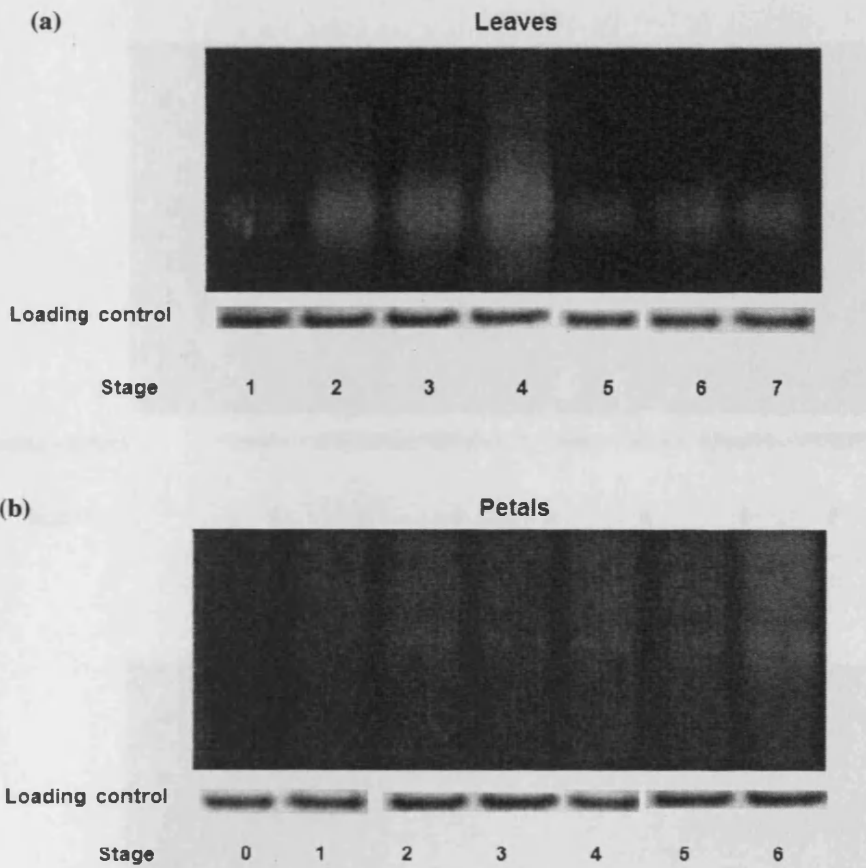
Figure 3-11. Ascorbate peroxidase (APX) zymograms of isoform activities present during wallflower (a) leaf and (b) petal development. Loading control gel images are shown beneath each zymogram.

Finally three isoforms with superoxide dismutase activity were detected in both leaves (~ 68 kDa, 60 kDa and 40 kDa) and petals (~ 72 kDa, 45 kDa and 38 kDa) (Fig. 3-12). All three SOD isoforms in leaves showed constant activities throughout leaf development (Fig. 3-12a). In petals, each isoform exhibited distinct expression pattern at different age. The two larger isoforms displayed reduced activities at the onset of senescence (stage 4) while the smallest isoform activity was unchanged (Fig. 3-12b).
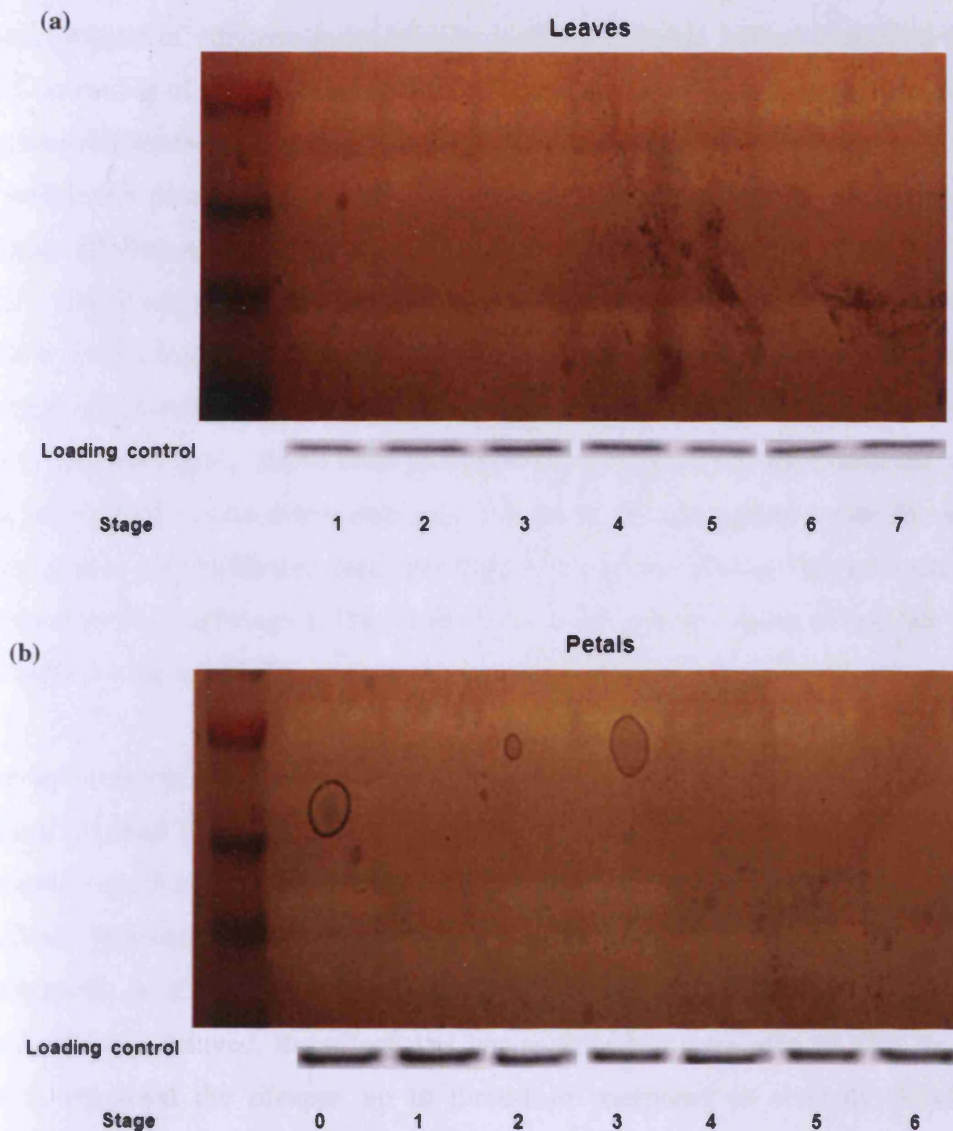
Figure 3-12. Superoxide dismutase (SOD) zymograms during wallflower (a) leaf and (b) petal development. Loading control gel images are shown beneath each zymogram

3.4 Discussion

Consistent with previous microarray transcript analysis of wallflowers, the results presented here clearly showed that the regulation of senescence in both petals and leaves is rather complex. The multifaceted network involves a tight control of hormonal balance, changes in ethylene and cytokinin regulated genes and also a role of ROS. Due to the close taxonomic relationship between wallflower and Arabidopsis, it seemed very likely that ethylene would be an important regulator of petal senescence in this species too (Price et al., 2008). Quantification of ethylene production in wallflower petals indeed supported this hypothesis. And the timing of the peak in endogenous ethylene production at stage 3, immediately before visible petal senescence suggests that ethylene has a regulatory function in initiating the onset of wallflower petal senescence. The maximum amount of ethylene production is comparable to other ethylene-sensitive flowers such as carnation (ten Have and Woltering, 1997; Shibuya et al., 2000) and is almost four fold higher than reported in *Alstroemeria* (Wagstaff et al., 2005). Interestingly, the ethylene production pattern exhibited by wallflower petals was slightly different compared to other ethylene sensitive flowers (ten Have and Woltering, 1997; Wagstaff et al., 2005) because ethylene production was also detected at earlier stages and not limited to late senescence and abscission. This suggests a role for ethylene also in early phases of wallflower petal development perhaps during flower opening that occurs between stage 0 and stage 1. Previously, ethylene has been shown to regulate flower opening in roses (Xue et al., 2008).

The involvement of ethylene in wallflower regulation was further confirmed when both timing of petal senescence and abscission was delayed up to two days compared to the control in cut flowers pulse-treated with ethylene receptor inhibitor; STS. This effect of STS on floral senescence in ethylene sensitive species is well-documented (Wagstaff et al., 2005; Hoeberichts et al., 2007b; van Doorn and Woltering, 2008). Although the timing of both processes was delayed, the effect was not as dramatic compared to STS-treated carnations which improved the lifespan up to three-fold compared to controls (Hoeberichts et al., 2007b). The large variation in the ethylene effect might be due to the difference in ethylene sensitivity or experimental setup between studied species.

In contrast to the STS-effect, continuous treatment with CEPA, an ethylene-producing compound hastened both petal senescence and abscission in cut wallflowers compared to controls. A dose-dependent treatment revealed that wallflower did not respond to a lower concentration of CEPA and only exhibited accelerated petal wilting and abscission at concentrations higher than 125 ppm. The CEPA concentration-response-range shown by wallflowers is very high compared to two *Alstroemeria* varieties which showed accelerated abscission even with 5 ppm CEPA (Wagstaff et al., 2005). This suggests that although wallflower senescence is regulated by ethylene it is less sensitive to ethylene than *Alstroemeria*. The ethylene sensitivity could also relate to the timing of CEPA treatment, where in wallflowers CEPA was applied at stage 1 (first opened flower), while in *Altsroemeria*, CEPA was applied a day prior to flower opening (Wagstaff et al., 2005).

Semi-quantitative RT-PCR showed that the rise in ethylene production during petal development was accompanied by the up-regulation of a putative ACC oxidase (*ACO*) wallflower homologue (*WLS73*) transcript in senescing petals, with the highest expression at stage 4 followed by a down-regulation coinciding with decrease in ethylene production. This gene was also slightly up-regulated in senescing leaves. This result is in agreement with the previous microarray data (Price et al., 2008) and further support the role of ethylene in both petal and leaf senescence in wallflower. Similar increase of *ACO* transcript was also reported in senescing petals of Arabidopsis (Wagstaff et al., 2009) and carnation (ten Have and Woltering, 1997). In some flowers ethylene biosynthetic genes are autocatalytically regulated (ten Have and Woltering, 1997). The reduction of *WLS73* expression in response to STS could indicate an autocatalytic response, however further experiments analysing the expression of *WLS73* in response to exogenous ethylene would be required to resolve this.

In addition to ethylene, cytokinins might also play a crucial role in wallflower petal senescence, either in an ethylene-dependent or ethylene-independent manner as established in other ethylene-sensitive species (Eisinger, 1977; Mor et al., 1983; ten Have and Woltering, 1997; Chang et al., 2003; Hoeberichts et al., 2007a). In Hharvested stage 1 flowers subjected to the cytokinin oxidase inhibitor, 6MP delayed senescence and abscission by 2 days. Similarly, continuous kinetin supply also resulted in improved lifespan and a delay in visible senescence, thus delaying both processes. Both treatments are presumed to result in increased endogenous cytokinin levels and have been previously been demonstrated to have a similar

effect in un-pollinated carnations (Eisinger, 1977; Mor et al., 1983). Despite the positive effect demonstrated by this hormone in wallflower regulation, no cytokinin oxidase transcripts could be detected by semi-quantitative RT-PCR in wallflower petals although a cytokinin oxidase homologue was previously identified by microarray analysis in wallflower petals (Price et al., 2008; Wagstaff et al., 2009). This could be due to low levels of expression of this gene. This may also suggest that cytokinin levels in wallflowers could possibly be regulated by other pathways such as O-glucosylation inactivation as previously reported in carnation (Taverner et al., 2000).

Both treatments that are likely to increase cytokinin levels (6MP and kinetin) prevented up-regulation of the senescence marker, *SAG12* in wallflower petals. *SAG12* repression and reduced ethylene sensitivity indicating delayed senescence-associated activities have also been reported in transgenic petunia overexpressing cytokinin confirming the role of this hormone in flower senescence (Chang et al., 2003). Moreover, cytokinin-ethylene interaction could also be demonstrated in wallflowers since exogenous treatment with kinetin/6MP exhibited lower expression of *ACO* thus preventing up-regulation of ethylene synthesis. This suggests that cytokinin might possibly mediate ethylene-regulated genes such as *SAG12* and *ACO*, thus affecting the time to senescence in wallflowers. The quantification of endogenous amount of cytokinin might lead to a clearer understanding of the contribution of cytokinins to the regulation of wallflower development and senescence.

Unlike ethylene and cytokinin, the role of auxin in wallflower senescence is less clear cut. Expression of an auxin-induced gene *DFL-1* wallflower homologue (*WPS46*) was up-regulated in both senescing petals and leaves, which is in agreement with the previous microarray data (Price et al., 2008). This gene encodes IAA amido synthetase that in Arabidopsis functions in auxin signal transduction (Nakazawa et al., 2001), preventing the accumulation of free IAA. A homologous gene was shown to be up-regulated in pollination-induced petunia corolla senescence (Bai et al., 2010) and Arabidopsis leaf senescence (Buchanan-Wollaston et al., 2005). Moreover, a transient increase in the expression of an *Aux/IAA* gene was also observed in carnation petals (Hoeberichts et al., 2007b) but down-regulated in Arabidopsis senescing petals (Wagstaff et al., 2009).

In addition to the IAA-regulated *WPS46* gene expression, the quantification of two endogenous IAA isoforms displayed an interesting pattern during wallflower petal development. Free active IAA increased significantly from stage 3 to stage 5 which coincides with the beginning of visible senescence and the ethylene rise. Conversely, inactive conjugated IAA exhibited almost the opposite production pattern displaying a sharp decrease with age. Information on endogenous level of IAA in petals is scarce making interpretation a difficult task. Nevertheless, IAA is a central regulator of auxin responses and could also act as a transcriptional repressor (Ellis et al., 2005; van Doorn and Woltering, 2008). The auxin effect also appears to be dose-dependent and can induce ethylene biosynthesis at higher concentrations in some ethylene-sensitive species (Rogers, 2006; Tripathi and Tuteja, 2007). Further studies with auxin inhibitors will help to expand our understanding on how auxin could regulate wallflower petal development and whether it is related to ethylene biosynthesis.

Besides phytohormones, hydrogen peroxide (H_2O_2) is regarded as a signalling molecule regulating various developmental processes including gene expression during senescence (Apel and Hirt, 2004; Rogers, 2006). Quantitative analysis of H_2O_2 production sampled at different stages revealed a distinct pattern in petals and leaves of wallflowers. In petals, the H_2O_2 level peaked twice: at stage 1 when the flower opened and stage 4 coinciding with the first stage where visible senescence was observed, followed by a gradual decrease. An increase in H_2O_2 level during flower opening was also previously reported in the following ethylene-insensitive species: daylily (Panavas et al., 1999), chrysanthemum (Chakrabarty et al., 2007) and tulip (Azad et al., 2008), implying that the rise in H_2O_2 at this stage might act as a common signal for triggering flower opening independently of ethylene. The second H_2O_2 peak in wallflowers appeared upon visible senescence (stage 4) one stage later compared to when the highest ethylene production was recorded (stage 3). This might suggest that ROS accumulation is merely a consequence of senescence (resulting from ethylene accumulation) rather than acting as a signal precursor. This result is in agreement with the second peak observed quite late in tulip petal senescence (Azad et al., 2008).

Wallflower leaves exhibited a slightly different pattern of endogenous H_2O_2 with a high level at earlier stages and peaking at stage 6 (56% chlorophyll loss) before it declined, indicating that the high production of ROS might be related to chloroplast degradation. Interestingly, a similar pattern was reported in the progression of senescing Arabidopsis leaves (Zimmermann et al., 2006) suggesting an increase in ROS level coupled with a decrease in antioxidant properties might trigger leaf senescence in these two species. In parallel with the general H_2O_2 profile, the H_2O_2 level in 6MP/STS-treated cut wallflowers was also quantified. In contrast to the increase of H_2O_2 level with age observed in controls, both treatments prevented H_2O_2 accumulation in agreement with the delay in morphological markers of flower senescence. Although a more detailed analysis is crucial to conclude the exact ROS role in wallflower petal senescence, these findings may suggest interactions between ROS, ethylene and cytokinin.

SAG21 was selected for analysis as it was one of the few genes identified from the microarray experiments whose expression was up-regulated in petals but not leaves (Price et al., 2008). In petals, *SAG21* peaked rather early with the highest expression at stage 1 when the flowers just opened followed by a gradual decrease with age which only partly agrees with the microarray data. The difference in the expression pattern between the RT-PCR and the array data is most likely due to the more specific stages being analysed in the RT-PCR analysis, as in the array experiments younger and older petal and leaf stages were pooled.. The senescence marker, *SAG12* which was previously quantified using a similar technique (Price et al., 2008), reached its highest expression two stages later (at stage 3) compared to *SAG21*. Conversely, in leaves, *SAG21* remained constant at all stages. This may suggest that *SAG21* plays a role in the early stages of petal senescence before visible senescence markers are evident, but might not play a significant role in leaf senescence development of wallflowers. In STS-treated flowers, *SAG21* expression was down-regulated while treatment with kinetin/6-MP did not significantly affect its expression. These results suggest that *SAG21* might probably be transcriptionally regulated by ethylene but not by cytokinin in wallflower petal senescence, although further experimental evidence is needed. *SAG21/LEA5* in Arabidopsis responds to ROS signals (Mowla et al, 2006). However H_2O_2 levels in petals at stage 1 were relatively low (although significantly higher than in closed buds) calling into question whether expression of this gene is ROS regulated in wallflower petals.

Since a higher concentration of H_2O_2 may stimulate senescence, it is important to determine the activity of enzymes that serve to regulate the overall H_2O_2 concentration. Non-denaturing PAGE coupled with activity localization revealed three catalase (CAT) isoforms in wallflower leaves. Catalases are mainly localized in the peroxisomes (Petrova et al., 2004; Mhamdi et al., 2010). All isoform activities remained high and unchanged in all stages of leaf development and senescence which is in agreement with the microarray data (Price et al., 2008). Conversely, CAT activity was detected at very low levels in petals, with the exception of the stage 0 (unopened buds) in contrast with the microarray transcript analysis which showed up-regulation in senescent petals (Price et al., 2008). Clearly the microarray data would require further verification through RT-PCR to establish whether there is regulation at the post-transcriptional or post-translational levels that result in the low catalase activity detected. This enzyme activity profile differs greatly compared to catalase isoforms in Arabidopsis leaves (Zimmermann et al., 2006) and other flowers such as daylily, carnation and chrysanthemum petals (Bartoli et al, 1995; Chakrabarty et al, 2007; Panavas and Rubinstein, 1998),which are differentially regulated at different ages of petals.

APX in-gel assays showed one and two isoforms in leaves and petals, respectively. In leaves, the APX activity peaked at stage 4, just before visible senescence (stage 5, 20% chlorophyll loss) and then declined in later stages. The down-regulation of APX activity in senescing leaves coincided with the higher concentration of H_2O_2 reported above. Interestingly, similar results were reported in senescing Arabidopsis leaves (Panchuk, Zentgraf and Volkov, 2005) and *Gladiolus* tepal senescence (Hossain et al, 2006) suggesting that the down-regulation of APX activity, which may enhance the concentration of endogenous H_2O_2 could be a prerequisite for inducing senescence and cell death. In contrast, the APX activity in wallflower petals seemed to increase progressively with senescence suggesting that APX might play a crucial role in scavenging H_2O_2 during petal senescence. Similar expression was also previously reported in senescing chrysanthemum florets (Chakrabarty et al, 2007).

Three SOD isoforms were detected in wallflower leaves, while in petals, four isoforms were observed. According to size comparison to other SOD isoforms previously detected in carnation petals (Droillard and Paulin, 1990; del Río et al., 2003) and pea leaves (del Río et al., 2003), different classes of SOD according to their metal cofactor were predicted for wallflowers with the smaller isoforms most probably representing Mn-SODs (mitochondrial

or peroxisomal) and the other two larger isoforms most likely Cu/Zn-SODs (located in plastids, cytosol, apoplast and peroxisomes) (Zelko, Mariani and Folz, 2002). Further microsomal fractionation analysis would be required in order to confirm the compartment-specific activities of the wallflower isoforms. In wallflower leaves, all isoform activities were constant at all stages. Conversely, each SOD petal isoform exhibited a distinct expression pattern with a representative from each group being down-regulated upon senescence. Similar increases in specific SOD isoform activities were previously reported in petunia (Bai et al., 2010), daylily and carnation flower senescence (Bartoli et al, 1995; Chakrabarty et al, 2007; Panavas and Rubinstein, 1998). Despite the presence of APX and SOD enzyme activities in both tissues, surprisingly no wallflower homologs were identified in the wallflower microarray transcript analysis studied previously. Besides the three antioxidative enzymes studied in this work, GSTs might also be contribute to wallflower redox regulation since GSTs represented a high proportion of up-regulated genes in senescing petals (Price et al., 2008).

The antioxidative signalling mechanism in wallflower petals and leaves is indeed complex. In leaves of other studied species, the activity of the main free-radical scavenging enzymes; CAT, APX and SOD tend to increase with age (Buchanan-Wollaston, 1997; Orendi et al., 2001; Buchanan-Wollaston et al., 2003; Panchuk et al., 2005; Zimmermann et al., 2006). However in petals, these anti-oxidative properties in many species have been assessed only crudely *in vitro*, hence might not represent the activity of individual isozymes, limiting their actual value (van Doorn and Woltering, 2008). Therefore, a quantitative measurement of different CAT, APX and SOD isoforms following compartment isolation would need to be done separately before the role of anti-oxidative enzymes in parallel with ROS production can be properly evaluated. However, clearly the role of APX and SOD in wallflower petal senescence is worthy of further investigation. Furthermore, fluorometric detection of different ROS in different cell compartments might give a clearer view on how the redox regulation coupled with other phytohormones regulates senescence in wallflower.

3.5 Summary

To gain a better insight into senescence regulation in wallflower, the characteristics of several phytohormones, senescence-associated genes, ROS and antioxidative enzymes were analysed in different stages of petals and leaves. The onset of petal senescence was accompanied by an increase in ethylene and auxin production, followed by ROS accumulation. Exogenous treatment with the ethylene receptor blocker, STS, the cytokinin oxidase inhibitor, 6MP, or cytokinin (kinetin) delayed petal senescence and time to abscission. In contrast, ethylene (produced by CEPA) hastened both processes. Several genes including *SAG12* (senescence marker), *WLS73* (ethylene synthesis) and *WPS46* (IAA-induced) were up-regulated in senescing petals and leaves. On the other hand, other genes such as *SAG21* might play a protective role in earlier stages. In treated flowers, *SAG12*, *WLS73* and *SAG21* displayed differential expression patterns, while *WPS46* transcript levels remained unaffected. The redox regulation in wallflower leaves might involve a balance of antioxidative enzyme activities contributed by catalase, ascorbate peroxidase and superoxide dismutase. In petals, the two latter enzymes might play a more significant role although further experimental evidence is crucial to support this proposed role. Clearly, a more detailed analysis is required in order to clarify the interaction between phytohormones and ROS in wallflower senescence regulation.

Chapter 4: *In silico* analysis and subcellular localization of the ROS-induced gene: *SAG21*

4.1 Introduction

Late embryogenesis abundant (LEA) proteins are extremely hydrophilic proteins and were first identified in plants (Tunnacliffe and Wise 2007). To date, multiple forms of LEA have also been identified in desiccation-tolerant animals from at least four phyla (Hand et al. 2010). LEA expression has been associated with water-stress caused by desiccation, salt or low temperatures in many studies (Wise 2003). Recent findings suggest that LEA proteins play various, possibly multiple roles in drying cells (Tunnacliffe et al. 2010). These include a protective role via protein-protein interactions, and membrane stabilization together with sugars like trehalose (Kovacs et al. 2008). Antioxidant and ion-binding properties have also been established in specific LEA groups such as dehydrins (Tunnacliffe and Wise 2007).

Due to their high hydrophilicity, most LEA proteins are predicted to be in the form of intrinsically disordered proteins (IDP) in aqueous solution (Kovacs et al. 2008). However, surprisingly, several LEA proteins adopt a defined α-helical structure during dehydration either by drying or freezing (Tompa and Kovacs 2010). In contrast, atypical LEAs with higher hydrophobicity such as the Lea5 Group to which SAG21/AtLEA5 (At4g02380; hereafter referred to as SAG21) are mostly not predicted to be IDPs (Tunnacliffe et al. 2010). However, the first structural characterization of this group member from *Lotus japonicus*; LjIDP1, which plays a role in nodule senescence and symbiotic interactions, indicated otherwise (Haaning et al. 2008). In contrast to *in silico* predictions, LjIDP1 was shown to be intrinsically disordered adopting a largely α-helical structure upon dehydration and in the presence of detergents, making it a suitable candidate for transient interactions. Moreover, recombinant LjIDP1 exhibits chaperone activity by effectively preventing inactivation of two model enzymes, citrate synthase and alcohol dehydrogenase upon freezing (Haaning et al. 2008). In addition, the atypical LEA protein, *Medicago truncatula* MtPM25, which is highly hydrophobic and belongs to the seed maturation protein group, is also largely disordered in the hydrated state and has an anti-aggregation property (Boucher et al. 2010). Hence it would seem that at least some of the atypical LEAs may be IDPs.

Typical plant LEAs such as Group 3 LEAs have an average hydrophathy score of -0.97 (Wise 2003) and most LEA proteins from animals score less than -1 (Hand et al. 2010), which is highly hydrophylic. Interestingly, a Group 3 LEA from the bdelloid rotifer *Adineta ricciae*, *Arlea1B*, displayed a slightly hydrophobic property compared to the other members (the Grand Average Hydrophathy Value or GRAVY = -0.46) and showed a strong propensity to interact with dry phospholipid membranes (Pouchkina-Stantcheva et al. 2007). Likewise, a similar membrane binding property to phospholipid liposomes was observed in Group 3 LEA *Pisum sativum* PsLEAm through its amphiphatic α-helices that formed upon dehydration (Grelet et al. 2005). A chloroplastic Arabidopsis LEA located in the stroma, COR15a (GRAVY: -0.554) coming from the same group also played a crucial role in altering the intrinsic curvature of the inner hydrophobic membrane of the chloroplast envelope upon freezing (Steponkus et al. 1998). These findings suggest that a hydrophobic region in LEA proteins promotes membrane-binding thus contributing an important role in membrane stabilization (Hand et al. 2010).

Multiple LEA proteins are frequently found within a single organism (Pouchkina-Stantcheva et al. 2007). In Arabidopsis, 51 LEA proteins have been identified and classified into nine different groups according to their conserved Pfam domains (Hundertmark and Hincha 2008). This pattern reflects subcellular targeting of LEA proteins to protect critical components from damage caused by various stresses. Experimental evidence demonstrated that LEA proteins are expressed in the cytoplasm, nucleus, chloroplast and mitochondria (Tunnacliffe and Wise 2007). SAG21 and three other Arabidopsis members of the same group are exclusively targeted to either plastids or mitochondria (Hundertmark & Hincha, 2008).

Mitochondria frozen with trehalose may preserve their outer membrane integrity thus retaining a number of biological functions (Yamaguchi et al. 2007). Mitochondria isolated from *Artemia franciscana* (brine shrimp) which contained the LEA protein, Afrlea3m exhibited resistance to freezing when frozen together with trehalose, proposing a role for LEA proteins in inner mitochondrial membrane protection (Menze et al. 2009). Furthermore, *in vitro* analysis showed that recombinant *PsLEAm* found in the pea seed mitochondrial matrix could prevent fumarase inactivation upon drying indicating an anti-aggregation property (Grelet et al. 2005).

Under stress conditions, mitochondria and chloroplasts accumulate ROS and can cause critical shifts in cell redox status because antioxidant systems ultimately require electrons from redox pairs such as NADP/NADPH, which connect many aspects of metabolism (Foyer et al. 2009; Rhoads et al. 2006). The citrus dehydrin, CuCOR19, a member of Group 2 LEAs (dehydrins) was shown to have potent antioxidative properties, which are important components of ROS modulation (Tunnacliffe and Wise 2007). CuCOR19, which is predominantly expressed in mitochondria could scavenge hydroxyl radicals and peroxyl radicals in soybean liposomes through the modifications of its amino acid residues, Gly, His and Lys, thus inhibiting lipid peroxidation (Hara et al. 2004).

Bioinformatics serves as a powerful tool to investigate structure-function relationships and gather all the useful information available on the databases before deciding on the best experimental approach. *In silico* analysis allows the identification of LEA protein characteristic profiles such as amino acid abundance composition, hydrophathy profile analysis, and secondary structure prediction. Another useful tool that is available online is the sub-cellular prediction software. Most LEA proteins are cytosolic and thus lack a peptide signal sequence (Tunnacliffe and Wise 2007). The peptide signal sequence located at the N-terminus of the protein usually consists of a majority of hydrophobic amino acids. The actual localization can then be further analysed either transiently, in transfected protoplasts, or in transgenic plants transformed with constructs expressing the signal peptide fused to a fluorescent reporter gene.

The aim of the work reported in this chapter, was the identification of SAG21 protein characteristics and subcellular localization. SAG21 primary amino acid sequence was subjected to several prediction programmes *in silico*. Further confirmation of its compartment-specific expression was obtained from Arabidopsis protoplasts and stable transgenic lines transformed with *SAG21*-YFP fusions driven by the 35S constitutive promoter.

4.2 Materials and methods

4.2.1 *In silico* analysis

A hydropathy plot was constructed using the Kyte and Doolittle algorithm (Kyte and Doolittle, 1982) (ProtScale program, http://au.expasy.org/tools/protscale.html). The Biology Workbench 3.2 site (http://workbench.sdsc.edu/) was used for multiple sequence alignments (CLUSTALW) and evaluation of amino acid abundance (AASTATS). Secondary structure analysis was performed with the SOPMA, GOR IV, and Porter programmes (http://au.expasy.org/tools/). Sub-cellular localization was predicted using: Mito Prot II (version 1.101) (http://ihg.gsf.de/ihg/mitoprot.html), TargetP (www.cbs.dtu.dk/services/TargetP), and iPSORT (http://www.psort.org/psortb/index.html).

4.2.2 Subcellular localization of SAG21

4.2.2.1 cDNA cloning of expression construct 35S::*SAG21*::YFP

Full-length *SAG21* cDNA was amplified from a pGEM-T Easy::*SAG21* ORF cloning template (section 2.3) using the *SAG21* YFP primer set containing the *Bam*H1 and *Not*1 restriction sites (section 2.5.2) and commercial GoTaq® DNA polymerase (Promega). The sequenced clone was inserted in the pGreen based vector 35S-YFP-nosT in frame with ATG-less YFP. PCR, digestion, ligation and phosphatase steps required for the directional cloning were carried out as described in section 2.12. The expression construct was either stably transformed into Arabidopsis as described in section 2.15 or transiently expressed in Arabidopsis protoplasts (see below). Two homozygous lines of the stable transformants were selected for further expression analysis.

4.2.2.2. Protoplast preparation and transient transfection

Three-week-old *in vitro* grown WT Arabidopsis seedlings were transferred to Petri dishes with approximately 20 mL of filter-sterilized enzyme solution mix (Yacult; 0.5% cellulase, 0.2% macerozyme in K3 medium). K3 medium composition is as follows: 10x B5 medium including vitamins (Melford, UK), 200x MES (0.1g/ml), 500x myo-inositol (0.05g/ml), 100x NH_4NO_3 (25 mg/ml), 100x $CaCl_2$ (75 mg/ml), 100x D-xylose (25mg/ml). Leaves were cut with a sterile scalpel, placed in the enzyme solution and incubated overnight in the dark at RT. The following day, the enzyme solution was removed carefully with a sterile Pasteur pipette without disturbing the cut leaves. K3 medium (10 mL) was added and the plates were gently swirled to release the protoplasts. The fresh medium containing the protoplasts was filtered through a 30 μM nylon filter and transferred into sterile round bottom tubes. After 1 hour incubation at RT, intact protoplasts floated to the top of the solution and were seen as a thin green layer. Protoplasts were transferred with a sterile Pasteur pipette into new tubes and another 5 mL of K3 medium were added. Protoplasts were allowed to float again and another wash with K3 medium was made to recover as many protoplasts as possible. The bottom layer was removed and 2 mL of protoplast suspension medium (0.4 M mannitol, 20 mM $CaCl_2*2H_2O$, 5 mM MES, pH 5.7) were added. Suspended protoplasts (250 μL) were mixed with 10-20 μg of plasmid DNA, and an equal volume of PEG solution (40 % (w/v) PEG 4000, 0.4 M Mannitol, 100 mM $Ca(NO_3)_2$, pH 7) was added. After 30 min incubation at RT, 2 mL of K3 medium were used to dilute the PEG solution and the tubes were allowed to stand for another 1-2 hours. Then, the solution beneath the protoplast layer was removed, followed by the final addition of 2 mL of K3 medium. The protoplasts were incubated overnight at RT in the dark. The next day, transient expression was studied under the confocal microscope.

4.2.2.3 Confocal analysis

YFP expression was recorded in 5d old seedlings or transiently transfected protoplasts by confocal laser scanning microscopy using either a Leica TCS SP2 AOBS spectral confocal microscope system (Leica Microsystems) or a Zeiss LSM 510 META confocal microscope system (Carl Zeiss Ltd.). YFP was excited at 514 nm and detected in the 525- to 583-nm range. Chlorophyll autofluorescence was excited simultaneously with the 514 nm laser and emission was detected at wavelengths longer than 650 nm. A plastidial marker containing a presequence transit peptide (TP) targeted to the plastids; TP-23K::GFP (Di Cola and Robinson 2005) was used as a control.

4.3 Results

4.3.1 SAG21 *in silico* analysis

To analyse the amino acid composition and hydrophathy profile of SAG21 protein, the primary sequence was subjected to *in silico* analysis using the ExPasy Proteomics Protscale tool, and the overall amino acid distribution in SAG21 protein was determined (Fig. 4-1). The primary sequence was found to be very rich in hydrophilic (59.8% of D, E, G, K, N, P, Q, R, S, T) and charged (22.7% of K, R, D, E) residues. Alanine (A) showed the highest proportion (14.4%) followed by serine (S) (13.4%). The primary sequence was devoid of cysteine (C) and histidine (H).

The Kyte and Doolittle hydropathy plot indicated a GRAVY score of -0.36, with the N-terminal being more hydrophobic than the C-terminal (Fig. 4-2). The more hydrophobic N-terminal could represent a signaling transit peptide.
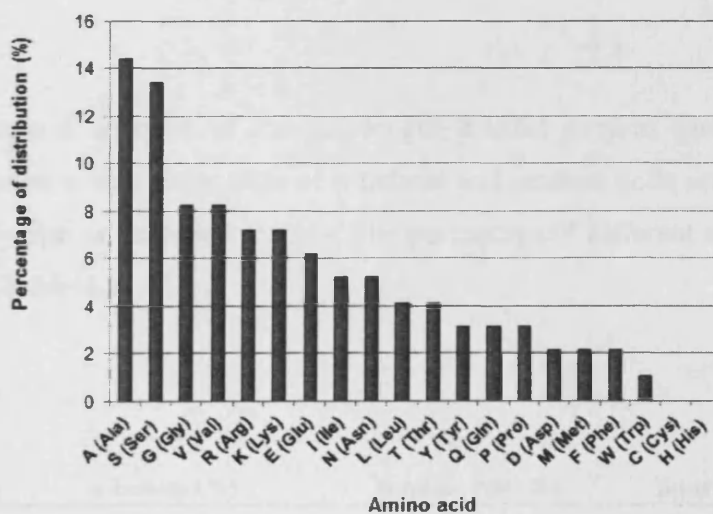
Figure 4-1: Amino acid abundance in *SAG21* protein.
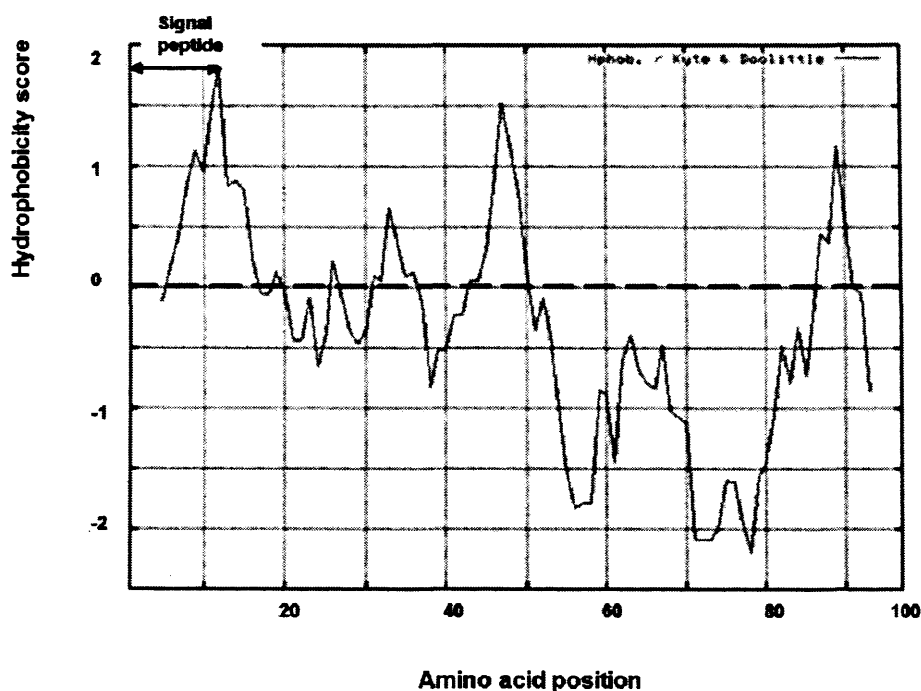
the zero line

ndow of nine

)w signals the

Secondary structural analysis of the full-length SAG21 protein carried out with several programs predicted a high proportion of α-helices and random coils accompanied by a small proportion of β-turns or extended strands. The percentage of different secondary structures is summarized in Table 4-1.

Program	α-helices (%)	random coil (%)	β-turns/Extended strands (%)
SOPMA	59.79	29.90	7.22
GOR IV	40.21	42.27	17.53
PROF	53.00	38.00	6.00

Two programmes (MitoProt, TargetP) predicted a high probability of mitochondrial localization for SAG21 with a further sub-mitochondrial localization to the mitochondrial matrix space. In contrast, another programme (iPSORT) ranked first a plastidial followed by a mitochondrial targeting probability. The prediction probability test is summarized in Table 4-2.

Table 4-2: Subcellular localization prediction of *SAG21*. Values indicate the probability of mitochondrial/plastid localization using different programmes.

Program	Mitochondrial	Plastid
MitoProt	0.9856 (0.819)[a]	-
TargetP	0.555	0.397
iPSORT	8.0	5.0

(a: submitochondrial localization probability to matrix space)

4.3.2 SAG21 subcellular localization

To clarify the subcellular localization of SAG21, Arabidopsis protoplasts transfected with the expression construct 35S::*SAG21*::YFP were analysed alongside a plastidial marker, TP-23K::GFP. Confocal microscopy revealed the GFP signal showed a clear targeting of the plastidial marker to the membrane, stroma and lumen of chloroplast, coinciding with the chloroplast autofluorescence (overlay picture in Fig. 4-3a). In contrast, the *SAG21* YFP localization was quite different, with the most prominent expression localized between the chloroplasts (white arrow in Fig. 4-3b), suggesting a possible mitochondrial localization.
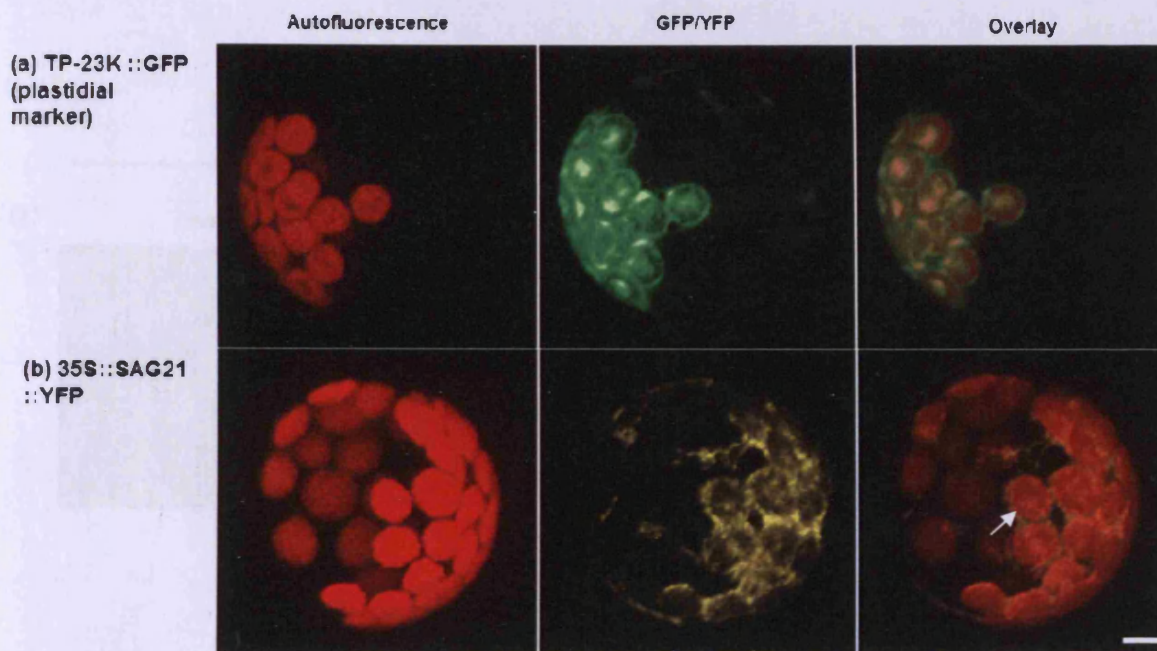
Figure 4-3: Confocal Analysis: Arabidopsis protoplasts transfected either with a plastid marker; TP-23K::GFP or with an expression construct; 35S::*SAG21*::YFP. Red, green and yellow indicate chloroplast autofluorescence, GFP signal and YFP signal respectively. (a) Green and red fluorescence co-localized in the overlay picture indicating a positive platidial expression for TP-23K::GFP. (b) Yellow fluorescence localized to the empty spaces between red fluorescence (white arrows) suggesting a mitochondrial localization. Scale bar = 5 μm.

Due to the ambiguity of the result from transient transfection, stable transformants were generated. In root tissues, SAG21 localized between the cell walls and the vacuoles (Fig. 4-4a) appearing as small subcellular compartments forming a punctate pattern. A similar localisation was detected in cotyledons (Fig 4-4b). Furthermore, the YFP signal clearly did not coincide with chloroplast autofluorescence, therefore a plastid localisation for SAG21 can be excluded.
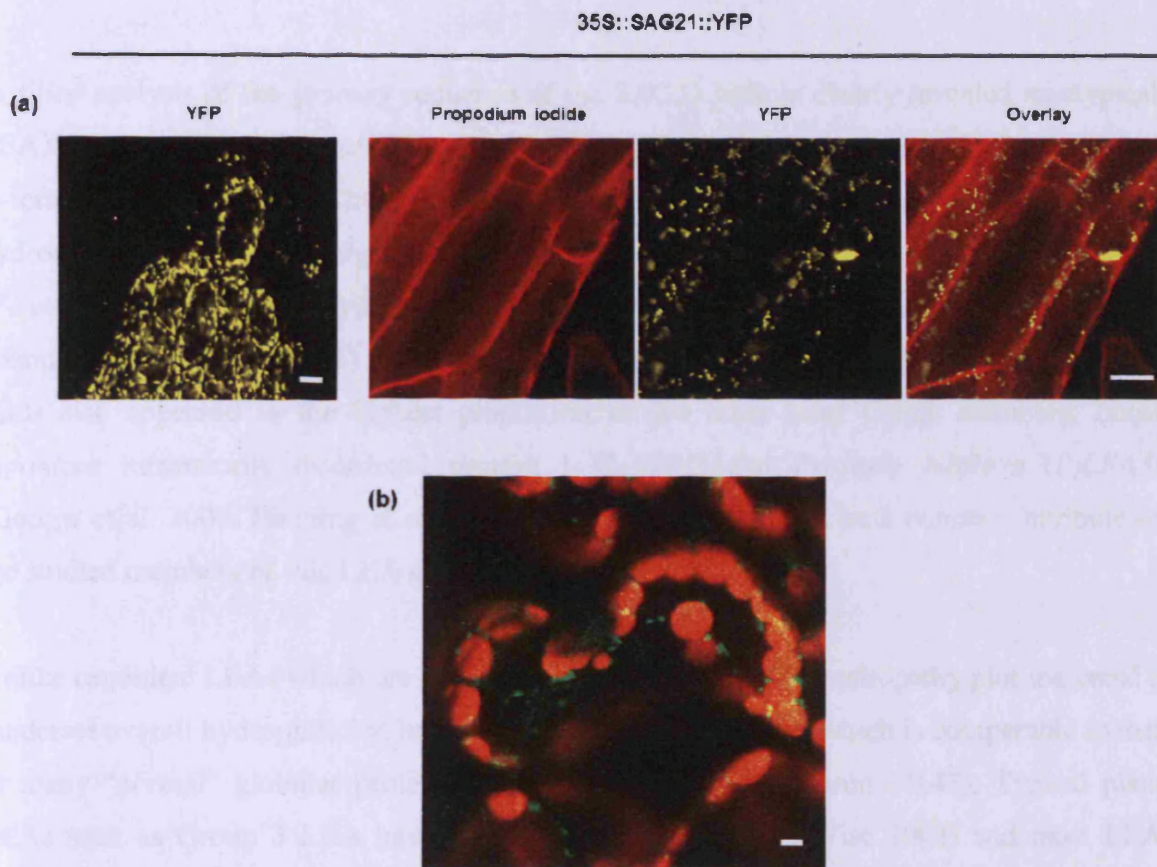
35S::SAG21::YFP

Figure 4-4: Confocal analysis: Stable Arabidopsis transgenic lines expressing 35S::*SAG21*::YFP. Red indicates propodium iodide cell wall staining (a) or chloroplast autofluorescence (b) and yellow/green fluorescence indicates *SAG21* YFP signal. (a) In root tissues, yellow fluorescence appears as small dots and did not co-localize with the cell wall. Scale bars = 20 μm. (b) In cotyledons, green fluorescence did not co-localize with the red chloroplast auto-fluorescence indicating a non-plastid localization. Scale bars = 5 μm.

4.4 Discussion

In silico analysis of the primary sequence of the SAG21 protein clearly revealed its atypical LEA features characteristic of Group Lea5 (Pfam 03242) and the presence of a hydrophobic N-terminal pre-sequence. The primary structure is highly enriched in amino acids with hydrophilic (59.8%) and charged (22.7%) residues. Cysteine is not found in the protein which is a common feature of many LEA proteins (Wise and Tunnacliffe 2004). Alanine is the most abundant amino acid (14.4%) in the SAG21 protein followed by serine (13.4%). Both amino acids also appeared as the highest proportion in two other Lea5 Group members; *Lotus japonicus* intrinsically disordered protein 1 (*LjIDP1*) and *Prosopis juliflora* (*PjLEA3*) (George et al. 2009; Haaning et al. 2008) suggesting that it might be a common attribute of the studied members of this LEA group.

Unlike canonical LEAs which are highly hydrophilic, the SAG21 hydropathy plot indicated a moderate overall hydrophilicity, having a GRAVY score of -0.36 which is comparable to that of many "normal" globular proteins such as bovine serum albumin (-0.43). Typical plant LEAs such as Group 3 LEA have an average score of -0.97 (Wise 2003) and most LEA proteins from animals score less than -1 (Hand et al. 2010) indicating that SAG21 is indeed a more hydrophobic LEA protein. Other members of Group Lea5 mentioned previously; *LjIDP1* and *PjLEA3* also exhibit an average negative hydropathy with GRAVY scores of -0.36 and -0.24, respectively (George et al. 2009; Haaning et al. 2008). Interestingly, several members from Group 3 LEAs also were slightly more hydrophobic compared to the other members of the group. These include bdelloid rotifer *Adineta ricciae*; Arlea1B, *Pisum sativum* PsLEAm and chloroplastic Arabidopsis COR15a with GRAVY values of -0.46, -0.571 and -0.554 respectively (Grelet et al. 2005; Pouchkina-Stantcheva et al. 2007; Steponkus et al. 1998). Notably, this slightly hydrophobic feature is not common in Group 3 LEA proteins. These more hydrophobic Group 3 LEA proteins showed a strong propensity to interact with phospholipid liposomes and inner membranes upon dehydration suggesting that a more hydrophobic region is a prequisite for binding to membranes which are mainly composed of phospholipid bilayers (Hand et al. 2010). The hydrophobic property of SAG21 protein mirrors atypical characteristics of the members of this group. This suggests a possible role of SAG21 in membrane stabilization.

SAG21 has an additional peculiar feature in that it contains only three proline residues which are all located within a proline-rich domain WVPDPKTGYYRP that also contains three other residues (Thr, Tyr and Tyr) capable of being phosphorylated (Kay et al. 2000). Proline is often found in regions engaging in phosphorylation-regulated transient protein-protein interaction and is also known to prevent protein aggregation (Kay et al. 2000; Rousseau et al. 2006). The presence of a similar domain in LjIDP1 which displayed transient hydrophobic interaction/chaperone-like activity by preventing aggregation of two model enzymes; citrate synthase and alcohol dehydrogenase (Haaning et al. 2008), suggests a possible protein protective role of SAG21. Two short peptides, iAb11 (RDLPFFPVPID), and YiAb11 (RDLPFYPVPID) which have anti-aggregation/fibrillation property in rats (Poduslo et al. 1999) also share sequence similarities with the proline-rich domain mentioned above. Furthermore, multiple alignment analysis with other Lea5 members showed that this domain is well conserved in the C-terminal region implying that it may act as an important feature contributing to Group Lea5's functional role.

Secondary structure analysis carried out with several programmes predicted a high proportion of α-helices and random coils in SAG21 in dry state. Although, members of Group Lea5 were mostly predicted not to be IDPs (Tunnacliffe et al. 2010) LjIDP1 was shown to adopt a largely α-helical structure upon water stress, which is reversible upon rehydration making it a suitable candidate for transient interactions (Haaning et al. 2008). Due to the striking similarities in physiochemical properties between LjIDP1 and SAG21, perhaps a similar structural change in SAG21 might occur upon water stress. Nevertheless, it will be essential to provide experimental evidence using several approaches like circular dichroism spectroscopy and FTIR to test this hypothesis.

SAG21 was originally suggested to be a plastid protein (Hundertmark and Hincha 2008; Mowla et al. 2006). *In silico* predictions with several programs indicated a high probability of mitochondrial or plastidial localization for SAG21. Since mitochondrial and plastidial transit peptide share common features in length and composition and similar import machinery, their discrimination remains difficult, and in addition some proteins are found to be dual targeted (Berglund et al. 2009; Peeters and Small 2001). The difficulty of predicting the mitochondrial localization of proteins was recently highlighted by a thorough examination of the Arabidopsis mitochondrial proteome in which only one-half of the proteins were correctly

predicted (Heazlewood et al. 2004). Transient transfection and stable transformation of 35S::*SAG21*::YFP construct into Arabidopsis revealed that the YFP signal was associated with small subcellular compartments which did not co-localize with chloroplast autoflourescence in both protoplast and cotyledon indicating that SAG21 is most likely localized to the mitochondria. Moreover, time lapse imaging of these compartments in root tissues reveals that their appearance and behaviour is characteristic of mitochondria. Taken together, these results therefore suggest that a plastid localization for SAG21 can be excluded. However, a co-expression with a mitochondrial marker such as Mitotracker red dye would be a crucial step to further confirm its exact subcellular specificity.

Several LEA proteins from both plants and other organisms are mitochondrially located specifically to the matrix space and are involved in protein protection during water stress (Grelet et al. 2005; Hand et al. 2010; Tunnacliffe et al. 2010). Evidence suggests that mitochondria containing LEA proteins frozen with trehalose could preserve outer membrane integrity thus retaining a number of their biological functions (Menze et al. 2009; Yamaguchi et al. 2007). Consistent with SAG21 as a mitochondrial protein and further submitochondrial targeting to the matrix space (Mitoprot: 0.819), SAG21 could play the same protective role in this compartment. SAG21 sub-mitochondrial localization could be determined by disrupting intact SAG21 mitochondria using an osmotic gradient (e.g mannitol) or detergent (e.g Triton X-100) followed by immunodetection with enzyme activity markers, fumarase and adenylate kinase, for the matrix space and intermembrane space, respectively (Grelet et al. 2005).

Under stress conditions, mitochondria as well as chloroplasts accumulate ROS and can cause critical shifts in cell redox status thus affecting redox-mediated gene expression (Foyer and Noctor 2005; Rhoads et al. 2006). The proposed localization of SAG21 to mitochondria is in parallel with its suggested role in protection upon oxidative stress and its up-regulation by abiotic stress (Mowla et al. 2006). In addition, plant mitochondria can also be a major source of ROS in dark and non-green tissues (Rhoads et al. 2006) which fits well with SAG21's predominant expression in non-photosynthetic tissues and light-repressed expression (Mowla et al. 2006; Weaver et al. 1998). Taken together, SAG21 might regulate the expression of redox-mediated genes during stress and normal development in a compartment and tissue-specific manner.

The SAG21 protein contains Lys and Gly residues which have been shown to modulate hydroxyl scavenging in the mitochondrial citrus dehydrin, CuCOR19 (Hara et al. 2004). Furthermore, the SAG21 protein also contains Tyr, Trp and Phe which are residues involved in metal-ion binding in the CuCOR15 dehydrin (Hara et al. 2005). This amino acid profile might suggest a possible antioxidative role for SAG21 by preventing the generation of hydroxyl radicals through the metal-catalysed Haber-Weiss reaction (Foyer and Noctor 2005) thus minimizing further oxidative damage to intracellular macromolecules such as mitochondrial DNA. His-rich domains and polylysine segment-containing domains participated in DNA-binding in dehydrins (Hara et al. 2009). The SAG21 protein lacks these domains suggesting that it is unlikely to bind directly to DNA. However, consistent with the previously proposed function in ROS scavenging and metal-binding, SAG21 might protect mitochondrial DNA indirectly by preventing oxidative damage caused by hydroxyl-DNA interactions.

Taken together, the SAG21 primary sequence analysis and mitochondrial localization suggest that SAG21 might function in oxidative stress regulation via antioxidative properties, chaperone-like protein-protein interaction and membrane stabilization. Nevertheless, further experimental evidence will be required to demonstrate the above proposed roles.

4.5 Summary

To gain a better insight of SAG21 characteristics as an atypical LEA and its predicted subcellular localization, SAG21 primary sequence was subjected to *in silico* analysis. Its hydropathy plot indicated that SAG21 has an average negative hydrophobicity with a more hydrophobic N-terminal pre-sequence targeting the protein to the mitochondria or plastids. SAG21 protein was also predicted to form α-helix secondary structures in the dehydrated state. Similar structural characteristics are reported in other Group Lea5 members and other slightly hydrophobic LEAs suggesting a proposed role in membrane and protein protection. In addition, SAG21 protein is also composed of amino acid residues previously shown to be involved in ROS scavenging and metal binding therefore suggesting antioxidant properties. Finally, transient and stable expression of a *SAG21*-YFP construct fused to a constitutive promoter indicates that SAG21 is most likely localized to the mitochondria and excluded from the plastid. As mitochondrial ROS increases upon stress, the mitochondrial localization is in agreement with a proposed role for SAG21 in oxidative stress protection.

Chapter 5: Cellular expression pattern and functional analysis of ROS-induced gene; *SAG21* during development

5.1 Introduction

Yeast complementation can be a powerful technique for functional screens of plant genes (d'Enfert, Minet and Lacroute, 1995). This approach was used to identify a previously unknown role for the previously identified SAG21 gene (Mowla et al., 2006). *YAP1* is a bZIP transcription factor in yeast (Apel and Hirt, 2004) required for transcriptional regulation of at least 32 oxidative-stress responsive genes. These genes mainly comprise ROS scavenging enzymes, and pentose phosphate pathway enzymes which are crucial for NADPH production (Kuge and Jones, 1994). Moreover, analysis of *yap1* mutants revealed that most ROS-induced gene expression in yeast is *YAP1*-dependent (Apel and Hirt, 2004).

Using this valuable functional information, a yeast complementation screen of *yap1* mutants using an Arabidopsis cDNA library enabled the isolation of a full-length LEA protein, *AtLEA5/SAG21*, which enhanced *yap1* cells' tolerance towards toxic concentrations of pro-oxidants of different chemistries including H_2O_2, diamide and menadione (Mowla et al., 2006). Previously, *SAG21* transcript levels were also shown to be up-regulated in ozone-induced leaf senescence (Miller, Arteca and Pell, 1999) and in ozone-treated plants (Tosti et al., 2006). This revealed a unique feature of *SAG21/AtLEA5* compared to other prototypical LEA proteins, which is an additional role in oxidative stress tolerance and ROS signaling.

At a tissue-specific level, *SAG21* transcripts were shown to be constitutively expressed in roots and reproductive organs but absent in the rosette and seeds (Mowla et al., 2006). In addition, *SAG21* expression was also induced in the dark and repressed by light (Weaver et al., 1998; Mowla et al., 2006). Although Mowla et al. (2006) could not detect any *SAG21* expression in whole rosette, Weaver et al. (1998) showed earlier that *SAG21* reached its highest expression just before full senescence, followed by a sharp decrease in detached leaves. The increase in transcript level shown by Weaver et al. (1998) might be due to a wound-induced effect introduced in the experimental setup of detached leaves (discussed further in Chapter 6). This could also be correlated with a transient ROS increase or a shift to

higher ROS levels seen in senescing leaves (Zimmermann and Zentgraf, 2005). However, no direct function of this protein in relation to senescence had been established to date.

The developmental, tissue-specific and stress-induced expression patterns observed for *SAG21* are presumed to be controlled by regulatory elements present within its promoter. There are various publicly available algorithm and bioinformatics tools that have been developed to facilitate *in silico* analysis of plant promoter sequences, for example TRANSFAC, PLACE, AGRIS, PlantCARE and JASPAR (Wingender et al., 2000; Hiro et al., 1999; Duvuluri et al., 2003; Lescot et al., 2002; Sandelin et al., 2004). These computer approaches estimate the probability of occurrence of short DNA motifs based on random sampling or statistical modelling of a background distribution (Priest et al., 2009). Using promoter constructs fused to reporter genes such as *β*-glucuronidase (GUS) serves as a powerful tool to further confirm the spatial and temporal expression of specific genes thus leading to a better understanding of the correlation between regulatory elements and gene expression (Jefferson, 1987).

Another powerful tool in functional studies besides knockout analysis is to create transgenic over-expressor and antisense lines in model organisms such as Arabidopsis. Using this method, a constitutive promoter, such as the Cauliflower mosaic virus 35S CaMV promoter is fused to the open reading frame in the sense (over-expressor) or antisense direction. This will result in the perturbation of total protein content with ectopic over-production in the over-expressor lines and repressed production in antisense lines respectively. These perturbations can result in different phenotypes under optimal conditions and or might result in altered responses to the presence or absence of specific internal or external stimuli compared to WT.

In this chapter, aimed at the elucidation of molecular mechanisms underlying the transcriptional control of *SAG21*, a search of plant promoter and transcription factor databases was utilized to predict the transcriptional regulatory elements within the 5' upstream region of *SAG21* following its tissue-specific, spatial and temporal expression during development. Furthermore, phenotypic characterization of the *SAG21* over-expressor (OEX), and *SAG21* antisense (AS) plants compared to WT plants grown under standard conditions were carried out to identify how *SAG21* perturbation affected growth and development.

5.2 Materials and methods

5.2.1 Plant material and phenotypic analysis

Arabidopsis thaliana (Col-O) plants were grown in a controlled environment as described in section 2.14.1 (*in vitro* growth) and section 2.14.2 (in soil). Soil grown plants were used for analysis of above-ground phenotype (plant size, flowering time, leaf number and leaf senescence). All parameters were recorded, and after 10 weeks, the six oldest leaves from each genotype were harvested for chlorophyll quantification. At least three replicate plants were used for each line.

Below-ground analysis was carried out *in vitro*. Seeds were sown in one row in the top third of 90 mm Petri dishes and grown vertically for 20 days and 8 days for root and root hair analysis, respectively. Roots grown synchronously were selected for further characterization. Primary root length was measured directly using a ruler. Seedlings were then fixed and subjected to Feulgen staining (section 2.18) to allow accurate phenotyping of the number of lateral roots and lateral root primordia using a dissecting microscope (Nikon SMZ-2T). For root hair analysis, images of seedling root hair zones were taken with a BH2 Olympus research microscope with a 4X objective and FUJI 1X Digital Camera HC-300Z. Size bars were embedded by software analysis (Sigmascan, Jandel Scientific).

5.2.2 *In silico* promoter analysis

A 1685 bp upstream region of *SAG21* was screened for *cis*-acting regulatory elements using the PLACE (Higo et al., 1999) and the PlantCARE (Lescot et al., 2002) database.

5.2.3 *SAG21* transgenic lines

For cellular expression analysis, two promoter constructs; *SAG21(1685)*::GUS and *SAG21(325)*::GUS were generated. For *SAG21(1685)*::GUS, 1685 bp 5' upstream *SAG21* was PCR amplified (section 2.11) from genomic DNA using primers containing *Sal*I and *Xba*I sites respectively: 5'-AATT<u>GTCGAC</u>TAATCTCCAAAACATTGTG and 5'-ACTG

TCTAGATTTCGAAGTAAGTGGTTTC, and cloned into pGEM-T Easy (Promega, UK). (all cloning steps are described in section 2.12). The insert was removed by restriction digestion and cloned into the pGPTV-KAN upstream of the *uid* (GUS) gene. For the *SAG21(325)*::GUS construct, the fragment was amplified using a pGEM-T Easy template containing *SAG21*(1685) (section 2.3) using primers containing the *att*B sites; 5'-GGGG ACAAGTTTGTACAAAAAAGCAGGCTTCGGGTCAAAAGACTCAAAG and 5'-GGGG ACCACTTTGTACAAGAAAGCTGGGTCTTTCGAAGTAAGTGGTTTC and cloned into Gateway vectors (Invitrogen). The *att*B-PCR product was introduced into the entry vector, pDONR221 by a BP clonase recombination reaction. This generated anentry clone, pENTRSAG21(325). An LR clonase recombination reaction was performed to transfer the DNA fragment from entry clones to destination vector; pMDC221. The BP and LR reactions were carried out according to manufacturer's instructions (Gateway, Invitrogen).

For phenotypical analysis, over-expressor (*SAG21*-OEX) transgenic lines were as described in Mowla *et al.* (2006). Antisense lines (*SAG21*-AS) were generated by PCR amplification of the entire *SAG21* open reading frame using primers: 5'-CAAGTCTAGACTTA CTTCGAAAATGGC and 5'-CCGGATCC TCTCCTCTTAAAGACC containing *Xba*I and *Bam*HI sites respectively and cloned into pBin19-35S (Höfgen & Willmitzer, 1990) in the reverse orientation as described in Mowla et al. (2006).

Constructs were transformed into *Agrobacterium tumefaciens* strain *GV3101* (section 2.12.5.2) and Arabidopsis plants were transformed by the floral dip method (section 2.15). Transformants were selected on 1 x MS, 1% agar plates containing 50 µg/ml kanamycin (*SAG21(1685)*::GUS, *SAG21*-OEX, *SAG21*-AS) or 50 µg/ml hygromycin (*SAG21(325)*::GUS). Primary transformants were tested by PCR followed by RT-PCR (section 2.11.1) or GUS assays (section 2.17) depending on the line. Several lines were selected for each experiment, and tested for expression; all experiments were performed with two selected homozygous lines for each transgene (details on transgenic lines used for each construct are provided in 2.4).

5.2.4 Chlorophyll content

Chlorophyll content was measured from 5 mm diameter leaf disc samples. Chlorophyll was extracted from three leaf discs placed in a microcentrifuge tube containing 0.5 ml of 70% acetone. The discs were homogenized with an Eppendorf grinder and centrifuged at 4000 rpm, RT for 5 min using a Eppendorf MiniSpin plus® microcentrifuge. The clear supernatant was transferred into a clean glass bottle. The pellet was re-extracted twice and topped up to a final volume of 10 ml with 70% acetone. Chlorophyll content was measured spectrophotometrically according to Bruinsma (1963). Each measurement included three replications.

5.3 Results

5.3.1 Analysis of *cis*-regulatory elements in the *SAG21* promoter

Sequence analysis showed that the investigated 1658 bp region upstream of *SAG21* (Fig. 5-1) contained several basal regulatory elements upstream of the transcriptional start point which includes a TATA-box (Zhu et al. 1995; Grace et al., 2004) for RNA polymerase binding and CAAT boxes (Shirsat et al., 1989) for transcriptional regulation. As seen in many other senescence/redox regulated genes such as *WRKY53*, *SAG21* contained several putative W-boxes. A group of two W-box elements were present in the *SAG21* promoter region between -360 and -316, while two others were present as single motifs further upstream at positions -1023 and -1623. Another likely candidate, the MYC recognition site, MYCCONSENSUS (Chinnusamy et al., 2003) was also identified at four different locations (-1007, -1163, -1175, -1481) within the promoter region was previously reported to be an important binding motif for the switch of *WRKY53* expression from a leaf age dependent to a systemic plant age dependent expression during bolting time (Miao et al., 2007)

The *cis*-acting light-regulating elements; GATA-box and GT1 (Lam and Chua, 1989; Villain, Mache and Zhou, 1996) were represented 16 and 21 times, respectively throughout the promoter region. In addition, a CIRCADIANLELHC (Piechulla, Merforth and Rudolph, 1998) element was also detected at 277 bp upstream of the putative translation site. For tissue-directed expression, seventeen ROOTMOTIFTAPOX1 (Elmayan and Tepfer, 1995), five OSE2ROOTNODULE (Vieweg et al., 2004) and eight POLLEN1LELAT52 (Bate and Twell, 1998) were identified within the investigated region. The number of occurrences of each *cis*-regulatory elements analysed within both promoter constructs; *SAG21(1685)::GUS* and *SAG21(325)::GUS* are summarized in Table 5-1.

-1685 TAATCTCCAAAACATTGTGAAAAATTGGGGGTTTTTTTTATCATTTAAATTGTCTATAGTGGTCAATCATTATTAAAAAA
                                            GATA-BOX   W-BOX

-1605 AATTGTTTTTTGTTGAAATTTTAAATTATAAAAAAAAAACACGTTTATACATAAAATGCAAAAACTTTTCTTAAACCAAA
                                                                          POLLEN

-1525 TTACAGAGAAAGGCTATCACCATCCTTGTCTTGATGCCAACCACACTTGTAATCCCAAAATACATACTTAAACTATACTA
              POLLEN   MYC

-1445 TACTAACATGAATTGGTTATACGATTATCTATCTAGTTAGCTACATAATTCATATAATTAGTTTTTTAAAATATACTTAT

-1365 GTAATGATAGTAACTAAAAAATATACTATCTCGAGAAATCCAACCAAAATGCTATGATAGTATATAAAATAAAATGAAAG
          GATA-BOX   ROOT

-1285 AAAGAGGAACCAAGTTGTGAAACCATTTACCAAGAAGAAGAAGAAAAAAACAAGATGGTCGAGTCTCGTGATAGTATGAA

-1205 GCTGGGGCCGAAACCACGAATCAAAGAACCATTTGACGGATCGCAAGTGCTCATCGATAACCAATCAATAGAAACTCCACCG
                              MYC   MYC

-1125 CCTCAAAATATCATAGTGCTATTTAATTTTTCATACTATCATTTATTGTAGGCTATAACATATTTTTGTATTGTAGATGG
                                                                  ROOT

-1045 ACGGCTAGTACACGCAAGTTAGTCAATAAACTTTTAACAAATGGCATCTTGACATGCTTAAACACATTTTATAATTCGAA
                       W-BOX   MYC

-965   CCTCACTTTGCCTACTTTACACACGTCTACTTATAGTAGATGAGCATCAATCATTGAACCGTTCGTATAATACAATTTTT

-885   TTTTTGTAATACGTTATAATTAGAAAGTAATGGAAAATAAGTTGAAACACAAATTTTCAACGGTTTTACTAAGATTTAAT

-805   TTTACAATTTTCAAAATATAACCGAATTATTTAAATCGTATTAAATTTATAATTAATTTTCTAAAAAAAAAACACAGATTA

-725   AAAAAATATATTAAAACTAATCATAAATATATTAATTTTTGTAATTTATATTTTTTATAACTTTAAACTAATAATATTC

-645   AATTATTTATCTTAAACTTTACAAATTATCAATAATAACTAATAAATAATGCATAAAAACTTTTTAAAAATTAACTTTTT

-565   GAAACAAATTTTTTTCTAAAAAATTAAATAATAAAGAACAGAAAAATATTATTCAACTAAAAATATTGGATAATAACTC

-485   TGAAAGTTTGCATTTTTCAAATAAATCATTGATTTTTTTTGTTTGACATAAAACATTAATTTCCCCTTGTAAATCACACA
                  CIRCADIANLEHLHC

-405   TTTAAAATCTAACTATATTTAAACAAAAAAAAAAAGTCCAATTTTGACTTTAATTATATAAAAAAAGCAAAGCTAATTAT
                                                                W-BOX

-325   CGGTCAAAGCACTCAAAGCCCAGAATTCACGCACCCGTTTATCACAAGTCAGAAGACAATTTCGGAGTCACTTCCTTTAT
       W-BOX

-245   TTCCTCTCTTCCTTCACTCTCTCCTATATAAACCTTCCTCTCCTCTTCCTCTCTTCTCATCTCTTCAAACCATTTTCGAA
                                                  ROOT(N)

-165   AGCCTTGAGAGAGAGAACACAGACGATACCAACTTTCTTCAATCTCGTTGCCGCAGTATAATTATCTCATTCCTCGGATA

-85   TATCTCTCCTTCTGCGGCGGCGACAAGAAGCTACAAGAATAAAAAGTCTGTTTTCTCTCTTTCAAGAAACCACTTACTT

-5   CCAAA **ATG**

Figure 5-1. *SAG21* upstream regions. Nucleotide sequences representing potential *cis*-regulatory elements present on the positive strand (underlined) and negative strand (dotted underlined) are labelled as follows: W-box and MYC motifs (yellow); GATA-box (red); Root motifs (ROOTMOTIFTAPOX1) and Root(N) motifs (OSE2ROOTNODULE) (blue) and POLLEN1LELA52 (green), CIRCADIANLEHLC (purple). Black arrow indicates the fragment included in the shorter construct (325 bp).

Table 5-1. Number of occurrences (n) of different *cis*-regulatory elements within *SAG21* upstream regions; 1685 bp and 325 bp respectively. These elements are known to be involved in redox/senescence-regulated, light-regulated and tissue-specific expression.

cis-element	sequence	1685 bp (n)	325 bp (n)
Redox/senescence-regulated			
W-BOX	TTGACY	4	1
MYC CONSENSUS	CANNTG	4	-
Light-regulated			
GATA-BOX	GATA	16	5
GT1CONSENSUS	GRWAAW	21	3
CIACADIANLELHC	CANNNNATG	1	1
Root-specific			
ROOTMOTIFTAPOX1	ATATT	17	-
OSE2ROOTNODULE	CTCTT	5	5
Pollen-specific			
POLLEN1LELAT52	AGAAA	8	1

(Y= C/T, N=A/T/G/C, R=A/G, W= A/T)

5.3.2 *SAG21* spatial and temporal expression

Homozygous transgenic Arabidopsis lines carrying promoter constructs (Fig. 5-2a, b), *SAG21(1685)*::GUS (lines: T3-2-6, T2-3-5) and *SAG21(325)*::GUS (lines: T2-5-6, T2-5-8) were selected for further analysis. As a first step in the functional analysis of *SAG21* , its spatial and temporal expression patterns during normal growth and developmental conditions were characterized.

(a)

Xba1   Sal1   Size (bp)

| | GUS | nosT | 1685

-1685   +1

(b)

attr1   attr2

| | GUS | nosT | 325

-325   +1
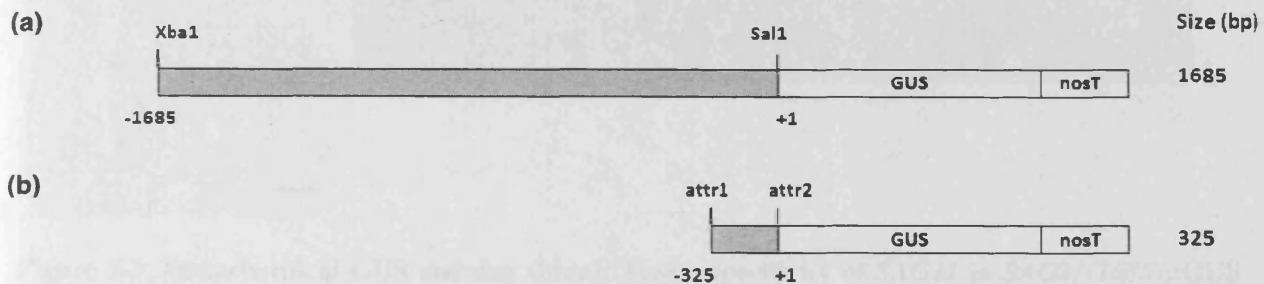
moter analysis.

ınd 325 bp (b) to

struct (a) and (b)

5.3.2.1 *SAG21* is constitutively expressed in roots, cotyledons and pollen and is light-repressed

To investigate the tissue-specific expression of *SAG21* during normal development and the effect of truncating the promoter on expression patterns, transgenic lines of *SAG21(1685)*::GUS and *SAG21(325)*::GUS seedlings and whole plants were subjected to GUS histochemical analysis. In *SAG21(1685)*::GUS seedlings, the highest expression was observed in roots and cotyledons (Fig. 5-3a). All the lines studied showed similar expression patterns. Higher magnification of the root section revealed a more distinct pattern with very low or no expression in either primary or lateral root tips (Fig. 5-3b, c) while a more intense blue could be clearly seen in the differentiation and elongation zone (Fig. 5-3c, d) where lateral roots and root hairs emerged. GUS expression was also clearly detected in root hairs (Fig. 5-3d). In the *SAG21(325)::*GUS lines, expression could be detected in whole rosette and cotyledons (Fig. 5-4a) in all transgenic lines. A lower expression but with similar pattern to

117

SAG21(1685)::GUS seedlings was observed in the primary root with higher expression in the lateral root initiation region (Fig. 5-4b, c).
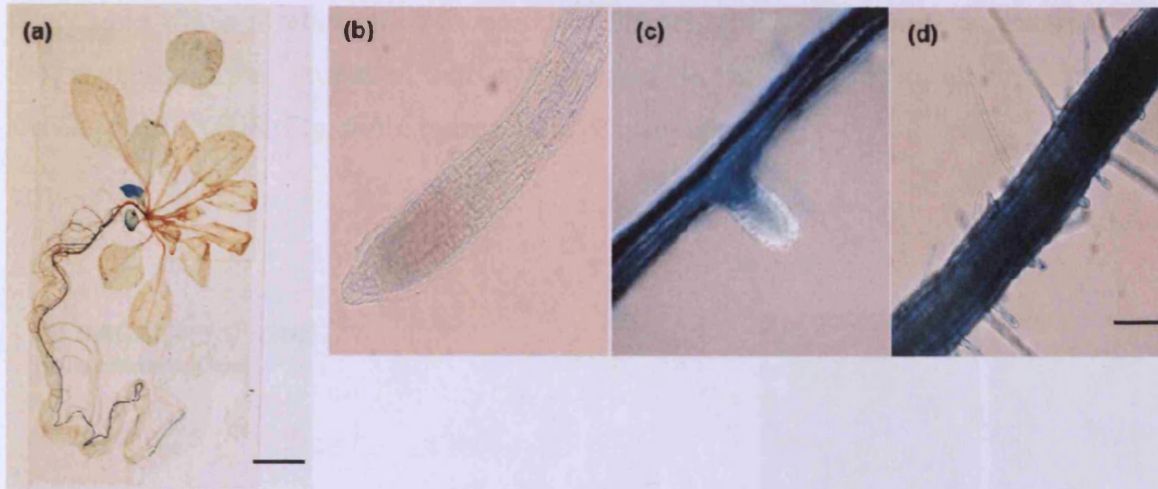
Figure 5-3. Histochemical GUS staining (blue): Tissue-specificity of *SAG21* in *SAG21(1685)*::GUS (line: T3-2-6) seedlings. (a) Whole seedlings (three-week-old). Expression was high in primary root and cotyledon, followed by a lower expression in lateral roots and absent in whole rosette. Scale bar = 1 cm. **(b-d)** Root tissues of seedlings 8 DAS; Higher magnification of the root section showed highest expression in the differentiation and elongation zone (c) and root hairs (d) but not present in the root tip (b) Scale bar = 100 μm.
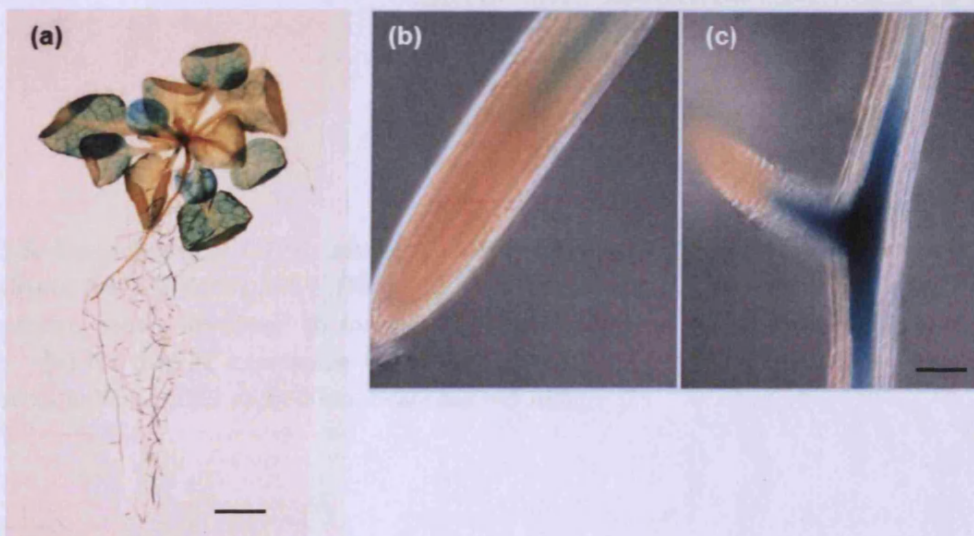
Figure 5-4. Histochemical GUS staining (blue): Tissue-specificity of *SAG21* in *SAG21(325)*::GUS (line: T2-5-6) seedlings. (a) Whole seedlings (three-week-old). Expression could be detected in whole rosette and cotyledon. A lower expression was observed in the primary root with higher expression in the laterals. Scale bar = 1 cm. **(b-d)** Root tissues of seedlings 8 DAS. Higher magnification of root section showed similar pattern observed in *SAG21(1685)*::GUS with a more localized expression at the base of lateral root initiation site (c). Scale bar = 100 μm.

118

Almost no GUS activity was detected in younger leaves of *SAG21(1685)::*GUS rosettes (Fig. 5-5b) but occasional expression was observed in early senescing leaves localized to the interface between green and yellowing tissue (Fig. 5-5a). However, three further attempts on 8-week-old whole rosettes failed to reproduce the pre-senescence expression pattern (Fig. 5-5b) suggesting the promoter activity appeared to be inactive in all leaf stages of *SAG21(1685)::*GUS (Fig. 5-5b) independent of plant age.

(a) *SAG21(1685)::GUS*
(early senescing leaf)
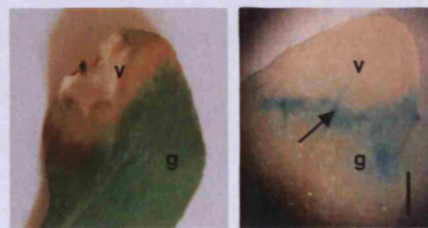
(b) *SAG21(1685)::GUS*
(whole rosette)

Figure 5-5. Histochemical GUS staining: Senescence-specificity of *SAG21* in senescing leaves of 8-week-old *SAG21(1685)::GUS* (line: T3-2-6) plants. (a) *SAG21* expression was detected in early senescing leaves localized to the interface between green (g) and yellowing/senescing (y) tissue. (b) No *SAG21* expression was detected in all leaf stages except at the wounding site. Black arrows indicate GUS expression. Scale bar = 5 mm.

In flowers of *SAG21(1685)::*GUS, expression was restricted to the male reproductive organs: anthers and pollen (Fig. 5-6a). The strongest pollen expression was observed upon anthesis and remained high in mature pollen. The pollen- floral specific expression was completely abolished in *SAG21(325)::*GUS flowers but with a noticeable expression in the anther filaments (Fig. 5-6b). Interestingly, *SAG21* expression could also be detected in other organs including sepals (all stages) and petals (at anthesis). Following petal abscission, a marked up-regulation of expression was seen localized to the style.

In addition to the root and floral expression, transgenic seedlings of both lines subjected to light/dark cycle revealed that the promoter activity was high in the dark but decreased rapidly upon illumination in the elongation and differentiation zones of roots (Fig. 5-7). However, no dark-induced expression was detected in the rosette of *SAG21(1685)::*GUS.
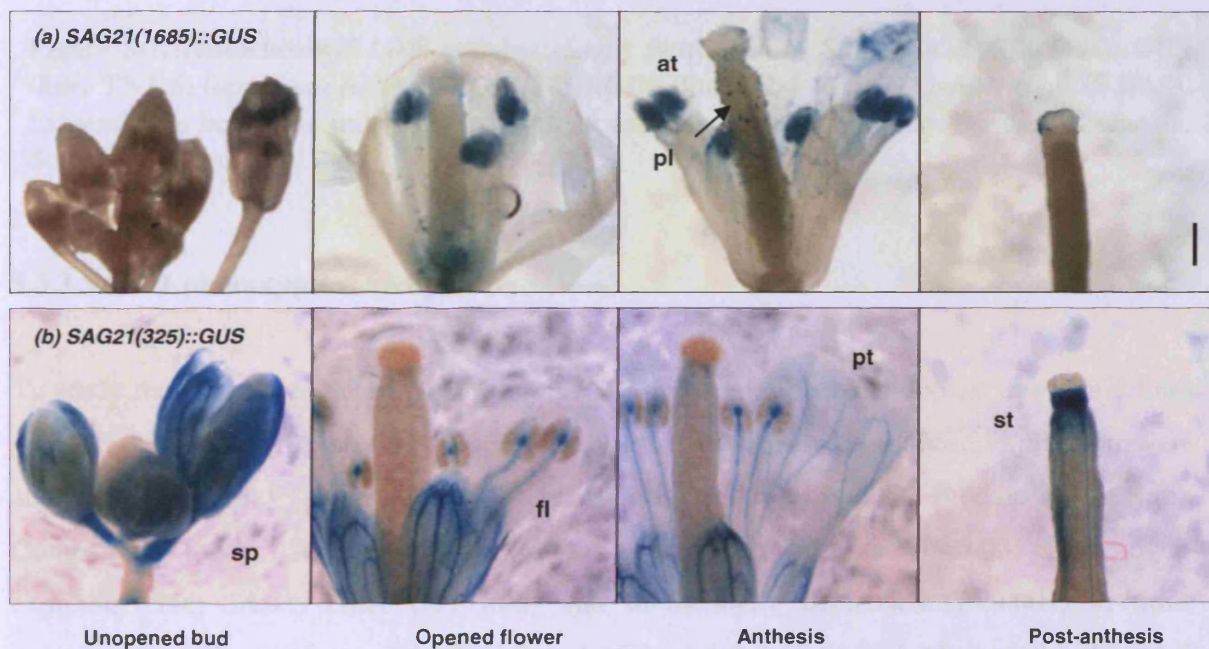
Figure 5-6. Histochemical GUS staining: organ-specificity of *SAG21* in *SAG21(1685)::GUS* (line: T3-2-6) and *SAG21(325)::GUS* (line: T2-5-6) flowers. (a) *SAG21(1685)::GUS;* expression was restricted to anther (at) with highest expression in pollen (pl) which could be clearly detected at anthesis. (b) *SAG21(325)::GUS*; expression could be detected in sepal (sp) at all stages, anther filaments (fl) of opened flowers, petal (pt) at anthesis, and style (st) post-anthesis. No expression was detected in the pollen any stage. Scale bar = 1 mm.
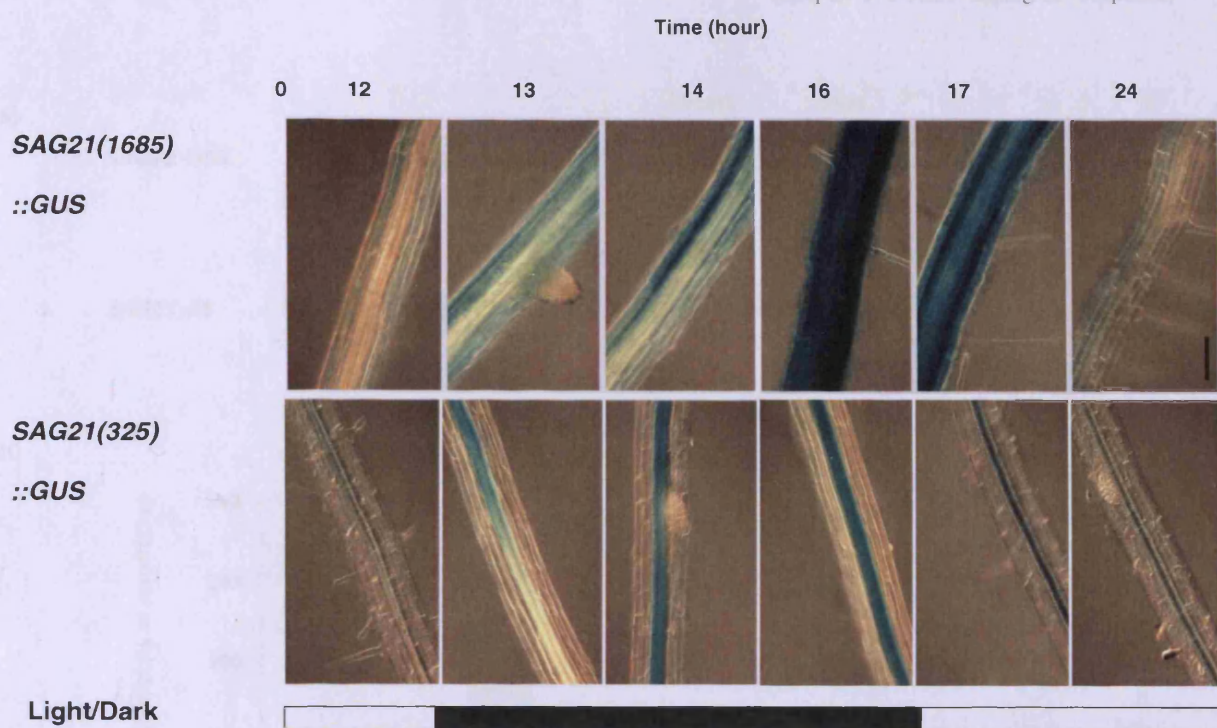
Figure 5-7. Histochemical GUS staining: Light repression of *SAG21* in *SAG21(1685)::*GUS (line: T3-2-6) *(upper panel)* **and *SAG21(325)*::GUS (line: T2-5-6)** *(lower panel)* **roots (8 DAS).** Expression in both lines was repressed by light and showed induction following dark incubation. Scale bar = 100 μm.

5.3.3 *SAG21* phenotypical analysis

To study the consequences of perturbing *SAG21* expression in Arabidopsis, transgenic lines with ectopically over-expressing *SAG21* and antisense lines with reduced expression were analysed (Fig. 5-8a) (Kindly gifted by Prof Christine Foyer and Dr Freddie Theodolou). Compared to the WT, the transcript level was significantly increased (P<0.001) in the over-expressor line; *SAG21*-OEX (2.5 fold) and dramatically decreased (P<0.001) in three independent antisense lines; *SAG21*-AS-1, *SAG21*-AS-2 and *SAG21*-AS-3 at 2.2, 8 and 5 fold, respectively (Fig. 5-8b). *SAG21*-AS-2 antisense line with the highest down-regulation was selected for further phenotypic analysis under controlled growth conditions, in parallel with *SAG21*-OEX and wild type (WT).

121
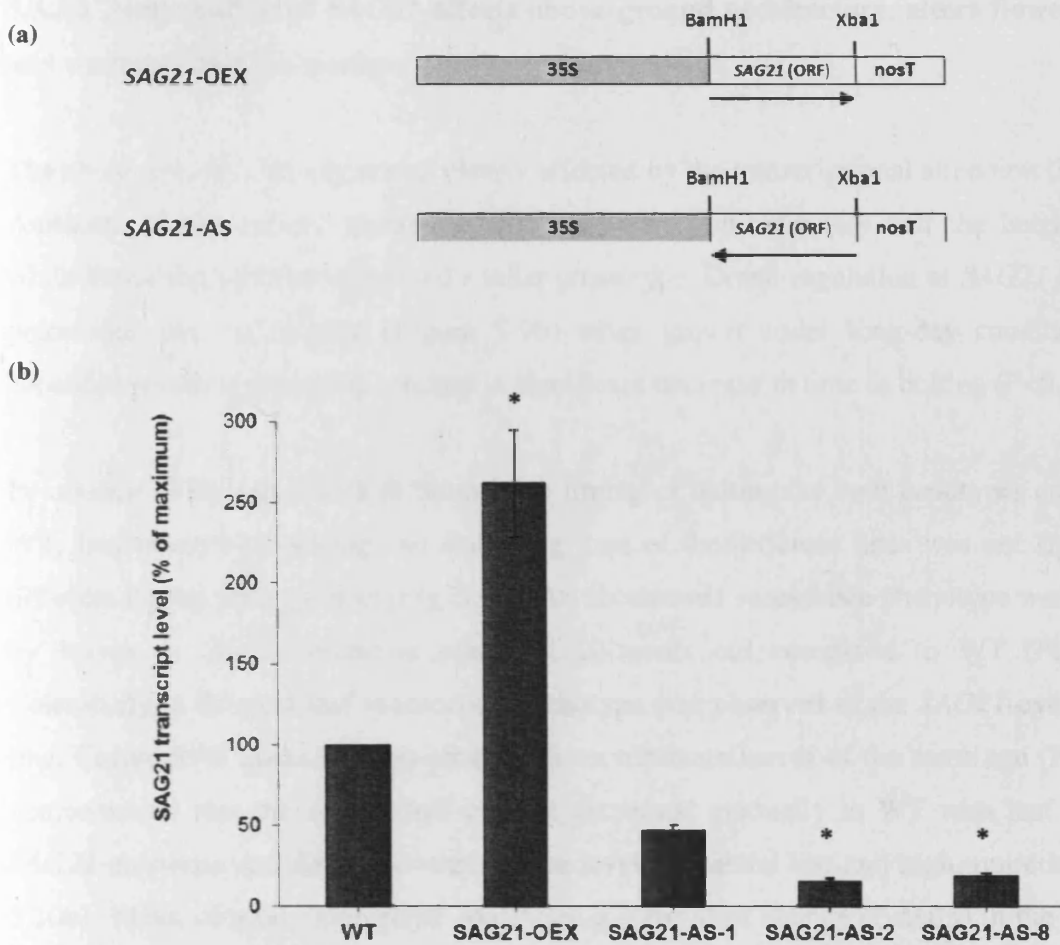
Figure 5-8. *SAG21* transcript levels of *SAG21*-AS and *SAG21*-OEX lines compared to WT. (a) Schematic representation of the constructs used for generating the transgenic lines used in the phenotypic analyses; *CamV35S* constitutive promoter was fused to *SAG21* open reading frame (ORF) either in sense (OEX) or anti-sense (AS) direction and terminated by *nos T*. (b) Mean (±SE, n=3) *SAG21* transcript levels of wild type (WT), over-expressor (*SAG21*-OEX) and three antisense lines (*SAG21*-AS-1, *SAG21*-AS-2, *SAG21*-AS-8). *SAG21* transcript levels were determined by semi-quantitative RT-PCR using At*SAG21*F and At*SAG21*R primers (section 2.5.2) and normalized using PUV primers (section 2.5.2) which targeted 18S rRNA. Transcript levels are expressed as a percentage of maximum. Significant differences of transcript level compared to WT is indicated by asterisk (*P<0.001).

5.3.3.1 Perturbation of *SAG21* affects above-ground architecture, alters flowering time and timing of leaf senescence

The above ground phenotype was clearly affected by the transcriptional alteration (Fig. 5-9a). Antisense plants showed stunted growth and were approximately half the height of WT, while the over-expressor displayed a taller phenotype. Down-regulation of *SAG21* resulted in precocious time to bolting (Figure 5-9b) when grown under long-day conditions while constitutive over-expression resulted in significant decrease in time to bolting (P<0.05).

In contrast to the significant differences in timing of bolting for both genotypes compared to WT, leaf number at bolting and flowering time of the different lines was not significantly different during plant growth (Fig. 5.9b). An accelerated senescence phenotype was exhibited by leaves of *SAG21*-antisense plants at 10-weeks old compared to WT (Fig. 5-10a). Conversely, a delayed leaf senescence phenotype was observed in the *SAG21*-overexpressor line. Chlorophyll quantification obtained from triplicate leaves of the same age (Fig. 5-10b) demonstrated that the chlorophyll content decreased gradually in WT with leaf age while *SAG21*-antisense and *SAG21*-overexpressor levels remained low and high, respectively (Fig. 5.10b). Mean of total chlorophyll confirmed a significant change (P<0.05) in the transgenic lines compared to WT. Although no quantitative data had been obtained, the antisense leaves appeared to be slightly thinner compared to WT and the over-expressor.

(a)
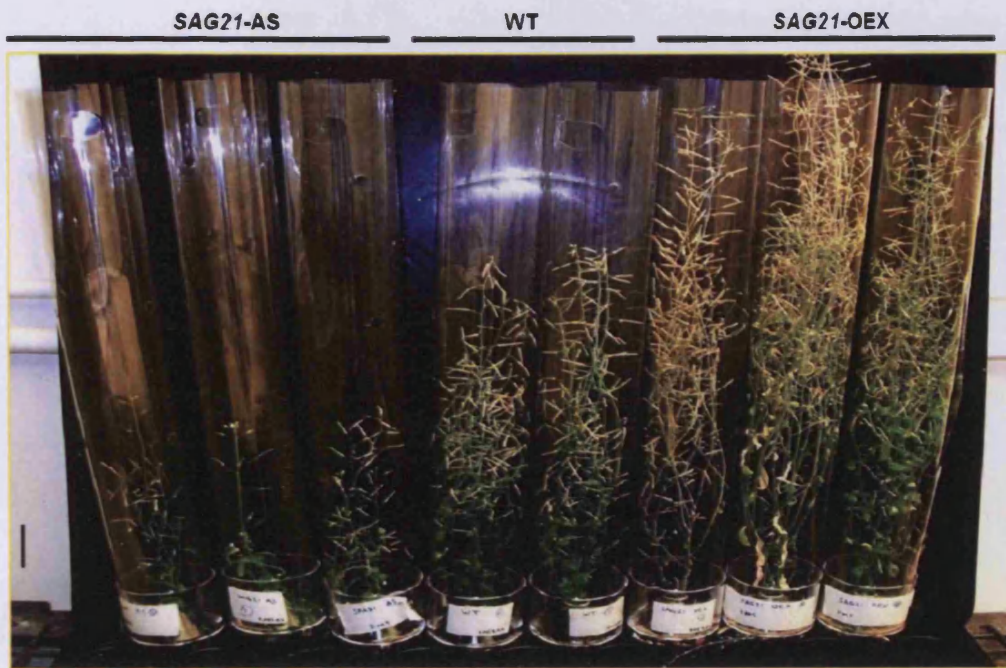
(b)
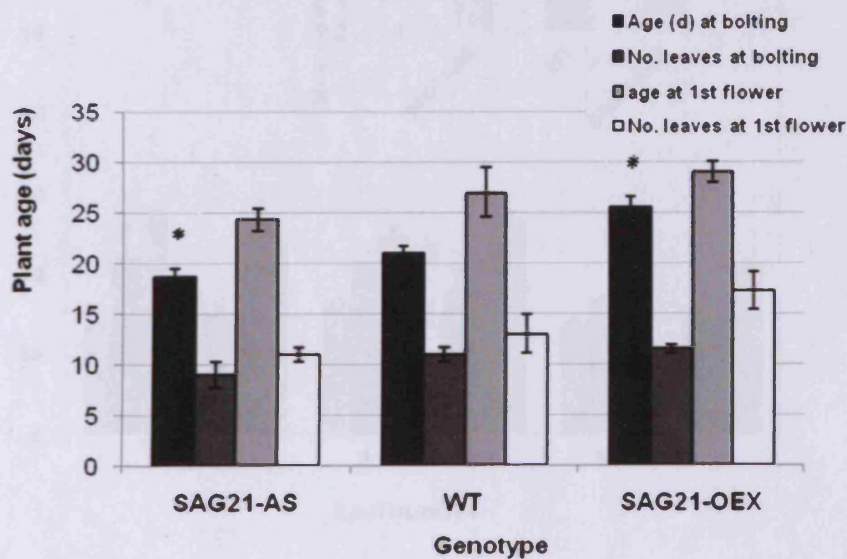
Figure 5-9. Whole plant phenotype of *SAG21*-AS and *SAG21*-OEX compared to WT. (a) Height comparison of 10-week-old soil-grown plants for each genotype. Scale bar = 5 cm. (b) Timing of bolting and flowering for each genotype (±SE, n=3). All parameters were recorded using number of days and were determined from three individual plants of each genotype. Significant differences of number of days compared to WT is indicated by asterisk (*P<0.05).

(a)

(b)
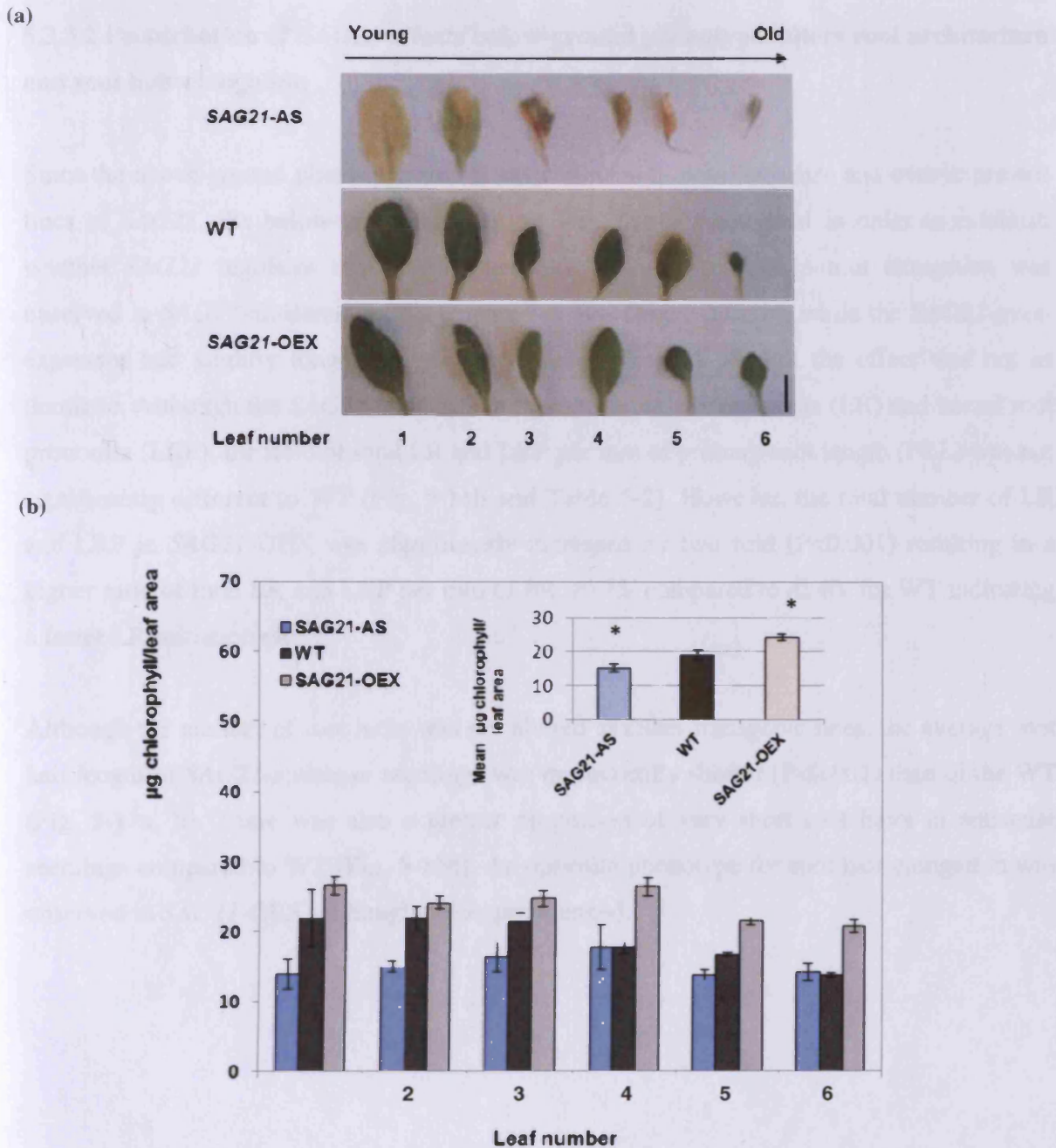
Figure 5-10. Leaf senescence pattern in *SAG21*-AS and *SAG21*-OEX compared to WT. (a) Leaf phenotype of the six oldest leaves (arranged from young to old) for 10-week-old plants for each genotype. Scale bars = 0.5 cm. (b) Mean (±SE, n=18) chlorophyll content extracted from the six oldest leaves. Significant differences of chlorophyll content compared to WT are indicated by asterisks (* P<0.05).

5.3.3.2 Perturbation of *SAG21* affects below-ground phenotype: alters root architecture and root hair elongation

Since the above ground phenotype was clearly affected in both antisense and over-expressor lines of *SAG21*, the below-ground phenotype was also characterized in order to establish whether *SAG21* regulates root development. A 70% suppression in root elongation was observed in *SAG21*-antisense roots compared to WT (Fig. 5-11a, b), while the *SAG21*-over-expressor had slightly longer primary roots than WT (P<0.05) but the effect was not as dramatic. Although the *SAG21*-antisense line produced less lateral roots (LR) and lateral root primordia (LRP), the ratio of total LR and LRP per mm of primary root length (PRL) was not significantly different to WT (Fig. 5-11b and Table 5-2). However, the total number of LR and LRP in *SAG21*-OEX was significantly increased by two fold (P<0.001) resulting in a higher ratio of total LR and LRP per mm of PR: /0.75/ compared to /0.40/ for WT indicating a faster LR initiation rate.

Although the number of root hairs was not altered in either transgenic lines, the average root hair length of *SAG21*-antisense seedlings was dramatically shorter (P<0.001) than of the WT (Fig. 5-12a, b). There was also a greater proportion of very short root hairs in antisense seedlings compared to WT (Fig. 5-12c). An opposite phenotype for root hair elongation was observed in *SAG21*-OEX, although not as pronounced.

(a)

(b)
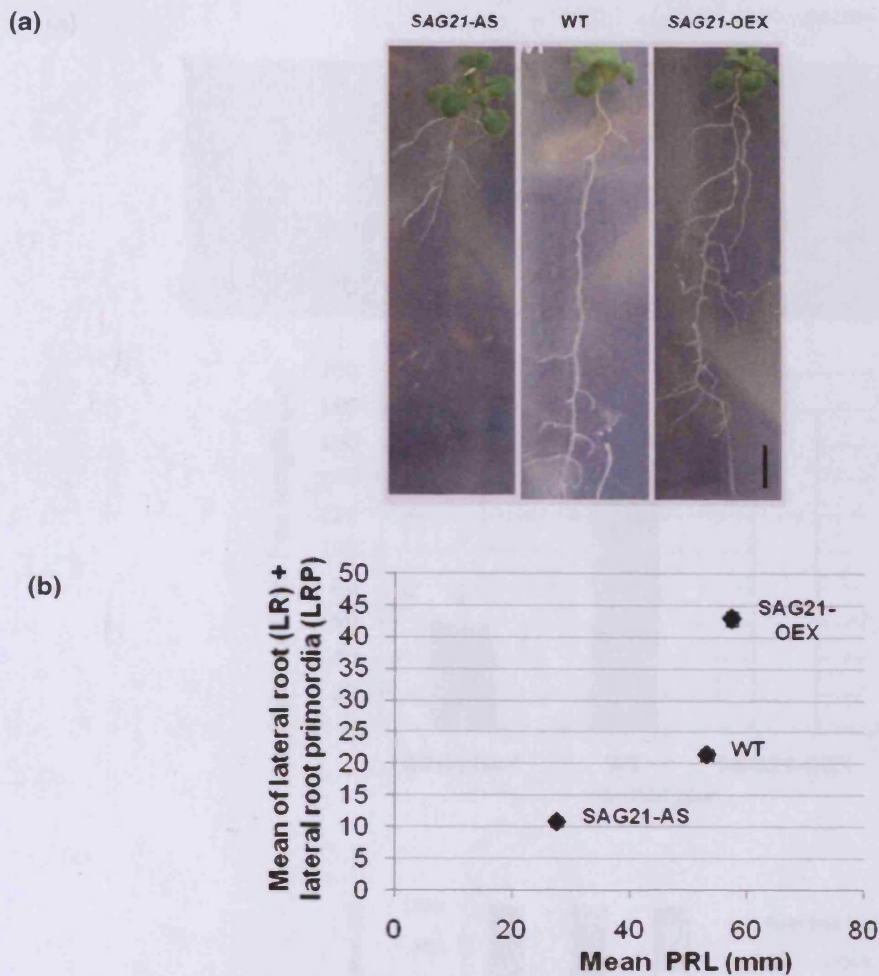
Figure 5-11. Root phenotype of *SAG21*-AS and *SAG21*-OEX compared to WT. (a) Root architecture of 20 DAS seedlings grown vertically on MS agar plates for each genotype. Scale bar = 5 mm. (b) Mean (±SE, n=20) of number of lateral roots (LR) and lateral root primordia (LRP) as a function of mean of primary root length (PRL) for each genotype.

Table 5-2. Mean (±SE, n=20) of primary root length (PRL) and mean (±SE, n=20) of lateral root (LR) and lateral root primordial (LRP) and their P-values.

Genotype	X: PRL(mm) (±SE)	P+	Y: Mean of LR +LRP (±SE)	P+	Ratio Y/X	P+ (±SE)
SAG21-AS	27.57 (±0.83)	<0.001	10.8 (±0.366)	<0.001	0.40 (±0.02)	NS
WT	53.03 (±1.16)	-	21.333 (±0.73)	-	0.40 (±0.02)	-
SAG21-OEX	57.40 (±0.70)	<0.05	42.833 (±1.10)	<0.001	0.75 (±0.01)	<0.001

127

(a)

WT   SAG21-OEX

(b)

(c)
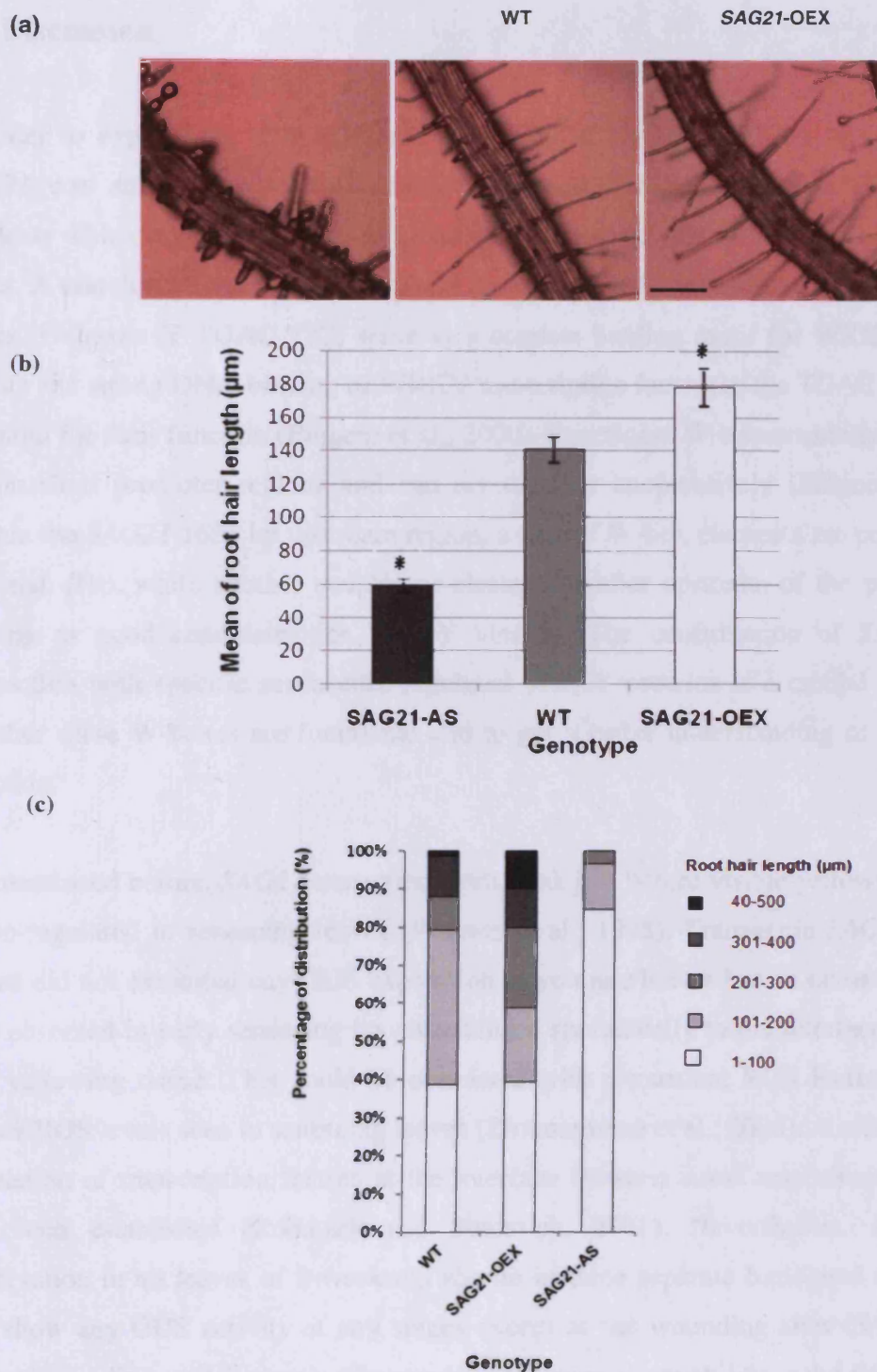
Figure 5-12. Root hair phenotype of *SAG21*-AS and *SAG21*-OEX compared to WT. (a) Root hair zone of vertically grown 8 DAS seedlings for each genotype. Scale bars = 100 µm. (b) Mean (±SE, n=150) of total root hair lengths for each genotype. (c) Root hair lengths for each genotype (grouped according to different length range) and represented as percentage of distribution. Significant differences of root hair length compared to WT are indicated by asterisks (* P<0.001).

5.4 Discussion

In order to explore the transcriptional regulation of *SAG21*, 1685 bp upstream region of *SAG21* was analysed to identify the presence and distribution of specific cis-regulatory elements which might contribute to its general expression and up-regulation upon oxidative stress. A search with the PLACE database revealed that the investigated region is rich in W-boxes. W-boxes (T TGAC T/C) serve as a cognate binding motif for WRKY transcription factors and strong DNA-binding of WRKY transcription factors to the TGAC core element is essential for their function (Eulgem et al., 2000). Functional W-boxes usually act in a cluster within short promoter regions and can act together cooperatively (Eulgem et al., 2000). Within the *SAG21* 1685 bp upstream region, a pair of W-box elements are present between -360 and -316, while another couple are clustered further upstream of the promoter region, serving as good candidates for WRKY binding. The confirmation of *SAG21* promoter interaction with specific senescence-regulated WRKY proteins is a crucial step to confirm whether these W-boxes are functional and to get a better understanding of their regulatory function.

As mentioned before, *SAG21* transcript levels peak just before visible yellowing and are then down-regulated in senescing leaves (Weaver et al., 1998). Transgenic *SAG21(1685)*::GUS plants did not exhibited any GUS expression in younger leaves but an occasional expression was observed in early senescing leaves localised sporadically to the interface between green and yellowing tissue. This could be correlated with a transient ROS increase or a shift to higher ROS levels seen in senescing leaves (Zimmermann et al., 2006). A role for ROS in the regulation of transcription factors at the interface between stress responses and senescence has been established (Robatzek and Somssich, 2001). Nevertheless, a more careful observation in all leaves of 8-week-old rosette in three separate biological experiments did not show any GUS activity at any stages except at the wounding sites (*SAG21* wounding induction is discussed further in Chapter 6). The cause of variability in the *SAG21* expression between plants is not known. Since *SAG21* is highly induced by oxidative stress, it is possible that an unintentional prime-stress in the earlier observation might have affected its later expression in leaves. The absence of *SAG21* expression in leaves in all developmental stages suggests that an important age-dependent expression regulator might be located further upstream of the investigated region (The *SAG21* upstream region extends up to ~3 kb).

Interestingly, in the shorter construct; *SAG21(325)*::GUS which contains only one W-box, promoter activity could be observed in all leaf stages suggesting that promoter elements between -325 and -1685 are acting as repressors of a basal leaf expression.

Perturbation of *SAG21* clearly has a dramatic effect on plant growth and development. Down-regulation of *SAG21* (*SAG21* antisense lines) resulted in earlier bolting time and earlier rosette senescence while the opposite effect was recorded for the over-expressors. An acceleration of flowering time and senescence was also observed in *wrky70* mutants (Ulker, et al., 2007) and over-expressor lines of *WRKY53* (Miao et al., 2004) suggesting that they might be candidates for positive and negative regulators of *SAG21*, respectively. An increase in ROS levels associated with bolting (Zimmerman et al., 2006) may be related to the effects of *SAG21* perturbation if the encoded protein has a role in protecting against ROS. Interestingly, knock-out plants of the antioxidative enzyme cytosolic ascorbate peroxidase (*APX1*), a main H_2O_2 scavenger, also had the same phenotype (Miller et al., 2007). Furthermore, constitutive expression of four proteins of obscure features (POF) which showed enhanced oxidative stress properties resulted in altered flowering time when grown under standard conditions (Luhua et al., 2008).

As well as accelerated senescence, *SAG21* antisense plants also exhibited a dwarf phenotype which has been previously reported in other oxidative stress mutants including *apx1* (Miller et al., 2007). More severe stunted growth was displayed in *mekk1* mutant plants (Nakagami et al., 2006), an upstream regulator of *WRKY53* (Miao et al., 2007). Growth suppression was also reported in leaf size of catalase-deficient plants (Vandenabeele et al., 2004). On the other hand, over-expression of *SAG21* resulted in biomass increase (Mowla et al., 2006). These results taken together suggest that the alteration of the cellular redox homeostasis (down-regulation of *SAG21*, *APX1*, *CAT2*, POFs and WRKYs) may enhance sensitivity towards stress, thus altering growth rate and finally resulting in stunted growth, earlier flowering, and premature senescence. Thus, the leaf senescence effect might be indirect due to elevated oxidative stress.

In addition to W-boxes, the *SAG21* promoter region also contains MYC recognition sites which regulate ABA signalling in abiotic stress responses (Shinozaki, Yamaguchi-Shinozaki and Seki, 2003). The MYC binding motif was also identified as the *cis*-element responsible for the binding of *MEKK1* to the *WRKY53* promoter (Miao et al., 2007). Recently, a microarray transcriptome analysis revealed that *SAG21* is up-regulated in *mekk1* plants as well as in knock-outs of its downstream regulators, *MKK1/2* and *MPK4* (Pitzschke et al., 2009) suggesting that *SAG21* might act downstream of WRKY TFs in the well-known H_2O_2 induced-MEKK1-MKK1/2-MPK4 signalling cascade. No evidence has been provided on whether the *SAG21* promoter interacts directly with any of the MAPK cascade components mentioned above. Figure 5-13 suggests a putative model regulating *SAG21*, with *MEKK1/2-MKK1-MPK4* and *WRKY53* as possible regulators.
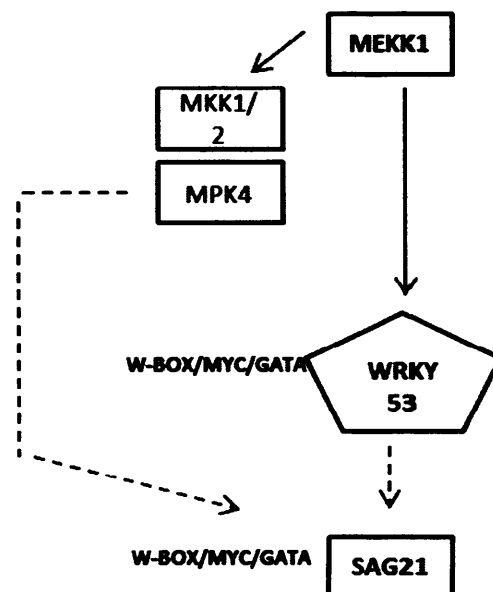
AG21 crosstalk.

arrows indicate

Another interesting phenotype was observed in *SAG21* antisense leaves. Although no qualitative data had been carried out, the antisense leaves appeared to be slightly thinner leaves compared to WT and the over-expressor. This phenomenon is consistent in both long-day and short-day grown plants. Different reactive oxygen intermediates (ROI) can alter cell wall properties mediating both cell wall loosening and tightening (Gapper and Dolan, 2006). H_2O_2 accumulation is correlated with lignification (Barceló et al., 2002) and cell wall rigidification by increasing cross-linking of polymers in differentiating tissues of many cell types including cellulose-rich cell walls in cotton fibres (Potikha et al., 1999). On the other hand, hydroxyl radicals which are abundant in cell walls of elongating organs (Liszkay, van der Zalm and Schopfer, 2004) regulate growth by promoting xyloglucan, pectin, and homogalacturonan depolymerisation hence allowing walls to expand (Gapper and Dolan, 2006). ROS-induced cell wall loosening is also involved in natural ripening of pear fruit (Fry, Miller and Dumville, 2002) which might have parallels to the mechanism governing senescence in leaves. A possible alteration of cell wall composition in *SAG21* antisense leaves suggests that this protein may be required indirectly in cell wall synthesis or biodegradation.

The effect of *SAG21* perturbation on below ground development is striking. The dosage series: over-expressor, WT, antisense, suggests that this gene is important even under optimal conditions for correct root development. Root hairs failed to elongate properly resulting in shorter root hairs in the antisense lines compared to the WT. Root hair elongation is driven by cell expansion, a process requiring efficient Ca^{2+} uptake (Carol and Dolan, 2006) and is also tightly regulated by localised ROS production by *RHD2* NADPH oxidase (Knight, 2007). A similar phenotype was observed in *rhd2* roots which were defective in ROS production and Ca^{2+} uptake hence compromising cell expansion (Foreman et al., 2003). Furthermore, knockouts of *MEKK1*, the upstream regulator of *MKK1/2* and *MPK4*, and *OXI1* kinase, the upstream upregulator of *MPK3/6*, that play major roles in oxidative-burst mediated signalling, also exhibited a short root hair phenotype. *SAG21* expression is independent of *OXI1* (Mowla et al., 2006) but might be regulated by the MEKK1-MKK1/2-MPK4 cascade (Pitzschke et al., 2009). These findings indicate that correct ROS regulation by redox-regulated proteins including *SAG21* is a pre-requisite for correct cell expansion in root hair elongation. Since ROS generation and signalling is essential for root hair growth (Gapper and Dolan, 2006), the role of *SAG21* may be in protecting cellular proteins against the ROS, thus a lack of *SAG21* may result in cellular damage thus reducing growth.

SAG21 is constitutively expressed in roots (consistent with previous northern analysis by (Mowla et al., 2006) mainly in the elongation and differentiation zone, but absent in the meristematic area (root tip). A similar expression pattern has also been reported in *RHD2* where its transcript is present in the elongation and differentiation zones, and during elongation of root hairs (Foreman et al., 2003; Takeda et al., 2008). Zone-specific expression appears crucial in determining *RHD2* function because Dunand, et al. (2007) showed that different ROS are located in different regions of the root and regulate different root development processes. H_2O_2 accumulates in the differentiation zone and cell wall of root hairs and plays a key role in root hair elongation, driven by cell expansion. Conversely, superoxide is more abundant in the meristematic area promoting primary root growth. The localisation of *SAG21* in the elongation zone and differentiation zone suggests that it is more involved in tissue growth regulated via cell expansion, resulting also in the root hair elongation defect in the antisense lines. However, a more detailed study of this expression pattern via cross-section may assist in further confirming this expression zone-function correlation. Constitutive root-expression was also reported in *OXI1::*GUS roots; however the specific expression region was not reported in detail (Rentel et al., 2004).

In addition to the root hair phenotype, *SAG21* antisense lines also exhibit shorter primary roots and less lateral roots compared to WT, while the opposite was observed in *SAG21*-OEX lines. Previously, Mowla et al. (2006) also showed that over-expression of *SAG21* resulted in increased primary root and lateral root length. Interestingly, *mekk1* mutants also showed slightly shorter roots and less lateral roots (Nakagami et al., 2006) consistent with the proposed role of *MEKK1* as an upstream regulator of *SAG21*. In *rhd2* mutants, the stunted root phenotype was more dramatic, 20% shorter than WT (Foreman et al., 2003) suggesting that ROS-regulated growth is not limited to tip-growing cells like root hairs. ROS have been shown to be present in rapidly growing cells of maize roots (Liszkay et al., 2004), cucumber and Arabidopsis seedlings (Renew et al., 2005). A real-time measurement of superoxide production in maize roots, which is then converted to the highly reactive hydroxyl (by peroxidation) revealed that the production of these ROS radicals is responsible for the cell wall loosening effect which leads to increased growth rate, hence resulting to up to a 50% increase in root cell length per hour (Liszkay et al., 2004). This evidence supports the participation of ROS in controlling rapid cell growth within the elongation zone of primary roots. However, the involvement of ROS in lateral root development has not been investigated to date.

Another possible explanation for the altered primary root and lateral root development in mutants of genes-encoding redox-regulated proteins is the involvement of growth-promoting hormones, such as auxin. ROS have been implicated as secondary messengers for auxin (Kwak, Nguyen and Schroeder, 2006). Auxin controls both cell division and cell expansion and thereby orchestrates many developmental events and environmental responses. Auxin regulates lateral root initiation, root and stem elongation and leaf expansion (Strader et al., 2010). Furthermore, auxin also induced ROS production in roots and the auxin transport inhibitor, N-1-napthylphthlamic acid (NPA) did not inhibit H_2O_2-induced root curvature, leading to the suggestion that ROS play a role downstream of transport in auxin signalling and gravitropism (Joo, Bae and Lee, 2001). Altered expression of several auxin-induced and auxin-responsive genes in the *mekk1* mutant (Nakagami et al., 2006) and repression of auxin responses in maize protoplast regulated by H_2O_2-MAPK (Joo et al., 2001) further support the crosstalk between ROS homeostasis and hormone responses.

Under optimal conditions, *SAG21* also exhibited a very high expression in cotyledons and pollen (Mowla et al., 2006) and also indicated by data presented here. The cotyledon-specific expression could be compared to root hair development because growth of both organs is driven by cell expansion which is regulated by ROS. In Arabidopsis, after germination, the cotyledons grow solely by cell expansion without cell division (Mansfield and Briarty, 1996). Strong pollen expression confirms reports from the microarray data (Affymetrix) and fits well with the classical role of LEAs in dehydrated tissues. Five other members of the LEA family in Arabidopsis are also expressed in pollen (*At4g20450, At1g54410, At1g76180, At2g23120, At2g40170*). The tip growth of pollen tubes parallels that of root hairs (Carol and Dolan, 2006). In fact, an important advance in the pollen tube growth field in recent years revealed a tight-regulation between tip-accumulation of ROS and a tip-focused Ca^{2+} gradient in tobacco (Lee and Yang, 2008). The suppression of *NtNOX* (*Nicotiana tabacum* NADPH oxidase) as well as treatment with its inhibitor, inhibited ROS production and pollen tube growth. It was also shown that *NtNOX* and ROS localized to the growing pollen tube tip (Potocký et al., 2007). Furthermore, exogenous application of H_2O_2 rescued the phenotype of *NtNOX*-suppressed plants (Potocký et al., 2007), mirroring the exogenous ROS effect (Foreman et al., 2003) observed in *rhd2* mutants discussed earlier. Pollen NADPH oxidase activity has also been previously reported in 10 weed species,10 grasses and 20 trees (Carol and Dolan, 2006). These discoveries imply that tip accumulation of ROS is an important hallmark of tip-growing cells and the NADPH oxidase-dependent ROS serves as a common regulatory

mechanism for tip-growth in plant cells (Lee and Yang, 2008). *SAG21* antisense plants appeared to be normally fertile. However it is well-known that the CamV 35S promoter is poorly expressed in pollen (Wilkinson, Twell and Lindsey, 1997). Further investigation of pollen tube growth and seed production in AS lines of *SAG21*, where expression is also reduced in the pollen, would be interesting to determine if the *SAG21* expression in pollen is a requirement for normal pollen tube growth.

In addition to the tissue-specific expression, *SAG21* also appears to be light-repressed. This confirms northern blot analyses from Mowla et al. (2006). This light-regulation correlates with the abundance of GATA-boxes and GT1 *cis*-elements within the 1685 bp upstream region. A CIRCADIANLELHC *cis*-element which regulates circadian-dependent expression in tomato (Piechulla et al., 1998) was also identified. However, *SAG21* does not appear to be subject to circadian regulation (Harmer et al., 2000). The transient expression observed in leaves prior to senescence is most likely caused by the oxidative burst (H_2O_2 accumulation) during bolting time (Zimmermann et al., 2006) or could be contributed by ROS accumulation caused by chloroplast degradation occurring at senescence.

5.5 Summary

To gain a better knowledge of the role of *SAG21* during normal plant development in *Arabidopsis*, the expression of two GUS constructs fused to *SAG21* upstream regions: *SAG21(1685)*::GUS and *SAG21(325)*::GUS was analysed in transgenic Arabidopsis lines followed by phenotypic characterization of over-expressor and antisense plants. Generally, *SAG21* is highly expressed in roots, cotyledons, and pollen but absent in the rosette. Its dark-induced promoter activity agrees with previous northern analysis. Under optimal growth conditions, down-regulation of *SAG21* resulted in stunted growth, earlier bolting time and earlier senescence. In addition, knock-down seedlings also have shorter roots and shorter root hairs. The opposite effects were observed in the over-expressor lines. Although no direct senescence-effect was observed, these phenotypes clearly indicate that *SAG21* is required for correct growth and development especially involving cell expansion/elongation. Furthermore, similar phenotypes were reported in several important redox-regulator and auxin mutants suggesting that *SAG21* may be involved in some way in a crosstalk between ROS and auxin pathways.

Chapter 6: Expression pattern and functional analysis of ROS-induced gene; *SAG21* during stress

6.1 Introduction

Consistent with the ROS-inducible property of *SAG21* and proposed function in oxidative stress protection, *SAG21* transcripts have also been shown to be up-regulated by all key phytohormones abscisic acid (ABA), salicylic acid (SA), jasmonic acid (JA), and ethylene (ET) (Weaver et al., 1998; Schenk et al., 2000; De Paepe et al., 2004; Mowla et al., 2006; Jung et al., 2007). Furthermore, microarray database and northern blot analysis indicate *SAG21* up-regulation upon abiotic (Weaver et al., 1998; Mowla et al., 2006; Hundertmark and Hincha, 2008), biotic (Pegadaraju et al., 2005; Pegadaraju et al., 2007) and oxidative stress (Miller, Arteca and Pell, 1999; Mowla et al., 2006; Tosti et al., 2006). Nevertheless, most of the studies done so far are mainly limited to gene expression studies and might not reflect the activity of the functioning protein and its main role in plant defence.

Plants undergo continuous exposure to various abiotic and biotic stresses in their natural environment. As sessile organisms, plants have evolved intricate mechanisms to perceive signals, allowing optimal responses to environmental conditions. Both biotic and abiotic stresses can result in increased synthesis of secondary metabolites such as phytoalexins, ion fluxes, an oxidative burst, and changes in the transcription of an array of genes (Cheong et al., 2002). Furthermore, biotic and abiotic stresses induce the expression of both distinct and overlapping set of genes (Schenk et al., 2000; Seki et al., 2002). ABA, SA, JA, and ET are endogenous, low molecular weight molecules that regulate the protective responses of plants via synergestic and antagonistic actions (Anderson et al., 2004; Yasuda et al., 2008), which are referred to as signalling crosstalk. ABA is extensively involved in responses to abiotic stresses such as drought, cold and osmotic stress. In contrast, SA, JA, and ET play central roles in biotic stress signalling upon pathogen infection. The generation of ROS has been proposed as a key process that is shared between both types of stresses thus acting as a common signal triggering downstream processes (Apel and Hirt, 2004; Fujita et al., 2006).

Plants respond to infection using a two-branched innate immune system (Jones and Dangl, 2006). The first branch recognizes and responds to a broad spectrum of slowly-evolving microbes, including non-pathogens referred to as pathogen-associated molecular patterns (PAMPs), such as flagellin and chitin (Gómez-Gómez, Felix and Boller, 1999; Gómez-Gómez and Boller, 2002). The activation of this basal defence results in PAMP-triggered immunity (PTI). The second layer requires the suppression of PTI by effector proteins (virulence factors) thus activating a stronger defence response: effector-triggered immunity (ETI). ETI results in disease resistance which is usually governed by the hypersensitive response (HR) at the infection site (Jones and Dangl, 2006). Two main pathogen groups are biotrophs and nectotrophs. Biotrophs infect plants by growing on living tissue while nectotrophs kill host tissue during colonization (Jones and Dangl, 2006). ETI is only effective against biotrophs but not necrotrophs (Glazebrook, 2005).

The flagellin (*flg22*) PAMP-triggered immunity signal transduction from receptors to downstream components is activated via the SA/redox-mediated MAPK cascade; MEKK1-MKK1/2-MPK4 (Mizoguchi et al., 1996; Suarez-Rodriguez et al., 2007). Loss-of-function in *mekk1*, *mkk1/2* and *mpk4* resulted in accumulation of SA, H_2O_2 and pathogenesis-related (*PR*) genes accompanied by enhanced pathogen resistance, dwarf phenotype and spontaneous cell death indicating a negative regulation of plant defence response by these genes (Nakagami et al., 2006; Su, Suarez-Rodriguez and Krysan, 2007; Gao et al., 2008). This cascade (Fig. 6-1) can regulate the production of the antimicrobial phytoalexin, camalexin. A complex that includes MPK4-MKSI-*AtWRKY33*, the downstream effectors of the MEKK1-MKK1/2 cascade, regulated the transcription of *PHYTOALEXIN DEFICIENT3 (PAD3)* (Qiu et al., 2008a; Qiu et al., 2008b). *PAD3* encodes the cytochrome P450 monoxygenase 7B15, an enzyme required in the last step of camalexin biosynthesis (Zhou, Tootle and Glazebrook, 1999). Upon *flg22* treatment, *AtWRKY33* is released from the complex and binds to the W-box of the *PAD3* promoter (Qiu et al., 2008a). Both *atwrky33* and *pad3* mutants exhibited increased susceptibility to the fungal necrotrophs, *Botrytis cinerea* and *Alternaria brassicicola* (Thomma et al., 1999b; Zhou et al., 1999; Zheng et al., 2006). However, no altered sensitivity was observed against the biotroph bacterium, *Pseudomonas syringae* in both mutants indicating that *PAD3*-derived camalexin is fungal/necrotroph-specific (Nafisi et al., 2007; Qiu et al., 2008a).
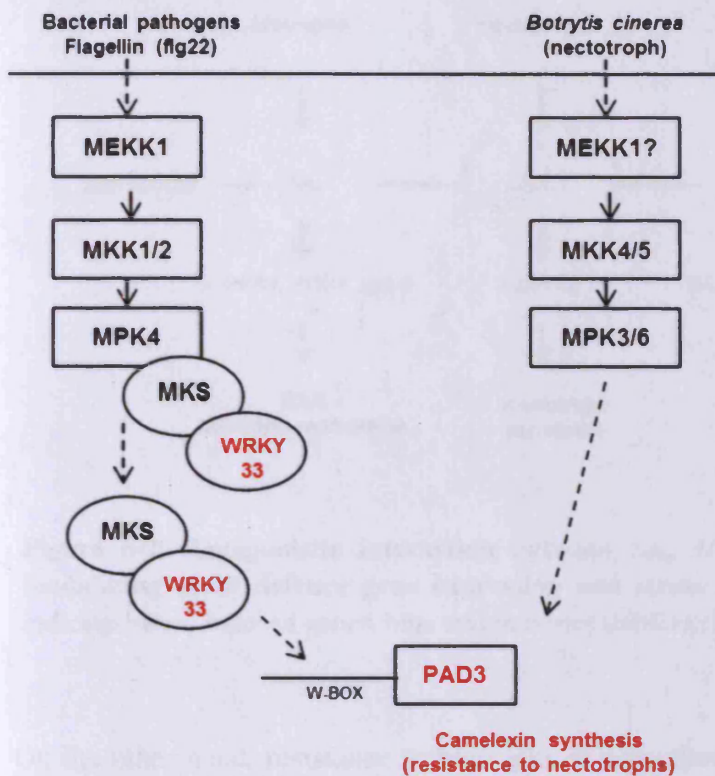
Figure 6-1. MAPK cascades mediates PAD3-dependent camalexin synthesis resulting in nectotroph resistance. In Arabidopsis, in response to flagellin (*flg22*), WRKY33 is released from the MPK4-MKS-WRKY33 complex, and then binds to and activates the transcription of the PAD3 promoter. Upon *Botrytis* infection, MPK3/MPK6 cascade upstream of PAD3 regulates camalexin production through transcriptional regulation of its biosynthetic genes.

In addition, the MKK4/5-MPK3/6 cascade also plays a key role in *PAD3*-camalexin synthesis (Figure 6-1). *mpk3/mpk6* mutants were compromised in camalexin production and consequently were more susceptible to *Botrytis cinerea* (Ren et al., 2008). Resistance to *Botrytis cinerea* regulated via the *PAD3*-camalexin pathway is independent of SA, JA and ET (Ferrari et al., 2007) and is strictly separated from the *Botrytis cinerea* resistance regulated via the JA/ET-regulated defence gene, *PDF1-2* (Thomma et al., 1999a) (Fig. 6.2). Furthermore, constitutive expression of SA-mediated genes resulting in systemic acquired resistance (SAR) promote *Botrytis* infection (Govrin and Levine, 2000), while mutants impaired in SA-signalling also do not appear to affect systemic responses towards *Botrytis* (Thomma et al., 1998) hence confirming that *Botrytis* resistance is not regulated by SA. *Botrytis* infection causes necrotic lesions accompanied by increased ROS levels but does not induce a form of programmed cell death (PCD) (Govrin and Levine, 2000).
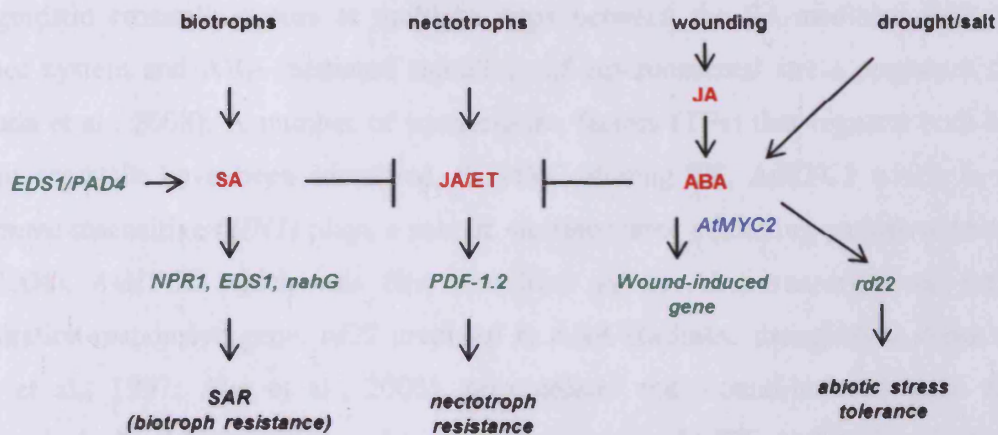
Figure 6-2. Antagonistic interaction between SA, JA/ET and ABA signalling pathways modulating plant defence gene expression and stress resistance in Arabidopsis. Green text indicates stress-induced genes, blue text indicates transcription factor.

On the other hand, resistance to biotrophs is dependent on SA-mediated plant defence gene activation (Ton et al., 2002). This involves both PTI and ETI which may lead to the resistance to a broad spectrum of pathogens often referred as systemic acquired resistance (SAR). SA negatively regulates JA/ET-regulated defence genes (involved in necrotroph resistance) (Fig. 6-2), thus perturbation of genes impaired in SA signalling like *NONEXPRESSOR OF PR-1* (*NPR1*), salicylate hydroxylase (*nahG*), *ENHANCED DISEASE SUBCEPTIBILITY-1* (*EDS1*) and *PHYTOALEXIN4* (*PAD4*) usually results in increased susceptibility towards biotrophs (Cao et al., 1994; Delaney et al., 1994; Zhou et al., 1998; Wiermer, Feys and Parker, 2005). *EDS1* could form a complex with *PAD4* which then activates SA signalling and mediates the antagonism between JA/ET signalling (Fig. 6-2). This complex was shown to tranduce redox signals in response to certain biotic and abiotic stresses (Mateo et al., 2004; Feys et al., 2005). Further studies indicated that *PAD4* could function independently of *EDS1* in aphid-phloem feeding defence. Interestingly, *PAD4* was also shown to regulate three SAGs: *SAG21, SAG13* and *SAG27* upon aphid infection (Pegadaraju et al., 2005; Pegadaraju et al., 2007). In addition, *PAD4* functions upstream of SA regulating bacterial-specific camalexin production in Arabidopsis (Zhou et al., 1998) and its expression is a prerequisite for *AtWRKY33* activation (Lippok et al., 2007).

Antagonistic crosstalk occurs at multiple steps between the SA-mediated SAR pathogen defence system and ABA-mediated signalling of environmental stress responses (Fig. 6-2) (Yasuda et al., 2008). A number of transcription factors (TFs) that regulate both biotic and abiotic crosstalk have been identified. A MYC-binding TF, *AtMYC2* which is allelic to jasmonate-insensitive *(JIN1)* plays a role in multihormone signalling pathways (Anderson et al., 2004). *AtMYC2* which was first identified as an ABA-transcriptional activator of dehydration-responsive gene, *rd22* involved in ABA-mediated drought/salt stress signalling (Abe et al., 1997; Abe et al., 2003), up-regulates the wound-induced gene expression regulated via the JA signalling and negatively regulates JA/ET-mediated pathogen defence genes (Abe et al., 1997; Abe et al., 2003; Anderson et al., 2004). Moreover, *atmyc2* mutants were less sensitive to ABA and displayed enhanced resistance to necrotrophs (Anderson et al., 2004; Lorenzo et al., 2004). Another key regulator of the stress crosstalk, JA-mediated *AtMYB108* (previously known as *BOTRYTIS SUSCEPTIBLE1; BOS1)* belongs to the *R2R3-MYB* TF family (binds to MYB *cis*-element). *bos1* mutants showed enhanced susceptibility to several necrotrophs, as well as serious impairment in responses to drought, salinity and oxidative stress (Mengiste et al., 2003).

As mentioned before, ROS elevation has been proposed as the common signal mediating both abiotic and biotic stress (Fujita et al., 2006). The ROS regulation is mainly governed by the redox status of the plant controlled by reactive oxygen intermediates (ROIs) and an effective antioxidative system (Apel and Hirt, 2004). The ability of ROS to interact with ABA (Guan, Zhao and Scandalios, 2000) and SA (Torres, Jones and Dangl, 2006) and other signalling pathways such as Ca^{2+} -mediated MAPK regulation (Jaspers and Kangasjärvi, 2010; Torres, 2010) has significantly contributed to the complexity of the regulation at the perception and transduction level. However, the identification of further possible targeting of downstream effectors involved in the execution process such as ROS-mediated TFs and stress-induced protein like LEA proteins is a crucial step on establishing the overall crosstalk occurring in ROS regulation of both abiotic and biotic stress.

Thus, in this chapter, transcriptional regulation of *SAG21* upon abiotic and biotic stress is reported. Furthermore, the effect of *SAG21* perturbation towards pathogen resistance was characterized in *SAG21* over-expressor (OEX) and *SAG21* antisense (AS) plants compared to WT in order to understand the function of *SAG21* in plant defence.

6.2 Materials and methods

6.2.1 *In silico* promoter analysis

1685 bp upstream region of *SAG21* was screened for *cis*-acting regulatory elements using the PLACE (Higo et al., 1999) and the PlantCARE (Lescot et al., 2002) database.

6.2.2 Arabidopsis lines

Homozygous transgenic Arabidopsis lines carrying promoter constructs *SAG21(1685)*::GUS (lines: T3-2-6, T2-3-5) and *SAG21(325)*::GUS (lines: T2-5-6, T2-5-8) were used for abiotic stress analysis. Additionally SAG21-OEX, SAG21-AS (2) and WT were used for biotic stress analysis (details of these lines are provided in section 2.4)

6.2.3 Abiotic stress treatments

To eliminate background (dark-induced) *SAG21* expression, seedlings were pretreated with continuous light. Seeds were germinated normally, but at 8 DAS (days after sowing), seedlings were exposed to 12 hours light (approx. 300-400 μmol m^{-2} s^{-1}) prior to stress treatments. Drought treatment was applied by removing the seedlings onto filter paper and subjecting them to 30 min air flow in a laminar air flow cabinet. For cold treatment Petri dishes were placed onto crushed ice for 30 min. For salt and oxidant treatments, Petri dishes were flooded with 1-2 ml of 150 mM NaCl, or 10 mM H_2O_2 respectively for 1 h prior to analysis. Untreated seedlings were used as controls. All treatments were under continuous light. In all experiments, at least three replicate plants for each line were used. Histochemical GUS staining and fluorometric GUS analysis were performed as described in section 2.17. Fluorometric H_2O_2 analysis using an Amplex-Red Hydrogen Peroxide/Peroxidase Assay Kit (Molecular probes, Eugene, USA) was performed as described in section 2.18.

6.2.4 Biotic stress treatments

6.2.4.1 Plant growth

Plants used for pathogen inoculation experiments were transferred from 1 x MS 1% agar to Levington Universal compost and placed in Polysec growth rooms (Polysec Cold Rooms Ltd., Worcester, Worcs, UK) fitted with six Sylvania Lynx Delux 840 fluorescent tubes (International lamps Ltd., UK) per shelf providing a light intensity of 160 μmol m^{-2} s^{-1} at shelf height, maintained at 24 °C with an 8 h photoperiod. In all experiments at least three replicate plants for each line were used.

6.2.4.2 Pathogen inoculation

Botrytis cinerea (strain iMi 169558, International Mycological Institute, Kew, U.K.) was maintained on potato dextrose agar (PDA; Oxoid Ltd., UK). *Botrytis cinerea* conidia were harvested from the surface of the plates in a carrier media with sterile PDB (Formedium, UK) and diluted accordingly to 1 x 10^5 spores mL^{-1} as determined using a Neybauer Haemocytometer. *B. cinerea* spores (5 μL) were applied onto the adaxial surface of the leaf of 5-week-old Arabidopsis rosettes. A relative humidity of 50-80 % was obtained by keeping the plants under Stewart Micropropagators (H. Smith plastics Ltd. UK).

Strains of *Pseudomonas syringae* pv. *tomato* DC3000 were cultured on nutrient agar (Sigma-Aldrich Ltd., UK) at 28 °C. A single colony was inoculated into 10 mL nutrient broth (Sigma-Aldrich Ltd., UK) and incubated overnight at 28 °C with shaking. Subsequently, the bacteria were harvested by centrifugation (650 x g for 10 min) and resuspended to a bacterial cell density of 10^6 cfu mL^{-1} determined spectrophotometrically (OD560=0.1). The bacterial suspension was injected into the abaxial side of Arabidopsis leaves using a 1 mL sterile needleless plastic syringe (BD plastipak, Madrid, Spain).

6.2.4.3 Pathogen growth analysis

Infected plants were assayed at time intervals of 3, 6, 12, 24 and 48 hours post inoculation (hpi). Inoculated leaves were stained for GUS as described in section 2.17.

For examining growth of *Botrytis cinerea* fungal hyphae, infected leaves were autoclaved at 121 ^{0}C in 1 M KOH for 2 min. Following rinsing three times in sterile distilled water, the samples were mounted on glass slides in several drops of freshly prepared 0.05% water soluble analine blue dye (Sigma-Aldrich Ltd., UK) in 0.067 M potassium buffer pH 9. Aniline blue stained leaves were observed using a fluorescence microscope (Olympus BX51 microscope (Olympus America Inc, PA, US) coupled with a Nikon Coolpix 990 camera (Nikon, Tokyo, Japan).

For determining bacterial growth in *Pseudomonas syringae*-infected leaves, single cores from three individual lesions were ground in 500 μL of 10 mM phosphate buffer (pH 7). Serial dilutions of the homogenous extract were plated onto nutrient agar (Sigma-Aldrich Ltd., UK) supplemented with 50 μgml^{-1} rifampicin. Following incubation at 28^{0}C for 2 days, colonies were counted and the original population size was determined. Bacterial populations were expressed as colony forming units (cfu) per leaf.

6.3 Results

6.3.1 Analysis of *cis*-regulatory elements in the *SAG21* promoter

As seen in many other stress-related genes such as *AtWRKY33*, the upstream region of *SAG21* contains several putative W-boxes, MYC binding sites (described in Chapter 5), two MYB binding sites (-786, -827) and two TGACG motifs (-298, -1172) (Fig. 6-3). In addition, the investigated region (1685 bp upstream of the ATG) also included four anaerobic ARE-elements (-17, -178, -1195, -1266, -1533) and 15 ozone-responsive Dofcore elements. Other stress responsive elements include a TCA SA-responsive element and TC-rich repeat at locations -1237 and -133 respectively. The number and occurrence of each *cis*-regulatory element included within the promoter constructs *SAG21(1685)::*GUS and *SAG21(325)::*GUS are summarized in Table 6-1.

6.3.2 *SAG21* promoter response to abiotic stress

GUS staining revealed strong up-regulation of *SAG21* expression in *SAG21(1685)::*GUS root seedlings exposed to all stresses (Fig. 6-4a). Expression was detected both in the elongation and differentiation zones of the root, but excluded from the lateral root tips and primordia. The strongest effect was exhibited by cold followed by a similar up-regulation level by drought, salt and H_2O_2. This observation was further confirmed quantitatively with cold inducing a 14 fold up-regulation compared to the control (Fig. 6-5). Drought, salt and H_2O_2 induced *SAG21* expression at 5, 10 and 6 fold, respectively compared to controls.

```
-1685  TAATCTCCAAAACATTGTGAAAAATTGGGGGTTTTTTTTATCATTTAAATTGTCTATAGTGGTCAATCATTATTAAAAAA
                                                                       W-BOX

-1605  AATTGTTTTTGTTGAAATTTTAAATTATAAAAAAAAAACACGTTTATACATAAAATGCAAAAACTTTTCTTAAACCAAA
                                                                                 ARE

-1525  TTACAGAGAAAGGCTATCACCATCCTTGTCTTGATGCCAACCACACTTGTAATCCCAAAATACATACTTAAACTATACTA
            DOFCORE                                 MYC

-1445  TACTAACATGAATTGGTTATACGATTATCTATCTAGTTAGCTACATAATTCATATAATTAGTTTTTTAAAATATACTTAT

-1365  GTAATGATAGTAACTAAAAAATATACTATCTCGAGAAATCCAACCAAAATGCTATGATAGTATATAAAATAAAATGAAAG

-1285  AAAGAGGAACCAAGTTGTGAAACCATTTACCAAGAAGAAGAAGAAAAAAACAAGATGGTCGAGTCTCGTGATAGTATGAA
                              ARE                          TCA

-1205  GCTGGGGCCGAAACCACGAATCAAAGAACCATTTGAACGATGCAACTGGTCATCGATAACCAATCAATAGAAACTCCACCG
                    ARE              MYC TGA   MYC

-1125  CCTCAAAATATCATAGTGCTATTTAATTTTTCATACTATCATTTATTGTAGGCTATAACATATTTTGTATTGTAGATGG

-1045  ACGGCTAGTACACGCAAGTTAGTCAATAAACTTTTAACAAATGGCATCTTGACATGCTTAAACACATTTTATAATTCGAA
                           W-BOX             MYC

-965   CCTCACTTTGCCTACTTTACACACGTCTACTTATAGTAGATGAGCATCAATCATTGAACCGTTCGTATAATACAATTTTT

-885   TTTTTGTAATACGTTATAATTAGAAAGTAATGGAAAATAAGTTGAAACACAAATTTTAACGGTTTACTAAGATTTAAT
                                                                 MYB

-805   TTTACAATTTTCAAAATATAACCGAATTATTTAAATCGTATTAAATTTATAATTAATTTTCTAAAAAAAAACACAGATTA
                         MYB

-725   AAAAAATATATTAAAACTAATCATAAATATATTAATTTTTGTAATTTATATTTTTTTATAACTTTAAACTAATAATATTC

-645   AATTATTTATCTTAAAGTTTACAAATTATCAATAATAACTAATAAATAATGCATAAAAACTTTTTAAAAATTAACTTTTT

-565   GAAACAAATTTTTTTCTAAAAAATTAAATAATAAAGAACAGAAAAAATATTATTCAACTAAAAATATTGGATAATAACTC

-485   TGAAAGTTTGCATTTTTCAAATAAATCATTGATTTTTTTTGTTTGACATAAAACATTAATTTCCCCTTGTAAATCACACA

-405   TTTAAAATCTAACTATATTTAAACAAAAAAAAAAAGTCCAATTTTGACTTTAATTATATAAAAAAAGCAAAGCTAATTAT
                                                 TTGACT
                                                 W-BOX

-325   CGGTCAAAAGACTCAAAGGCCAGAATTGACGCAGCCGTTTATGAGAAGTGAGAAGACAATTTCGGAGTCACTTCCTTTAT
         W-BOX              TGACG
         W-BOX              TGA

-245   TTCCTCTCTTCCTTCACTCTCTCCTATATAAACCTTCCTCTCCTCTTCCTCTCTTCTCATCTCTTCAAACCATTTTCGAA
                                                                         ARE

-165   AGCCTTGAGAGAGAGAACACAGACGATACCAACTTTCTTCAATCTCGTTGCCGCAGTATAATTATCTCATTCCTCGGATA
                                     TC-RICH

-85    TATCTCTCCTTCTGCGGCGGCGACAAGAAGCTACAAGAATAAAAAGTCTGTTTTCTCTCTTTTCAAGAAACCACTTACTT
                                                                         ARE

-5     CGAAA ATG
```

Figure 6-3. *SAG21* upstream regions of ATG. Nucleotide sequences representing potential *cis*-regulatory elements present on the positive strand (underlined) and negative strand (dotted underlined) are labelled as follows: W-box (yellow box); and MYC/MYB motifs (cyan box); TGACG motifs (green text); ARE-elements (red text); Dofcore elements (gray box); TCA SA-responsive element (light blue text); and TC-rich repeats (dark blue text). Black arrow indicates the fragment included in the shorter construct (325 bp).

Table 6-1. Number (n) of different *cis*-regulatory elements within *SAG21* upstream regions; 1685 bp and 325 bp respectively. These elements are known to be involved in stress-responsive and oxidative stress regulation.

cis-element	sequence	1685 bp (n)	325 bp (n)
Abiotic/biotic stress-responsive elements			
W-BOX	TTGACY	4	1
MYC CONSENSUS	CANNTG	4	-
MYB CONSENSUS	YAACKG	2	-
TGACG motif	TGACG	2	1
TCA	CCATCTTTT	1	-
TC-rich repeats	ATTTTCTTCA	1	1
Anaerobic/ozone responsive elements			
ARE-element	AAACCA	5	2
Dofcore element	AAAG	15	4

(Y= C/T, N=A/T/G/C, K=G/T)

*SAG21(325)::*GUS roots displayed a slightly different response towards specific stresses. Notably, the GUS expression was only detected specifically in the stele, but neither in the epidermal nor cortex layers (Fig. 6-4b; black arrow). Despite the massive deletion in the promoter construct, a strong response towards drought was detected (Fig. 6-4b). However, only mild expression was observed following salt and cold stress treatments. Almost no GUS staining was detected by exogenous application of H_2O_2. Quantitative GUS activity analysis indicated that the up-regulation by drought was significantly higher than the control (19-fold) though similar to drought-treated seedlings of the *SAG21(1685)::*GUS line (Fig. 6-5). In addition, both cold and salt also elicited 9- and 11-fold increases in activity, respectively, compared to the control, although these increases were less pronounced than with the 1685 bp promoter construct.. However, expression following H_2O_2 treatment did not induce any significant GUS activity in the 325 bp construct line compared to control. In parallel with the GUS activity analysis, the relative H_2O_2 produced in whole seedlings in control and stressed

conditions were also determined using fluorometric detection methods (Amplex Red). The results indicated clear ROS accumulation upon all stresses compared to the control (Fig. 6-6).

SAG21(1685)::GUS
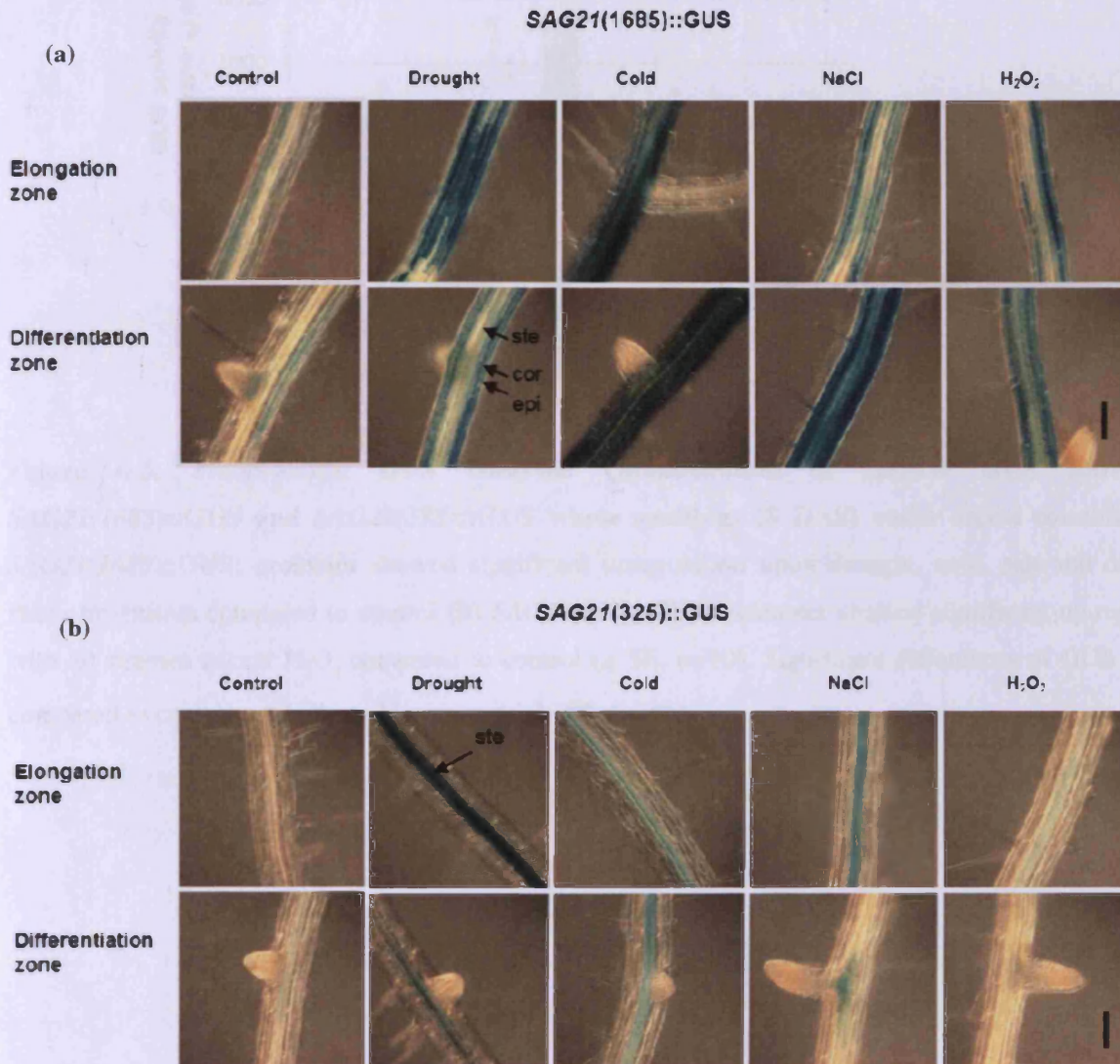
SAG21(325)::GUS

Figure 6-4. Histochemical GUS staining: response of *SAG21* promoter to abiotic stress in *SAG21(1685)*::GUS and *SAG21(325)*::GUS root seedlings (8 DAS). (a) *SAG21(1685)*::GUS; promoter responded to all stresses with highest expression detected in cold-treated roots. The expression could only be observed in stele (ste), cortex (cor) and epidermis (epi) tissue layers **(b)** *SAG21(325)*::GUS; promoter showed strong response towards drought but a milder up-regulation could also be detected in cold and salt-treated roots. No expression was detected with oxidative stress (H_2O_2). The expression could be only be observed in the stele (ste) tissues. Scale bar = 100 μm.

148
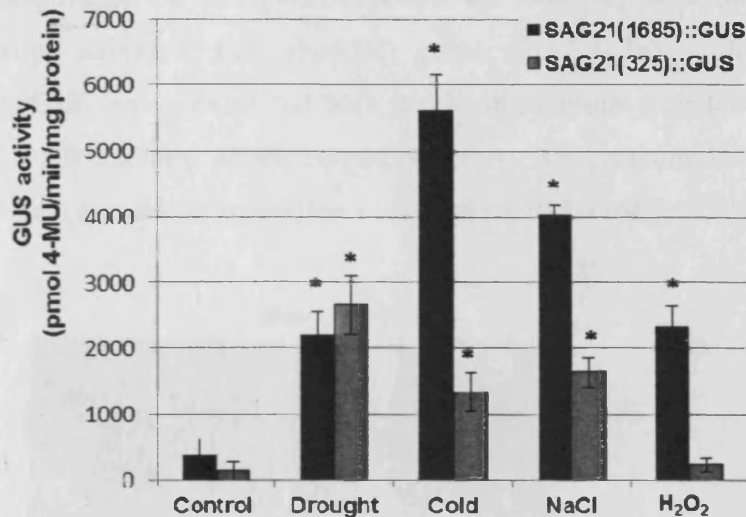
Figure 6-5. Fluorometric GUS analysis: Quantification of relative GUS activity in *SAG21(1685)*::GUS **and** *SAG21(325)*::GUS **whole seedlings (8 DAS) under stress conditions. (a)** *SAG21(1685)*::GUS; promoter showed significant upregulation upon drought, cold, salt and oxidative stress treatments compared to control **(b)** *SAG21(325)*::GUS; promoter showed significant up-regulation with all stresses except H_2O_2 compared to control (± SE, n=10). Significant differences of GUS activity compared to control are indicated by an asterisk (*$P<0.001$).
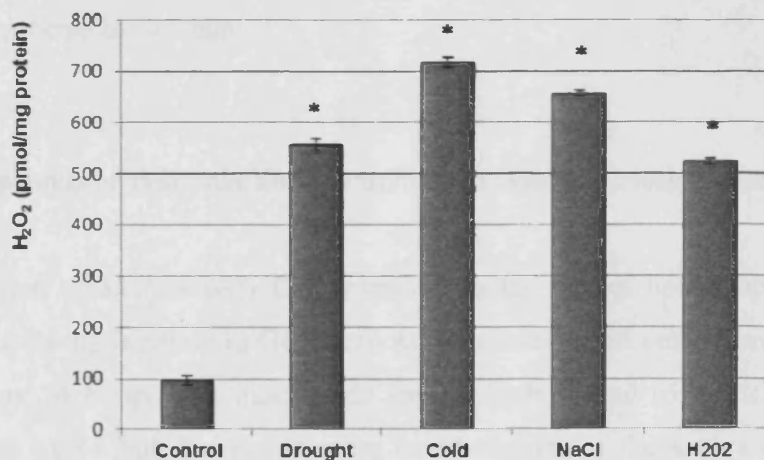

Figure 6-6. Fluorometric Amplex Red analysis: Quantification of relative H_2O_2 levels in whole seedlings (8 DAS) under control and stress conditions. Mean (±SE, n=9) H_2O_2 levels were significantly higher in all stress-treated seedlings compared to control. Significant differences of H_2O_2 level compared to control are indicated by an asterisk (*$P<0.001$).

Similar experiments with young leaves did not result in up-regulation of the *SAG21* expression in either of the two lines (Appendix-C). However, wounding *SAG21(1685)::*GUS leaves locally activated the reporter gene (Fig. 6-7a). Interestingly, wounded *SAG21(325)::*GUS leaves exhibited both local and systemic activation of the reporter gene. In addition, DAB staining which corresponded to H_2O_2 accumulation coincided with the GUS localization around the wounding sites in the *SAG21(1685)::*GUS leaves (Fig. 6-7b).
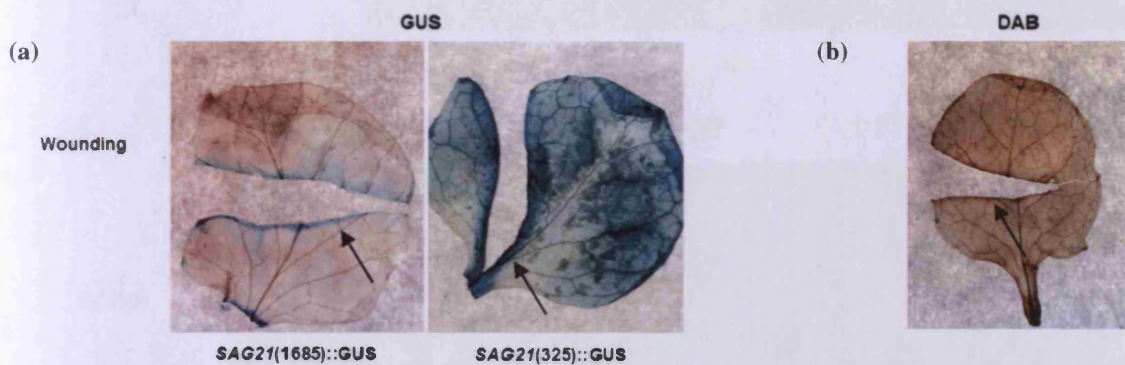

Figure 6-7. Histochemical GUS and DAB staining: Effect of wounding on *SAG21* promoter activity (GUS staining) and on H_2O_2 levels (DAB staining) in *SAG21(1685)*::GUS and *SAG21(325)*::GUS mature leaves. (a) *SAG21(1685)*::GUS promoter activity was localized to the wound sites (left panel) while *SAG21(325)*::GUS activity was both localized and systemic (right panel) (b) H_2O_2 level were up-regulated and localized to wounding sites. Black arrows indicate leaf wounding sites. Scale bar = 5 mm.

6.3.3 *SAG21* promoter response and perturbation effect to biotic stress

Upon inoculation of *SAG21(1685)*::GUS plants with the fungal necrotroph; *Botrytis cinerea* (*B. cinerea*), a strong increase in GUS activity was detected in cells immediately around the necrotic lesions 24 hours post inoculation (hpi) which spread to a wider area around the inoculation site by 48 hpi, but not to more distal regions of the leaves (Fig. 6-8a). To test whether perturbation of *SAG21* expression affected pathogen growth, growth of fungal hyphae was investigated in *SAG21*-OEX and *SAG21*-AS lines compared to WT. Whilst fungal germination and growth was observed in WT and the *SAG21*-AS plants after 24 h, very little was found in the *SAG21*-OEX line (Fig. 6-8b). Nevertheless, by 48 h, equivalent hyphal development was observed in WT and the transgenic lines.
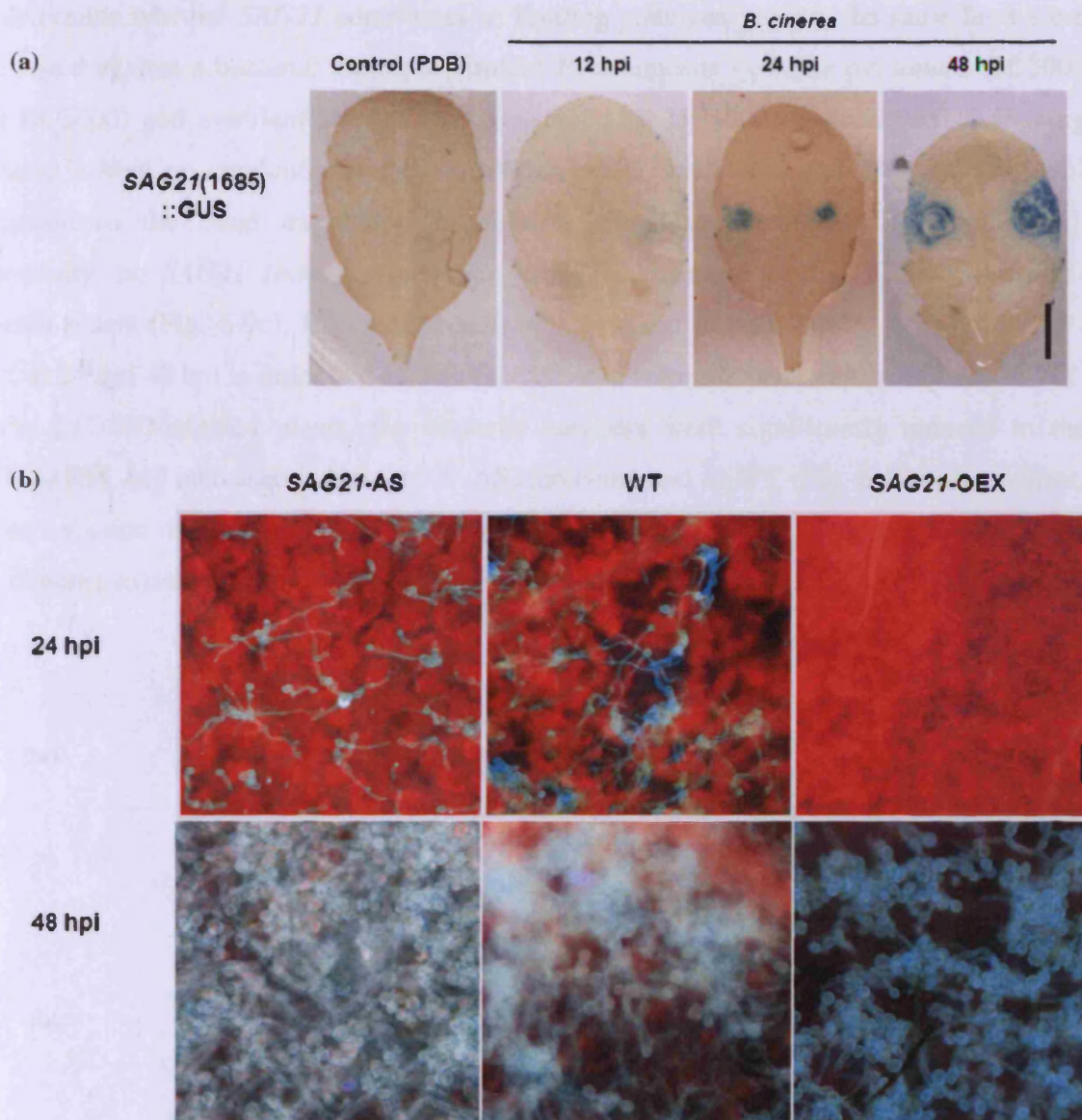
Figure 6-8. Histochemical GUS and aniline blue staining: Response of *SAG21* promoter to *Botrytis cinerea inoculation* and effects of *SAG21* expression on *Botrytis cinerea* growth (a) GUS expression (*SAG21(1685)*::GUS) was detected at inoculation sites at 12, 24 and 48 hours post inoculation (hpi). Scale bar = 10 mm. **(b)** *SAG21*-AS displayed growth of more fungal hyphae at 24 hpi compared to WT. The opposite effect was observed in *SAG21*-OEX transgenic plants. Scale bar = 50 µm.

To determine whether *SAG21* contributes to limiting pathogen growth, the same lines were also tested against a bacterial biotroph: virulent *Pseudomonas syringae* pv. *tomato* DC3000 (*Pst* DC3000) and avirulent *Pst* DC3000 *avrRpm1* (*Pst* DC3000 *avrRpm1*). GUS staining revealed a high up-regulation in *Pst* DC3000-infected plants at 6 and 24 hpi (Fig. 6-9b) compared to the basal expression in controls (inoculated with MgCl$_2$) (Fig. 6-9a). Conversely, no *SAG21* promoter induction could be detected in *Pst* DC3000 *avrRpm1*-infected plants (Fig. 6-9c). Bacterial growth was assessed in both *SAG21*-AS and *SAG21*-OEX at 24 and 48 hpi in order to establish their disease response phenotype compared to WT. In *Pst* DC3000-infected plants, the bacterial numbers were significantly reduced in the *SAG21*-OEX and increased in the *SAG21*-AS line compared to WT (Fig. 6-10a). In contrast, the perturbation of *SAG21* did not show any clear altered responses compared to WT in the HR-eliciting avirulent strain (Fig. 6-10b).
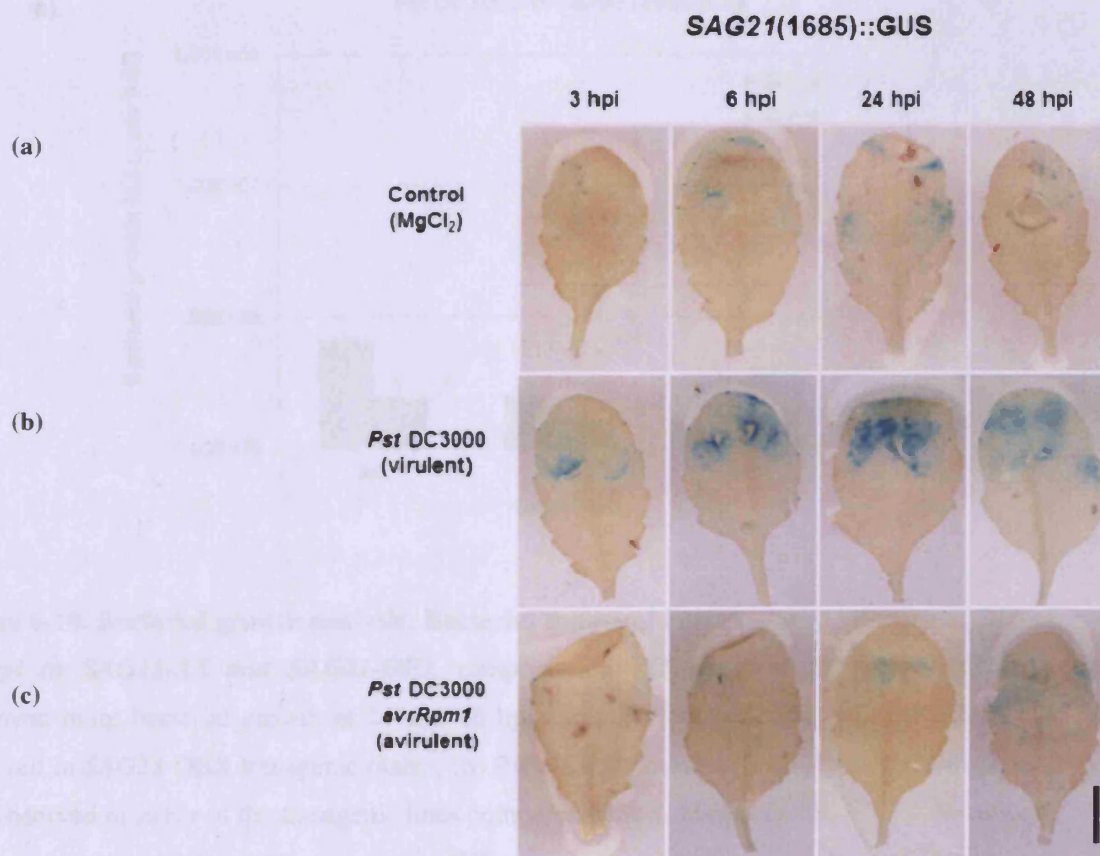
SAG21(1685)::GUS

Figure 6-9. Histochemical GUS staining: Response of *SAG21* promoter to virulent *Pseudomonas syringae* pv. *tomato* DC3000 (*Pst DC3000*) and *Pst DC3000* avirulent *Rpm1* (*Pst DC3000 avrRpm1*) bacterial strains in *SAG21(1685)*::GUS plants. GUS expression was up-regulated by *Pst DC3000* at 3, 6, 24 and 48 hpi compared to the basal expression exhibited by the control. No clear expression pattern was detected upon *Pst DC3000 avrRpm1* inoculation compared to control. Scale bar = 10 mm.

(a)

Pst DC3000 (virulent)

■ 24 hpi
■ 48 hpi

Bacterial growth (c.f.u. per leaf)

1.00E+08

1.00E+07

1.00E+06

1.00E+05

AS   WT   OEX

Genotype

(b)

Pst DC3000 *avrRpm1* (avirulent)

■ 24 hpi
■ 48 hpi

Bacterial growth (c.f.u. per leaf)

1.00E+08

1.00E+07

1.00E+06

1.00E+05

AS   WT   OEX

Genotype
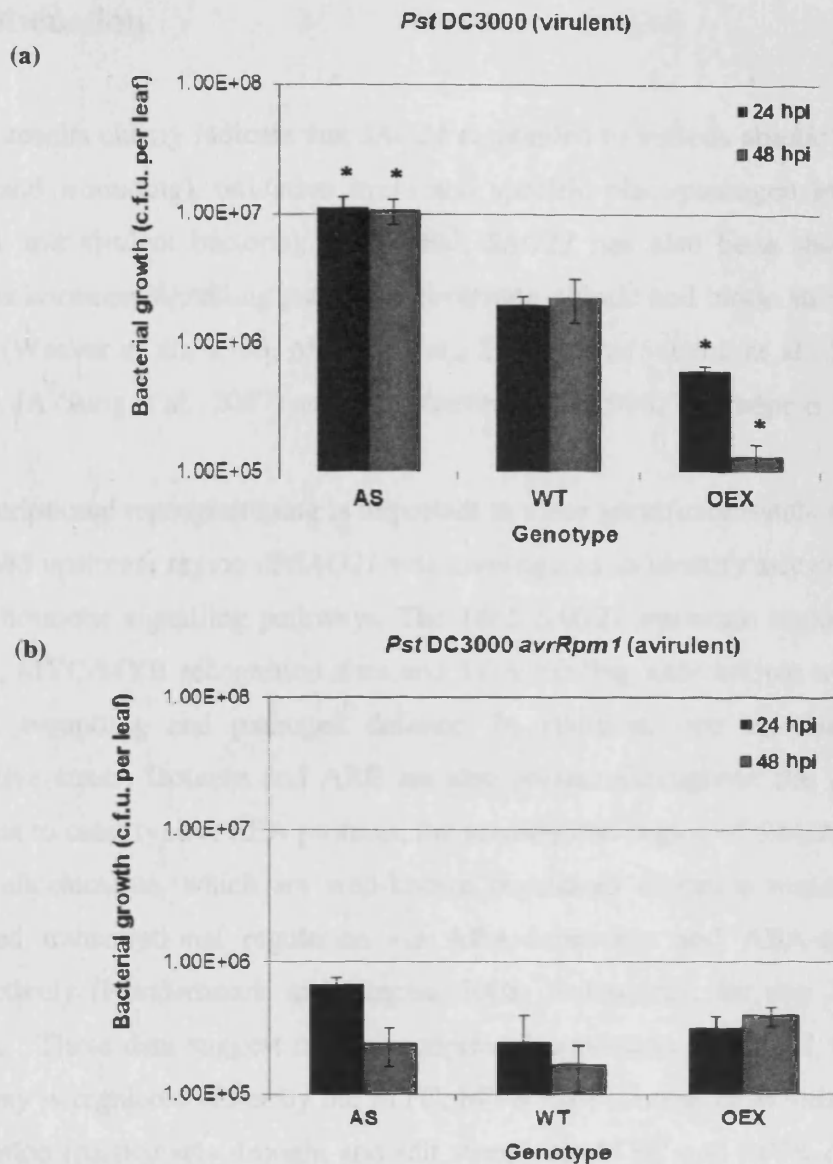
Figure 6-10. Bacterial growth analysis: Bacterial counts of *Pseudomonas syringae* at 24 and 48 hpi in *SAG21*-AS and *SAG21*-OEX compared to WT. (a) *Pst DC3000*: *SAG21*-AS displayed more bacterial growth at 24 and 48 hpi compared to WT. The opposite effect was observed in *SAG21*-OEX transgenic plants. (b) P*st DC3000 avrRpm1*: No clear growth pattern was observed in either of the transgenic lines compared to WT. Means (± SE, n=12). Significant differences in bacterial growth compared to WT are indicated by an asterisk (*P<0.01).

153

6.4 Discussion

These results clearly indicate that *SAG21* responded to various abiotic stresses (drought, salt, cold, and wounding), oxidative stress and specific plant-pathogen interactions (necrotroph fungal and virulent bacteria). In parallel, *SAG21* has also been shown to be induced by various hormone signalling pathways governing abiotic and biotic stress responses including ABA (Weaver et al., 1998; Mowla et al., 2006), SA (Schenk et al., 2000; Pitzschke et al., 2009), JA (Jung et al., 2007) and ET (Weaver et al., 1998; De Paepe et al., 2004).

Transcriptional reprogramming is important in these specific crosstalk stress responses, hence the 1685 upstream region of *SAG21* was investigated to identify any *cis*-elements targeted by these hormone signalling pathways. The 1685 *SAG21* upstream region contains several W-boxes, MYC/MYB recognition sites and TGA binding sites known to play a role in abiotic stress, wounding and pathogen defence. In addition, two cis-elements which regulate oxidative stress; Dofcore and ARE are also present throughout the investigated region. In contrast to most typical LEA proteins, the investigated region of *SAG21* lacks any ABRE and DRE *cis*-elements, which are well-known regulatory elements required for abiotic stress-induced transcriptional regulation via ABA-dependent and ABA-independent pathways, respectively (Hundertmark and Hincha, 2008; Nakashima, Ito and Yamaguchi-Shinozaki, 2009). These data suggest that transcriptional regulation of *SAG21* via the ABA-mediated pathway is regulated either by the MYC, MYB *cis*-elements or W-boxes. The abiotic stress regulation (particularly drought and salt stress) via MYC and MYB *cis*-elements in *SAG21* may be governed by the ABA-transcriptional activator *AtMYC2/JIN1* and *AtMYB2* (Abe et al., 1997; Abe et al., 2003) because both TFs are also induced by drought and salt and so far are the best studied TFs from the MYC and MYB family, respectively. In addition, *SAG21* transcripts were up-regulated in *atmyb60-1* leaves (Cominelli et al., 2005). *AtMYB60* is a TF which is downregulated by drought and ABA. Thus, all three TFs might possibly act upstream of *SAG21* abiotic stress regulation via the MYC/MYB pathway (Fig. 6-11). This unique *cis*-element feature of *SAG21* (Hundertmark and Hincha, 2008) might suggest a less direct up-regulation by abiotic stress compared to other LEA proteins.

Four W-boxes present within the 1685 kb upstream *SAG21*, with two boxes clustered together are excellent candidates for WRKY TF binding. Coincidentally, two similarly spaced functional W-boxes were also identified in ABA-mediated *AtWRKY33* (Lippok et al., 2007) and its homologue *PcWRKY1* (Eulgem et al., 2000). Like *SAG21*, *AtWRKY33* is also up-regulated by paraquat (ROS), wounding and both abiotic stress (Jiang and Deyholos, 2009) and biotic stress (Zheng et al., 2006; Lippok et al., 2007) suggesting that *AtWRKY33* might act as one of the direct WRKY TF regulators of *SAG21*.
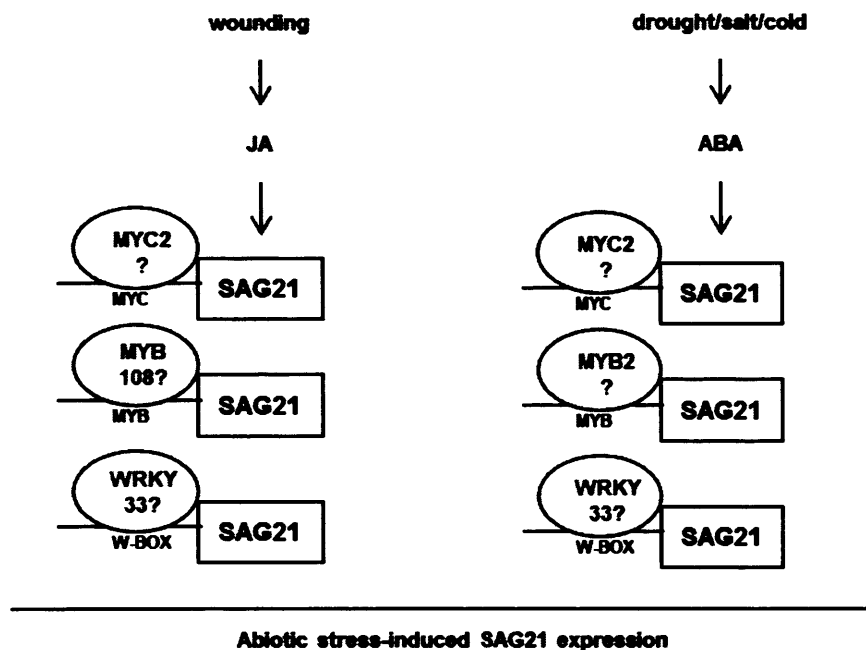
Figure 6-11. Proposed transcriptional regulation of *SAG21* upon various abiotic stresses in Arabidopsis.

Compared to the *SAG21*(1685)::GUS construct, the shorter construct, *SAG21*(325)::GUS only contains one W-box. However, *SAG21* was still induced by wounding and certain abiotic stresses in a line expressing this construct indicating that a single W-box is sufficient for *SAG21* activation. Furthermore, it has been shown that reporter gene constructs driven solely by W-box elements in transgenic *Arabidopsis* plants were strongly activated by diverse stresses (Rushton et al., 2002). The localized promoter activity at wounding sites was lost resulting in a systemic wound response thus inferring that an additional element required for localized *SAG21* wound activation is present further upstream of the 325 region. The wound-induced expression also coincides with H_2O_2 staining suggesting that the ROS could be mediating the *SAG21* activation.

PR-1 activation is a reasonably robust marker for SAR. DNA microarray analysis showed that *SAG21* is one of the candidate genes belonging to the *PR-1* regulon and most likely to function during SAR (Maleck et al., 2000). Despite the proposed role of *SAG21* as a positive regulator of SA-mediated SAR, its upstream region lacks G-boxes which are present in the *PR1* promoter, specifically involved in positive regulation of *PR1* by a bZip TF interacting with *NPR1* for SAR activation (Zhang et al., 1999). However, the presence of TGA binding sites which are positive regulators of *PR-1* expression (Maleck et al., 2000) supports the role of *SAG21* in SAR activation. Interestingly, MPK4 which was previously proposed as an upstream regulator of *SAG21* (Pitzschke et al., 2009), also lacks the G-boxes and negatively regulates the SA-mediated defences independently of *NPR1* (Petersen et al., 2000). These distinct features suggest that SA-mediated SAR by *SAG21* is most likely acting downstream or independently of *NPR1*, although further confirmation is needed. In addition, *PAD4*, another putative upstream regulator of *SAG21* upon phloem-feeding aphid infection in *Arabidopsis* (Pegadaraju et al., 2005; Pegadaraju et al., 2007), is also regulated by SA accumulation but independent of *NPR1* (Zhou et al., 1998; Jirage et al., 1999) supporting a NPR1 independent route for SA up-regulation of *SAG21*.

The absence of a GCC-box which is a prerequisite for *ETHYLENE-RESPONSE-FACTOR1* (*ERF1*) activation, a critical TF for JA/ET defence response against necrotrophs (Berrocal-Lobo, Molina and Solano, 2002) within the *SAG21* 1685 upstream region suggests that *SAG21* induction exhibited upon *Botrytis cinerea* (fungal necrotroph) inoculation in *SAG21*(1685)::GUS plants is not regulated via the JA/ET regulated defence response genes, *PDF1.2* (Thomma et al., 1999b). Instead, the resistance may be mediated via the fungal-specific camalexin biosynthesis pathway (*PAD3*) (Fig. 6-12) either via the MKK4/5-MPK3/MPK6 cascade which is independent of SA, JA and ET (Ferrari et al., 2003; Ferrari et al., 2007; Ren et al., 2008) or via the MEKK1-MKK1/2-MPK4 cascade which regulates the downstream JA-independent *AtWRKY33* (Zheng et al., 2006) by binding to the *PAD3* promoter (Qiu et al., 2008a). In addition to the camalexin pathway regulation via the W-Box, the *SAG21* induction by *Botrytis cinerea* could also be modulated through the MYB pathway. Mutants in a *R2R3MYB*-type TF; *AtMYB108/BOS1* increased susceptibility towards this necrotroph and various other abiotic stresses (Mengiste et al., 2003). This might target *SAG21* via its *MYB* cis-elements.
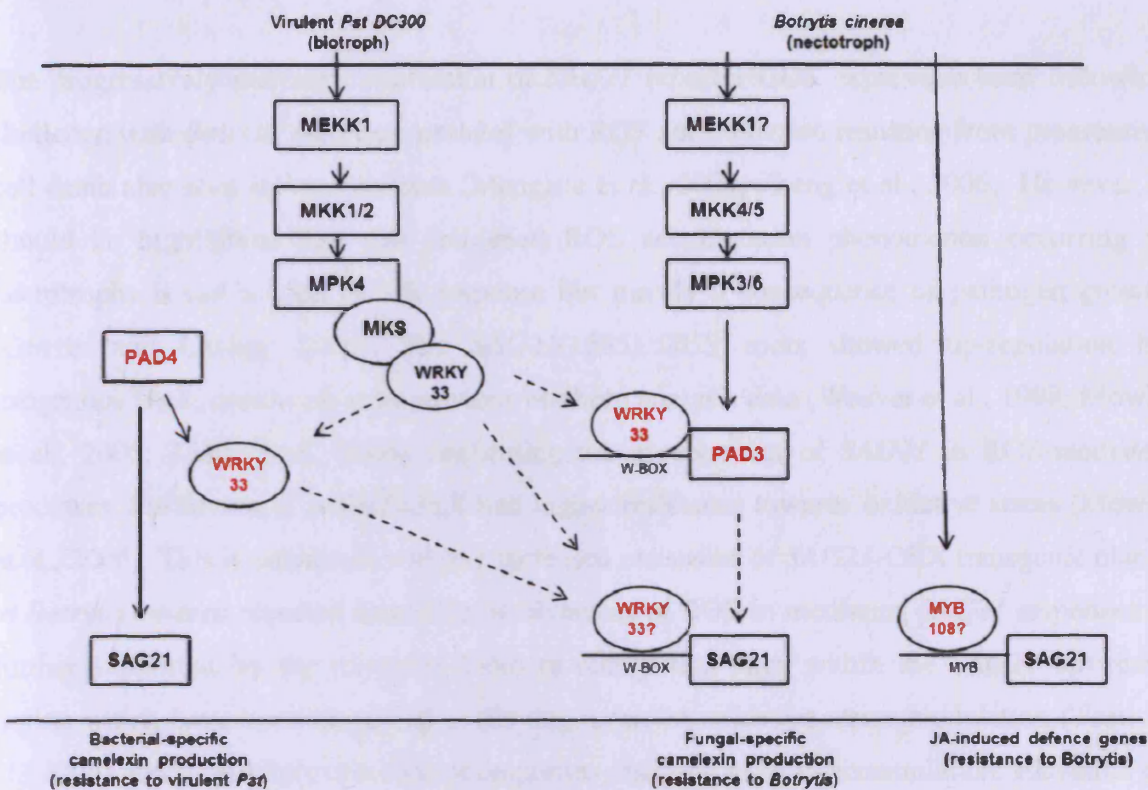
Figure 6-12. Proposed transcriptional regulation of *SAG21* upon pathogen infection by virulent biotroph bacteria: *Pst. DC3000* and fungal nectotroph: *Botrytis cinerea.*

A functional role for the up-regulation of *SAG21* when challenged with the fungal necrotroph, *Botrytis cinerea*, was further supported by the effect of *SAG21* perturbation in over-expressor and antisense lines. Hyphal growth was not seen at 24 hours after inoculation in *SAG21*-OEX plants compared to WT. This suggests that the initial infection phase before cell death initiation is compromised in this line, resulting in plant resistance. Conversely, antisense lines appeared more susceptible to this necrotroph with increased fungal growth detected 24 hours after inoculation compared to WT. Enhanced susceptibility to necrotrophs was also observed in the fungal camalexin-defective *Arabidopsis* mutants, *wrky33/mpk4* (Qiu et al., 2008a), *mpk3/mpk6* (Ren et al., 2008) and in *R2R3*-MYB defective *bos1* mutants (Mengiste et al., 2003). Furthermore, overexpression of *AtWRKY33* accompanied by increased camalexin production resulted in enhanced resistance to necrotrophs (Zheng et al., 2006). These similar pathogen defence mechanisms suggest their possible role as upstream regulators of *SAG21*. Besides, *AtWRKY33* expression is dependent on *PAD4* (Lippok et al., 2007), suggesting the possibility of a *PAD4-AtWRKY33-SAG21* regulon.

The progressively increased expression of *SAG21* reporter GUS expression seen following challenge with *Botrytis cinerea* correlates with ROS accumulation resulting from progressive cell death also seen in *bos1* mutants (Mengiste et al., 2003; Zheng et al., 2006). However, it should be highlighted that this cell death-ROS accumulation phenomenon occurring in necrotrophs is not a form of HR response but merely a consequence of pathogen growth (Govrin and Levine, 2000). The *SAG21*(1685)::GUS roots showed up-regulation by exogenous H_2O_2; consistent with previous northern analysis data (Weaver et al., 1998; Mowla et al., 2006; Tosti et al., 2006) confirming the involvement of *SAG21* in ROS-mediated processes. Furthermore, *SAG21*-OEX had higher resistance towards oxidative stress (Mowla et al., 2006). This is consistent with the increased resistance of *SAG21*-OEX transgenic plants to *Botrytis cinerea* reported here. The involvement of ROS in mediating *SAG21* responses is further supported by the recurring Dofcore recognition sites within the *SAG21* upstream region which have been identified as playing a role in oxidative stress modulation (Tosti et al., 2006) and most likely other stress responses resulting in ROS accumulation. Elevation of ROS levels was confirmed in young *SAG21*(1685)::GUS seedlings treated with various stresses. In addition, the presence of ARE-elements, which correspond to anaerobic functional genes found in maize (Olive et al., 1990), is another signature of both *SAG21* and *AtWRKY33* upstream regions, which might act as an important mediator of crosstalk between abiotic and biotic stress responses.

To test *SAG21* pathogen-specificity, *SAG21* transgenic plants were also subjected to both virulent (*Pst* DC3000) and avirulent strains (*Pst avrRpm1*) of the bacterial biotroph, *Pseudomonas syringae pv. tomato (Pst)* DC3000. Only the virulent line induced a rapid up-regulation of *SAG21* GUS activity. Consistent with these findings, the growth of virulent bacteria *Pst* DC3000 appeared to be inversely proportional to *SAG21* expression with increased resistance in the over-expressor lines and vice versa. In contrast, infection elicited with avirulent *Pst avrRpm1* was not significantly different in *SAG21* transgenic lines compared to WT suggesting that *SAG21* does not affect the HR response. Similarly enhanced disease symptoms in response to inoculation with virulent biotroph bacteria were also detected in two potential upstream regulators of *SAG21*: *mpk4* (Petersen et al., 2000; Pitzschke et al., 2009) and *pad4* mutants (Zhou et al., 1998; Pegadaraju et al., 2005). In *pad4* mutants (which lack bacterial-specific camalexin production), susceptibility was observed in response to another bacterium, *Pseudomonas syringae pv. maculicola ES4326 (Psm ES4326)*

but not in response to its avirulent strain, *avrRpt2 (Zhou et al., 1998)*. This would support a function of *SAG21* in HR-independent SA-mediated SAR and virulent-specific pathogen defence regulated through the *MPK4-PAD4* and *PAD4*-bacterial-specific-camalexin regulation network (Fig. 6-12).

SAG21 transcript was up-regulated by almost four-fold in over-expressor lines of *AtWRKY70* (Li, Brader and Palva, 2004). The positive regulation of *SAG21* by this TF which appears to be an important convergence point in fine-tuning the balance between SA and JA-defence dependent pathways (Li et al., 2004; AbuQamar et al., 2006; Li et al., 2006; Ulker, Shahid Mukhtar and Somssich, 2007) suggests a functional role for *SAG21*. *MEKK1* regulated-*AtWRKY53*, an SA-induced gene (Miao and Zentgraf, 2007) might also serve as an additional potential WRKY TF candidate for *SAG21* since *MEKK1* has also been proposed as an upstream regulator of SA-induced *SAG21* (Pitzschke et al., 2009).

Since host defences to necrotroph *Botrytis cinerea* and virulent bacteria *Pst* DC3000 were influenced by *SAG21* modulation, basal resistance mechanisms might be affected. Microarray online databases revealed that the elicitor *flg22* could trigger *SAG21* expression (Zimmermann et al., 2004). Some facets of the basal resistance mechanism via *flg22* are regulated by the redox-mediated MEKK1-MKK1/2-MPK4 cascade (Suarez-Rodriguez et al., 2007) and so it may be that the H_2O_2-responsive *SAG21* is a component in this mechanism and underlines the requirement to precisely define its function.

Despite the altered susceptibly/resistance observed in *SAG21* transgenic lines toward biotic stress, the effect on abiotic stress tolerance appeared to be less clear. In preliminary results, germination rate and stress tolerance were not compromised in younger seedlings in either lines (Appendix-D). Previously, soil-grown *SAG21*-OEX plants were instead shown to be more susceptible to drought (Mowla et al., 2006). Moreover, *atwrky33* mutants (which also exhibited increased susceptibility to pathogens) showed only a moderate increase in salt-sensitivity (Jiang and Deyholos, 2009). This may suggest functional redundancy with other stress-related proteins such as other members of WRKY TFs and LEA proteins. This correlates with the atypical feature of the *SAG21* upstream region compared to other typical LEA proteins in Arabidopsis which are mainly composed of the ABRE and DRE elements (Hundertmark and Hincha, 2008), as these are critical *cis*-elements required for rapid abiotic stress tolerance (Nakashima et al., 2009). Taken together, this may suggest that

SAG21/AtLEA5 might play a less important role in abiotic stress tolerance compared to biotic stress, and its induction by abiotic stress observed in this work might be due to ROS accumulation which plays key roles in the crosstalk between both stresses.

ROS can stimulate the production of phytoalexins and other secondary metabolites that arrest pathogen growth (Thoma et al., 2003). ROS in association with SA were proposed to mediate the establishment of SAR (Torres et al., 2006). This is consistent with ROS regulation of SA-induced bacterial resistance in *SAG21* over-expressor lines. Furthermore, ROS could also form complex regulatory circuits with calmodulin signalling and MAPK phosphorylation cascades thus affecting the activity of transcription factors and other downstream signalling (Jaspers and Kangasjärvi, 2010; Torres, 2010). Up-regulation of *SAG21* transcripts in *mekk1*, *mkk1/2*, *mpk4* mutants (Pitzschke et al., 2009) and upon transient cellular Ca^{2+} (Kaplan et al., 2006) clearly support a possible ROS-mediated role of up-regulation in response to various stresses.

6.5 Summary

To gain a better understanding of the role of *SAG21* during stress responses in *Arabidopsis*, two transgenic lines expressing GUS fused to the *SAG21* upstream regions *SAG21(1685)*::GUS and *SAG21(325)*::GUS were subjected to various abiotic stresses and specific pathogens. Stress tolerance/susceptibility of over-expressor and antisense plants was also characterized. *SAG21* responded to various abiotic stresses, wounding and exogenous ROS (H_2O_2) agreeing with previous northern analysis. In pathogen defence, *SAG21* responded specifically to a fungal nectotroph, *Botrytis cinerea* and the virulent biotroph bacterium, *Pst* DC3000. Over-expression of *SAG21* resulted in reduced growth of both pathogens. The opposite effect was observed in the antisense line. Preliminary results suggest perturbation of *SAG21* did not alter abiotic stress tolerance indicating a more important role in biotic tolerance. Similar responses were observed in regulators of ROS-mediated MAPK components independent of HR suggesting that *SAG21* may be involved in basal defence through the PAMP-triggered immunity and may possibly play a role in the downstream antimicrobial camalexin signaling.

Chapter 7: General Discussion and Future perspectives

The basis of the work presented in this thesis was to investigate the regulation of reactive oxygen species (ROS) during plant growth, stress and senescence. One aspect of my research was focused on the hormonal and redox regulation in wallflower petal (*Erysimum linifolium*) senescence **(Chapter 3)**. Of particular interest, *SAG21*, a senescence associated gene was previously identified to be up-regulated in senescent petals (Price et al., 2008). The roles of key plant growth regulators (ethylene, cytokinin and auxin) were determined by quantifying their endogenous production and the effects of their inhibitors toward petal abscission time and senescence progression. In parallel, the differential expression pattern of *SAG12* (a senescence marker), *SAG21*, an ethylene biosynthetic gene and an auxin-induced gene were also characterized. In order to understand the role of ROS in this developmental process, hydrogen peroxide levels were measured and the activities of several antioxidative enzymes were assayed by zymograms.

Another aspect of my work was dedicated to further elucidating the function of the ROS-induced gene, *SAG21* (Mowla et al., 2006) in Arabidopsis. First, the subcellular localization of this gene was confirmed by transient and stable transformation of 35S-*SAG21*-YFP construct into protoplast or plants, respectively **(Chapter 4)**. Secondly, using transgenic lines transformed with *SAG21* promoter-GUS, its tissue-specific, spatial and temporal expression during development **(Chapter 5)** and stress conditions **(Chapter 6)** were defined. Finally, greater insights into the role of *SAG21* in growth, senescence and plant defence were achieved by analysing the effect of *SAG21* perturbation on these developmental processes in *SAG21* over-expressor (OEX) and *SAG21* antisense (AS) plants compared to WT plants grown under standard conditions **(Chapter 5)** as well as various abiotic and biotic stress conditions **(Chapter 6)**. Using these findings, tentative models for signalling pathways regulating *SAG21* expression during development and stress responses were proposed.

In the following sections, the main findings from different chapters of this thesis are summarized and discussed, including perspectives for future work.

7.1 Hormonal and redox regulation in wallflowers

In Arabidopsis, leaf senescence has been extensively studied due to the availability of genomic resources and mutants (Buchanan-Wollaston, 1997; Buchanan-Wollaston et al., 2003; Buchanan-Wollaston et al., 2005). However, its small flowers and difficulties in staging of flowers accurately limit the progression of petal senescence research in this model plant. Recently, a microarray analysis was undertaken comparing senescence in petals and leaves of a bigger ornamental plant, the wallflower, which is closely related to Arabidopsis and *Brassica*. The microarray data revealed a number of common and distinct patterns of gene expression with a large proportion of genes up-regulated during senescence in both tissues including genes involved in remobilization, hormonal regulation and ROS signalling (Price et al., 2008). Consistent with the microarray analysis, the senescence regulation in wallflowers by specific phytohormones and ROS signalling components was established in this work. The onset of petal senescence exhibited by petal wilting was accompanied by an increase in ethylene and auxin production, followed by ROS accumulation. This finding suggests a crucial role for ethylene rise as a signal precursor while ROS accumulation might act as downstream signal. The increase in ethylene production was accompanied by the up-regulation of an ethylene biosynthetic gene, *WLS73* at about the same stage in both petals and leaves. A similar pattern in ethylene production alongside differential expression of ethylene biosynthetic genes has also been reported in a number of ethylene-sensitive flowers such as carnation, rose and Arabidopsis (ten Have and Woltering, 1997; Xue et al., 2008; Wagstaff et al., 2009).

Exogenous treatment of detached flowers with ethylene (produced by CEPA) hastened the time to petal abscission and senescence progression in wallflowers. In contrast, treatment with the ethylene receptor blocker, silver thio-sulphate (STS) confirmed that the reduction in endogenous ethylene signalling was able to delay both processes. In fact, the up-regulation of *WLS73* transcripts was also delayed in these STS-treated flowers indicating a possible autocatalytic response. Further experiments analysing the expression of WLS73 in response to exogenous ethylene would be a crucial step to clarify this. Up-regulation of the senescence marker, *SAG12*, which normally increased with age (Price et al., 2008) was also reduced in these STS-treated flowers hence confirming the delay in senescence progression. On the contrary, the expression of an auxin-induced gene, *WPS46*,which was normally elevated with

age (Price et al., 2008) remained unchanged in all treatments suggesting that its expression might not be directly regulated by ethylene or cytokinin. Exogenous treatments with auxin inhibitors might reveal some useful insights towards its functional role during wallflower petal senescence.

In addition to ethylene, exogenous treatment of detached flowers with cytokinin (kinetin) or 6-methyl purine, an inhibitor of cytokinin oxidase, an enzyme involved in cytokinin degradation, also delayed petal senescence, time to abscission and prevented up-regulation of *SAG12* and *WLS73* transcripts in wallflower petals. Both treatments are presumed to result in increased endogenous cytokinin levels and have been previously been demonstrated to have a similar effect in un-pollinated carnations (Eisinger, 1977; Mor, Spiegelstein and Halevy, 1983). *SAG12* repression and reduced ethylene sensitivity indicating delayed senescence-associated activities, have also been reported in transgenic petunia overproducing cytokinin confirming the role of this hormone in flower senescence (Chang et al., 2003). Further quantification of wallflowers' endogenous cytokinin content and transcript levels of genes involved in cytokinin signalling is the next step to dissect the role of cytokinin in this developmental process.

Unlike *SAG12*, *WLS73* and *WPS46* which increased with age, *SAG21* transcript levels peaked rather early in petals then were down-regulated even before the first sign of visible senescence could be observed. Conversely, in leaves, *SAG21* remained constant at all stages. This may suggest that *SAG21* plays a role in the early stages of petal senescence before visible senescence markers are evident, but might not play a significant role in leaf senescence in wallflowers. Treatment with STS and kinetin suggests that *SAG21* might be transcriptionally regulated by ethylene but not by cytokinin in wallflower petal senescence, although further experimental evidence is needed.

SAG21/AtLEA5 in Arabidopsis responds to ROS signals (Mowla et al., 2006). However H_2O_2 levels in earlier petal stages were relatively low thus questioning whether in wallflower petals expression of this gene is ROS regulated. The redox regulation in wallflower leaves might involve a balance of antioxidative enzyme activities contributed by catalase, ascorbate peroxidase and superoxide dismutase. In leaves, the H_2O_2 level peaked at bolting time and some of the isoform activity profiles for ROS related enzymes in wallflower leaves

resembled the expression patterns reported in Arabidopsis (Orendi et al., 2001; Panchuk, Zentgraf and Volkov, 2005; Zimmermann et al., 2006). Nevertheless, not much can be concluded at this stage since the isoforms identified in this work require further characterization. Therefore, a quantitative measurement of different CAT, APX and SOD isoforms following compartment isolation would be needed separately before the role of anti-oxidative enzymes in parallel with ROS production can be properly evaluated. In petals, APX and SOD might play a more significant role although further experimental evidence is crucial to support this proposed role and clarify the interaction between phytohormones and ROS in wallflower senescence regulation. Figure 7-1 is a proposed tentative model regulating petal senescence in wallflowers. Figure 7-2 classified the studied genes according to their possible hormonal regulation in wallflower petals.
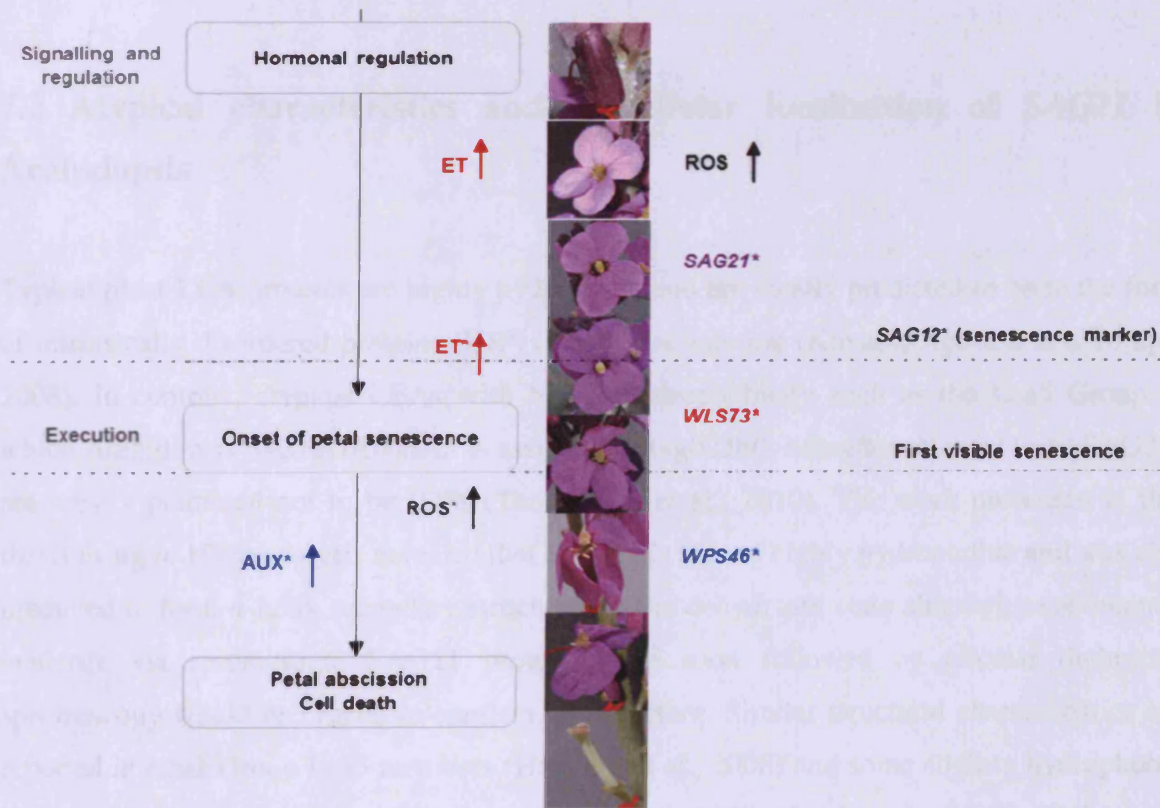

Figure 7-1. Tentative model regulating the onset of petal senescence in wallflowers. Red text indicates ethylene (ET) and ethylene-biosynthetic gene; blue text indicates auxin (AUX) and auxin-induced gene; senescence associated gene (SAG); reactive oxygen species (ROS). Asterisk (*) indicates peak of expression/production.
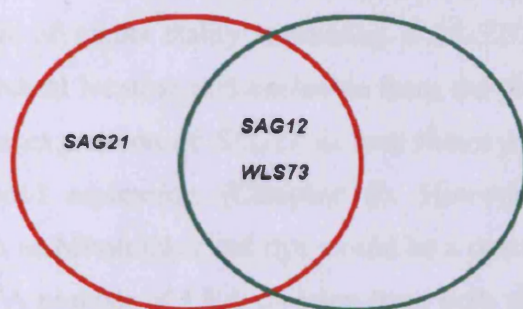
Figure 7-2. Hormonally regulated genes. Red circle indicates ethylene-regulated genes; green circle indicates cytokinin-regulated genes.

7.2 Atypical characteristics and subcellular localization of *SAG21* in Arabidopsis

Typical plant LEA proteins are highly hydrophilic and are mostly predicted to be in the form of intrinsically disordered proteins (IDP) in aqueous solution (Kovacs, Agoston and Tompa, 2008). In contrast, atypical LEAs with higher hydrophobicity such as the Lea5 Group to which Arabidopsis SAG21/AtLEA5 is assigned (At4g02380; hereafter referred to as SAG21) are mostly predicted not to be IDPs (Tunnacliffe et al., 2010). The work presented in this thesis using *in silico* analysis revealed that SAG21 is indeed highly hydrophobic and was also predicted to form α-helix secondary structures in the dehydrated state although experimental evidence via recombinant SAG21 protein purification followed by circular dichroism spectroscopy would be crucial to confirm the structure. Similar structural characteristics are reported in other Group Lea5 members (Haaning et al., 2008) and some slightly hydrophobic Group 3 LEA proteins (Pouchkina-Stantcheva et al., 2007; Hand et al., 2010). These more hydrophobic LEA proteins showed a strong propensity to interact with phospholipid liposomes and inner membranes upon dehydration suggesting that a more hydrophobic region is a prerequisite for binding to membranes which are mainly composed of phospholipid bilayers (Hand et al., 2010). This may suggest a proposed role of SAG21 in membrane and protein protection through transient interactions.

It was originally suggested that SAG21 might be a plastid protein (Mowla et al., 2006), however, confocal analysis of plants stably expressing a SAG21-YFP fusion protein was consistent with a mitochondrial location and exclusion from the plastids (**Chapter 4**) which fits well with predominant expression of *SAG21* in non-photosynthetic tissues (pollen and roots) and its light-induced repression (**Chapter 5**). However, co-expression with a mitochondrial marker such as Mitotracker red dye would be a crucial step to further confirm its subcellular specificity. A number of LEA proteins from both plants and other organisms are mitochondrially located and may be involved in protecting mitochondrial proteins from aggregation during stress (Grelet et al, 2005; Menze et al, 2009). As mitochondrial ROS increases upon stress (Rhoads et al., 2006), the mitochondrial localization is in agreement with a proposed role for SAG21 in oxidative stress protection. In addition, SAG21 protein is also composed of amino acid residues previously shown to be involved in ROS scavenging and metal binding of the mitochondrial citrus dehydrin, *CuCOR19* (Hara, Fujinaga and Kuboi, 2004) therefore suggesting possible antioxidant properties.

7.3 *In vivo* function of *SAG21* during plant development in Arabidopsis

As well as identifying the structural characteristics and SAG21 subcellular localization, it is of great importance to identify the *in vivo* functions of *SAG21* and the consequence of *SAG21* expression in plants. The expression of two GUS constructs fused to *SAG21* upstream promoter regions: *SAG21(1685)*::GUS and *SAG21(325)*::GUS were analysed in transgenic Arabidopsis lines followed by phenotypic characterization of over-expressor (*SAG21*-OEX) and antisense (*SAG21*-AS) plants. Generally, *SAG21* is highly expressed in primary roots (differentiation and elongation zones), root hairs, cotyledons, and pollen but almost absent in the rosette. In addition, *SAG21* is also repressed by light. Its strong expression in pollen fits well with the classical role of LEAs in dehydrated tissues (Tunnacliffe and Wise, 2007). This expression pattern supports earlier reports based on northern analysis although previously *SAG21* was also detected in rosettes (Weaver et al, 1998; (Mowla et al., 2006). The shorter construct lost the pollen-specific expression and age-regulated expression in leaves hence suggesting important *cis*-elements might be present further upstream in the promoter region, positively regulating pollen expression and negatively regulating leaf expression in non-senescent leaves. This could be determined by generating several deletion constructs

consisting of different promoter regions or specific *cis*-elements followed by assessment of their temporal expression pattern in a tissue-specific manner.

The most striking phenotype of the *SAG21* transgenic lines was the effect on root architecture, particularly the number and length of lateral roots, relative to the primary root and root hair elongation. Antisense seedlings had shorter primary roots and less lateral roots, which is in agreement with previous reports (Mowla et al., 2006) as well as shorter root hairs. The opposite effects were observed in the over-expressor lines. The exclusion of the GUS staining from the root tips and lateral meristems is interesting in relation to the effect on lateral root development in the antisense and over-expressor lines, suggesting perhaps that the effects on lateral root development are not directly related to changes in *SAG21* levels in the meristem. ROS moieties are differentially localized in the root (Dunand et al, 2007) with $O_2^{\cdot-}$ mainly localized in the cell elongation zone, whereas H_2O_2 was mainly in the differentiation zone. They also seem to perform different roles, with $O_2^{\cdot-}$ favouring root elongation while H_2O_2 restricts growth. *SAG21* is expressed in both regions and thus may be responding to both ROS moieties and might explain the root phenotype. However, a more detailed study of this expression pattern via cross-section may assist in further confirming this expression-zone function correlation.

It is now well-established that redox regulation plays an important role in maintaining root meristem formation, root hair formation and the transition from proliferation to differentiation in the root (Vernoux et al., 2000; Foreman et al., 2003; Dunand et al., 2007; Tsukagoshi et al., 2010). The data presented here strongly implicate the redox-regulated LEA, *SAG21* in the control of root architecture. The short root hair phenotype of AS plants is strikingly similar to that of the *root hair defective 2* (*rhd2*) mutant, which lack the plasma membrane-located respiratory burst oxidase, *AtrbohC* (Foreman et al., 2003; Carol and Dolan 2006; Dolan and Davies 2004; Gapper & Dolan 2006). The mitochondrial location of *SAG21* might suggest that sources of ROS other than *AtrbohC* may be important in the pathways/signal transduction network that controls elongation.

Mitochondria are found at high densities in tip-growing cells and are associated with the initiation bulge during root hair formation (Ciamporova et al., 2003). Although this has been typically associated with the energetic demands of tip growth, there may also be redox-

related roles for mitochondria in this process. The tip-growth of pollen tubes parallels that of root hairs (Carol and Dolan, 2006). However, it is worth noting that *SAG21* over-expression in this work was driven by the 35S promoter which is not active in pollen (Wilkinson, Twell and Lindsey, 1997) A detailed phenotyping of cotyledon development in *SAG21* transgenic lines would however be interesting to establish if *SAG21* plays a general role in cell expansion. Further experiments expressing *SAG21* under control of a promoter active in pollen such as LAT52 (Bate and Twell, 1998) would also be interesting to see if pollen tube growth is affected.

As described in **Chapter 5**, perturbation of *SAG21* also affected the above ground phenotype. Previously, Mowla et al. (2006) showed that *SAG21* over-expression resulted in biomass increase. In the work presented here, shoot biomass was dramatically changed in *SAG21* transgenic lines confirming previous findings. In addition, leaf number and time to flowering was significantly increased in *SAG21* over-expressors, while it was decreased in the antisense lines. This mirrors effects on both biomass and flowering time noted in perturbations of ascorbate peroxidase expression (Miller et al., 2007). In catalase deficient plants leaf area was also reduced (Vandenabeele et al. 2004), and flowering time was perturbed in transgenic plants over-expressing three proteins of unknown function that confer enhanced tolerance to oxidative stress (Luhua et al, 2008). Thus the alteration of biomass and flowering time in the *SAG21* transgenic lines is consistent with a role for this protein in ROS responses. There is also an important link between life-span and oxidative stress. Delayed senescence mutants *ore1*, *ore3* and *ore9* are also more tolerant of oxidative stress (Woo et al. 2004) as is the late flowering mutant, *gigantea* (Kurepa et al. 1998), and ascorbate deficiency is linked to a perturbation of senescence timing (Barth et al. 2004). This is again consistent with the delayed and accelerated leaf senescence seen respectively in lines where *SAG21* was over-expressed or down-regulated. The mechanisms regulating the link between ROS, flowering and senescence are complex, but altering expression levels of the senescence-linked transcription factors, *WRKY53* and *WRKY70*, affects both flowering time and senescence (Miao et al., 2004; Ulker, Shahid Mukhtar and Somssich, 2007) and a peak in H_2O_2 levels coinciding with bolting (Zimmerman et al, 2006) may activate senescence-associated transcription factors such as *WRKY53*, coordinating developmentally regulated leaf senescence.

Recently, a microarray transcriptome analysis revealed that *SAG21* is up-regulated in *mekk1* plants as well as in knock-outs of its downstream regulators, *MKK1/2* and *MPK4* (Pitzschke et al., 2009). *MEKK1* acts as an upstream regulator of *WRKY53* either by direct interaction or by binding to the MYC region of the *WRKY53* promoter (Miao et al., 2007). The presence of several W-boxes and MYC binding sites within the 1685 bp upstream regions of *SAG21* suggest that *SAG21* might act downstream of *WRKY* TFs in the well-studied *MEKK1-MKK1/2-MPK4* signalling cascade. To date, no evidence has been provided on whether the *SAG21* promoter interacts directly with any of the MAPK cascade components mentioned above. Hence, the identification of proteins interacting with the *SAG21* promoter via yeast-one-hybrid system or gel retardation using candidate oligos from the promoter sequence is possibly the next crucial step to confirm this proposed signalling mechanism. Furthermore, identification of proteins interacting with SAG21 protein itself via yeast two-hybrid will expand our understanding on the possible signalling pathways involving SAG21. However, SAG21's atypical structural properties as a sticky LEA protein will make these *in vitro* experiments more challenging. Figure 7-3 suggests a putative model regulating *SAG21*, with *MEKK1/2-MKK1-MPK4* and *WRKY53* as possible regulators.
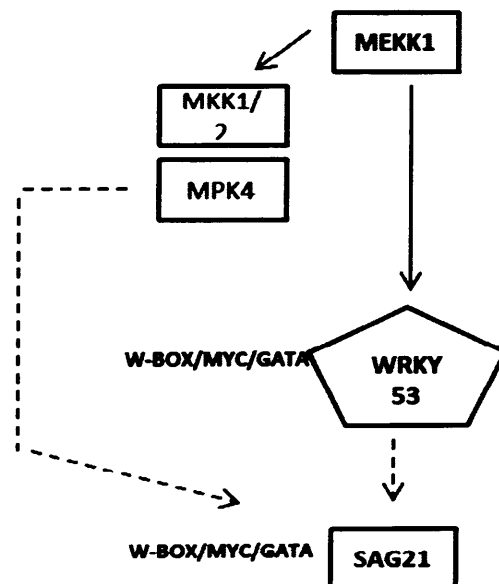

nd *SAG21*

ion. Dashed

7.4 *In vivo* function of *SAG21* during stress in Arabidopsis

As highlighted several times throughout the thesis, *SAG21* is a ROS-inducible gene that has a proposed role in oxidative stress. Numerous reports, including data from publicly available microarrays indicate that *SAG21* expression is also up-regulated by a range of other stresses such as ozone (Miller et al., 1999), cold (Seki et al, 2001), low nitrate (Wang et al, 2000), and pathogen infection (Pegadaraju et al., 2005; Pegadaraju et al., 2007)) as well as the hormones ethylene, abscissic acid (Weaver et al, 1998; De Paepe et al. 2004), jasmonate (Jung et al, 2007) and salicylic acid (Schenk et al., 2000). The role of SAG21 in plant stress regulation is evident from the analysis of *SAG21* transgenic plants presented in this work (**Chapter 6**). *SAG21* responded strongly to drought, salt, cold, wounding as well as exogenous ROS (H_2O_2). However, preliminary results suggest perturbation of *SAG21* did not alter abiotic stress tolerance. This suggests that SAG21 protein might not play a primary role in abiotic stress protection which might be due to the high redundancy of overlapping functions played by the various members of the LEA protein family.

In pathogen defence, *SAG21* responded to a fungal nectotroph, *Botrytis cinerea* and the virulent biotroph bacterium, *Pseudomonas syringae* (*Pst*) DC3000. Over-expression of *SAG21* resulted in reduced growth of both pathogens. The opposite effect was observed in the antisense line. Similar phenotypes were observed in Arabidopsis mutants defective in the production of antifungal camalexin; *mpk3/mpk6*, *atwrky33* and *pad3* (Ferrari et al., 2003; Zheng et al., 2006; Ferrari et al., 2007; Qiu et al., 2008a; Ren et al., 2008) and antibacterial camalexin, *pad4* and *mpk4* (Zhou et al., 1998; Lippok et al., 2007), respectively. *AtWRKY33* and *PAD3* are downstream effectors of the *MEKK1/2-MKK1*-MPK4 cascade (Qiu et al., 2008a; Qiu et al., 2008b), the upstream regulator of *SAG21*. On the other hand, *PAD4* was shown to regulate both *AtWRKY33* and *SAG21* (Pegadaraju et al., 2005; Lippok et al., 2007). Furthermore, ROS has been shown to stimulate camalexin production (Thoma et al., 2003).
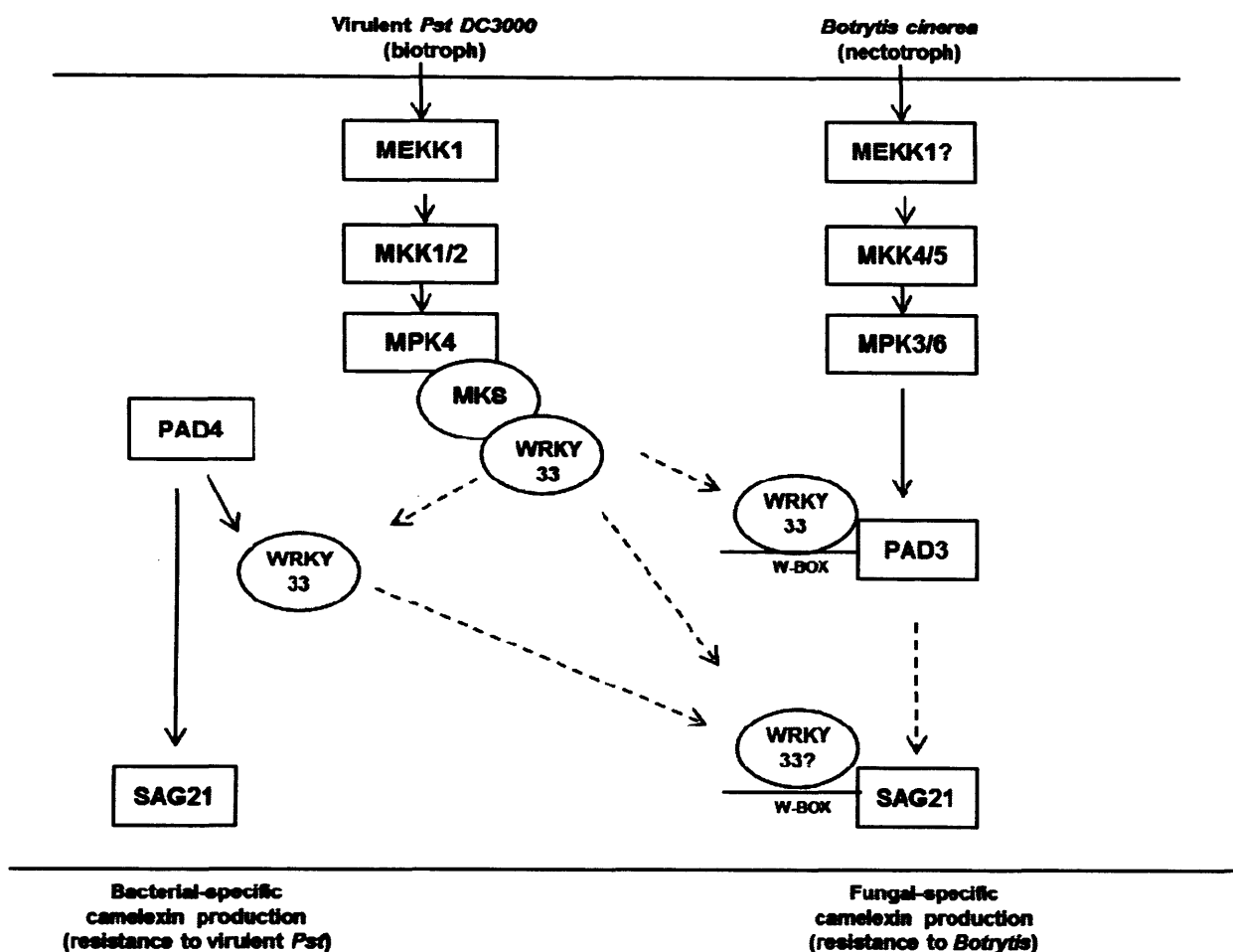
According to these observations, a tentative model suggesting a potential regulation of ROS-induced *SAG21* pathogen resistance involving these camelexin-regulating genes is proposed in Figure 7-4. Confirmation of *SAG21* interaction with these potential candidates and quantification of camalexin content in *SAG21* transgenic lines will contribute to a better understanding of its role in camalexin-regulated plant defence. As host defences to *Botrytis cinerea* and *Pst* DC3000 were modulated by *SAG21* expression, this suggests that basal resistance mechanisms were being affected. Some facets of the basal resistance mechanism are mediated by oxidative stress (Suarez-Rodriguez et al., 2007) and it may be that the ROS-induced *SAG21* is a component in this mechanism and underlines the requirement to precisely define its function. Complementation studies with other ROS-regulated mutants

involved in both biotic stress and growth such as *mekk1* might improve our understanding of *SAG21* function in growth, stress and plant defence.

As mentioned several times in the thesis, redox regulation during plant stress and senescence is clearly a complex process integrating various networks involving ROS, phytohormones, transcription factors, SAGs, other stress-induced proteins including LEA proteins as well as secondary metabolites (Fujita et al., 2006; Yasuda et al., 2008). Identifying the function of downstream individual proteins such as SAG21 and their interacting partners which might play a crucial role in regulating the crosstalk between these two processes is crucial to pin down the critical points converging different signalling networks.

REFERENCES

Abe H, Urao T, Ito T, Seki M, Shinozaki K, and Yamaguchi-Shinozaki K (2003) Arabidopsis AtMYC2 (bHLH) and AtMYB2 (MYB) function as transcriptional activators in abscisic acid signaling. *Plant Cell* 15: 63-78.

Abe H, Yamaguchi-Shinozaki K, Urao T, Iwasaki T, Hosokawa D, and Shinozaki K (1997) Role of arabidopsis MYC and MYB homologs in drought- and abscisic acid-regulated gene expression. *Plant Cell* 9: 1859-1868.

AbuQamar S, Chen X, Dhawan R, Bluhm B, Salmeron J, Lam S, Dietrich R A et al. (2006) Expression profiling and mutant analysis reveals complex regulatory networks involved in Arabidopsis response to Botrytis infection. *Plant J* 48: 28-44.

Alpert P (2006) Constraints of tolerance: why are desiccation-tolerant organisms so small or rare? *J Exp Biol* 209: 1575-1584.

Anderson J P, Badruzsaufari E, Schenk P M, Manners J M, Desmond O J, Ehlert C, Maclean D J et al. (2004) Antagonistic interaction between abscisic acid and jasmonate-ethylene signaling pathways modulates defense gene expression and disease resistance in Arabidopsis. *Plant Cell* 16: 3460-3479.

Apel K, and Hirt H (2004) Reactive oxygen species: metabolism, oxidative stress, and signal transduction. *Annu Rev Plant Biol* 55: 373-399.

Azad A K, Ishikawa T, Sawa Y, and Shibata H (2008) Intracellular energy depletion triggers programmed cell death during petal senescence in tulip. *J Exp Bot* 59: 2085-2095.

Bahrndorff S, Tunnacliffe A, Wise M J, McGee B, Holmstrup M, and Loeschcke V (2009) Bioinformatics and protein expression analyses implicate LEA proteins in the drought response of Collembola. *J Insect Physiol* 55: 210-217.

Bai S, Willard B, Chapin L J, Kinter M T, Francis D M, Stead A D, and Jones M L (2010) Proteomic analysis of pollination-induced corolla senescence in petunia. *J Exp Bot* 61: 1089-1109.

Barceló A R, Pomar F, Ferrer M A, Martínez P, Ballesta M C, and Pedreño M A (2002) In situ characterization of a NO-sensitive peroxidase in the lignifying xylem of Zinnia elegans. *Physiol Plant* 114: 33-40.

Bartels D (2005) Desiccation Tolerance Studied in the Resurrection Plant Craterostigma plantagineum. *Integrative and Comparative Biology* 45: 696-701.

Barth C, Moeder W, Klessig D F, and Conklin P L (2004) The timing of senescence and response to pathogens is altered in the ascorbate-deficient Arabidopsis mutant vitamin c-1. *Plant Physiol* 134: 1784-1792.

Bate N, and Twell D (1998) Functional architecture of a late pollen promoter: pollen-specific transcription is developmentally regulated by multiple stage-specific and co-dependent activator elements. *Plant Mol Biol* 37: 859-869.

Battaglia M, Olvera-Carrillo Y, Garciarrubio A, Campos F, and Covarrubias A A (2008) The enigmatic LEA proteins and other hydrophilins. *Plant Physiol* 148: 6-24.

Berglund A K, Spånning E, Biverståhl H, Maddalo G, Tellgren-Roth C, Mäler L, and Glaser E (2009) Dual targeting to mitochondria and chloroplasts: characterization of Thr-tRNA synthetase targeting peptide. *Mol Plant* 2: 1298-1309.

Berri S, Abbruscato P, Faivre-Rampant O, Brasileiro A C, Fumasoni I, Satoh K, Kikuchi S et al. (2009) Characterization of WRKY co-regulatory networks in rice and Arabidopsis. *BMC Plant Biol* 9: 120.

Berrocal-Lobo M, Molina A, and Solano R (2002) Constitutive expression of ETHYLENE-RESPONSE-FACTOR1 in Arabidopsis confers resistance to several necrotrophic fungi. *Plant J* 29: 23-32.

Boter M, Ruíz-Rivero O, Abdeen A, and Prat S (2004) Conserved MYC transcription factors play a key role in jasmonate signaling both in tomato and Arabidopsis. *Genes Dev* 18: 1577-1591.

Boucher V, Buitink J, Lin X, Boudet J, Hoekstra F A, Hundertmark M, Renard D et al. (2010) MtPM25 is an atypical hydrophobic late embryogenesis-abundant protein that dissociates cold and desiccation-aggregated proteins. *Plant Cell Environ* 33: 418-430.

Bray E A (1993) Molecular Responses to Water Deficit. *Plant Physiol* 103: 1035-1040.

Browne J, Tunnacliffe A, and Burnell A (2002) Anhydrobiosis: plant desiccation gene found in a nematode. *Nature* 416: 38.

Browne J A, Dolan K M, Tyson T, Goyal K, Tunnacliffe A, and Burnell A M (2004) Dehydration-specific induction of hydrophilic protein genes in the anhydrobiotic nematode Aphelenchus avenae. *Eukaryot Cell* 3: 966-975.

Buchanan-Wollaston V (1997) The molecular biology of leaf senescence. *J. Exp. Bot.* 48: 181-199.

Buchanan-Wollaston V, Earl S, Harrison E, Mathas E, Navabpour S, Page T, and Pink D (2003) The molecular analysis of leaf senescence--a genomics approach. *Plant Biotechnol J* 1: 3-22.

Buchanan-Wollaston V, Page T, Harrison E, Breeze E, Lim P O, Nam H G, Lin J F et al. (2005) Comparative transcriptome analysis reveals significant differences in gene expression and signalling pathways between developmental and dark/starvation-induced senescence in Arabidopsis. *Plant J* 42: 567-585.

Bucholc M, Ciesielski A, Goch G, Anielska-Mazur A, Kulik A, Krzywińska E, and Dobrowolska G (2011) SNF1-related Protein Kinases 2 Are Negatively Regulated by a Plant-specific Calcium Sensor. *J. of Biol.Chem.*286: 3429-3441.

Buitink J, and Leprince O (2004) Glass formation in plant anhydrobiotes: survival in the dry state. *Cryobiology* 48: 215-228.

Butenko M A, Stenvik G E, Alm V, Saether B, Patterson S E, and Aalen R B (2006) Ethylene-dependent and -independent pathways controlling floral abscission are revealed to converge using promoter::reporter gene constructs in the ida abscission mutant. *J Exp Bot* 57: 3627-3637.

Cacela C, and Hincha D K (2006) Low amounts of sucrose are sufficient to depress the phase transition temperature of dry phosphatidylcholine, but not for lyoprotection of liposomes. *Biophys J* 90: 2831-2842.

Cao H, Bowling S A, Gordon A S, and Dong X (1994) Characterization of an Arabidopsis Mutant That Is Nonresponsive to Inducers of Systemic Acquired Resistance. *Plant Cell* 6: 1583-1592.

Carol R J, and Dolan L (2006) The role of reactive oxygen species in cell growth: lessons from root hairs. *J Exp Bot* 57: 1829-1834.

Cary A J, Liu W, and Howell S H (1995) Cytokinin action is coupled to ethylene in its effects on the inhibition of root and hypocotyl elongation in Arabidopsis thaliana seedlings. *Plant Physiol* 107: 1075-1082.

Chae M-J, Lee J-S, Nam M-H, Cho K, Hong J-Y, Yi S-A, Suh S-C et al. (2007) A rice dehydration-inducible SNF1-related protein kinase 2 phosphorylates an abscisic acid responsive element-binding factor and associates with ABA signaling. *Plant Mol. Bio.*63: 151-169.

Chakrabarty D, Chatterjee J, and Datta S (2007) Oxidative stress and antioxidant activity as the basis of senescence in chrysanthemum florets. *Plant Growth Reg.* 53: 107-115.

Chakrabortee S, Boschetti C, Walton L J, Sarkar S, Rubinsztein D C, and Tunnacliffe A (2007) Hydrophilic protein associated with desiccation tolerance exhibits broad protein stabilization function. *Proc Natl Acad Sci U S A* 104: 18073-18078.

Chang H, Jones M L, Banowetz G M, and Clark D G (2003) Overproduction of cytokinins in petunia flowers transformed with P(SAG12)-IPT delays corolla senescence and decreases sensitivity to ethylene. *Plant Physiol* 132: 2174-2183.

Cheong Y H, Chang H S, Gupta R, Wang X, Zhu T, and Luan S (2002) Transcriptional profiling reveals novel interactions between wounding, pathogen, abiotic stress, and hormonal responses in Arabidopsis. *Plant Physiol* 129: 661-677.

Chichkova N V, Kim S H, Titova E S, Kalkum M, Morozov V S, Rubtsov Y P, Kalinina N O et al. (2004) A plant caspase-like protease activated during the hypersensitive response. *Plant Cell* 16: 157-171.

Chinnusamy V, Ohta M, Kanrar S, Lee B H, Hong X, Agarwal M, and Zhu J K (2003) ICE1: a regulator of cold-induced transcriptome and freezing tolerance in Arabidopsis. *Genes Dev* 17: 1043-1054.

Chinnusamy V, Schumaker K, and Zhu J K (2004) Molecular genetic perspectives on cross-talk and specificity in abiotic stress signalling in plants. *J Exp Bot* 55: 225-236.

Choi H, Hong J, Ha J, Kang J, and Kim S Y (2000) ABFs, a family of ABA-responsive element binding factors. *J Biol Chem* 275: 1723-1730.

Close T J (1996) Dehydrins: Emergence of a biochemical role of a family of plant dehydration proteins. *Physiol. Plant.* 97: 795-803.

Colcombet J, and Hirt H (2008) Arabidopsis MAPKs: a complex signalling network involved in multiple biological processes. *Biochem J* 413: 217-226.

Cominelli E, Galbiati M, Vavasseur A, Conti L, Sala T, Vuylsteke M, Leonhardt N et al. (2005) A guard-cell-specific MYB transcription factor regulates stomatal movements and plant drought tolerance. *Curr Biol* 15: 1196-1200.

Crowe J H, Carpenter J F, and Crowe L M (1998) The role of vitrification in anhydrobiosis. *Annu Rev Physiol* 60: 73-103.

Cutler S R, Rodriguez P L, Finkelstein R R, and Abrams S R (2010) Abscisic acid: emergence of a core signaling network. *Annu Rev Plant Biol* 61: 651-679.

d'Enfert C, Minet M, and Lacroute F (1995) Cloning plant genes by complementation of yeast mutants. *Methods Cell Biol* 49: 417-430.

De Paepe A, Vuylsteke M, Van Hummelen P, Zabeau M, and Van Der Straeten D (2004) Transcriptional profiling by cDNA-AFLP and microarray analysis reveals novel insights into the early response to ethylene in Arabidopsis. *Plant J* 39: 537-559.

del Río L A, Sandalio L M, Altomare D A, and Zilinskas B A (2003) Mitochondrial and peroxisomal manganese superoxide dismutase: differential expression during leaf senescence. *J Exp Bot* 54: 923-933.

Delaney T P, Uknes S, Vernooij B, Friedrich L, Weymann K, Negrotto D, Gaffney T et al. (1994) A central role of salicylic Acid in plant disease resistance. *Science* 266: 1247-1250.

Denekamp N Y, Thorne M A, Clark M S, Kube M, Reinhardt R, and Lubzens E (2009) Discovering genes associated with dormancy in the monogonont rotifer Brachionus plicatilis. *BMC Genomics* 10: 108.

Di Cola A, and Robinson C (2005) Large-scale translocation reversal within the thylakoid Tat system in vivo. *J Cell Biol* 171: 281-289.

Dolan L, and Davies J (2004) Cell expansion in roots. *Curr Opin Plant Biol* 7: 33-39.

Droillard M J, and Paulin A (1990) Isozymes of Superoxide Dismutase in Mitochondria and Peroxisomes Isolated from Petals of Carnation (Dianthus caryophyllus) during Senescence. *Plant Physiol* 94: 1187-1192.

Dunand C, Crèvecoeur M, and Penel C (2007) Distribution of superoxide and hydrogen peroxide in Arabidopsis root and their influence on root development: possible interaction with peroxidases. *New Phytol* 174: 332-341.

Dure L, Crouch M, Harada J, Ho T-H D, Mundy J, Quatrano R, Thomas T et al. (1989) Common amino acid sequence domains among the LEA proteins of higher plants. *Plant Mol.r Biology* 12: 475-486.

Dure L, and Galau G A (1981) Developmental Biochemistry of Cottonseed Embryogenesis and Germination : XIII. Regulation of biosynthesis of principal storage proteins. *Plant Physiol* 68: 187-194.

Eisinger W (1977) Role of cytokinins in carnation flower senescence. *Plant Physiol* 59: 707-709.

Ellis C M, Nagpal P, Young J C, Hagen G, Guilfoyle T J, and Reed J W (2005) AUXIN RESPONSE FACTOR1 and AUXIN RESPONSE FACTOR2 regulate senescence and floral organ abscission in Arabidopsis thaliana. *Development* 132: 4563-4574.

Elmayan T, and Tepfer M (1995) Evaluation in tobacco of the organ specificity and strength of the rolD promoter, domain A of the 35S promoter and the 35S2 promoter. *Transgenic Res* 4: 388-396.

Eulgem T, Rushton P J, Robatzek S, and Somssich I E (2000) The WRKY superfamily of plant transcription factors. *Trends Plant Sci* 5: 199-206.

Ferrari S, Galletti R, Denoux C, De Lorenzo G, Ausubel F M, and Dewdney J (2007) Resistance to Botrytis cinerea induced in Arabidopsis by elicitors is independent of salicylic acid, ethylene, or jasmonate signaling but requires PHYTOALEXIN DEFICIENT3. *Plant Physiol* 144: 367-379.

Ferrari S, Plotnikova J M, De Lorenzo G, and Ausubel F M (2003) Arabidopsis local resistance to Botrytis cinerea involves salicylic acid and camalexin and requires EDS4 and PAD2, but not SID2, EDS5 or PAD4. *Plant J* 35: 193-205.

Feys B J, Wiermer M, Bhat R A, Moisan L J, Medina-Escobar N, Neu C, Cabral A et al. (2005) Arabidopsis SENESCENCE-ASSOCIATED GENE101 stabilizes and signals within an ENHANCED DISEASE SUSCEPTIBILITY1 complex in plant innate immunity. *Plant Cell* 17: 2601-2613.

Finkelstein R R, Gampala S S, and Rock C D (2002) Abscisic acid signaling in seeds and seedlings. *Plant Cell* 14 Suppl: S15-45.

Foreman J, Demidchik V, Bothwell J H, Mylona P, Miedema H, Torres M A, Linstead P et al. (2003) Reactive oxygen species produced by NADPH oxidase regulate plant cell growth. *Nature* 422: 442-446.

Foyer C H, Bloom A J, Queval G, and Noctor G (2009a) Photorespiratory metabolism: genes, mutants, energetics, and redox signaling. *Annu Rev Plant Biol* 60: 455-484.

Foyer C H, Faragher R, and Thornalley P (2009b) Redox metabolism and longevity relationships in animals and plants. Preface. *SEB Exp Biol Ser* 62: xix-xx.

Foyer C H, and Noctor G (2005) Redox homeostasis and antioxidant signaling: a metabolic interface between stress perception and physiological responses. *Plant Cell* 17: 1866-1875.

Foyer C H, and Noctor G (2009) Redox regulation in photosynthetic organisms: signaling, acclimation, and practical implications. *Antioxid Redox Signal* 11: 861-905.

Fry S, Miller J, and Dumville J (2002) A proposed role for copper ions in cell wall loosening. *Plant and Soil* 247: 57-67.

Fujita M, Fujita Y, Noutoshi Y, Takahashi F, Narusaka Y, Yamaguchi-Shinozaki K, and Shinozaki K (2006) Crosstalk between abiotic and biotic stress responses: a current view from the points of convergence in the stress signaling networks. *Curr Opin Plant Biol* 9: 436-442.

Fujita Y, Fujita M, Satoh R, Maruyama K, Parvez M M, Seki M, Hiratsu K et al. (2005) AREB1 is a transcription activator of novel ABRE-dependent ABA signaling that enhances drought stress tolerance in Arabidopsis. *Plant Cell* 17: 3470-3488.

Gadjev I, Vanderauwera S, Gechev T S, Laloi C, Minkov I N, Shulaev V, Apel K et al. (2006) Transcriptomic footprints disclose specificity of reactive oxygen species signaling in Arabidopsis. *Plant Physiol* 141: 436-445.

Gal T Z, Glazer I, and Koltai H (2004) An LEA group 3 family member is involved in survival of C. elegans during exposure to stress. *FEBS letters* 577: 21-26.

Galau G A, Wang H Y, and Hughes D W (1993) Cotton Lea5 and Lea14 encode atypical late embryogenesis-abundant proteins. *Plant Physiol* 101: 695-696.

Gao M, Liu J, Bi D, Zhang Z, Cheng F, Chen S, and Zhang Y (2008) MEKK1, MKK1/MKK2 and MPK4 function together in a mitogen-activated protein kinase cascade to regulate innate immunity in plants. *Cell Res* 18: 1190-1198.

Gapper C, and Dolan L (2006) Control of plant development by reactive oxygen species. *Plant Physiol* 141: 341-345.

George S, Usha B, and Parida A (2009) Isolation and characterization of an atypical LEA protein coding cDNA and its promoter from drought-tolerant plant Prosopis juliflora. *Appl Biochem Biotechnol* 157: 244-253.

Glazebrook J (2005) Contrasting mechanisms of defense against biotrophic and necrotrophic pathogens. *Annu Rev Phytopathol* 43: 205-227.

Govrin E M, and Levine A (2000) The hypersensitive response facilitates plant infection by the necrotrophic pathogen Botrytis cinerea. *Curr Biol* 10: 751-757.

Goyal K, Walton L J, and Tunnacliffe A (2005) LEA proteins prevent protein aggregation due to water stress. *Biochem J* 388: 151-157.

Grace M L, Chandrasekharan M B, Hall T C, and Crowe A J (2004) Sequence and spacing of TATA box elements are critical for accurate initiation from the beta-phaseolin promoter. *J Biol Chem* 279: 8102-8110.

Grelet J, Benamar A, Teyssier E, Avelange-Macherel M H, Grunwald D, and Macherel D (2005) Identification in pea seed mitochondria of a late-embryogenesis abundant protein able to protect enzymes from drying. *Plant Physiol* 137: 157-167.

Guan L M, Zhao J, and Scandalios J G (2000) Cis-elements and trans-factors that regulate expression of the maize Cat1 antioxidant gene in response to ABA and osmotic stress: H2O2 is the likely intermediary signaling molecule for the response. *Plant J* 22: 87-95.

Guiltinan M J, Marcotte W R, and Quatrano R S (1990) A plant leucine zipper protein that recognizes an abscisic acid response element. *Science* 250: 267-271.

Guo Y, and Gan S (2005) Leaf senescence: signals, execution, and regulation. *Curr Top Dev Biol* 71: 83-112.

Gómez-Gómez L, and Boller T (2002) Flagellin perception: a paradigm for innate immunity. *Trends Plant Sci* 7: 251-256.

Gómez-Gómez L, Felix G, and Boller T (1999) A single locus determines sensitivity to bacterial flagellin in Arabidopsis thaliana. *Plant J* 18: 277-284.

Haaning S, Radutoiu S, Hoffmann S V, Dittmer J, Giehm L, Otzen D E, and Stougaard J (2008) An unusual intrinsically disordered protein from the model legume Lotus japonicus stabilizes proteins in vitro. *J Biol Chem* 283: 31142-31152.

Hand S C, Menze M A, Toner M, Boswell L, and Moore D (2010) LEA Proteins During Water Stress: Not Just for Plants Anymore. *Annu Rev Physiol*. Vol. 73: 115-134

Hara M, Fujinaga M, and Kuboi T (2004) Radical scavenging activity and oxidative modification of citrus dehydrin. *Plant Physiol Biochem* 42: 657-662.

Hara M, Fujinaga M, and Kuboi T (2005) Metal binding by citrus dehydrin with histidine-rich domains. *J Exp Bot* 56: 2695-2703.

Hara M, Shinoda Y, Tanaka Y, and Kuboi T (2009) DNA binding of citrus dehydrin promoted by zinc ion. *Plant Cell Environ* 32: 532-541.

Hara M, Terashima S, Fukaya T, and Kuboi T (2003) Enhancement of cold tolerance and inhibition of lipid peroxidation by citrus dehydrin in transgenic tobacco. *Planta* 217: 290-298.

Harmer S L, Hogenesch J B, Straume M, Chang H S, Han B, Zhu T, Wang X et al. (2000) Orchestrated transcription of key pathways in Arabidopsis by the circadian clock. *Science* 290: 2110-2113.

Heazlewood J L, Tonti-Filippini J S, Gout A M, Day D A, Whelan J, and Millar A H (2004) · Experimental analysis of the Arabidopsis mitochondrial proteome highlights signaling and regulatory components, provides assessment of targeting prediction programs, and indicates plant-specific mitochondrial proteins. *Plant Cell* 16: 241-256.

Higo K, Ugawa Y, Iwamoto M, and Korenaga T (1999) Plant cis-acting regulatory DNA elements (PLACE) database: 1999. *Nucleic Acids Res* 27: 297-300.

Hinderhofer K, and Zentgraf U (2001) Identification of a transcription factor specifically expressed at the onset of leaf senescence. *Planta* 213: 469-473.

Hirayama T, and Shinozaki K (2010) Research on plant abiotic stress responses in the post-genome era: past, present and future. *Plant J* 61: 1041-1052.

Hoeberichts F A, van Doorn W G, Vorst O, Hall R D, and van Wordragen M F (2007a) Sucrose prevents up-regulation of senescence-associated genes in carnation petals. *J. Exp. Bot.* 58: 2873-2885.

Hoeberichts F A, van Doorn W G, Vorst O, Hall R D, and van Wordragen M F (2007b) Sucrose prevents up-regulation of senescence-associated genes in carnation petals. *J Exp Bot* 58: 2873-2885.

Hoekstra F A, Golovina E A, and Buitink J (2001) Mechanisms of plant desiccation tolerance. *Trends Plant Sci* 6: 431-438.

Honjoh K, Shimizu H, Nagaishi N, Matsumoto H, Suga K, Miyamoto T, Iio M et al. (2001) Improvement of freezing tolerance in transgenic tobacco leaves by expressing the hiC6 gene. *Biosci Biotechnol Biochem* 65: 1796-1804.

Hunault G, and Jaspard E (2010) LEAPdb: a database for the late embryogenesis abundant proteins. *BMC Genomics* 11: 221.

Hundertmark M, Dimova R, Lengefeld J, Seckler R, and Hincha D K (2011) The intrinsically disordered late embryogenesis abundant protein LEA18 from Arabidopsis thaliana modulates membrane stability through binding and folding. *Biochim Biophys Acta* 1808: 446-453.

Hundertmark M, and Hincha D K (2008) LEA (late embryogenesis abundant) proteins and their encoding genes in Arabidopsis thaliana. *BMC Genomics* 9: 118.

Hörtensteiner S, and Feller U (2002) Nitrogen metabolism and remobilization during senescence. *J Exp Bot* 53: 927-937.

Imai R, Chang L, Ohta A, Bray E A, and Takagi M (1996) A lea-class gene of tomato confers salt and freezing tolerance when expressed in Saccharomyces cerevisiae. *Gene* 170: 243-248.

Jackson S, Gascón J, Carrera E, Monte E, and Prat S (1997) Cloning and expression analysis of a gene that shows developmental regulation upon tuberization in potato. *Plant Mol Biol* 33: 169-174.

Jaspers P, and Kangasjärvi J (2010) Reactive oxygen species in abiotic stress signaling. *Physiol Plant* 138: 405-413.

Jefferson R (1987) Assaying chimeric genes in plants: The GUS gene fusion system. *Plant Mol. Bio. Rep.* 5: 387-405.

Jiang Y, and Deyholos M K (2009) Functional characterization of Arabidopsis NaCl-inducible WRKY25 and WRKY33 transcription factors in abiotic stresses. *Plant Mol Biol* 69: 91-105.

Jirage D, Tootle T L, Reuber T L, Frost L N, Feys B J, Parker J E, Ausubel F M et al. (1999) Arabidopsis thaliana PAD4 encodes a lipase-like gene that is important for salicylic acid signaling. *Proc Natl Acad Sci U S A* 96: 13583-13588.

Jones J D, and Dangl J L (2006) The plant immune system. *Nature* 444: 323-329.

Jones M L, Chaffin G S, Eason J R, and Clark D G (2005) Ethylene-sensitivity regulates proteolytic activity and cysteine protease gene expression in petunia corollas. *J Exp Bot* 56: 2733-2744.

Jones M L, and Woodson W R (1999) Differential expression of three members of the 1-aminocyclopropane-1-carboxylate synthase gene family in carnation. *Plant Physiol* 119: 755-764.

Joo J H, Bae Y S, and Lee J S (2001) Role of auxin-induced reactive oxygen species in root gravitropism. *Plant Physiol* 126: 1055-1060.

Jung C, Lyou S, Yeu S, Kim M, Rhee S, Kim M, Lee J et al. (2007) Microarray-based screening of jasmonate-responsive genes in <i>Arabidopsis thaliana</i&gt. *Plant Cell Reports* 26: 1053-1063.

Kang J Y, Choi H I, Im M Y, and Kim S Y (2002) Arabidopsis basic leucine zipper proteins that mediate stress-responsive abscisic acid signaling. *Plant Cell* 14: 343-357.

Kanias T, Wong K, and Acker J P (2007) Determination of Lipid Peroxidation in Desiccated Red Blood Cells. *Cell Preservation Technology* 5: 165-174.

Kaplan B, Davydov O, Knight H, Galon Y, Knight M R, Fluhr R, and Fromm H (2006) Rapid transcriptome changes induced by cytosolic Ca2+ transients reveal ABRE-related sequences as Ca2+-responsive cis elements in Arabidopsis. *Plant Cell* 18: 2733-2748.

Kay B K, Williamson M P, and Sudol M (2000) The importance of being proline: the interaction of proline-rich motifs in signaling proteins with their cognate domains. *FASEB J* 14: 231-241.

Kikawada T, Nakahara Y, Kanamori Y, Iwata K, Watanabe M, McGee B, Tunnacliffe A et al. (2006) Dehydration-induced expression of LEA proteins in an anhydrobiotic chironomid. *Biochem Biophys Res Commun* 348: 56-61.

Knight M R (2007) New ideas on root hair growth appear from the flanks. *Proc Natl Acad Sci U S A* 104: 20649-20650.

Kovacs D, Agoston B, and Tompa P (2008a) Disordered plant LEA proteins as molecular chaperones. *Plant Signal Behav* 3: 710-713.

Kovacs D, Kalmar E, Torok Z, and Tompa P (2008b) Chaperone activity of ERD10 and ERD14, two disordered stress-related plant proteins. *Plant Physiol* 147: 381-390.

Kruger C, Berkowitz O, Stephan U W, and Hell R (2002) A metal-binding member of the late embryogenesis abundant protein family transports iron in the phloem of Ricinus communis L. *J Biol Chem* 277: 25062-25069.

Kwak J M, Nguyen V, and Schroeder J I (2006) The role of reactive oxygen species in hormonal responses. *Plant Physiol* 141: 323-329.

Kyte J, and Doolittle R F (1982) A simple method for displaying the hydropathic character of a protein. *J Mol Biol* 157: 105-132.

Lal S, Gulyani V, and Khurana P (2008) Overexpression of HVA1 gene from barley generates tolerance to salinity and water stress in transgenic mulberry (Morus indica). *Transgenic Res* 17: 651-663.

Lam E, and Chua N H (1989) ASF-2: a factor that binds to the cauliflower mosaic virus 35S promoter and a conserved GATA motif in Cab promoters. *Plant Cell* 1: 1147-1156.

Lapinski J, and Tunnacliffe A (2003) Anhydrobiosis without trehalose in bdelloid rotifers. *FEBS Lett* 553: 387-390.

Lee Y J, and Yang Z (2008) Tip growth: signaling in the apical dome. *Curr Opin Plant Biol* 11: 662-671.

Leprince O, Colson P, Houssier C, and Deltour R (1995) Changes in chromatin structure associated with germination of maize and their relation with desiccation tolerance. *Plant, Cell Env.* 18: 619-629.

Lescot M, Déhais P, Thijs G, Marchal K, Moreau Y, Van de Peer Y, Rouzé P et al. (2002) PlantCARE, a database of plant cis-acting regulatory elements and a portal to tools for in silico analysis of promoter sequences. *Nucleic Acids research* 30: 325-327.

Leverentz M K, Wagstaff C, Rogers H J, Stead A D, Chanasut U, Silkowski H, Thomas B et al. (2002) Characterization of a novel lipoxygenase-independent senescence mechanism in Alstroemeria peruviana floral tissue. *Plant Physiol* 130: 273-283.

Li J, Brader G, Kariola T, and Palva E T (2006) WRKY70 modulates the selection of signaling pathways in plant defense. *Plant J* 46: 477-491.

Li J, Brader G, and Palva E T (2004) The WRKY70 transcription factor: a node of convergence for jasmonate-mediated and salicylate-mediated signals in plant defense. *Plant Cell* 16: 319-331.

Lim P O, Kim H J, and Nam H G (2007) Leaf senescence. *Annu Rev Plant Biol* 58: 115-136.

Lippok B, Birkenbihl R P, Rivory G, Brümmer J, Schmelzer E, Logemann E, and Somssich I E (2007) Expression of AtWRKY33 encoding a pathogen- or PAMP-responsive WRKY transcription factor is regulated by a composite DNA motif containing W box elements. *Mol Plant Microbe Interact* 20: 420-429.

Liszkay A, van der Zalm E, and Schopfer P (2004) Production of reactive oxygen intermediates (O(2)(.-), H(2)O(2), and (.)OH) by maize roots and their role in wall loosening and elongation growth. *Plant Physiol* 136: 3114-3123.

Litts J C, Colwell G W, Chakerian R L, and Quatrano R S (1987) The nucleotide sequence of a cDNA clone encoding the wheat Em protein. *Nucleic Acids Research* 15: 3607-3618.

Liu L, Zhou Y, Szczerba M W, Li X, and Lin Y (2010) Identification and application of a rice senescence-associated promoter. *Plant Physiol* 153: 1239-1249.

Liu Q, Kasuga M, Sakuma Y, Abe H, Miura S, Yamaguchi-Shinozaki K, and Shinozaki K (1998) Two transcription factors, DREB1 and DREB2, with an EREBP/AP2 DNA binding domain separate two cellular signal transduction pathways in drought- and low-temperature-responsive gene expression, respectively, in Arabidopsis. *Plant Cell* 10: 1391-1406.

Lorenzo O, Chico J M, Sánchez-Serrano J J, and Solano R (2004) JASMONATE-INSENSITIVE1 encodes a MYC transcription factor essential to discriminate between different jasmonate-regulated defense responses in Arabidopsis. *Plant Cell* 16: 1938-1950.

Luhua S, Ciftci-Yilmaz S, Harper J, Cushman J, and Mittler R (2008) Enhanced tolerance to oxidative stress in transgenic Arabidopsis plants expressing proteins of unknown function. *Plant Physiol* 148: 280-292.

Maleck K, Levine A, Eulgem T, Morgan A, Schmid J, Lawton K A, Dangl J L et al. (2000) The transcriptome of Arabidopsis thaliana during systemic acquired resistance. *Nat Genet* 26: 403-410.

Maruyama K, Sakuma Y, Kasuga M, Ito Y, Seki M, Goda H, Shimada Y et al. (2004) Identification of cold-inducible downstream genes of the Arabidopsis DREB1A/CBF3 transcriptional factor using two microarray systems. *Plant J* 38: 982-993.

Mateo A, Mühlenbock P, Rustérucci C, Chang C C, Miszalski Z, Karpinska B, Parker J E et al. (2004) LESION SIMULATING DISEASE 1 is required for acclimation to conditions that promote excess excitation energy. *Plant Physiol* 136: 2818-2830.

Mengiste T, Chen X, Salmeron J, and Dietrich R (2003) The BOTRYTIS SUSCEPTIBLE1 gene encodes an R2R3MYB transcription factor protein that is required for biotic and abiotic stress responses in Arabidopsis. *Plant Cell* 15: 2551-2565.

Menze M A, Boswell L, Toner M, and Hand S C (2009) Occurrence of mitochondria-targeted Late Embryogenesis Abundant (LEA) gene in animals increases organelle resistance to water stress. *J Biol Chem* 284: 10714-10719.

Mhamdi A, Queval G, Chaouch S, Vanderauwera S, Van Breusegem F, and Noctor G (2010) Catalase function in plants: a focus on Arabidopsis mutants as stress-mimic models. *J. Exp. Bot.* 61: 4197-4220.

Miao Y, Laun T, Zimmermann P, and Zentgraf U (2004) Targets of the WRKY53 transcription factor and its role during leaf senescence in Arabidopsis. *Plant Mol Biol* 55: 853-867.

Miao Y, Laun T M, Smykowski A, and Zentgraf U (2007) Arabidopsis MEKK1 can take a short cut: it can directly interact with senescence-related WRKY53 transcription factor on the protein level and can bind to its promoter. *Plant Mol Biol* 65: 63-76.

Miao Y, and Zentgraf U (2007) The antagonist function of Arabidopsis WRKY53 and ESR/ESP in leaf senescence is modulated by the jasmonic and salicylic acid equilibrium. *Plant Cell* 19: 819-830.

Miller G, Suzuki N, Rizhsky L, Hegie A, Koussevitzky S, and Mittler R (2007) Double mutants deficient in cytosolic and thylakoid ascorbate peroxidase reveal a complex mode of interaction between reactive oxygen species, plant development, and response to abiotic stresses. *Plant Physiol* 144: 1777-1785.

Miller J D, Arteca R N, and Pell E J (1999) Senescence-associated gene expression during ozone-induced leaf senescence in Arabidopsis. *Plant Physiol* 120: 1015-1024.

Mizoguchi T, Irie K, Hirayama T, Hayashida N, Yamaguchi-Shinozaki K, Matsumoto K, and Shinozaki K (1996) A gene encoding a mitogen-activated protein kinase kinase kinase is induced simultaneously with genes for a mitogen-activated protein kinase and an S6 ribosomal protein kinase by touch, cold, and water stress in Arabidopsis thaliana. *Proc Natl Acad Sci U S A* 93: 765-769.

Moons A, De Keyser A, and Van Montagu M (1997) A group 3 LEA cDNA of rice, responsive to abscisic acid, but not to jasmonic acid, shows variety-specific differences in salt stress response. *Gene* 191: 197-204.

Mor Y, Spiegelstein H, and Halevy A H (1983) Inhibition of ethylene biosynthesis in carnation petals by cytokinin. *Plant Physiol* 71: 541-546.

Morris P C, Kumar A, Bowles D J, and Cuming A C (1990) Osmotic stress and abscisic acid induce expression of the wheat Em genes. *Eur J Biochem* 190: 625-630.

Mowla S B, Cuypers A, Driscoll S P, Kiddle G, Thomson J, Foyer C H, and Theodoulou F L (2006) Yeast complementation reveals a role for an Arabidopsis thaliana late embryogenesis abundant (LEA)-like protein in oxidative stress tolerance. *Plant J* 48: 743-756.

Mukhopadhyay P, Zheng M, Bedzyk L A, LaRossa R A, and Storz G (2004) Prominent roles of the NorR and Fur regulators in the Escherichia coli transcriptional response to reactive nitrogen species. *Proc Natl Acad Sci U S A* 101: 745-750.

Mundy J, Yamaguchi-Shinozaki K, and Chua N H (1990) Nuclear proteins bind conserved elements in the abscisic acid-responsive promoter of a rice rab gene. *Proc Natl Acad Sci U S A* 87: 1406-1410.

Nafisi M, Goregaoker S, Botanga C J, Glawischnig E, Olsen C E, Halkier B A, and Glazebrook J (2007) Arabidopsis cytochrome P450 monooxygenase 71A13 catalyzes the conversion of indole-3-acetaldoxime in camalexin synthesis. *Plant Cell* 19: 2039-2052.

Nakagami H, Soukupová H, Schikora A, Zársky V, and Hirt H (2006) A Mitogen-activated protein kinase kinase kinase mediates reactive oxygen species homeostasis in Arabidopsis. *J Biol Chem* 281: 38697-38704.

Nakashima K, Ito Y, and Yamaguchi-Shinozaki K (2009) Transcriptional regulatory networks in response to abiotic stresses in Arabidopsis and grasses. *Plant Physiol* 149: 88-95.

Nakashima K, Kiyosue T, Yamaguchi-Shinozaki K, and Shinozaki K (1997) A nuclear gene, erd1, encoding a chloroplast-targeted Clp protease regulatory subunit homolog is not only induced by water stress but also developmentally up-regulated during senescence in Arabidopsis thaliana. *Plant J* 12: 851-861.

Nakazawa M, Yabe N, Ichikawa T, Yamamoto Y Y, Yoshizumi T, Hasunuma K, and Matsui M (2001) DFL1, an auxin-responsive GH3 gene homologue, negatively regulates shoot cell elongation and lateral root formation, and positively regulates the light response of hypocotyl length. *Plant J* 25: 213-221.

Naot D, Ben-Hayyim G, Eshdat Y, and Holland D (1995) Drought, heat and salt stress induce the expression of a citrus homologue of an atypical late-embryogenesis Lea5 gene. *Plant Mol Biol* 27: 619-622.

Narusaka Y, Nakashima K, Shinwari Z K, Sakuma Y, Furihata T, Abe H, Narusaka M et al. (2003) Interaction between two cis-acting elements, ABRE and DRE, in ABA-dependent expression of Arabidopsis rd29A gene in response to dehydration and high-salinity stresses. *Plant J* 34: 137-148.

Navabpour S, Morris K, Allen R, Harrison E, A-H-Mackerness S, and Buchanan-Wollaston V (2003) Expression of senescence-enhanced genes in response to oxidative stress. *J Exp Bot* 54: 2285-2292.

NDong C, Danyluk J, Wilson K E, Pocock T, Huner N P, and Sarhan F (2002) Cold-regulated cereal chloroplast late embryogenesis abundant-like proteins. Molecular characterization and functional analyses. *Plant Physiol* 129: 1368-1381.

Nylander M, Svensson J, Palva E T, and Welin B V (2001) Stress-induced accumulation and tissue-specific localization of dehydrins in Arabidopsis thaliana. *Plant Mol Biol* 45: 263-279.

Olive M R, Walker J C, Singh K, Dennis E S, and Peacock W J (1990) Functional properties of the anaerobic responsive element of the maize Adh1 gene. *Plant Mol Biol* 15: 593-604.

Orendi G, Zimmermann P, Baar C, and Zentgraf U (2001) Loss of stress-induced expression of catalase3 during leaf senescence in Arabidopsis thaliana is restricted to oxidative stress. *Plant Sci* 161: 301-314.

Panavas T, Pikula A, Reid P D, Rubinstein B, and Walker E L (1999) Identification of senescence-associated genes from daylily petals. *Plant Mol Biol* 40: 237-248.

Panchuk I I, Zentgraf U, and Volkov R A (2005) Expression of the Apx gene family during leaf senescence of Arabidopsis thaliana. *Planta* 222: 926-932.

Patterson S E, and Bleecker A B (2004) Ethylene-dependent and -independent processes associated with floral organ abscission in Arabidopsis. *Plant Physiol* 134: 194-203.

Peeters N, and Small I (2001) Dual targeting to mitochondria and chloroplasts. *Biochim Biophys Acta* 1541: 54-63.

Pegadaraju V, Knepper C, Reese J, and Shah J (2005) Premature leaf senescence modulated by the Arabidopsis PHYTOALEXIN DEFICIENT4 gene is associated with defense against the phloem-feeding green peach aphid. *Plant Physiol* 139: 1927-1934.

Pegadaraju V, Louis J, Singh V, Reese J C, Bautor J, Feys B J, Cook G et al. (2007) Phloem-based resistance to green peach aphid is controlled by Arabidopsis PHYTOALEXIN DEFICIENT4 without its signaling partner ENHANCED DISEASE SUSCEPTIBILITY1. *Plant J* 52: 332-341.

Petersen M, Brodersen P, Naested H, Andreasson E, Lindhart U, Johansen B, Nielsen H B et al. (2000) Arabidopsis map kinase 4 negatively regulates systemic acquired resistance. *Cell* 103: 1111-1120.

Petrova V Y, Drescher D, Kujumdzieva A V, and Schmitt M J (2004) Dual targeting of yeast catalase A to peroxisomes and mitochondria. *Biochem J* 380: 393-400.

Piechulla B, Merforth N, and Rudolph B (1998) Identification of tomato Lhc promoter regions necessary for circadian expression. *Plant Mol Biol* 38: 655-662.

Pitzschke A, Djamei A, Bitton F, and Hirt H (2009) A major role of the MEKK1-MKK1/2-MPK4 pathway in ROS signalling. *Mol Plant* 2: 120-137.

Pitzschke A, and Hirt H (2006) Mitogen-activated protein kinases and reactive oxygen species signaling in plants. *Plant Physiol* 141: 351-356.

Pitzschke A, and Hirt H (2009) Disentangling the complexity of mitogen-activated protein kinases and reactive oxygen species signaling. *Plant Physiol* 149: 606-615.

Poduslo J F, Curran G L, Kumar A, Frangione B, and Soto C (1999) Beta-sheet breaker peptide inhibitor of Alzheimer's amyloidogenesis with increased blood-brain barrier permeability and resistance to proteolytic degradation in plasma. *J Neurobiol* 39: 371-382.

Potikha T S, Collins C C, Johnson D I, Delmer D P, and Levine A (1999) The involvement of hydrogen peroxide in the differentiation of secondary walls in cotton fibers. *Plant Physiol* 119: 849-858.

Potocký M, Jones M A, Bezvoda R, Smirnoff N, and Žárský V (2007) Reactive oxygen species produced by NADPH oxidase are involved in pollen tube growth. *New Phytol* 174: 742-751.

Pouchkina-Stantcheva N N, McGee B M, Boschetti C, Tolleter D, Chakrabortee S, Popova A V, Meersman F et al. (2007) Functional divergence of former alleles in an ancient asexual invertebrate. *Science* 318: 268-271.

Price A M, Aros Orellana D F, Salleh F M, Stevens R, Acock R, Buchanan-Wollaston V, Stead A D et al. (2008) A comparison of leaf and petal senescence in wallflower reveals common and distinct patterns of gene expression and physiology. *Plant Physiol* 147: 1898-1912.

Puhakainen T, Hess M W, Mäkelä P, Svensson J, Heino P, and Palva E T (2004) Overexpression of multiple dehydrin genes enhances tolerance to freezing stress in Arabidopsis. *Plant Mol Biol* 54: 743-753.

Qin F, Sakuma Y, Li J, Liu Q, Li Y-Q, Shinozaki K, and Yamaguchi-Shinozaki K (2004) Cloning and Functional Analysis of a Novel DREB1/CBF Transcription Factor Involved in Cold-Responsive Gene Expression in Zea mays L. *Plant Cell Physi.* 45: 1042-1052.

Qiu J L, Fiil B K, Petersen K, Nielsen H B, Botanga C J, Thorgrimsen S, Palma K et al. (2008a) Arabidopsis MAP kinase 4 regulates gene expression through transcription factor release in the nucleus. *EMBO J* 27: 2214-2221.

Qiu J L, Zhou L, Yun B W, Nielsen H B, Fiil B K, Petersen K, Mackinlay J et al. (2008b) Arabidopsis mitogen-activated protein kinase kinases MKK1 and MKK2 have overlapping functions in defense signaling mediated by MEKK1, MPK4, and MKS1. *Plant Physiol* 148: 212-222.

Quirino B F, Noh Y S, Himelblau E, and Amasino R M (2000) Molecular aspects of leaf senescence. *Trends Plant Sci* 5: 278-282.

Rabbani M A, Maruyama K, Abe H, Khan M A, Katsura K, Ito Y, Yoshiwara K et al. (2003) Monitoring expression profiles of rice genes under cold, drought, and high-salinity stresses and abscisic acid application using cDNA microarray and RNA gel-blot analyses. *Plant Physiol* 133: 1755-1767.

Radivojac P, Iakoucheva L M, Oldfield C J, Obradovic Z, Uversky V N, and Dunker A K (2007) Intrinsic disorder and functional proteomics. *Biophys J* 92: 1439-1456.

Radivojac P, Obradovic Z, Smith D K, Zhu G, Vucetic S, Brown C J, Lawson J D et al. (2004) Protein flexibility and intrinsic disorder. *Protein Sci* 13: 71-80.

Ratnakumar S, and Tunnacliffe A (2006) Intracellular trehalose is neither necessary nor sufficient for desiccation tolerance in yeast. *FEMS Yeast Res* 6: 902-913.

Ren D, Liu Y, Yang K Y, Han L, Mao G, Glazebrook J, and Zhang S (2008) A fungal-responsive MAPK cascade regulates phytoalexin biosynthesis in Arabidopsis. *Proc Natl Acad Sci U S A* 105: 5638-5643.

Renew S, Heyno E, Schopfer P, and Liszkay A (2005) Sensitive detection and localization of hydroxyl radical production in cucumber roots and Arabidopsis seedlings by spin trapping electron paramagnetic resonance spectroscopy. *Plant J* 44: 342-347.

Rentel M C, Lecourieux D, Ouaked F, Usher S L, Petersen L, Okamoto H, Knight H et al. (2004) OXI1 kinase is necessary for oxidative burst-mediated signalling in Arabidopsis. *Nature* 427: 858-861.

Rhoads D M, Umbach A L, Subbaiah C C, and Siedow J N (2006) Mitochondrial reactive oxygen species. Contribution to oxidative stress and interorganellar signaling. *Plant Physiol* 141: 357-366.

Robatzek S, and Somssich I E (2001a) A new member of the Arabidopsis WRKY transcription factor family, AtWRKY6, is associated with both senescence- and defence-related processes. *Plant J* 28: 123-133.

Robatzek S, and Somssich I E (2001b) A new member of the Arabidopsis WRKY transcription factor family, AtWRKY6, is associated with both senescence- and defence-related processes. *Plant J* 28: 123-133.

Robatzek S, and Somssich I E (2002) Targets of AtWRKY6 regulation during plant senescence and pathogen defense. *Genes Dev* 16: 1139-1149.

Rodriguez M C, Petersen M, and Mundy J (2010) Mitogen-activated protein kinase signaling in plants. *Annu Rev Plant Biol* 61: 621-649.

Rogers H J (2006) Programmed cell death in floral organs: how and why do flowers die? *Ann Bot* 97: 309-315.

Rousseau F, Serrano L, and Schymkowitz J W (2006) How evolutionary pressure against protein aggregation shaped chaperone specificity. *J Mol Biol* 355: 1037-1047.

Rubinstein B (2000) Regulation of cell death in flower petals. *Plant Mol Biol* 44: 303-318.

Rushton P J, Reinstädler A, Lipka V, Lippok B, and Somssich I E (2002) Synthetic plant promoters containing defined regulatory elements provide novel insights into pathogen- and wound-induced signaling. *Plant Cell* 14: 749-762.

Rushton P J, Somssich I E, Ringler P, and Shen Q J (2010) WRKY transcription factors. *Trends Plant Sci* 15: 247-258.

Schenk P M, Kazan K, Wilson I, Anderson J P, Richmond T, Somerville S C, and Manners J M (2000) Coordinated plant defense responses in Arabidopsis revealed by microarray analysis. *Proc Natl Acad Sci U S A* 97: 11655-11660.

Seki M, Narusaka M, Abe H, Kasuga M, Yamaguchi-Shinozaki K, Carninci P, Hayashizaki Y et al. (2001) Monitoring the expression pattern of 1300 Arabidopsis genes under drought and cold stresses by using a full-length cDNA microarray. *Plant Cell* 13: 61-72.

Seki M, Narusaka M, Ishida J, Nanjo T, Fujita M, Oono Y, Kamiya A et al. (2002) Monitoring the expression profiles of 7000 Arabidopsis genes under drought, cold and high-salinity stresses using a full-length cDNA microarray. *Plant J* 31: 279-292.

Serafini-Fracassini D, Del Duca S, Monti F, Poli F, Sacchetti G, Bregoli A M, Biondi S et al. (2002) Transglutaminase activity during senescence and programmed cell death in the corolla of tobacco (Nicotiana tabacum) flowers. *Cell Death Differ* 9: 309-321.

Shen Q, and Ho T H (1995) Functional dissection of an abscisic acid (ABA)-inducible gene reveals two independent ABA-responsive complexes each containing a G-box and a novel cis-acting element. *Plant Cell* 7: 295-307.

Shen Q, Zhang P, and Ho T H (1996) Modular nature of abscisic acid (ABA) response complexes: composite promoter units that are necessary and sufficient for ABA induction of gene expression in barley. *Plant Cell* 8: 1107-1119.

Shen Q J, Casaretto J A, Zhang P, and Ho T H (2004) Functional definition of ABA-response complexes: the promoter units necessary and sufficient for ABA induction of gene expression in barley (Hordeum vulgare L.). *Plant Mol Biol* 54: 111-124.

Shibuya K, Yoshioka T, Hashiba T, and Satoh S (2000) Role of the gynoecium in natural senescence of carnation (Dianthus caryophyllus L.) flowers. *J Exp Bot* 51: 2067-2073.

Shih M d, Hoekstra F A, and Hsing Y I C (2008) Chapter 4 Late Embryogenesis Abundant Proteins. *Adv. Bot. Res.* pp. 211-255.

Shih M D, Lin S C, Hsieh J S, Tsou C H, Chow T Y, Lin T P, and Hsing Y I (2004) Gene cloning and characterization of a soybean (Glycine max L.) LEA protein, GmPM16. *Plant Mol Biol* 56: 689-703.

Shinozaki K, and Yamaguchi-Shinozaki K (2007) Gene networks involved in drought stress response and tolerance. *J Exp Bot* 58: 221-227.

Shinozaki K, Yamaguchi-Shinozaki K, and Seki M (2003) Regulatory network of gene expression in the drought and cold stress responses. *Curr Opin Plant Biol* 6: 410-417.

Shirsat A, Wilford N, Croy R, and Boulter D (1989) Sequences responsible for the tissue specific promoter activity of a pea legumin gene in tobacco. *Mol Gen Genet* 215: 326-331.

Simpson S D, Nakashima K, Narusaka Y, Seki M, Shinozaki K, and Yamaguchi-Shinozaki K (2003) Two different novel cis-acting elements of erd1, a clpA homologous Arabidopsis gene function in induction by dehydration stress and dark-induced senescence. *Plant J* 33: 259-270.

Singh K, Foley R C, and Oñate-Sánchez L (2002) Transcription factors in plant defense and stress responses. *Curr Opin Plant Biol* 5: 430-436.

Singh S, Cornilescu C C, Tyler R C, Cornilescu G, Tonelli M, Lee M S, and Markley J L (2005) Solution structure of a late embryogenesis abundant protein (LEA14) from Arabidopsis thaliana, a cellular stress-related protein. *Protein Sci* 14: 2601-2609.

Sivamani E, Bahieldin1 A, Wraith J M, Al-Niemi T, Dyer W E, Ho T D, and Qu R (2000) Improved biomass productivity and water use efficiency under water deficit conditions in transgenic wheat constitutively expressing the barley HVA1 gene. *Plant Sci* 155: 1-9.

Smith M T, Saks Y, and Staden J V (1992) Ultrastructural Changes in the Petals of Senescing flowers of Dianthus caryophyllus L. *Ann Bot* 69 (3): 277-285.

Smykowski A, Zimmermann P, and Zentgraf U (2010) G-Box binding factor1 reduces CATALASE2 expression and regulates the onset of leaf senescence in Arabidopsis. *Plant Physiol* 153: 1321-1331.

Steponkus P L, Uemura M, Joseph R A, Gilmour S J, and Thomashow M F (1998) Mode of action of the COR15a gene on the freezing tolerance of Arabidopsis thaliana. *Proc Natl Acad Sci U S A* 95: 14570-14575.

Strader L C, Culler A H, Cohen J D, and Bartel B (2010) Conversion of endogenous indole-3-butyric acid to indole-3-acetic acid drives cell expansion in Arabidopsis seedlings. *Plant Physiol* 153: 1577-1586.

Su S H, Suarez-Rodriguez M C, and Krysan P (2007) Genetic interaction and phenotypic analysis of the Arabidopsis MAP kinase pathway mutations mekk1 and mpk4 suggests signaling pathway complexity. *FEBS Lett* 581: 3171-3177.

Su W, and Howell S H (1992) A Single Genetic Locus, Ckr1, Defines Arabidopsis Mutants in which Root Growth Is Resistant to Low Concentrations of Cytokinin. *Plant Physiol* 99: 1569-1574.

Suarez-Rodriguez M C, Adams-Phillips L, Liu Y, Wang H, Su S H, Jester P J, Zhang S et al. (2007) MEKK1 is required for flg22-induced MPK4 activation in Arabidopsis plants. *Plant Physiol* 143: 661-669.

Svensson J, Palva E T, and Welin B (2000) Purification of recombinant Arabidopsis thaliana dehydrins by metal ion affinity chromatography. *Protein Expr Purif* 20: 169-178.

Swire-Clark G A, and Marcotte W R (1999) The wheat LEA protein Em functions as an osmoprotective molecule in Saccharomyces cerevisiae. *Plant Mol. Biol* 39: 117-128.

Takeda S, Gapper C, Kaya H, Bell E, Kuchitsu K, and Dolan L (2008) Local positive feedback regulation determines cell shape in root hair cells. *Science* 319: 1241-1244.

Tanaka S, Ikeda K, and Miyasaka H (2004) Isolation of a new member of group 3 late embryogenesis abundant protein gene from a halotolerant green alga by a functional expression screening with cyanobacterial cells. *FEMS Microbiol Lett* 236: 41-45.

ten Have A, and Woltering E J (1997) Ethylene biosynthetic genes are differentially expressed during carnation (Dianthus caryophyllus L.) flower senescence. *Plant Mol Biol* 34: 89-97.

Thoma I, Loeffler C, Sinha A K, Gupta M, Krischke M, Steffan B, Roitsch T et al. (2003) Cyclopentenone isoprostanes induced by reactive oxygen species trigger defense gene activation and phytoalexin accumulation in plants. *Plant J* 34: 363-375.

Thomas H, Huang L, Young M, and Ougham H (2009) Evolution of plant senescence. *BioMed Central.* Vol. 9:163.

Thomas H, Ougham H J, Wagstaff C, and Stead A D (2003) Defining senescence and death. *J Exp Bot* 54: 1127-1132.

Thomashow M F (1998) Role of cold-responsive genes in plant freezing tolerance. *Plant Physiol* 118: 1-8.

Thomma B P, Eggermont K, Penninckx I A, Mauch-Mani B, Vogelsang R, Cammue B P, and Broekaert W F (1998) Separate jasmonate-dependent and salicylate-dependent defense-response pathways in Arabidopsis are essential for resistance to distinct microbial pathogens. *Proc Natl Acad Sci U S A* 95: 15107-15111.

Thomma B P, Eggermont K, Tierens K F, and Broekaert W F (1999a) Requirement of functional ethylene-insensitive 2 gene for efficient resistance of Arabidopsis to infection by Botrytis cinerea. *Plant Physiol* 121: 1093-1102.

Thomma B P, Nelissen I, Eggermont K, and Broekaert W F (1999b) Deficiency in phytoalexin production causes enhanced susceptibility of Arabidopsis thaliana to the fungus Alternaria brassicicola. *Plant J* 19: 163-171.

Tolleter D, Hincha D K, and Macherel D (2010) A mitochondrial late embryogenesis abundant protein stabilizes model membranes in the dry state. *Biochim Biophys Acta* 1798: 1926-1933.

Tolleter D, Jaquinod M, Mangavel C, Passirani C, Saulnier P, Manon S, Teyssier E et al. (2007) Structure and function of a mitochondrial late embryogenesis abundant protein are revealed by desiccation. *Plant Cell* 19: 1580-1589.

Tompa P (2002) Intrinsically unstructured proteins. *Trends Biochem Sci* 27: 527-533.

Tompa P, Bánki P, Bokor M, Kamasa P, Kovács D, Lasanda G, and Tompa K (2006) Protein-water and protein-buffer interactions in the aqueous solution of an intrinsically unstructured plant dehydrin: NMR intensity and DSC aspects. *Biophys J* 91: 2243-2249.

Tompa P, and Kovacs D (2010) Intrinsically disordered chaperones in plants and animals. *Biochem Cell Biol* 88: 167-174.

Ton J, Van Pelt J A, Van Loon L C, and Pieterse C M (2002) Differential effectiveness of salicylate-dependent and jasmonate/ethylene-dependent induced resistance in Arabidopsis. *Mol Plant Microbe Interact* 15: 27-34.

Torres M A (2010) ROS in biotic interactions. *Physiol Plant* 138: 414-429.

Torres M A, Jones J D, and Dangl J L (2006) Reactive oxygen species signaling in response to pathogens. *Plant Physiol* 141: 373-378.

Tosti N, Pasqualini S, Borgogni A, Ederli L, Falistocco E, Crispi S, and Paolocci F (2006) Gene expression profiles of O3-treated Arabidopsis plants. *Plant Cell Environ* 29: 1686-1702.

Tran L S, Nakashima K, Sakuma Y, Simpson S D, Fujita Y, Maruyama K, Fujita M et al. (2004) Isolation and functional analysis of Arabidopsis stress-inducible NAC transcription factors that bind to a drought-responsive cis-element in the early responsive to dehydration stress 1 promoter. *Plant Cell* 16: 2481-2498.

Tripathi S K, and Tuteja N (2007) Integrated signaling in flower senescence: an overview. *Plant Signal Behav* 2: 437-445.

Tunnacliffe A, Hincha D, Leprince O, and Macherel D (2010) LEA Proteins: Versatility of Form and Function. In: Lubzens E, Cerda J, and Clark M [eds.] *Dormancy and Resistance in Harsh Environments*. Vol. 21. Springer Berlin / Heidelberg, pp. 91-108.

Tunnacliffe A, and Wise M J (2007) The continuing conundrum of the LEA proteins. *Naturwissenschaften* 94: 791-812.

Ulker B, Shahid Mukhtar M, and Somssich I E (2007) The WRKY70 transcription factor of Arabidopsis influences both the plant senescence and defense signaling pathways. *Planta* 226: 125-137.

Ulker B, and Somssich I E (2004) WRKY transcription factors: from DNA binding towards biological function. *Curr Opin Plant Biol* 7: 491-498.

Uno Y, Furihata T, Abe H, Yoshida R, Shinozaki K, and Yamaguchi-Shinozaki K (2000) Arabidopsis basic leucine zipper transcription factors involved in an abscisic acid-dependent signal transduction pathway under drought and high-salinity conditions. *Proc Natl Acad Sci U S A* 97: 11632-11637.

Urano K, Kurihara Y, Seki M, and Shinozaki K (2010) 'Omics' analyses of regulatory networks in plant abiotic stress responses. *Curr Opin Plant Biol* 13: 132-138.

van der Graaff E, Schwacke R, Schneider A, Desimone M, Flügge U I, and Kunze R (2006) Transcription analysis of arabidopsis membrane transporters and hormone pathways during developmental and induced leaf senescence. *Plant Physiol* 141: 776-792.

van Doorn W G, Balk P A, van Houwelingen A M, Hoeberichts F A, Hall R D, Vorst O, van der Schoot C et al. (2003) Gene expression during anthesis and senescence in Iris flowers. *Plant Mol Biol* 53: 845-863.

van Doorn W G, and Woltering E J (2008) Physiology and molecular biology of petal senescence. *J Exp Bot* 59: 453-480.

Vandenabeele S, Vanderauwera S, Vuylsteke M, Rombauts S, Langebartels C, Seidlitz H K, Zabeau M et al. (2004) Catalase deficiency drastically affects gene expression induced by high light in Arabidopsis thaliana. *Plant J* 39: 45-58.

Vieweg M F, Frühling M, Quandt H J, Heim U, Bäumlein H, Pühler A, Küster H et al. (2004) The promoter of the Vicia faba L. leghemoglobin gene VfLb29 is specifically activated in the infected cells of root nodules and in the arbuscule-containing cells of mycorrhizal roots from different legume and nonlegume plants. *Mol Plant Microbe Interact* 17: 62-69.

Villain P, Mache R, and Zhou D X (1996) The mechanism of GT element-mediated cell type-specific transcriptional control. *J Biol Chem* 271: 32593-32598.

Wagstaff C, Chanasut U, Harren F J, Laarhoven L J, Thomas B, Rogers H J, and Stead A D (2005) Ethylene and flower longevity in Alstroemeria: relationship between tepal senescence, abscission and ethylene biosynthesis. *J Exp Bot* 56: 1007-1016.

Wagstaff C, Malcolm P, Rafiq A, Leverentz M, Griffiths G, Thomas B, Stead A et al. (2003) Programmed cell death (PCD) processes begin extremely early in Alstroemeria petal senescence. *New Phyto* 160: 49-59.

Wagstaff C, Yang T J, Stead A D, Buchanan-Wollaston V, and Roberts J A (2009) A molecular and structural characterization of senescing Arabidopsis siliques and comparison of transcriptional profiles with senescing petals and leaves. *Plant J* 57: 690-705.

Weaver L M, and Amasino R M (2001) Senescence is induced in individually darkened Arabidopsis leaves, but inhibited in whole darkened plants. *Plant Physiol* 127: 876-886.

Weaver L M, Froehlich J E, and Amasino R M (1999) Chloroplast-targeted ERD1 protein declines but its mRNA increases during senescence in Arabidopsis. *Plant Physiol* 119: 1209-1216.

Weaver L M, Gan S, Quirino B, and Amasino R M (1998) A comparison of the expression patterns of several senescence-associated genes in response to stress and hormone treatment. *Plant Mol Biol* 37: 455-469.

Wiermer M, Feys B J, and Parker J E (2005) Plant immunity: the EDS1 regulatory node. *Curr Opin Plant Biol* 8: 383-389.

Wilkinson J E, Twell D, and Lindsey K (1997) Activities of CaMV 35S and nos promoters in pollen: implications for field release of transgenic plants. *Journal of Experimental Botany* 48: 265-275.

Wise M J (2003) LEAping to conclusions: a computational reanalysis of late embryogenesis abundant proteins and their possible roles. *BMC Bioinformatics* 4: 52.

Wise M J, and Tunnacliffe A (2004) POPP the question: what do LEA proteins do? *Trends Plant Sci* 9: 13-17.

Xu D, Duan X, Wang B, Hong B, Ho T, and Wu R (1996) Expression of a Late Embryogenesis Abundant Protein Gene, HVA1, from Barley Confers Tolerance to Water Deficit and Salt Stress in Transgenic Rice. *Plant Physiol* 110: 249-257.

Xu Q, and Zhang L (2009) Plant caspase-like proteases in plant programmed cell death. *Plant Signal Behav* 4.

Xue J, Li Y, Tan H, Yang F, Ma N, and Gao J (2008) Expression of ethylene biosynthetic and receptor genes in rose floral tissues during ethylene-enhanced flower opening. *J Exp Bot* 59: 2161-2169.

Yamada T, Ichimura K, and van Doorn W G (2006a) DNA degradation and nuclear degeneration during programmed cell death in petals of Antirrhinum, Argyranthemum, and Petunia. *J Exp Bot* 57: 3543-3552.

Yamada T, Takatsu Y, Kasumi M, Ichimura K, and van Doorn W G (2006b) Nuclear fragmentation and DNA degradation during programmed cell death in petals of morning glory (Ipomoea nil). *Planta* 224: 1279-1290.

Yamaguchi R, Andreyev A, Murphy A N, Perkins G A, Ellisman M H, and Newmeyer D D (2007) Mitochondria frozen with trehalose retain a number of biological functions and preserve outer membrane integrity. *Cell Death Differ* 14: 616-624.

Yamaguchi-Shinozaki K, and Shinozaki K (1993) Characterization of the expression of a desiccation-responsive rd29 gene of Arabidopsis thaliana and analysis of its promoter in transgenic plants. *Mol Gen Genet* 236: 331-340.

Yamaguchi-Shinozaki K, and Shinozaki K (1994) A novel cis-acting element in an Arabidopsis gene is involved in responsiveness to drought, low-temperature, or high-salt stress. *Plant Cell* 6: 251-264.

Yamaguchi-Shinozaki K, and Shinozaki K (2005) Organization of cis-acting regulatory elements in osmotic- and cold-stress-responsive promoters. *Trends Plant Sci* 10: 88-94.

Yasuda M, Ishikawa A, Jikumaru Y, Seki M, Umezawa T, Asami T, Maruyama-Nakashita A et al. (2008) Antagonistic interaction between systemic acquired resistance and the abscisic acid-mediated abiotic stress response in Arabidopsis. *Plant Cell* 20: 1678-1692.

Yoshida T, Fujita Y, Sayama H, Kidokoro S, Maruyama K, Mizoi J, Shinozaki K et al. (2010) AREB1, AREB2, and ABF3 are master transcription factors that cooperatively regulate ABRE-

dependent ABA signaling involved in drought stress tolerance and require ABA for full activation. *Plant J* 61: 672-685.

Zelko I N, Mariani T J, and Folz R J (2002) Superoxide dismutase multigene family: a comparison of the CuZn-SOD (SOD1), Mn-SOD (SOD2), and EC-SOD (SOD3) gene structures, evolution, and expression. *Free Radic Biol Med* 33: 337-349.

Zentgraf U (2007) *Oxidative Stress and Leaf Senescence*. Blackwell Publishing Ltd.

Zentgraf U, Laun T, and Miao Y (2010) The complex regulation of WRKY53 during leaf senescence of Arabidopsis thaliana. *Eur J Cell Biol* 89: 133-137.

Zhang Y, Fan W, Kinkema M, Li X, and Dong X (1999) Interaction of NPR1 with basic leucine zipper protein transcription factors that bind sequences required for salicylic acid induction of the PR-1 gene. *Proc Natl Acad Sci U S A* 96: 6523-6528.

Zheng Z, Qamar S A, Chen Z, and Mengiste T (2006) Arabidopsis WRKY33 transcription factor is required for resistance to necrotrophic fungal pathogens. *Plant J* 48: 592-605.

Zhou N, Tootle T L, and Glazebrook J (1999) Arabidopsis PAD3, a gene required for camalexin biosynthesis, encodes a putative cytochrome P450 monooxygenase. *Plant Cell* 11: 2419-2428.

Zhou N, Tootle T L, Tsui F, Klessig D F, and Glazebrook J (1998) PAD4 functions upstream from salicylic acid to control defense responses in Arabidopsis. *Plant Cell* 10: 1021-1030.

Zhou Y, Wang C-Y, Ge H, Hoeberichts F A, and Visser P B (2005) Programmed Cell Death in Relation to Petal Senescence in Ornamental Plants. *J Integ Plant Biol* 47: 641-650.

Zimmermann P, Heinlein C, Orendi G, and Zentgraf U (2006) Senescence-specific regulation of catalases in Arabidopsis thaliana (L.) Heynh. *Plant Cell Environ* 29: 1049-1060.

Zimmermann P, Hirsch-Hoffmann M, Hennig L, and Gruissem W (2004) GENEVESTIGATOR. Arabidopsis microarray database and analysis toolbox. *Plant Physiol* 136: 2621-2632.

Zimmermann P, and Zentgraf U (2005) The correlation between oxidative stress and leaf senescence during plant development. *Cell Mol Biol Lett* 10: 515-534.

Appendix A

A Comparison of Leaf and Petal Senescence in Wallflower Reveals Common and Distinct Patterns of Gene Expression and Physiology[1][W]

Anna Marie Price[2], Danilo F. Aros Orellana, Faezah Mohd Salleh, Ryan Stevens, Rosemary Acock, Vicky Buchanan-Wollaston, Anthony D. Stead, and Hilary J. Rogers*
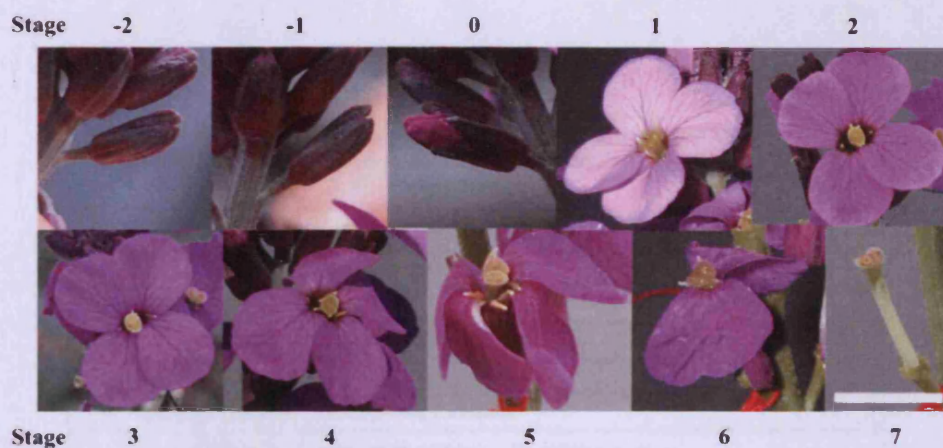
Figure 1. Stages of wallflower flower development. Stage −2 and stage −1, Two sequential buds below the lowest unopened bud on the raceme. Sepals completely cover petals. Stage 0, Lowest unopened bud on raceme. Petals are dark purple in color, tightly curled within sepals. Stage 1, Flower fully opened. Petals are pale purple, with sepals folded back midway along their length. Stigma is yellow and fuzzy in appearance, four of six anthers are visible, all undehisced, positioned close to the stigma with the tips curled over the stigma. Stage 2, As stage 1, but petals are darker in color. All six anthers are visible, two newly emerged anthers are dehisced and curled back from the stigma. Stage 3, The flower is not as tightly held together as previously. Petals are wilting slightly and darker again in color. Fuzz on stigma is not as fine as previously. All six anthers are dehisced and curled back from the stigma. Stage 4, The flower is loosely held together. Petals are limp and curled over at the tips. Flower appearance has deteriorated. Stage 5, As stage 4, but more extreme. Petals are wilted, stigma is discolored with dark purple areas. Stage 6, Sepals, petals, and stamens are beginning to abscise. Remaining petals look withered and dry. Stage 7, All sepals, petals, and stamens are abscised; only the stigma remains. Bar = 10 mm.
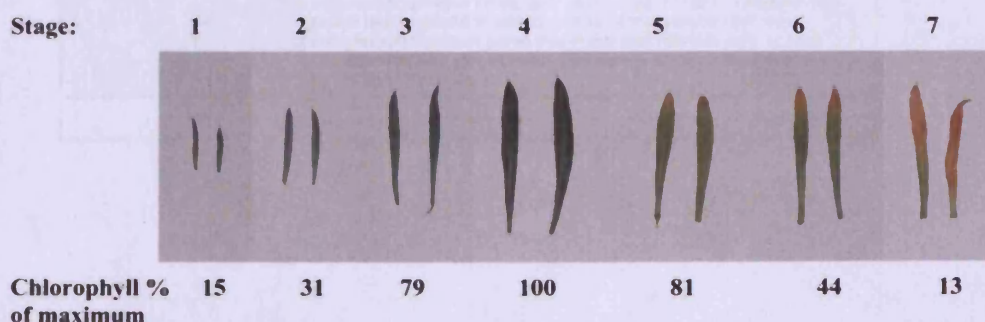

Figure 2. Stages of wallflower leaf development. Stage 1, Very young leaves, less than 50% expanded. Stage 2, Very young leaves, 50% to 75% expanded. Stage 3, Young leaves, 75% to 100% expanded. Stage 4, Mature green leaves. Stage 5, Older mature leaves, green with signs of yellowing on the tip. Stage 6, Old leaves, up to 50% of leaf area yellow. Stage 7, Very old leaves, mostly or all yellow. Below each image is the total chlorophyll for that leaf stage expressed as a percentage of maximum.

Appendix B

Manuscript accepted for publication in Plant, Cell and Environment Journal on 08/06/2011.

Plant, Cell &
Environment

PC
E

A novel function for a redox-related LEA protein (SAG21/AtLEA5) in root development and biotic stress responses.

| Journal:	Plant, Cell & Environment
Manuscript ID:	Draft
Wiley - Manuscript type:	Original Article
Environment Keywords:	oxidative stress, pathogens
Physiology Keywords:	development, hormones
Other Keywords:	senescence, root hair, LEA proteins, ROS
Abstract:	SAG21/AtLEA5 belongs to the late embryogenesis-associated (LEA) protein family, implicated in growth and redox responses. Over-expression (OEX) of SAG21/AtLEA5 resulted in increased root and shoot biomass, whereas antisense (AS) lines exhibited reduced biomass. Root and shoot development was altered in transgenic lines, with earlier flowering and senescence in aerial parts of AS lines. Primary root length was reduced in AS lines, as was the number of laterals relative to the primary root. Transgenic lines exhibited marked root hair phenotypes, with longer root hairs in OEX lines and shorter root hairs in AS, relative to wild type. Abiotic stress (drought, cold, NaCl, H2O2) induced SAG21/AtLEA5 expression in roots but not leaves. SAG21/AtLEA5 expression was also induced in roots by salicylic acid, ethylene and methyl jasmonate. Biotic stress (Botrytis cinerea inoculation) induced expression in leaves. Growth of B. cinerea and of a virulent bacterial pathogen (Pseudomonas syringae pv. tomato) was affected by SAG21/AtLEA5 expression, however growth of an avirulent P.syringae strain was unaffected. A SAG21/AtLEA5-YFP fusion was localised to mitochondria. We conclude that this mitochondrial protein plays and important role not only in root development but also in biotic and abiotic stress responses in a tissue-specific manner.

Appendix C

SAG21(1685)::GUS

| Control (water) | NaCl |
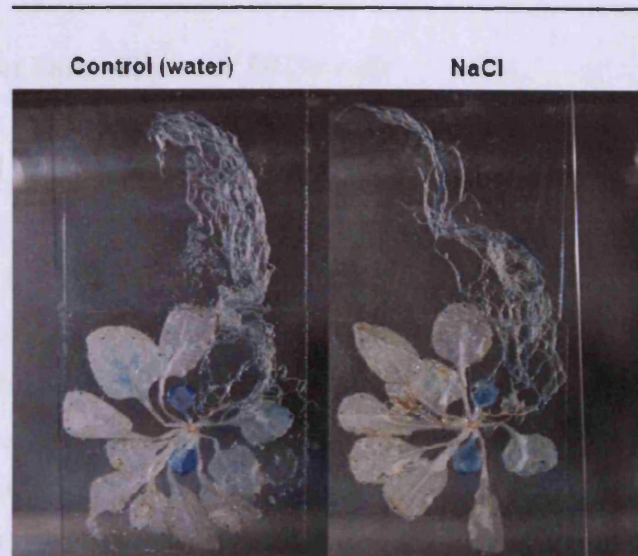
Appendix D

Mannitol

| WT | SAG21-AS | SAG21-OEX |
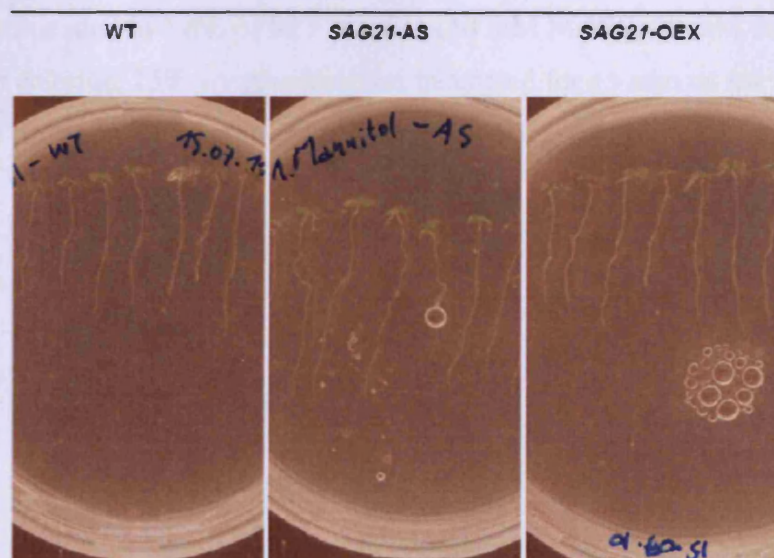
Appendix E

Preparation of competent Escherichia coli *DH5α cells*

E.coli DH5α competent cells were prepared with minor modification of the procedure of Hanahan (1983). Twenty mL of SOC medium (20 g L^{-1} tryptone, 5 g L^{-1} yeast extract, 0.5 g L^{-1} NaCl, 100 mL L^{-1} 1 M MgCl$_2$, 10 mL L^{-1} 2 M glucose) were inoculated in a 250 mL flask with a single colony of *E.coli* DH5α and were incubated overnight at 37°C, in a Gallenkamp orbital incubator set at 200 rpm. Then 0.625 mL of the overnight culture were inoculated in 500 mL flasks containing 62.5 mL of 2YT medium (16 g L^{-1} tryptone, 10 g L^{-1} yeast extract, 5 g L^{-1} NaCl) . The cultures were incubated at 37°C in a Gallenkamp orbital incubator set at 200 rpm, until an OD$_{600}$ of 0.5 (1 to 3 h) was reached. The cells were harvested by centrifugation for 10 min at 1°C, in a Beckman Coulter Avanti® J-E centrifuge fitted with a JA-14 rotor set at 5000 rpm. The pellets were resuspended in 20.75 mL of RF1 solution (10 mM MOPS, 10mM rubidium chloride, 50 mM manganese chloride, 30 mM potassium acetate, 10 mM calcium chloride, 15% w/v glycerol pH 5.8). The cells were incubated for 1 h on ice at 4°C and harvested by centrifugation for 10 min at 1°C in a Beckman Coulter Avanti® J-E centrifuge fitted with a JA-14 rotor set at 5000 rpm. The pellets were resuspended in 5 mL of RF2 solution (10 mM MOPS, 10 mM rubidium chloride, 75 mM calcium chloride, 15% v/v glycerol) and incubated for 15 min on ice at 4°C. Aliquots of 100 μL were frozen in liquid nitrogen and stored at -80°